Targeting neuroinflammation in Parkinson's disease

by Sarah Thomas Broome

Thesis submitted in fulfilment of the requirements for the degree of

Doctor of Philosophy

under the supervision of Alessandro Castorina

University of Technology Sydney
Faculty of Science

May 2022

Certificate of Original Authorship

I, *Sarah Thomas Broome* declare that this thesis, is submitted in fulfilment of the requirements for the award of *Doctor of Philosophy*, in the *Faculty of Science* at the University of Technology Sydney.

This thesis is wholly my own work unless otherwise referenced or acknowledged. In addition, I certify that all information sources and literature used are indicated in the thesis.

This document has not been submitted for qualifications at any other academic institution.

Production Note:
Signature: Signature removed prior to publication.

Date: 15/01/2022

Acknowledgments

First and foremost, I am extremely grateful to my supervisor, Associate Professor Alessandro Castorina, for taking a chance on me as a second-year transfer student and providing invaluable advice, unfaltering support and patience during my PhD study. It has truly been an honour and privilege to be your student and part of the LCMN. This achievement was made possible because of you.

I would also like to express my sincere gratitude to Professor Hui Chen, Dr Jeremy Chan, Ms Fiona Ryan, Dr Ghaith Al-Badri and past LCMN members for their insightful suggestions, technical support, lab chats and coffee breaks.

Finally, I would like to thank my friends and family for their unwavering and unconditional support. To my friends who were always there to drag me out of the lab and give me a break. To my grandparents, Yvette and David Broome, who are unfailingly generous and kind and my inspiration for becoming a neuroscientist. To my brother, Daniel, for his exceptional music suggestions, sense of humour and expert editing skills and advice. To my father, Brian, for his generosity, chauffeur services, attempts at science jokes and foundation, and my mother, Marisa, who is my ultimate inspiration and guidepost for everything.

Impact of Covid-19 pandemic

Unfortunately, I commenced my PhD in a lab group that was not able to create a productive and supportive environment to complete my research and after one year I changed supervisors and projects. The data in my thesis is the product of the research done in the Laboratory of Cellular and Molecular Neuroscience (LCMN).

During the two remaining years of my PhD candidature the Covid-19 pandemic caused several disruptions. From March to June 2020 the lab was closed, as per government health order. As such no lab work could be conducted during this time. The next lockdown, from the end of June to October 2021 resulted in significant disruptions accessing and learning new techniques including immunohistochemistry and microscopy. During these lockdowns I focused on developing my writing skills, with previously collected data from the LCMN, as well as analysing and curating data I had already collected. The second lockdown resulted in a dramatic downscale of experiments planned for microscopy due to lack of access and technical support. Despite these obstacles, the resulting body of work, obtained within two years amid two lockdowns was possible due to the support of my supervisor and sacrifice of my family who did everything possible to keep our household virus free.

Table of Contents

List of Figures

List of Tables

List of Abbreviations

5-HT	Serotonin/5-hydroxytrptamine
5HT1a	Serotonin receptor 1a
5HT2a	Serotonin receptor 2a
6-OHDA	6-hydroxydopamine
A1	Classically activated astrocytes
A2	Alternatively activated astrocytes
ADNP	Activity-dependent neuroprotective protein
Arg1	Arginase-1
BBB	Blood brain barrier
BDNF	Brain derived neurotrophic factor
BW	Body weight
CNS	Central nervous system
COMT	Catechol-O-methyltransferase
CRISPR	Clustered regularly interspaced short palindromic repeats
CSF	Cerebrospinal fluid
D2R	Dopamine-2-receptor
D3R	Dopamine-3receptor
D4R	Dopamine-4-receptor
DBS	Deep brain stimulation
DR	Dopamine receptor
Drd3	Gene encoding the dopamine-3-receptor
DRT	Dopamine replacement therapy
FDA	Food and Drug Administration (United States of America)
Fizz1	Found in inflammatory zone/Retnla

GABA	Gamma-aminobutyric acid
GFAP	Glial fibrillary acidic protein
GIT	Gastrointestinal tract
Htr1a	Gene encoding serotonin receptor 1a
IBD	Irritable bowel syndrome
IFN-γ	Interferon-gamma
IL-1β	Interleukin-1 beta
IL-4	Interleukin-4
IL-6	Interleukin-6
IL-10	Interleukin-10
iPSCs	Induced pluripotent stem cells
iNOS	Inducible nitric oxide synthase
KO	Knockout
L-Dopa	Levodopa
LPS	Lipopolysaccharide
Mθ	Resting microglia
M1	Classically activated microglia
M2	Alternatively activated microglia
MAO	Monoamine oxidase
MPTP	1-methyl-4-phenyl-1,2,3,6-tetrahydropyridine
MPP+	1-methyl-4-phenylpyridinium
NMDA	N-methyl-D-aspartic acid
NMS	Non-motor symptoms
NO	Nitric oxide
NSAIDs	Non-steroidal anti-inflammatory agents

PACAP	Pituitary adenylate cyclase-activating polypeptide
PD	Parkinson's disease
PET	Positron emission tomography
ROS	Reactive oxygen species
SNpc	*Substantia nigra pars compacta*
TGF-β	Transforming growth factor beta
TH	Tyrosine hydroxylase
TNF-α	Tumour necrosis factor-alpha
VIP	Vasoactive intestinal peptide

Publications

Publications arising from thesis

Submitted:

Thomas Broome, S. and Castorina, A. **Neurotoxicity of Rotenone in the Central Nervous System of C57BL/6 mice**. *Scientific reports*. Submitted on: 18/11/2021. Current status: Editors invited 12/01/2022

Published:

Thomas Broome, S., & Castorina, A. (2022). **The Anxiolytic Drug Buspirone Prevents Rotenone-Induced Toxicity in a Mouse Model of Parkinson's Disease**. *International journal of molecular sciences*, *23*(3), 1845. https://doi.org/10.3390/ijms23031845

Broome, S. T., Musumeci, G., & Castorina, A. (2022). **PACAP and VIP Mitigate Rotenone-Induced Inflammation in BV-2 Microglial Cells**. *Journal of molecular neuroscience : MN*, 10.1007/s12031-022-01968-1. Advance online publication. https://doi.org/10.1007/s12031-022-01968-1

Thomas Broome, S., Fisher, T., Faiz, A., Keay, K. A., Musumeci, G., Al-Badri, G., & Castorina, A. (2021). **Assessing the Anti-Inflammatory Activity of the Anxiolytic Drug Buspirone Using CRISPR-Cas9 Gene Editing in LPS-Stimulated BV-2 Microglial Cells**. *Cells*, *10*(6), 1312. https://doi.org/10.3390/cells10061312

Thomas Broome, S., Louangaphay, K., Keay, K. A., Leggio, G. M., Musumeci, G., & Castorina, A. (2020). **Dopamine: an immune transmitter**. *Neural regeneration research*, *15*(12), 2173–2185. https://doi.org/10.4103/1673-5374.284976

Published conference abstracts:

Thomas Broome, S. and Castorina, A. (2021). **Repurposing the anxiolytic drug buspirone to counteract inflammation in cellular and animal models of Parkinson's disease**. Life Sciences, Medicine, and Biomedicine (ISSN 2600-7207).

Other publications

Jansen, M. I., **Thomas Broome, S.,** & Castorina, A. (2022). **Exploring the Pro-Phagocytic and Anti-Inflammatory Functions of PACAP and VIP in Microglia: Implications for Multiple Sclerosis**. *International Journal of Molecular Sciences*, *23*(9), 4788.

Jansen, M[+].; **Thomas Broome, S**[+].; Castorina, A. (2021). **Targeting the neurological comorbidities of multiple sclerosis: the beneficial effects of VIP and PACAP neuropeptides**. *J. Integr. Neurosci*
(+ denotes equal contribution first authors)

Karunia, J.; Niaz, A.; Mandwie, M.; **Thomas Broome, S**.; Keay, K.A.; Waschek, J.A.; Al-Badri, G.; Castorina, A. (2021). **PACAP and VIP Modulate LPS-induced Microglial Activation and Trigger Distinct Phenotypic Changes in Murine BV2 Microglial Cells**. *Int. J. Mol. Sci,* 22, 10947. doi:
https://doi.org/10.3390/ijms222010947

Thomas Broome, S.; Musumeci, G.; Castorina, A. (2021). **Doxycycline and Minocycline Act as Positive Allosteric Modulators of the PAC1 Receptor and Induce Plasminogen Activators in RT4 Schwann Cells**. *Appl. Sci*. 11, 7673.
https://doi.org/10.3390/app11167673

Conference presentations

Invited oral presentations:

<u>Thomas Broome, S</u>. and Castorina, A. Repurposing the anxiolytic drug buspirone to counteract inflammation in cellular and animal models of Parkinson's disease, *University of Sydney, Conjoint Neuroscience Meeting* (2021)

<u>Thomas Broome, S</u>. My career journey and doctoral research, *Students of Brain Research* (2021)

<u>Thomas Broome, S</u>. and Castorina, A. Targeting neuroinflammation in Parkinson's disease, *Australasian Neuroscience Society, Early Career Researcher Webinar Series* (2020)

Oral presentations:

<u>Thomas Broome, S</u>. and Castorina, A. Repurposing the anxiolytic drug buspirone to counteract inflammation in cellular and animal models of Parkinson's disease, *International Society of Neuroimmunology Congress* (2021)

<u>Thomas Broome, S</u>. and Castorina, A. Assessing the anti-inflammatory activity of Buspirone, *Australian Society of Medical Research NSW Scientific Meeting* (2021*), First place*

<u>Thomas Broome, S</u>. and Castorina, A. Aspirin for Parkinson's disease, *Australian Society of Medical Research, Victoria Student Symposium*, Flash talk (2021), *Second place*

<u>Thomas Broome, S</u>. and Castorina, A. Repurposing buspirone for Parkinson's disease, *Australasian Neuroscience Society*, Flask talk (2020), *Finalist*

<u>Thomas Broome, S</u>. Aspirin for Parkinson's disease, University of Technology Sydney, *3-minute-thesis competition* (2020)

Thomas Broome, S. Aspirin for Parkinson's disease, *BioMed Link Conference*, University of Melbourne, Australia, 3-minute-thesis (2019), *First place*

Poster presentations:

Thomas Broome, S. and Castorina, A. *Students of Brain Research Symposium* (2021), *Second place*

Thomas Broome, S. and Castorina, A. Repurposing the anxiolytic drug buspirone to counteract inflammation in cellular and animal models of Parkinson's disease, *Graduate Research Symposium*, Taylor's University, Malaysia (2021)

Thomas Broome, S. and Castorina, A. Targeting neuroinflammation in Parkinson's disease, *European Molecular Biology Laboratory (EMBL) PhD Symposium* (2020)

Thomas Broome, S. and Castorina, A. Targeting neuroinflammation in Parkinson's disease, *BioMed Link Conference*, University of Melbourne (2019)

Awards and Scholarships

Paper of the Month (Jan-Feb 2022)

Thomas Broome, S., & Castorina, A. (2022). **The Anxiolytic Drug Buspirone Prevents Rotenone-Induced Toxicity in a Mouse Model of Parkinson's Disease**. *International journal of molecular sciences*, *23*(3), 1845.
https://doi.org/10.3390/ijms23031845
School of Life Sciences, University of Technology Sydney

Vice Chancellor's Conference Award (2021)

Travel fund to attend the 15th International Society of Neuroimmunology Congress, November 2021.

Second place poster (2021)

Students of Brain Research (SOBR) Symposium.

First place PhD Student Presentation (2021)

Australian Society of Medical Research (ASMR) NSW Annual Scientific Meeting.

Second place flash talk (2021)

Australian Society of Medical Research (ASMR) Victoria Student Symposium.

First Place Three-minute-thesis (2019)

BioMed Link Conference, University of Melbourne.

BioMed Link Conference Travel Award, Melbourne, Australia (2019)

Travel fund to attend the BioMed Link Conference in Melbourne.

UTS Research Excellence PhD Scholarship (July 2018 – December 2021)

Financial support during my PhD candidature.

Professional experience

Manuscript Peer Reviewer (Since 2021)

Neuroscience (IF 3.59), Frontiers in Molecular Neuroscience (IF 5.693), Scientific Reports (IF 4.379)

Deputy Convener Gala Dinner (2021) and Convener Annual Scientific Meeting (2022)

Australian Society of Medical Research, NSW Committee

NSW Representative (2021-2022)

Australasian Neuroscience Society, Student Committee

#ThisIsMyField Team member (2021)

Pint of Science Australia

Organising Committee and Translational Research Session Chair (2020)

EMBL Australia Postgraduate Symposium

EMBL Australia PhD Course, Hobart (2019)

European Molecular Biology Laboratory (EMBL) Australia

SOUL Award (2019-2021)

University of Technology Sydney

Parkinson's NSW Collaboration with UTS Business School (2019-2020)

Team Leader, Parkinson's NSW and University of Technology Sydney

Accomplish Award (2020)

University of Technology Sydney

Vice-President and Volunteers and Engagement Coordinator (2020)

batyr @ University of Technology Sydney

Postgraduate Student Representative, Research Committee (2019-2020)

University of Technology Sydney

Mentor (Since
2019)

Women's College, The University of Sydney, Australia

PROFESSIONAL MEMBERSHIPS

Students of Brain Research	From 2021
Australian Society of Medical Research	From 2020
Australasian Neuroscience Society	From 2020

Abstract

Parkinson's disease (PD) is a chronic neurodegenerative disease characterised by the progressive loss of midbrain dopaminergic neurons. No one knows how or why dopamine neurons are lost but several studies confirm the presence of neuroinflammation as a critical pathological component of the disease. As such, disease-modifying strategies that can reduce/halt neuroinflammation are likely to ameliorate PD progression and reduce severity.

Considerable evidence suggests that blockade of the dopamine D3 receptor (D3R) is neuroprotective and reduces inflammation in animal models of PD. However, to date there are no selective D3R antagonists in the market. Recently, computational analyses have demonstrated that buspirone, an FDA-approved anxiolytic drug with serotonin 1A (Htr1a) agonist activity, also functions as a potent D3R antagonist. Therefore, we aimed to test in cellular and animal models of PD if buspirone's D3R antagonism exerts anti-inflammatory and, therefore, neuroprotective activities.

In vitro, CRISPR-Cas9 gene deletion of the D3R and/or buspirone treatment in BV2 microglial cells attenuated microglial polarisation after LPS challenge. To determine if this result translated *in vivo,* we generated a rotenone mouse model of PD. Systemic administration of rotenone replicated several pathogenic and behavioural features of PD, including significant locomotor and exploratory impairments, dopaminergic degeneration, widespread alterations of mitochondrial function, increased oxidative stress, glial activation and heightened expression of inflammatory mediators in the midbrain and several extra-nigral CNS sites.

Accordingly, we used this model to assess the ability of buspirone to mitigate rotenone-induced toxicity. Buspirone prevented rotenone-induced behavioural deficits and mitigated dopaminergic degeneration. Drug treatment also prevented astrocyte and microglial activation, which was paralleled by a global downregulation of pro-inflammatory markers and the upregulation of anti-inflammatory markers and neurotrophic factors in several brain regions.

Interestingly, throughout our studies we also report disruptions in the expression levels of the neuroprotective and immune modulatory peptides pituitary adenylate cyclase-activating polypeptide (PACAP) and vasoactive intestinal peptide (VIP) following rotenone intoxication, which were rescued by buspirone. This prompted us to test whether these neuropeptides elicited anti-inflammatory activities against rotenone toxicity in BV2 microglia. Both peptides reliably suppressed microglial activation, suggesting an indirect involvement in the anti-inflammatory machinery triggered by buspirone.

In conclusion, our findings indicate that buspirone mitigates rotenone-induced neurotoxicity and inflammation via the activation of multiple protective and anti-inflammatory pathways, perhaps including PACAP and VIP neuropeptides. Altogether, these findings support the notion that targeting the D3R, PACAP or VIP may be a promising therapeutic strategy to reduce inflammation in PD.

Chapter 1:

General Introduction

1.1 Parkinson's disease

Parkinson's disease (PD) is the second most common progressive neurodegenerative disorder, affecting around 1% of the population over 60 years old [1]. Neurodegenerative diseases like PD present a significant health, economic and social burden on an aging society [2]. Increasing life expectancy means that a larger proportion of our population will become susceptible to neurodegenerative disorders, including PD [3].

PD characterised by the loss of dopamine neurons along the nigrostriatal pathway which originates in the *substantia nigra pars compacta* (*SNpc*) and results in a lack of dopamine available in the striatum [4]. This produces the classical parkinsonian motor symptoms, of bradykinesia, rigidity, tremor and postural instability, as this pathway is responsible for voluntary movement (**Figure 1.1**) [5]. The diagnosis is confirmed following a positive response to dopamine replacement therapy [6]. However, PD is now recognised as a more complex disease that is associated with a myriad of non-motor symptoms (NMS) [7]. NMS include depression, sleep disturbances, sensory abnormalities, autonomic dysfunction and cognitive decline and contribute to increasing disability and poor quality of life [7]. The prevalence of NMS suggests that PD pathology extends beyond the dopamine system.

Dopaminergic neurons project to a wide range of brain regions, including into the prefrontal cortex via the mesocortical pathway and to the hippocampus and amygdala via the mesolimbic pathway (**Figure 1.1**) [8]. These regions are associated with learning and memory, reward, motivation, emotion and cognition, which are all commonly reported NMS [9]. It is still not known how PD pathogenesis spreads, but it could be that the selective degeneration of dopamine neurons along these pathways results in damage to other neurotransmitter systems

including glutamatergic, cholinergic, serotoninergic and noradrenergic [10]. Braak and colleagues attempted to define the pathogenesis of PD, accounting for widespread neurodegeneration and a peripheral origin of disease [4]. Braak staging postulates a peripheral origin, starting in the nasal cavity and the gastrointestinal tract (GIT) and subsequently progressing by a specific pattern via olfactory tract and vagal nerve towards the CNS, excluding the spinal cord [11]. This theory aligns with the clinical appearance of NMS prior to motor symptoms [12] but does not account for the majority of clinical presentations as well as reported disruptions within the spinal cord [13].
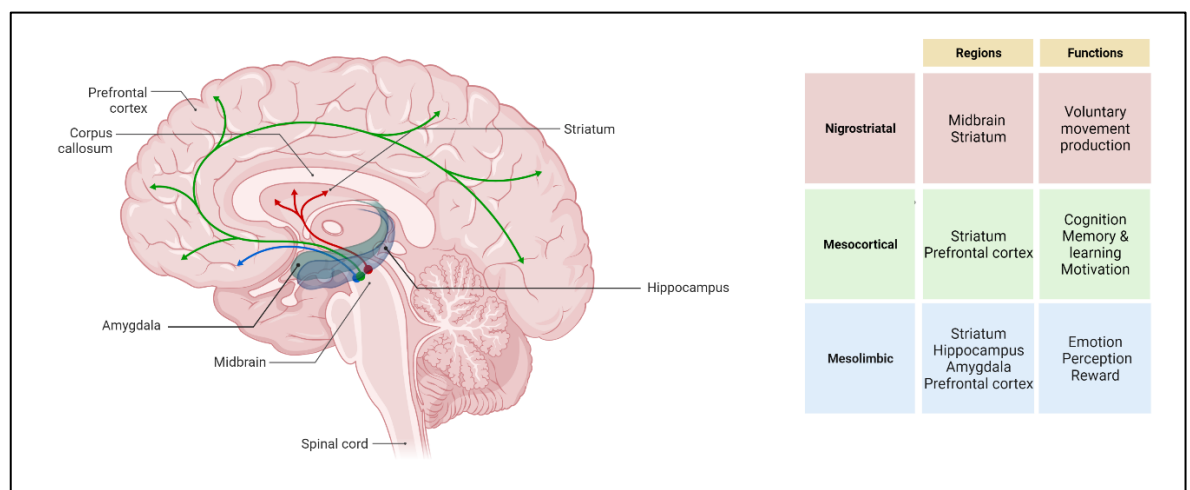
Figure 1.1 Dopaminergic pathways and regions affected in Parkinson's disease. Dopamine neuronal pathways extend beyond the midbrain and striatum (nigrostriatal pathway, shown in red) and encompass several brain regions. The mesocortical pathway (green) describes the neurons projecting from the striatum towards the prefrontal cortex and is involved in cognition, learning and memory as well as motivation. The mesolimbic pathway (blue) defines the projection of neurons from the striatum to the hippocampus, amygdala and prefrontal cortex and contributes to remotion, perception and reward pathways.

Accordingly, it is still not known how or why dopamine neurons are lost. Nevertheless, several pathological hallmarks have been consistently linked to dopaminergic degeneration observed in PD including, neuroinflammation, mitochondrial dysfunction and oxidative stress and the accumulation of α-synuclein aggregations in the form of Lewy bodies [14].

The accumulation of α-synuclein in Lewy bodies has been observed not only throughout the CNS but also in peripheral organs resulting in the appearance of some NMS, including GIT disorders [15]. The presence of α-synuclein Lewy bodies is also used as a diagnostic tool for PD [16]. A potential mechanism of PD has been proposed, in which the accumulation of Lewy bodies disrupts dopamine production and transmission [17]. This causes a build-up of dopamine which can be readily oxidised to form reactive oxygen species (ROS), resulting in oxidative stress [18]. Oxidative stress is detrimental to mitochondrial function and can result in mitophagy and increase susceptibility to excitotoxicity and other cell death pathways [19]. Furthermore, oxidative stress, ROS, excitotoxicity, Lewy bodies and signals of damaged neurons can activate glial cells and enhance neuroinflammation, which promotes further neurodegeneration [20]. **Figure 1.2** demonstrates how these pathological hallmarks are interrelated and create a self-propagating, vicious cycle that ultimately leads to neurodegeneration.
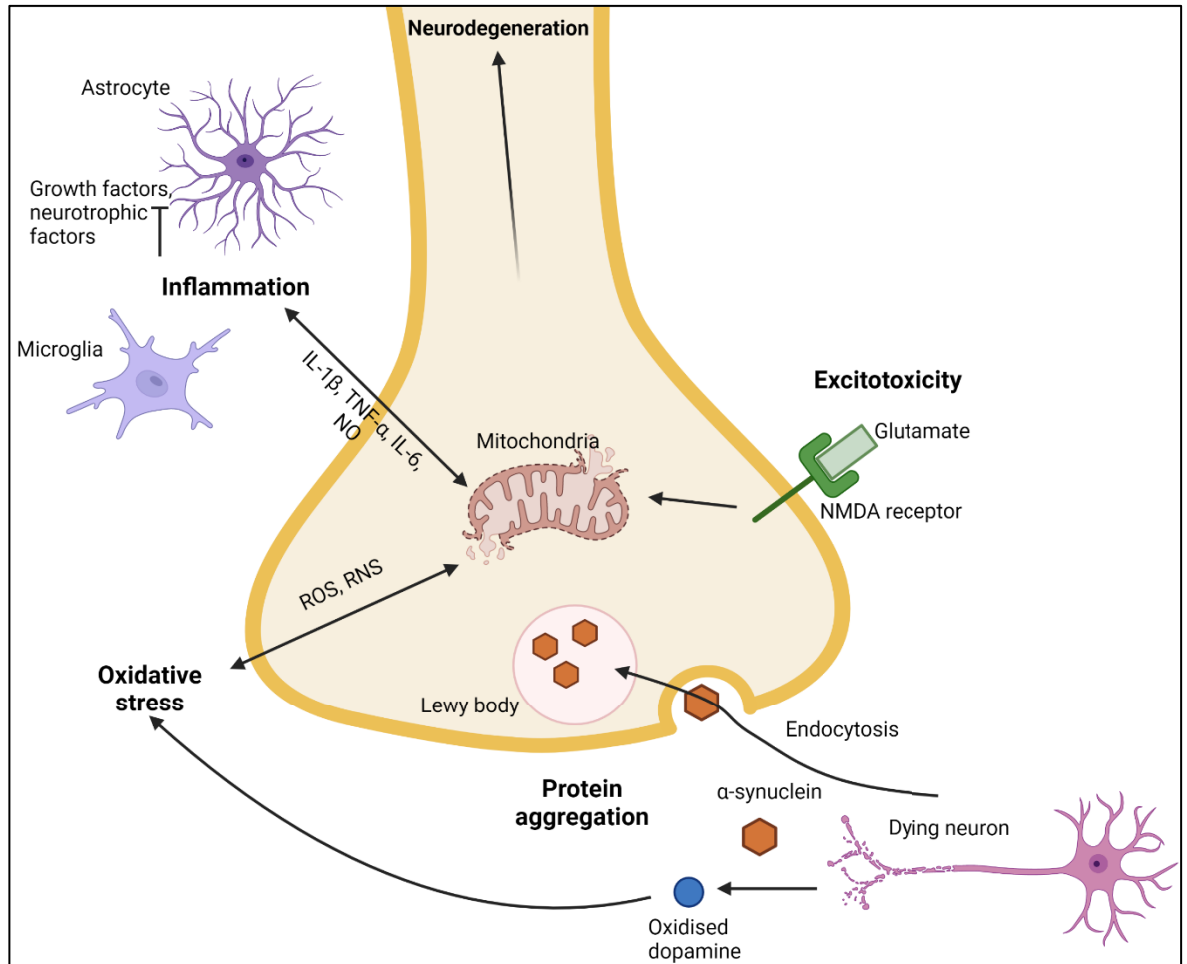
Figure 1.2 Pathological mechanisms of neurodegeneration in Parkinson's disease. As we still don't know how dopamine neurons are compromised, one popular theory is the transfer of α-synuclein aggregates from damaged to healthy neurons that starts the degenerative cascade. The damaged neuron releases a range of factors, including free radicals from oxidised dopamine, which damage mitochondria further contributing to oxidative stress. Damaged mitochondria can contribute to excitotoxicity that leads to the induction of more free radicals. Dying neurons and free radicals can activate glial cells and trigger pro-inflammatory processes that promote neurodegeneration.

Interestingly, the mutations associated with some variants of PD are associated with these pathological hallmarks, particularly α-synuclein and mitochondrial dysfunction. Several autosomal dominant and autosomal recessive gene mutations that increase an individual's risk of developing certain variants of PD have been identified (**Table 1**). However, these genetic risk factors are only relevant for early onset PD, with most cases (~90%) being of sporadic origin.

Table 1. Summary of the main genetic mutations associated with PD.

Gene	Associated pathological hallmark	Mode of inheritance	Age of onset (years)
SNCA	α-synuclein	Autosomal dominant	20-85
LRRK2	Enzymatic activity	Autosomal dominant	32-79
PRKN	Mitochondrial dysfunction	Autosomal recessive	16-72
PINK1	Mitochondrial dysfunction	Autosomal recessive	20-40
DJ-1	Oxidative stress	Autosomal recessive	20-40

1.1.1 Current approaches to treatment

Due to gaps in our understanding of both the origin and progression of PD, treatment for this disease has remained relatively unchanged for the past four decades. The mainstay treatment targets the only definitive pathological hallmark of PD, the loss of dopamine. As such the current gold standard treatment is dopamine replacement therapy (DRT), which simply aims to replace the dopamine that is lost. There are several therapeutics available that target different points of dopamine synthesis and metabolism (**Figure 1.3**). The most common of which is levodopa (L-dopa), a dopamine precursor that can cross the blood brain barrier (BBB) to promote dopamine synthesis [21]. Dopamine is synthesised from the amino acid tyrosine in dopaminergic neurons [22]. Tyrosine is converted to dopamine by the rate limiting enzyme tyrosine hydroxylase (TH) which produces, L-dopa, which is rapidly converted to dopamine by dopa decarboxylase [22]. As such, the administration of L-dopa also bypasses the rate limiting step of dopamine synthesis, TH, allowing for the quick production of dopamine required to maintain

homeostatic dopaminergic activity [23]. L-dopa remains the most effective
medication and primary treatment of PD despite only providing short term
symptomatic relief and the development of several adverse effects like orthostatic
hypotension, nausea, impulse control disorders and dyskinesia with long term use
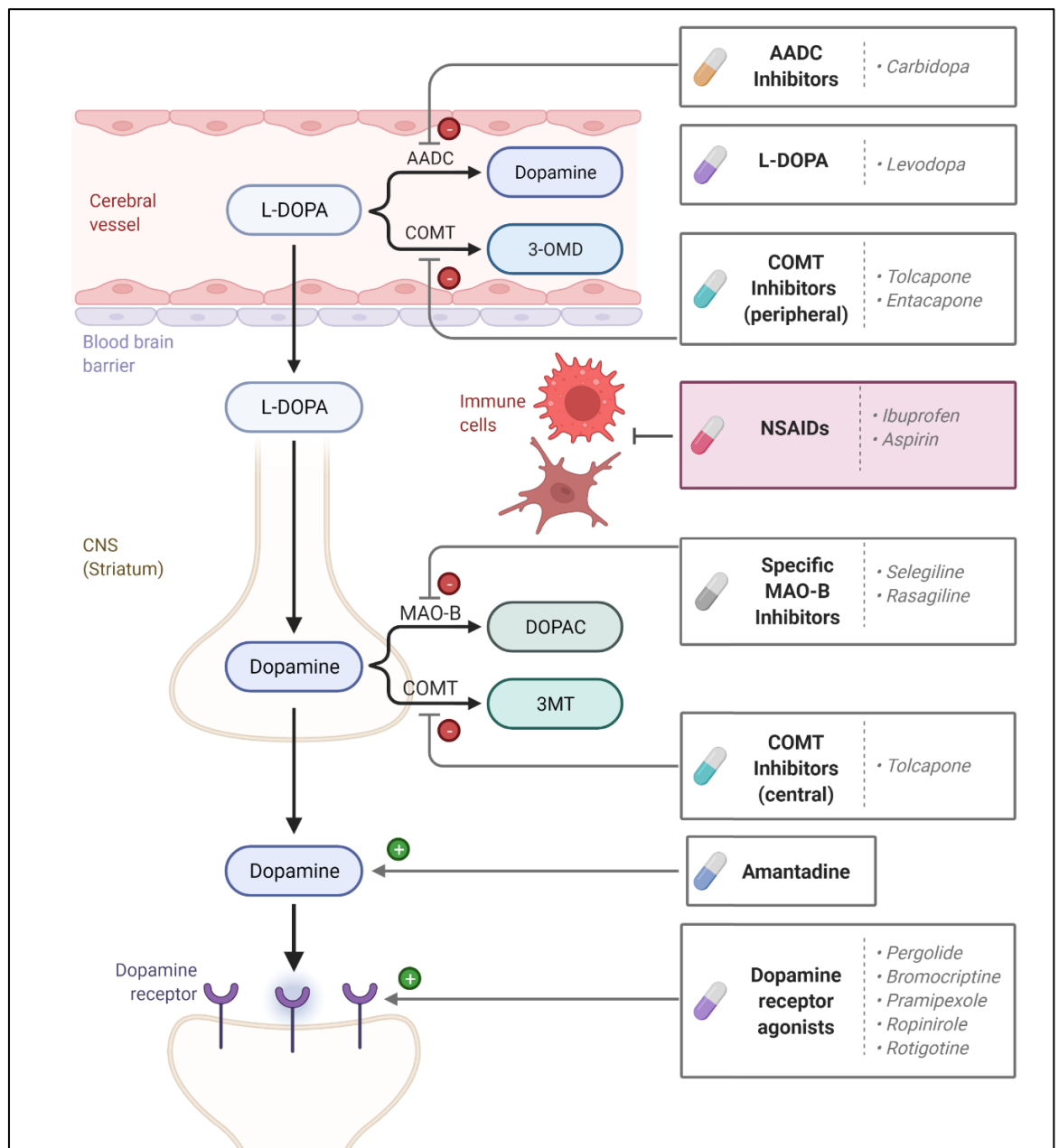[24].

Figure 1.3. Therapies for Parkinson's disease. Summary of therapies available for PD
therapy (white boxes) and example NSAIDs trialled for PD that target inflammation (red
box).

Monoamine oxidase (MAO) and catechol-O-methyltransferase (COMT) inhibitors have been introduced as adjuvant therapy to DRT, to reduce the breakdown of L-dopa and dopamine. These have been shown to reduce motor fluctuations associated with waning L-dopa responsiveness and dyskinesia [25]. The NMDA antagonist, amantadine is also used to treat dyskinesia and other motor symptoms but is associated with nausea, hypotension, hallucinations and confusion [26].

The last main class of PD therapeutics are dopamine receptor agonists that mimic endogenous dopamine. Dopamine receptors (DRs) govern distinct functions due to their unique location (**Table 2**) [27]. Currently available dopamine agonists can only distinguish between D1-like (D1 and D5) and D2-like (D2, D3 and D4) subtypes and not within each subtype. These receptors are discussed in greater detail in Section 1.4, but from **Table 2**, it is obvious that activating these receptors is associated with severe behavioural dysfunctions, despite some beneficial effects on motor function [28]. The expression of DRs is also reduced during PD pathogenesis [29], with the use of DR agonists also being shown to promote downregulation. For example, one study revealed that the use of dopamine agonists in PD cause downregulation of D2 receptors which is reversed following withdrawal of dopamine agonists [30]. Therefore, DR agonists are now only used as adjuvant therapy in advanced disease to limit these adverse effects.

Table 2. Characteristics of dopamine receptor subtypes.

Dopamine receptor	Location	Function	Affinity for dopamine	Inflammation
D1	Striatum, nucleus accumbens, amygdala, hippocampus, substantia nigra, frontal cortex	Locomotion, learning and memory, attention, impulse control, sleep	#	Anti-inflammatory

D2	Striatum, VTA, cerebral cortex	Locomotion, learning and memory, attention, sleep	##	Anti-inflammatory
D3	Striatum, cortex	Locomotion, cognition, attention, impulse control, sleep, regulation of food intake	#####	Pro-inflammatory
D4	Frontal cortex, amygdala, nucleus accumbens	Cognition, impulse control, attention, sleep	###	Anti-inflammatory
D5	Cortex, substantia nigra	Cognition, attention, decision making, motor learning	####	Pro-inflammatory

Current therapeutics are associated with several adverse effects and their effectiveness wanes over time and therefore cannot be used throughout the entire disease progression. A recent approach to diminish the need of medication is a surgical treatment that involves the deep brain stimulation (DBS) of the subthalamic nucleus, which has shown to improve motor function, reduce motor fluctuations and dyskinesia [31]. However, this is a very invasive technique which comes with a unique set of risks due to the surgical nature of the therapy and may not be suitable for patients with certain co-morbidities [32].

Due to the insidious nature of the neurodegeneration in PD, the actual onset of disease has not been clearly defined. Furthermore, there is limited knowledge on the underlying pathogenic mechanisms of the disease and subsequently, there are no effective therapies to slows or arrest disease progression, representing a large unmet medical need. There is an urgent need to develop disease modifying therapies that not only provide relief of motor symptoms but may help relieve the burden of both motor and non-motor symptoms.

1.1.2 Modelling Parkinson's disease

Adding further complexity in the development of disease modifying therapies, is that fact that like most neurodegenerative disorders, PD is predominantly sporadic, and the aetiology remains unknown. However, aging, genetics and exposure to environmental toxins, like pesticides, have been identified as risk factors for PD [33]. Since it is still not known how dopaminergic neurons are lost and why PD develops, it is not surprising that developing viable disease-modifying therapies is a daunting task. However, several pathophysiological mechanisms have been repeatedly associated with PD pathogenesis, namely mitochondrial damage, protein aggregation and neuroinflammation [25].

Analyses of PD pathophysiological traits in humans, alone or in combination with genetic risk factors, have been exploited to develop reliable pre-clinical models of PD. Various toxins have been reported to induce several of these traits, along with parkinsonian motor deficits in several cellular and animal models of PD [34-36]. These have been instrumental in advancing our understanding of the disease, as well as identifying and testing novel therapeutics.

Neurotoxins

The most common PD models are toxin-based models that have been shown to induce a range of PD pathological characteristics including dopaminergic degeneration, oxidative stress and neuroinflammation. The most frequently studied neurotoxins include 1-methyl-4-phenyl-1,2,3,6-tetrahydropyridine (MPTP) and 6-hydroxydopamine (6-OHDA) [37]. All of these have been shown to inhibit mitochondrial complex I, either directly or indirectly, producing a cascade of events including the generation of reactive oxygen species (ROS), oxidative stress,

neuroinflammation and neuron cell death (**Figure 1.4**) [34, 38]. A strength of these

models is the selective uptake of each neurotoxin by DA neurons and the ability to

recapitulate several pathological hallmarks [39]. However, MPTP is extremely toxic

and requires specialised facilities to prevent human toxic exposure. Additionally, 6-

OHDA requires direct administration to the brain via stereotaxic injection. This

technique not only requires special equipment and expertise but produces a

unilateral injury in which one brain hemisphere remains unharmed. Furthermore,

the use of an injection also creates a lesion which, alone also causes neuronal

death and inflammation, thereby creating uncertainty if the changes observed in

this model are the result of the lesion or toxin, which require the use of additional

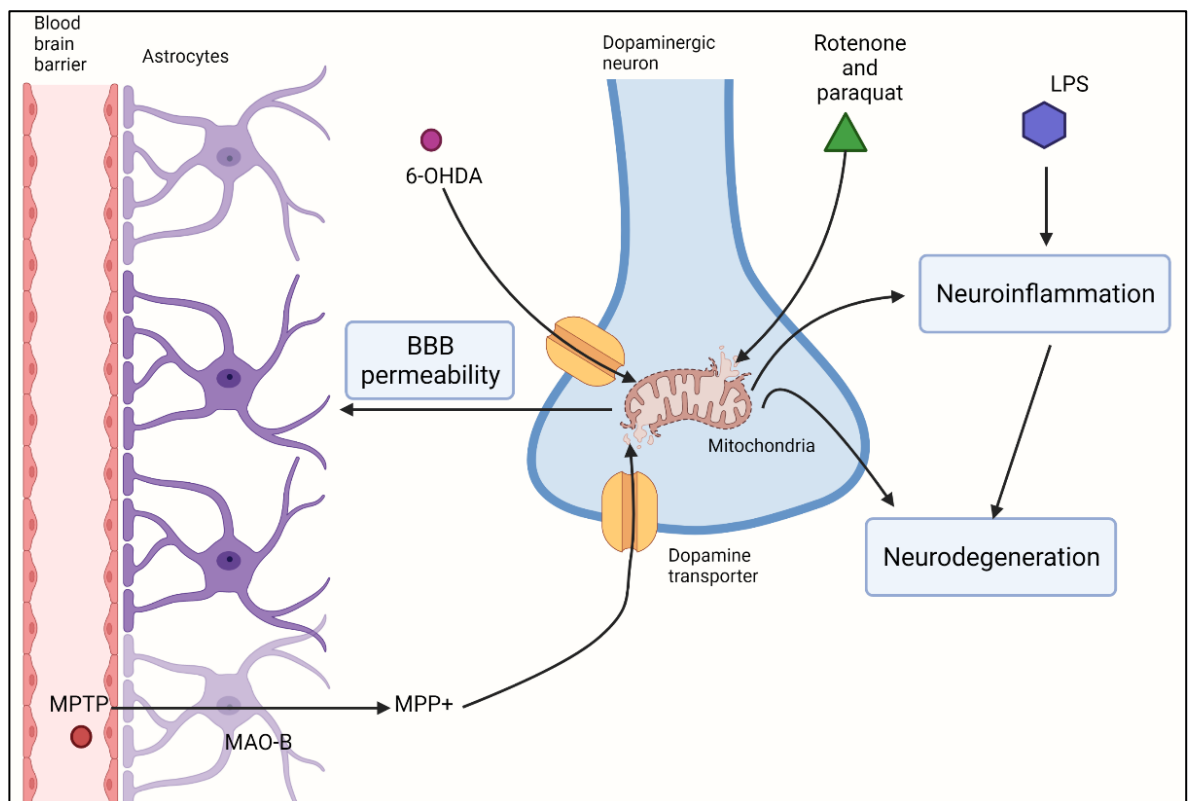animals to control for this (sham surgery).

Figure 1.4. Mechanism of Parkinson's disease mimetics. MPTP can cross the blood brain barrier where it is metabolised in astrocytes by MAO-B producing MPP+. MPP+ is taken up by neurons via the dopamine transporter where it targets the mitochondrial respiratory chain, as do rotenone and paraquat. 6-OHDA is administered directly into the brain where it also is taken up by neurons via the dopamine transporter and targets mitochondria. LPS can get into the brain where it activates glial cells resulting in neuroinflammation which results in neurodegeneration.

Herbicides/pesticides

The herbicide paraquat and pesticide rotenone have both been identified as risk factors for developing PD due to their ability to cross the blood brain barrier and destroy dopaminergic neurons [40, 41]. A study by Tanner and colleagues revealed that exposure to rotenone in farming communities increased the incidence of PD by 2-3-fold [38]. Similar epidemiological studies have not yet elucidated the how rotenone and other pesticides increase the risk of PD, however the ability of rotenone to disrupt mitochondrial function in vulnerable neuronal populations is a strong possibility [42].

Dopaminergic neurons are highly vulnerable due to the ability of dopamine to be oxidized to toxic reactive quinones [43, 44]. These reactive by-products can also promote mitochondrial dysfunction, resulting in the generation of more ROS and exacerbating oxidative stress [45]. It is this property of dopaminergic neurons that are exploited in preclinical neurotoxin models of PD [39]. For example, rotenone-mediated dopaminergic degeneration occurs via the inhibition of mitochondrial complex I which results in the formation and accumulation of ROS, which has been shown to be critical in PD pathogenesis in human *post-mortem* brain tissue [46-48].

Another useful characteristic of rotenone, which may contribute to its exposure as a risk factor for PD, is its highly lipophilic nature [49]. This lipophilicity enables

rotenone to readily cross the BBB allowing for the systemic administration of rotenone to be utilized in preclinical models [41, 50, 51].

The systemic administration of rotenone has been shown induce several pathophysiological aspects of PD. Chronic daily intraperitoneal injections of rotenone in rats, induced L-Dopa responsive locomotor behaviour deficits and neurochemical abnormalities consistent with PD [52, 53]. Additionally, in mice, systemic administration, including intraperitoneal injection of low doses of rotenone was sufficient to induce behavioural deficits, dopaminergic degeneration, mitochondrial impairment and neuroinflammation [54-57]. Additionally, rotenone can be combined with genetic PD models to elucidate disease specific pathology and test novel treatments. For example, a study exposed LRRK2 (gene associated with PD) mutant knock-in mice to rotenone via oral gavage which made mice more susceptible to dopaminergic cell death and resulted in the development of more robust locomotor deficits [58].

Rotenone is a good neurotoxin to exploit as a PD mimetic due to its ability to be used in technically simple and reproducible experimental paradigms via systemic administration. This combined with its ability to target dopamine neurons allows for many aspects of PD including both behaviour and pathophysiology to be studied, making it an ideal platform to study the effects of novel therapeutics for PD [40, 53, 59-61].

Inflammatory models

Lipopolysaccharide (LPS) has also been used to induce PD-like pathology as it has been shown that inflammation precedes dopaminergic cell death [62]. However, there are several limitations to the LPS model. Firstly, the systemic administration

of LPS can activate peripheral immune responses and cause additional inflammatory pathologies. On the other hand, stereotaxic injection of LPS produces a lesion which contributes to the neuropathology observed, similar to 6-OHDA model. Secondly, LPS produces inflammation which is known to contribute to the pathology of several neurological diseases and is not specific to PD [63]. Therefore, this model is not a specific PD model, but rather useful for researching neuroinflammation in general.

1.2 Neuroinflammation

Neuroinflammation describes the inflammatory processes of both the innate and adaptive immune systems, occurring within the central nervous system (CNS) [63]. Neuroinflammation has been consistently linked to neurodegeneration in a variety of contexts, including PD [64], Alzheimer's disease [65], stroke [66], and multiple sclerosis [67].

The involvement of inflammation in PD has gained increasing attention and general consensus, with studies showing that inflammation alone is sufficient to trigger the degeneration of dopaminergic neurons, culminating in the development of PD [44]. For example, injection of lipopolysaccharide (LPS) into the rodent brain results in increased levels of inflammatory mediators, including COX-2 and iNOS, events that occur prior to the loss of dopaminergic neurons [68]. These studies pinpoint the key role of neuroinflammation in the detrimental neurodegenerative cascade that leads to PD.

Direct evidence from patient-imaging [69], plasma [70], *post-mortem* studies [71] and preclinical models [72] has revealed an increase in pro-inflammatory cells,

cytokines and mediators in PD. For example, elevated levels of pro-inflammatory cytokines, including IL-1β, IL-6 and TNF-α were found in the striatum and *SNpc* in *post-mortem* PD brains [73]. More recently, increased plasma concentrations of IL-6 and IL-1β have been found in PD patients compared to healthy controls [74]. This correlated with elevated levels of the same pro-inflammatory cytokines in cerebrospinal fluid (CSF) which more closely mirrors the pathological alterations observed in the CNS [70].

Furthermore, neuroinflammation is consistently linked to both disease progression and clinical severity, making it an attractive therapeutic target for PD [68]. However, whether inflammation is directly involved in PD aetiology or just a secondary consequence of dopaminergic neuronal injury has not been elucidated. Despite this, studies inhibiting neuroinflammation, and in particular, microglia activation, have been shown to be beneficial in slowing disease progression in preclinical models of PD [75].

Lastly, neuroinflammation is a common pathological hallmark of several neurological diseases and non-motor symptoms/comorbidities of PD [76]. This includes dementia [77], stroke [78], depression [79], anxiety [80], abuse and addiction disorders [81]. The complex nature of PD and its co-morbidities often leads to multiple diagnoses, uncoordinated and fragmented care and polypharmacy [82]. Investigating ways to reduce the inflammatory burden in PD could reduce or resolve the degree of comorbidities associated with PD or be repurposed to treat other neuroinflammatory and neurodegenerative disorders.

1.2.1 Microglia

Microglia are the main contributors to neuroinflammation and are the main cell type responsible for monitoring and maintaining a healthy CNS [83]. In healthy brains,

microglia monitor synaptic activity, clear apoptotic cells and debris and provide

trophic support for neurons [20]. Recent investigations into microglia have revealed

the presence of distinct activated phenotypes that favour neurotoxic or

neuroprotective activities [84]. Resting microglia, or MØ, are those seen under

homeostatic conditions while, upon an inflammatory or neurotoxic insult microglia

can switch to a M1 or M2 activated phenotype. M1 describes the classically

activated, pro-inflammatory and neurotoxic microglia; while M2 defines the

alternatively activated, anti-inflammatory and neuroprotective microglia [75]. These

distinct activated phenotypes are associated with specific cytokines, chemokines

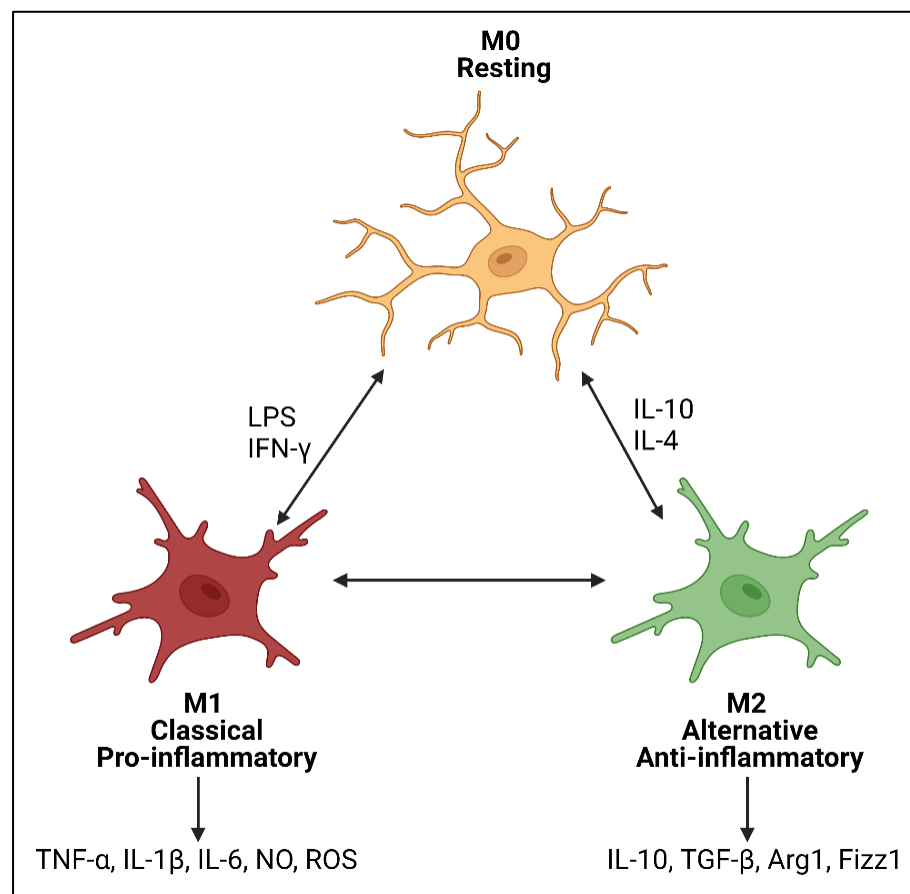and inflammatory mediators, summarised in **Figure 1.5**.

Figure 1.5. Microglia phenotypes. Microglia exist in three main phenotypic states; resting microglia (MØ), seen under homeostatic conditions. Depending on the stimulus MØ microglia can be classically activated by LPS or IFN-γ and become M1 phenotype or M2

phenotype via alternate activation from IL-4 or IL-10. M1 represent the classical activation of microglia that exhibit a pro-inflammatory phenotype due to the production and secretion of inflammatory cytokines and mediators like TNF-α, IL-1β, IL-6, NO, ROS. M2 are alternatively activated and display an anti-inflammatory phenotype due to the production of IL-10, TGF-β, Arg1 and Fizz1. Furthermore, under homeostatic conditions, M1 microglia can promote M2 activity to maintain physiological levels of inflammation and M2 are able to block excess neurotoxic activity of M1. In chronic neuroinflammation this balance and autocrine control is lost and the M1 phenotype dominates creating a neurotoxic and pro-inflammatory environment, as observed in PD.

Several lines of evidence have confirmed that in PD [85], microglia exhibit an uncontrolled pro-inflammatory M1 phenotype, with studies suggesting that the lack of an appropriate M2 phenotype response might be an important mechanism underlying neurodegeneration [86]. This was confirmed using positron emission tomography (PET) imaging studies with a ligand that is specifically expressed by activated microglia (PK-11195) that revealed PD patients had significantly higher levels of PK-11195 binding compared to healthy controls [69].

The toxicity of microglia to dopamine neurons has been demonstrated both *in vitro* and *in vivo*. In fact, dopaminergic neurons express a wide range of cytokine and chemokine receptors, meaning they are directly responsive to inflammatory mediators released from activated microglia [1]. The hyperactivation of M1 microglia contributes to dopaminergic cell death and the increase of neurotoxic mediators including ROS and pro-inflammatory cytokines [87]. For example, microglia have been implicated in promoting both behavioural changes [88] observed in PD as well as the degeneration and associated PD pathology in preclinical models [54]. Therefore, it is well accepted that inhibiting microglial activation reduces inflammation and neurodegeneration, therefore slowing disease progression [54, 80].

1.2.2 Astrocytes

Astrocytes are the most common glial cells in the brain and are involved in a range of functions, including synaptic plasticity, neuronal energy and trophic support, BBB maintenance which contribute to the maintenance of normal healthy brain function [89, 90]. Similar to microglia, astrocytes can exert both deleterious and beneficial functions within the brain and exist in two functional phenotypes with respect to their neurotoxic and neuroprotective activity [66]. Analogous to microglia nomenclature, Liddelow and colleagues termed these A1 and A2 astrocytes, for their neurotoxic and neuroprotective phenotypes respectively [90]. It has been found that reactive astrocytes lose their supportive, neuroprotective role and gain toxic function in the progression of neurodegenerative diseases like PD [89]. The role of astrocytes in PD is further confirmed in pathological examination of PD brains that show an increased number of astrocytes and elevated GFAP expression, an astrocytic activation marker, particularly in the *SNpc* [91]. The role of astrocytes in PD is strengthened by their key role of astrocytes in promoting MPTP neurotoxicity, as astrocytes metabolise MPTP to its toxic form MPP+ which is detrimental to dopaminergic neurons [89].

1.2.3 Other immune cells

The chronic activation of microglia and astrocytes disturbs BBB integrity, which allows the infiltration of peripheral immune cells, all of which aggravate neuroinflammation [92] (**Figure 1.6**). The infiltration of peripheral immune cells, especially lymphocytes is considered detrimental to disease progression [92, 93].

Several preclinical and *post-mortem* studies have revealed the presence of CD8+ and CD4+ T cells in the PD brain [93]. A recent study by Bhatia and colleagues,

reported phenotypic changes of T cells in PD; however, these also correlated to changes seen in healthy aging, making it difficult to discern their impact on disease [94]. Nonetheless, the analysis of peripheral blood samples did reveal a reduction in total CD3+ T cells in PD that was associated with disease severity [94].

Interestingly, mice deficient in both T and B lymphocytes are more resistant to MPTP toxicity [87]. Analysis of circulating lymphocyte populations revealed a continued loss of T and B cells, suggesting that disease progression may be influenced by disturbances to these cellular populations [95]. This is validated by Li and colleagues, who also demonstrated a reduction in total B-cell count and reduced B-cell proliferation in PD patients compared to matched neurologically healthy controls [96]. However, more research is required to understand the role of peripheral immune cells in PD pathogenesis and their potential as biomarkers to aid in the early detection of disease [97].
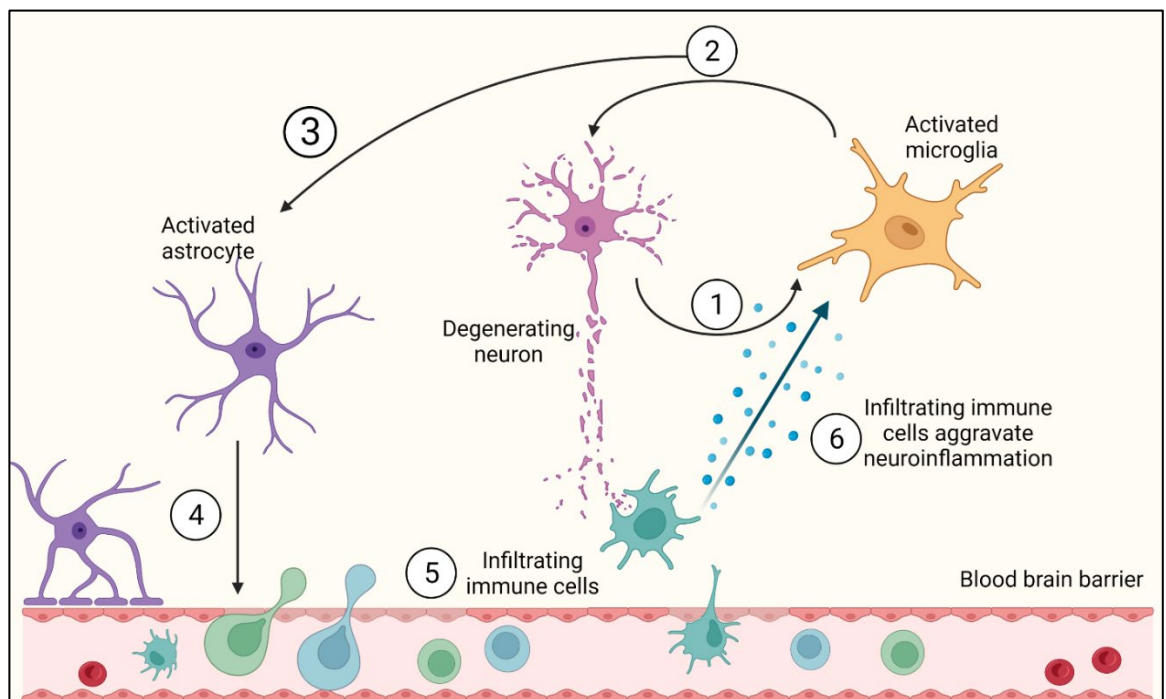

Figure 1.6. Overview of neuroinflammation observed in Parkinson's disease.
A chronic neuroinflammatory response is observed in Parkinson's disease whereby (1) degenerating neurons release factors that activate microglia (2), creating a

vicious cycle whereby activated microglia release neurotoxic and pro-inflammatory mediators that promote the further degeneration of dopamine neurons. Simultaneously, microglia and neurons activate astrocytes (3) which further promote neuroinflammation by releasing pro-inflammatory cytokines and disturbing the blood brain barrier (4). This allows for the infiltration of excess peripheral immune cells into the brain (5) which further aggravate inflammation (6). In Parkinson's disease the balance between protective and harmful activated glial cells is lost and they exist in a neurotoxic and inflammatory state that is harmful to neurons and neuronal function.

1.3 Attempts to target neuroinflammation

There have been several attempts made to target the immune response in PD; however, despite their promising results in preclinical trials, they have been disappointing in a clinical setting.

Non-steroidal anti-inflammatory agents (NSAIDs), including ibuprofen and aspirin were suggested to reduce the risk of developing PD, with chronic use of either NSAID associated with a 66% reduced incidence risk, as reported in one study [98]. Furthermore, the use of NSAIDs was found to be neuroprotective against dopamine cell loss in a MPTP mouse model [99]. Unfortunately, this did not translate into the clinic, which was limited by the lack of specificity of NSAIDs in inhibiting only the chronic neuroinflammatory response observed in PD, which resulted in a global downregulation of the immune system.

More recently, several studies have revealed the ability of minocycline, a tetracycline antibiotic commonly used to treat respiratory tract infections, to reduce microglial activation and neuronal cell death in preclinical models of PD [80, 100, 101]. This was validated in a phase 2 clinical trial, where minocycline ameliorated PD progression by inhibiting microglial polarization [102]. The potential of

minocycline as an anti-inflammatory agent is also promising in co-morbidities of PD, including depression and anxiety. For example, minocycline alleviated behavioural and cognitive changes induced by chronic stress through reducing the M1 microglial phenotype [103]. This strengthens the notion that targeting neuroinflammation can not only reduce PD pathogenesis but dampen overall disease burden by alleviating pathology associated with PD comorbidities.

Other studies have aimed to repurpose immune therapies used in other diseases for PD. For example, irritable bowel syndrome (IBD) patients are highly susceptible to develop PD and within this population, it was shown that those on anti-TNF therapy had a 78% reduction in PD incidence compared to those who were not [99]. This correlated with elevated TNF levels in the brain, CSF and blood of PD patients, suggesting anti-TNF treatment could be considered a potential disease-modifying therapy in PD [99].

Additionally, there have been several compounds targeting immune cells involved in PD pathophysiology. Sargramostium and azathioprine are two compounds targeting T cells that have entered Phase 1 clinical trials for PD [104]. However, the role of T cells in PD pathophysiology remains largely unclear. There are a few compounds that target glial cells directly implicated in neuroinflammation. Firstly, inzomelid inhibits NLRP3 inflammasome, which prevents microglial activation and pro-inflammatory cytokine release [104]. Secondly, NLY01 was shown to be protective against dopaminergic loss and abnormal behaviour in a sporadic PD mouse model, which was attributed to the inhibition of the mechanisms driving the conversion of astrocytes to the neurotoxic phenotype [91].

Unfortunately, despite a diverse range of immunomodulatory compounds under investigation, none have made it into the clinic for PD. This is due to several

reasons, including the lack of translation from preclinical success to human studies. For example, simvastatin appeared to protect dopaminergic neurons and maintain motor behaviour in rodents, primarily through immune suppression. However, this did not translate into significant disease-modifying effects in PD patients in a phase II study [104]. Accordingly, more research is required to understand the exact role of inflammation in PD to develop more targeted therapies that specifically disrupt the chronic neuroinflammatory response observed in PD. One possible explanation is the recent discovery that neurotransmitters, including dopamine, serotonin, glutamate, acetylcholine, norepinephrine and γ-aminobutyric acid (GABA), can modulate inflammation [105]. The ability of dopamine to control neuroinflammation adds further complexity in the context of PD as the loss of dopamine will not only impact neurotransmission but contribute to chronic neuroinflammation observed in PD. For example, both astrocytes [106] and microglia [107] have been found to respond to dopamine. Dopamine 2 receptor (D2R) signalling in astrocytes is associated with an anti-inflammatory response with D2R agonists attenuating MPTP-induced neurodegeneration [108]. Fan et al. demonstrated that dopamine impacts the phagocytic activity and motility of microglia, and this was dependent on the activation state of microglia at the time of dopamine stimulation [109]. This ability of dopamine to control the immune response been shown to influence disease pathogenesis in several pathologies including PD, schizophrenia, multiple sclerosis and cognitive disorders.

1.4 Dopamine: an immune transmitter

Dopamine has been implicated in regulating the inflammation which is discussed in **Section 1.4**.
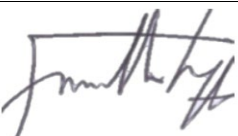
This section is published as:
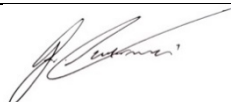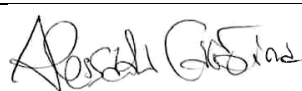
Thomas Broome, S., Louangaphay, K., Keay, K. A., Leggio, G. M., Musumeci, G., & Castorina, A. (2020). Dopamine: an immune transmitter. *Neural regeneration research*, 15(12), 2173–2185. https://doi.org/10.4103/1673-5374.284976

Contribution:

- Drafted the manuscript and prepared images
- Finalised the manuscript

Signature of co-authors:

Name	Signature
Sarah Thomas Broome	
Krystal Louangaphay	
Kevin A. Keay	
Gian Marco Leggio	

Giuseppe Musumeci	
Alessandro Castorina	

Dopamine: an *immune* transmitter

Sarah Thomas Broome[1], Krystal Louangaphay[1], Kevin A. Keay[2], Gian Marco Leggio[3], Giuseppe Musumeci[4], Alessandro Castorina[1,2*]

1 Laboratory of Cellular and Molecular Neuroscience (LCMN), School of Life Science, Faculty of Science, University of Technology Sydney, P.O. Box 123, Broadway, Sydney NSW 2007, Australia.

2 Laboratory of Neural Structure and Function (LNSF), School of Medical Sciences, (Anatomy and Histology), Faculty of Medicine and Health, University of Sydney, Sydney NSW 2006, Australia.

3 Section of Pharmacology, Department of Biomedical and Biotechnological Sciences, "Torre Biologica", University of Catania, via S. Sofia, 97, 95123 Catania, Italy.

4 Section of Human Anatomy and Histology, Department of Biomedical and Biotechnological Sciences, University of Catania, via S. Sofia, 87, 95123 Catania, Italy.

ABSTRACT

The dopaminergic system controls several vital central nervous system (CNS) functions, including the control of movement, reward behaviours and cognition. Alterations of dopaminergic signalling are involved in the pathogenesis of neurodegenerative and psychiatric disorders, in particular Parkinson's disease (PD), which are associated with a subtle and chronic inflammatory response. A substantial body of evidence has demonstrated the non-neuronal expression of dopamine (DA), its receptors and of the machinery that governs synthesis, secretion and storage of DA across several immune cell types. This review aims to surmise current knowledge on the role and expression of DA in immune cells. One of the goals is to decipher the complex mechanisms through which these cell types respond to DA, in order to address the impact this has on neurodegenerative and psychiatric pathologies such as PD. A further aim is to illustrate the gaps in our understanding of the physiological roles of DA to encourage more targeted research focused on understanding the consequences of aberrant DA production on immune regulation. These highlights may prompt scientists in the field to consider alternative functions of this important neurotransmitter when targeting neuroinflammatory/neurodegenerative pathologies.

INTRODUCTION

Dopamine (DA) is one of the most well-known and well-studied neurotransmitters in the brain. This is because DA controls several vital functions, including the control of movement, reward-related behaviours [110]. It is also involved in regulating several aspects of cognition by modulating the expression of several plasticity-associated molecular substrates [111-114]. DA exerts its function through distinct neural pathways, with abnormalities of DA and DA signalling in these pathways leading to a range of neurodegenerative, psychiatric and autoimmune disorders [115]. Many of these pathologies are accompanied by ongoing neuroinflammation, which is the localised inflammatory response of the central nervous system (CNS). Recently, a key role of DA in the regulation of immunity has been proposed. It has been shown that peripheral immune cells as well as microglia and astrocytes express all the elements of the machinery to synthesise [107, 116-118], metabolise and store DA [119], as well as expressing functional dopamine receptors (DRs) to control immune cell functions [120].

The emerging evidence confirming DA as an immune transmitter adds another layer of complexity to CNS physiology and disease pathology. As DA is involved in the control of several vital functions, it is conceivable that abnormal DA signalling may cause important neurological dysfunctions. For example, Parkinson's disease (PD) is characterised by a hypo-DAergic environment and is also linked to a chronic state of neuroinflammation [121]. As will be shown in this review, all inflammatory cell types found to be abnormally expressed in PD patients and *post-mortem* brains express DRs [120]. Since the mainstay treatment for PD is to replace the lost DA, it is important to consider how this restoration of DA affects the immune response associated with PD.

Despite a large body of evidence that suggests a role of DA in regulating inflammation, there are conflicting results and viewpoints on how DA might function as an immune regulator. These differences are due to differences in experimental models and the biological samples investigated (cell lines, animal tissue, and human samples), as well as differences in methodologies and experimental design. We will highlight some examples that illustrate DA's regulatory activity of inflammation, which seems to depend on the immune cell subtype, activation state of the target cell and DA-releasing cell subtype, abundance of DRs and ligand availability. Since comparing these studies is challenging due to the significant impact that each of these factors have on DA utilisation, research in this area has stagnated. This is detrimental as this dual role for DA has implications in how we study and manage DA-ergic and inflammatory pathologies. To illustrate the complexity of DA's actions, we conducted a pilot study in which we analysed the mRNA expression of all five DRs in BV2 microglial cells in response to a well-known inflammatory mediator (lipopolysaccharide, LPS) or to the PD mimetics, rotenone and 6-hydroxydopamine (6-OHDA) (**Figure 1**). We show that, compared with control cells, acute exposure (24h) to inflammation (LPS) or PD-like conditions (rotenone and 6-OHDA) triggers a differential and abnormal regulation of DR mRNA expression. Given the modulatory activities of DRs in these cells, the results suggest that dysregulated expression of DRs on microglial cells could participate, either directly or indirectly, in PD pathogenesis and the establishment of neuroinflammation. Furthermore, these results highlight the complex adaptive responses of the DA system, as the transcriptional regulation of each receptor subtype appears distinct for each insult, stressing the importance of dissecting the specific role/s for each receptor in different pathological contexts.
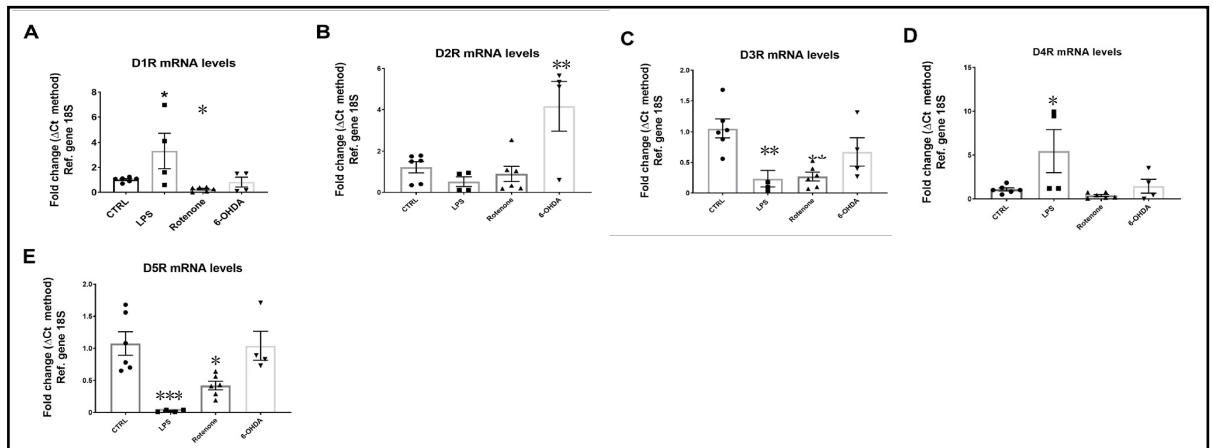
Figure 1: Dysregulated DRs mRNA levels in BV-2 microglial cells exposed to PD mimetics (Lipopolysaccharide, Rotenone and 6-OHDA) after 24h. BV-2 cells were plated at a density of 1.5×10^5 cells in 6-well plates with 10% FGM until 80% confluent and then incubated for further 24h in the presence of either LPS (1µg/µl), rotenone (0.01uM) and 6-OHDA (25uM) in 1% FGM. mRNA was quantified using the ΔCt method and normalised using the 18S gene. Data are the mean ± S.E.M n=4-6. Bar graphs depicting mRNA levels of (**A**) the dopamine D1 receptor, (**B**) the dopamine D2 receptor, (**C**) the dopamine D3 receptor, (**D**) the dopamine D4 receptor and (**E**) the dopamine D5 receptor. *p<0.05 or **p<0.01 vs Control (one-way ANOVA followed by a Sidak *post-hoc* test). D1R: Dopamine D1 receptor, D2R: Dopamine D2 receptor, D3R: Dopamine D3 receptor, D4R: Dopamine D4 receptor, D5R: Dopamine D5 receptor, 18S: ribosomal protein 18S (housekeeping gene).

Evidence of the expression of DA has been reviewed previously [122, 123]. In this review, our goal is to introduce new important insights into DA's biological role as an immune transmitter. The idea is to prompt further investigation into this area of

research and to highlight novel, non-neuronal activities of DA with regards to several DA- and neuroinflammation-related pathologies.

The current scientific literature was searched using PubMed with the keywords: DA, dopamine receptors AND immune cell, receptor expression, glia, inflammation, neuroinflammation, CNS immune response. Papers were then screened and assessed for inclusion according to their significance for the field of dopamine as an immune transmitter.

DOPAMINE METABOLISM AND TRANSPORT IN THE IMMUNE SYSTEM

DA is derived from the hydroxylation of L-tyrosine by the rate limiting enzyme, tyrosine hydroxylase (TH), forming l-3,4-dihydroxyphenylalanine (L-DOPA), which is then de-carboxylated by the aromatic amino acid decarboxylase (AADC) to form DA (**Figure 2**). This process has been well-described in immune cells, specifically T lymphocytes [124] and dendritic cells [125]. In a prior study, Musso and colleagues showed that the addition of L-tyrosine and L-DOPA to lymphocyte cultures increased catecholamine levels in a dose dependent manner [126].
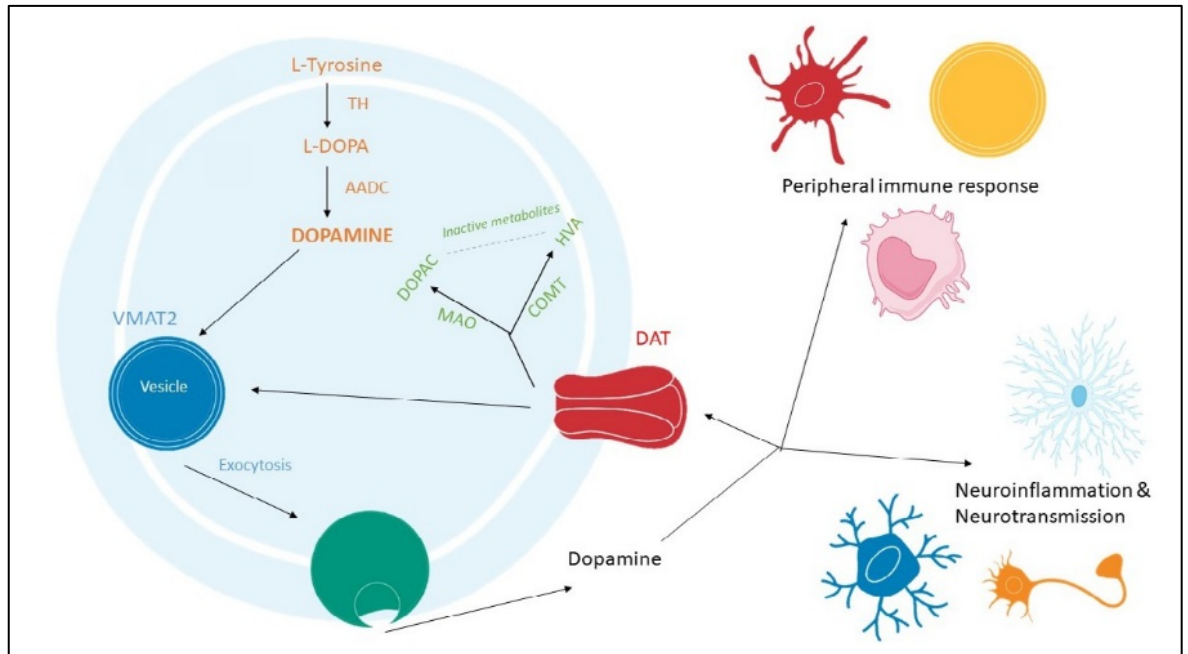
Figure 2. Dopamine biosynthesis, storage and metabolism pathways.

Dopamine is derived from the hydroxylation of L-tyrosine by the rate limiting enzyme, tyrosine hydroxylase (TH), forming l-3,4-dihydroxyphenylalanine (L-DOPA), which is then de-carboxylated by the aromatic amino acid decarboxylase (AADC) to form dopamine (orange). Dopamine is stored in vesicles through vesicular monoamine transporter 2 (VMAT2) and in neurons upon stimulation dopamine is released via exocytosis (blue). Dopamine is taken up by cells via the dopamine transporter (DAT) (yellow). Once dopamine re-enters the cell it can be incorporated back into vesicles by VMAT2 or dopamine can be inactivated through several metabolic pathways including oxidative deamination by monoamine oxidase (MAO) or by O-methylation by catechol-O-methyltransferase (COMT), leading to the formation of two catabolic products, 3,4-Dihydroxyphenylacetic acid (DOPAC) and homovanillic acid (HVA) respectively (green).

Several independent research groups have shown that astrocytes and microglia are able to synthesise and metabolise DA [106, 107, 119, 127-132]. This is particularly important as these cells are in direct contact with DAergic neurons. It is therefore possible that glial cells could play a role in sustaining DA levels in the brain, in both normal homeostatic and pathological states. This suggestion has been raised by Asanuma & Miyazaki [106], who showed that striatal astrocytes can act as a reservoir for L-DOPA and that, in turn, L-DOPA increased the neurotrophic action of astrocytes thereby protecting neurons from neurotoxic insult. This attribute of astrocytes could be exploited to enhance current PD therapies, as L-DOPA is the gold standard treatment for PD. For example, Asanuma and colleagues showed that L-DOPA immunoreactivity was increased on the side of a 6-OHDA lesion compared to the unlesioned, control side suggesting that when DAergic neurons are damaged excess L-DOPA is taken up by astrocytes [133]. However, this study also demonstrated that despite expressing the enzymes required for metabolism, astrocytes were unable to convert L-DOPA to DA. This step could be a therapeutic target to restore DA lost in PD pathogenesis, it also suggests a cell-specific ability to synthesise DA. It would be interesting determine how the rapid metabolism of dopamine and inability of astrocytes to convert L-DOPA to DA affects L-DOPA therapy in PD patients as targeting astrocytes themselves may not have a therapeutic benefit but could aid in current and future PD therapies.

In neurons, DA is typically stored in synaptic vesicles through vesicular monoamine transporter 2 (VMAT2) [134]. It has been shown that VMAT2 is expressed in immune cells as treatment of cultured cells with reserpine, a drug that typically inhibits the re-uptake and storage of DA into vesicles, reduced the intracellular concentration of DA while increasing DA accumulation in the cell culture supernatant of reserpine-treated immune cells [135].

In the brain, reuptake of excess DA by neurons occurs via the DA transporter (DAT). DAT mRNA and protein, as well as VMAT2 immunoreactivity have been detected on cell membranes and in vesicle-like structures of human lymphocytes [136], suggesting that immune cells are also able to store DA (**Figure 2**). In lymphocytes, intracellular DA levels increase following an increase in extracellular DA, supporting the idea that cells of the adaptive immune system exhibit a functional cellular uptake mechanism [117]. This is important during the progression of PD when peripheral immune cells are recruited to the site of DAergic degeneration as these immune cells could further reduce available DA levels via VMAT2 activity.

When DA stores are at capacity, DA can be inactivated through several metabolic pathways, including oxidative deamination by monoamine oxidase (MAO) or by O-methylation by catechol-O-methyltransferase (COMT), leading to the formation of two catabolic products, 3,4-Dihydroxyphenylacetic acid (DOPAC) and homovanillic acid (HVA), respectively [137, 138]. It should be noted that COMT is predominantly expressed by glial cells, particularly in microglia. In neurons, COMT is either missing or found at very low levels. MAO-B is predominantly found in astrocytes [139]. MAO-B activity in astrocytes has been proposed as a potential biomarker for chronic neuroinflammation, as increased astrocytic MAO-B expression is associated with cellular ageing and age-related neurodegeneration [130]. In humans, Bidart et al. (1983) discovered that both T and B lymphocytes exhibit COMT immunoreactivity, and Balsa and collaborators later confirmed MAO activity in human lymphocytes and granulocytes [140, 141].

These results indicate that both glial and immune cells capable of producing, inactivating and transporting DA, but that they do this independently of the neuronal

system (**Table 1**). Despite evidence demonstrating that most immune cells possess each of the elements required to synthesise, metabolise and store DA, further investigations are warranted [142-145]. In particular, studies are needed to unveil how these cells can be manipulated to promote the recovery of lost DA, which characterises PD, or perhaps more generally to rescue normal DA signalling, as seen in mood and other psychiatric disorders [146, 147].

Additional Table 1 Non-neuronal expression of the machinery required for dopamine synthesis, storage, uptake and metabolism

Cell type	Synthesis	Storage	Uptake	Metabolism
Microglia	Mastroeni et al., 2009; Morales et al., 2017	n/a	Mastroeni et al., 2009	Redell et al., 2007; Meiser et al., 2013
Astrocytes	Asanuma and Miyazaki, 2016; Morales et al., 2017	Petrelli et al., 2018; Matt and Gaskill, 2019	Morales et al., 2017; Matt and Gaskill, 2019	Bisaglia et al., 2013; Schain et al., 2017; Winner et al., 2017; Petrelli et al., 2018
Monocyte	Gaskill et al., 2012; Mackie et a., 2018; Gopinath et al., 2020	Gaskill et al., 2012; Gopinath et al., 2020	Gaskill et al., 2012; Mackie et a., 2018; Gopinath et al., 2020	n/a
Macrophages	(Gaskill et al., 2012)	Gaskill et al., 2012	Gaskill et al., 2012; Mackie, et al., 2018	n/a
T-lymphocytes	Musso et al., 1996; Cosentino, et al., 2006; Wang et al., 2016	Cosentino, et al., 2006; Amenta et al., 2001	Amenta et al., 2001	Balsa et al., 1989
B-lymphocytes	Talhada et al., 2018	Pacheco et al., 2014	n/a	Balsa et al., 1989
Dendritic cells	Nakano et al., 2009; Prado et al., 2012; Pacheco et al., 2014	Nakano et al., 2009; Prado et al., 2012	Prado et al., 2012	Prado et al., 2012
Neutrophils	Cosentino et al., 1999	Cosentino et al., 1999	Cosentino et al., 1999	Bidart et al., 1983
Eosinophils	n/a	n/a	n/a	Bidart et al., 1983
Mast cells	Ronneberg et al., 2012	Anlauf et al., 2006	n/a	n/a

Literature evidence describing the expression of the genes that are critical for the synthesis (TH), storage (VMAT2), uptake (DAT) and metabolism (COMT and/or MAO) of dopamine. Several non-neuronal cell types are able to produce, transport and metabolise dopamine in a manner independent of dopamine neurotransmission. COMT: Catechol-O-methyltransferase; DAT: DA transporter; MAO: monoamine oxidase; TH: tyrosine hydroxylase; VMAT2: vesicular monoamine transporter 2.

Table 1. Non-neuronal expression of the machinery required for dopamine synthesis, storage, uptake and metabolism. Literature evidence describing the expression of the genes that are critical for the synthesis (TH), storage (VMAT2), uptake (DAT) and metabolism (COMT and/or MAO) of dopamine. Several non-neuronal cell types are able to produce, transport and metabolise dopamine in a manner independent of dopamine neurotransmission.

DOPAMINE RECEPTORS IN THE IMMUNE SYSTEM

DA mediates its functions *via* interactions with one or more of the five DRs (DRs) expressed on the membrane of target cells. A large body of evidence confirms the presence of DRs on specific immune cell types [107, 119, 122, 148-150]. In 2002, McKenna and colleagues conducted the first study aimed at identifying the expression of all five DR subtypes across multiple cell types [120]. Peripheral blood leukocytes from healthy volunteers were investigated using flow cytometry and a panel of DR sub-type-specific antibodies. They found that T-lymphocytes and monocytes exhibited low levels of DR expression, whereas neutrophils and eosinophils had moderate expression levels while B-lymphocytes and natural killer (NK) cells had higher and more consistent expression of DRs [120]. The cell-specific expression profile of each DR is summarised in **Table 2**.

Additional Table 2 Dopamine receptor expression in non-neuronal cells

| Cell type | DA receptors | | | | | Reference |
| | D1-like | | D2-like | | | |
	D1R	D5R	D2R	D3R	D4R	
Microglia	+		+	+	+	Mastroeni et al., 2009
	#		#	#	#	
Astrocytes	+	+	+	+	+	Miyazaki et al., 2004
	#	#	#	#	#	
Oligodendrocytes			+	+		Rosin et al., 2005
			#	#		
Monocyte	+	+	+	+	+	Matt and Gaskill, 2019
	#	#	#	#	#	
Macrophages	+	+	+	+	+	Gaskill et al., 2012
T-lymphocytes	+	+	+	+	+	(Arce-Sillas et al., 2019)
	#	#	#	#	#	
B-lymphocytes	+	+	+	+	+	Arce-Sillas et al., 2019
	#	#	#	#	#	
Dendritic cells	+	+	+	+	+	Nakano et al., 2008
Neutrophils	+	+	+	+	+	McKenna et al., 2002
	#	#	#	#	#	
Eosinophils	+	+	+	+	+	McKenna et al., 2002
	#	#	#	#	#	
Natural killer (NK) cells	+	+	+	+	+	McKenna et al., 2002
	#	#	#	#	#	

Summary of evidence showing either protein (+) and/or mRNA (#) expression of each dopamine receptor subtype in non-neuronal cells.

Table 2. Dopamine receptor expression in non-neuronal cells. Summary of evidence showing either protein (+) and/or mRNA (#) expression of each dopamine receptor subtype in non-neuronal cells.

DRs are also present on resident glia (microglia and astrocytes) and other non-neuronal CNS cell types, like oligodendrocytes and macrophages (**Table 2**). DRs belong to the G protein-coupled receptor (GPCR) superfamily and have been divided into two main subclasses, D1-like and D2-like based on their ability to regulate cyclic adenosine monophosphate (cAMP) levels, with D1-like receptors increasing cAMP production and D2-like receptors inhibiting the formation of cAMP [151]. D1-like receptors are coupled to $G_{\alpha s}$ protein that increases the intracellular concentration of the second messenger cAMP through the activation of adenylyl cyclase (AC) [152]. AC activates protein kinase A (PKA) and protein kinase C (PKC), which both promote the transcription of cAMP response element binding protein (CREB), favouring an anti-inflammatory environment [153]. D2-like receptors, via coupling to $G_{\alpha i/o}$ decrease the levels of cAMP [146]. D2-like receptors activate β-arrestin pathway which downstream stimulates Akt (PKB) signalling which regulates inflammation through Phosphoinositide 3-kinases (PI3K)-Akt and glycogen synthase kinase 3 beta (GSK3β) targets.

Both classes of DRs control the activity of classical pro-inflammatory pathways, including the nuclear translocation of the transcription factor-β (NF-κβ) [123] (**Figure 3**), with D2-like receptors promoting the transcription of CREB regulated proteins that promote neuronal survival and increase anti-inflammatory cytokines. The signalling of DRs is further complicated by evidence showing the occurrence of an heterodimerisation process, which recapitulates in a different pharmacological profile if compared with that of the monomers that constitute them[154].
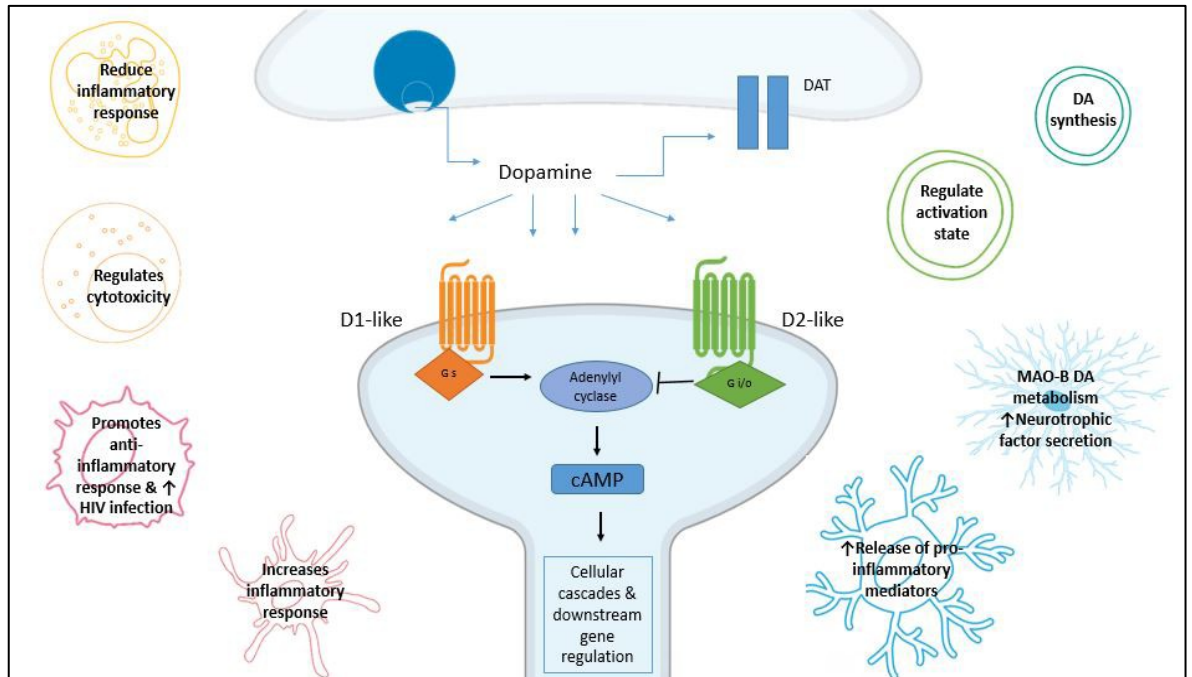
Figure 3. Dopamine receptor signalling pathways. Dopamine receptors (DRs)
belong to the G protein-coupled receptor (GPCR) superfamily and have been
divided into two main subclasses, D1-like and D2-like based on their ability to
regulate cAMP levels. This figure illustrates the commonly reported pathways for
both receptors. D1-like receptors are coupled to Gαs protein which activates
adenylyl cyclase (AC) which increases cAMP production. cAMP activates PKA
(blue). PKA activates several targets including DARPP-32 which inhibits PP1
subsequently inhibiting CREB activity (orange). D2-like receptors inhibit the activity
of AC through Gαi/o therefore reduce cAMP production. D2-like receptors bind to
β-arrestin/PP2A complex which inhibits Akt. This promotes PI3K-Akt signalling,
including GSK3β-β-catenin mediated anti-inflammatory pathway (green) through
this inhibition of NF-κβ (yellow). NF-κβ is known as a pro-inflammatory mediator.

Furthermore, there is evidence suggesting that the expression of DRs on resident
glial cells may be context specific, with an increase in DR expression during

pathological stimuli [115, 155, 156]. As such, it is of no surprise that the abnormal

DA signalling observed in PD and schizophrenia could be contributing not only to

abnormal DA neurotransmission, but also to an altered immune response [115,

157]. Rangel-Barajas et al. showed that DRs display different affinities for DA [115].

Studies of the effects of DA on the immune response have shown that both the

bioavailability of DA and the expression of specific DR subtypes determines

whether DA will trigger pro- or anti-inflammatory responses.
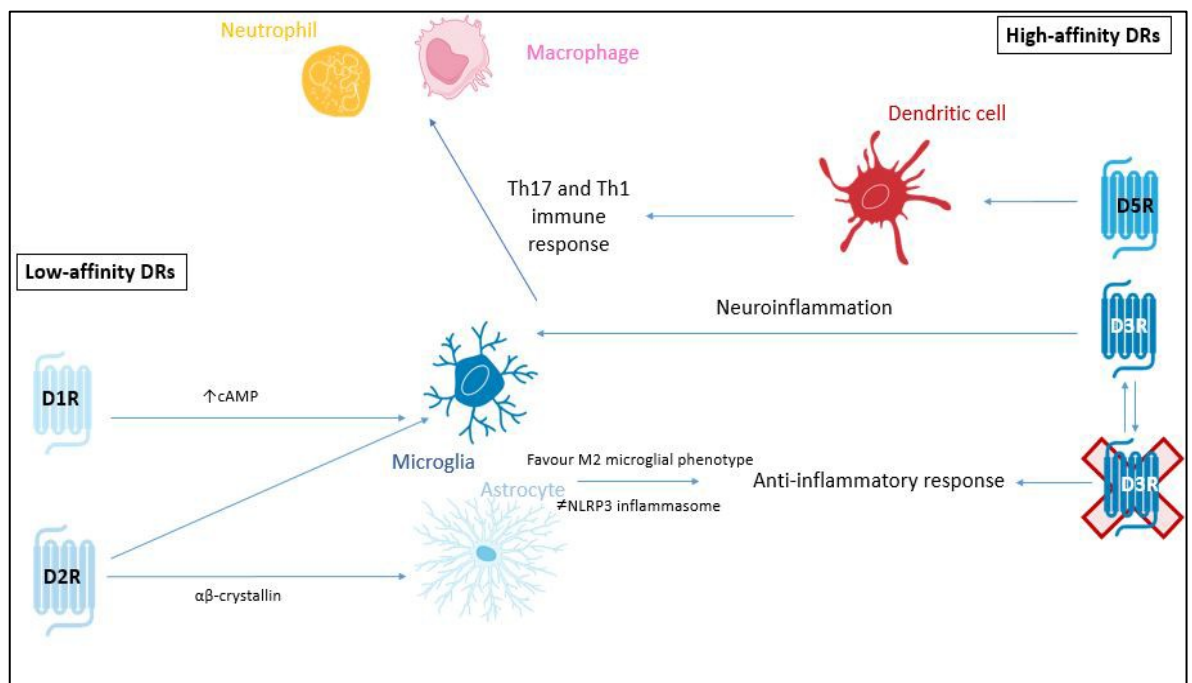
Figure 4 Summary of low-affinity and high-affinity actions of dopamine

receptors. In Parkinson's disease and PD models pro-inflammatory signalling has

been shown to be mediated by high affinity D3 and D5 receptors. The RHS of the

image shows the signalling of high-affinity receptors D3R and D5R. D3Rs on glial

cells promote neuroinflammation but also secrete pro-inflammatory cytokines that

activate Th17 and Th1 immune responses in CD4+ T cells which promotes the

recruitment of neutrophils and macrophages to the inflammatory site. Furthermore,

dopamine acting on D5R stimulates dendritic cells to acquire the Th17 pro-inflammatory phenotype. Moreover, in Parkinson's disease it has been shown that D1 agonism promotes anti-inflammatory response through increase of cAMP and favouring of M2 microglia phenotype and inhibition of NLRP3 inflammasome. Also, D2 agonists acting on astrocytes and microglia inhibits NLRP3 inflammasome (via ab crystallin signalling in astrocytes). The inhibition of D3R has been shown to attenuate inflammation and subsequent degeneration in MPTP mouse models of PD.

Furthermore, Pacheco deduced that low affinity DRs (i.e. D1R and D2R, respectively) are coupled to anti-inflammatory mechanisms, thereby DA binding to these receptors can dampen inflammation [158] (**Figure 4**). Conversely, signalling generated by high-affinity DRs (D3R and D5R) have been found to promote inflammation [158] (**Figure 4**).

Using PD as an example, we can better validate this concept. In a recent study, Elgueta et al, showed that D3R signalling promoted the development of PD by favouring neuroinflammation and the pathogenic CD4+ T cell response [159]. Contreras and colleagues subsequently confirmed these findings demonstrating that D3Rs expressed on CD4+ T cells promote Th1 and Th17 mediated immunity [160]. Th1 and Th17 mediated immunity stimulates the activation of pro-inflammatory pathways through the recruitment neutrophils and macrophages to the inflammation site [161]. However, it was also shown that D2R-signalling in astrocytes promotes an anti-inflammatory response mediated by αβ-crystallin [108]. In this study, Shao and colleagues demonstrated that astrocytic D2R-deficiency exacerbated susceptibility to 1-methyl-4-phenyl-1,2,3,6-tetrahydropyridine (MPTP)-

induced neurodegeneration and that wild-type mice treated with a D2R agonist displayed attenuated neurodegeneration of the nigrostriatal pathway [108]. Additionally, in the MPTP model of PD in the mouse, D1R-signalling in microglial cells and astrocytes was shown to promote an anti-inflammatory effect, which was mediated by an increase in cAMP levels, ultimately promoting the degradation of the NLRP3 inflammasome [162].

Taken together, these studies suggest that high DA levels, such as those found in the nigrostriatal pathway under homeostatic conditions, would promote the stimulation of low-affinity DRs (D1R and D2R), thus inducing anti-inflammatory effects. Conversely, pathological conditions that cause depletion of DA levels, such as PD, would induce a selective stimulation of high-affinity DRs, specifically D3Rs, thereby triggering pro-inflammatory responses, establishing CNS inflammation and consequently, neurodegeneration [163].

DOPAMINE-MEDIATED NEUROINFLAMMATION

DA is involved in the CNS-immune system interplay and in the autocrine/paracrine communication that exists between different immune cells. The effects of DA have been extensively studied in relation to the adaptive immune response and, in particular, how DA modulates T-lymphocyte activity [123] [164]. Comparatively little is known however, about how DA signalling regulates neuroinflammation and innate immunity. This is particularly important as evidence has shown that inflammatory responses from non-neuronal cells alone are sufficient to cause loss of DAergic neurons, as shown in studies of LPS-mediated neurotoxicity [1]. Injection of LPS into the rodent brain results in increased levels of inflammatory mediators, including cyclooxygenase-2 (COX-2) and inducible nitric oxide

synthetase (iNOS), prior to the loss of DAergic neurons [68]. This suggests that inflammation precedes neurodegeneration that ultimately results in PD.

We will take a closer look at evidence for each non-neuronal cell type to illustrate the complexity of DA's immune regulation and highlight the significance of the role DA has on the immune response.

DOPAMINE AND INNATE IMMUNITY

The innate immune response is the first line of defence and involves a fast, non-specific response. Innate immunity involves the coordinated responses of macrophages, natural killer (NK) cells, dendritic cells (DCs), neutrophils and more. We will focus on these four innate immune cell types as they are commonly found in the CNS following injury or in disease states.

Neutrophils

Neutrophils produce reactive oxygen species (ROS) and cytokines in response to pathogenic insult [165]. As described above, McKenna et al. revealed the presence of all five DRs on neutrophils with D5R being the most abundantly expressed [120]. In a mouse model of inflammation, DA agonists acting on neutrophils reduced their Th17-induced (pro-inflammatory) response [166]. It was also recently reported that L-DOPA treatment led to neutropenia in a patient with PD. This patient was shown to have reduced mRNA levels of all D2-like DRs and increased mRNA levels of TH and D5R [117].

Macrophages

Macrophages have been described as the vacuum cleaners of the body due to their ability to engulf foreign and toxic substances. They clean up the inflammatory

site removing anything that might be detrimental to the resident cells. DA suppresses the production of the pro-inflammatory interleukin-12 (IL-12) and promotes the secretion of IL-10, a key anti-inflammatory cytokine in macrophages in the mouse [110]. In addition, it has been consistently shown that D2R promotes an increase in viral replication in human immunodeficiency virus (HIV)-infected macrophages [167]. Recent studies have suggested a significant role of DA in regulating HIV-associated neurological disorders (HAND) [168].

Dendritic cells

Studies of DCs revealed they express the whole machinery to synthesise and store DA, which may act in an autocrine manner to stimulate DRs [169]. A preclinical mouse model of multiple sclerosis (MS) has shown that stimulation of D5R on DCs exacerbates Th-17 driven experimental autoimmune encephalomyelitis (EAE) [170]. A DA-mediated paracrine loop has been established between DCs and T cells [171]. DA stored in human DCs following its release acts on D1Rs present on naïve T cells to promote Th2 driven immunity. However, in the absence of DA, T cell differentiation shifts towards Th1 immunity [164]. Nakano also suggested that since stimulation of cAMP increases DA concentration in DCs and because DA by acting through its D1Rs can increase cAMP concentration, it is possible that the released DA auto-regulates its synthesis in these cells by acting through D1Rs present in these cells [149].

Natural killer cells

NK cells play a crucial role in the host-rejection of both tumours and virally infected cells. They act like cytotoxic T cells, destroying any cell that does not contain the "self" label. NK cells respond differently to DA depending on the specific DRs expressed on their membrane [155]. For example, activation of D1-like receptors

with the agonist SFK-38393 enhanced NK cell cytotoxicity but activation of D2-like receptors with the agonist quinpirole attenuated NK cells cytotoxic functions [155].

DOPAMINE AND ADAPTIVE IMMUNITY

Data demonstrating the influence of DA on innate immunity, supports strongly the emerging view that the CNS and immune systems share signalling pathways previously thought to be system specific. The adaptive immune response is usually activated when the innate immune response is insufficient to eliminate the pathogen and there is a slower, more targeted, antigen specific response involving T and B lymphocytes. T lymphocytes (T cells) are involved in the destruction and elimination of pathogens while B lymphocytes (B cells) provide antigen memory through the production of antibodies. Considerable work has been done by Talhada and Pacheco to dissect how dopamine regulates T-cell function [155, 169], driven by the observations that T cells are altered in several disease pathologies including autoimmune diseases, several cancers and inflammatory disorders. This work highlights the importance of determining how DA might contribute to T-cell abnormalities and whether DA could itself be harnessed as a therapeutic target to reduce disease burden and severity.

T lymphocytes

Most studies investigating DA control of immunity has focussed on T-cells. The complexity and context specificity of DA signalling is illustrated by the fact that the ultimate response of a T cell depends on the combined effects of DA concentration, DR sub-type expression, T-cell subtypes and T-cell activation state. For example, DA at physiological concentrations can evoke opposite functional responses in T cells. DA activates resting effector T cells (Teffs) resulting in their proliferation and

cytokine production [123]. However, if Teffs are already activated, DA will inhibit their function. Furthermore, D3R activation on human naïve T cells promotes inflammation through the selective secretion of tumour necrosis factor alpha (TNF-α), whereas, within the same population of cells, D2R activation selectively stimulates the release of IL-10, an anti-inflammatory cytokine [155]. These examples highlight the duplicity of DA's actions in immune responses. Regulatory T cells are also capable of releasing high amounts of DA that acts in an autocrine DR-mediated manner to inhibit their suppressive activity [169].

B-lymphocytes

B cells have been shown to produce DA which is upregulated upon mitogen induced activation, as shown by increased TH mRNA expression [155]. Additionally, intracellular vesicles containing DA in B cells are released in a calcium (Ca^{2+}) dependent manner [169].

Studies investigating the role of the peripheral immune system on CNS disorders are becoming more predominant because the infiltration of peripheral immune cells is usually present at a more severe stage of the disease [172]. Since peripheral immune cells are recruited by neuroinflammatory processes that originate in the brain, it is important to determine whether DA secreted by resident microglia and astrocytes interacts with immune cells and contributes to the altered blood brain barrier and recruitment of the innate and adaptive immune systems.

Neuroinflammation

Central neuroinflammation refers to the inflammatory processes occurring within neural tissues of the CNS which are mediated by the production of cytokines, chemokines, reactive oxygen species and secondary messengers by microglia and astrocytes [173]. Neuroinflammation has been repeatedly linked to most CNS

pathologies characterised by abnormal DA signalling, including PD, schizophrenia and mood disorders [147] [174] [175]. The chronic or sustained neuroinflammation seen in these diseases promotes the infiltration of peripheral immune cells, from both the adaptive and innate immune systems to the inflammatory site. It is critical to understand the role of DA in both glial and peripheral immune cells, as DA's critical role both as a neurotransmitter and immune transmitter in these pathologies requires a careful balancing act when developing drug targets to ensure they have a beneficial action on both functions.

Microglia

Microglia are specialised scavengers of the CNS. When chronically activated, these cells become the main contributors to neuroinflammation, which in turn is responsible for the progression of neurodegeneration [176]. It has been shown that human microglia are immunoreactive for all five DRs [120]. Microglia exist in four main phenotypic states in addition to the resting state, seen under homeostatic conditions which is referred to as the M0 phenotype. Under "activating" conditions, microglia can present with distinct phenotypes: M1 (classical activated, neurotoxic, pro-inflammatory) and M2a (alternatively activated, neuroprotective, anti-inflammatory) alternative type II activation (M2b), and acquired deactivation (M2c) [84] (**Figure 5**). Importantly, it has been suggested that specific DR subtypes can influence whether microglia are either M1 or M2 activated, thereby controlling whether a pro- or anti-inflammatory response occurs. Strong support for this idea arises from several studies including data from Wang et al, (2019) which showed that DA alters LPS-induced NO production in microglia via D1-like mediated AC/cAMP-PKA-ERL1/2-NF-κβ-iNOS axis [177]. Additionally, it has been shown that microglia activation was prevented in D3R deficient mice in an MPTP model of

PD [159]. Furthermore, the anti-PD drug rasagiline, a brain selective MAO inhibitor significantly reduced both ROS and NO secretion, as well as cytokine release in DA stimulated microglia. Collectively, these results suggest that DA can affect the ability of microglia to secrete cytokines, and importantly DR activation directs the shift towards specific microglial phenotypes. Since inflammation is associated with several DAergic pathologies, the ability of DA to determine the phenotype of microglia is very important to consider in attempting to understand the pathology of disease. Microglia are the key drivers of neuroinflammation and as such determining how DA can regulate these cells is crucial. For example, in PD it is well accepted that neuroinflammation drives progressive neurodegeneration. In fact, neuronal damage and uncontrolled inflammation amplify each other neurodegenerative and induce a feed-forward cycle driving chronic progression of PD and other diseases [178]. These observations underpin the substantial experimental efforts in exploring the potential utility of traditional anti-inflammatories in slowing, reversing and preventing PD. However, due to the peripheral effects of long-term anti-inflammatory drugs use, novel targets are needed specifically to counteract CNS inflammation.
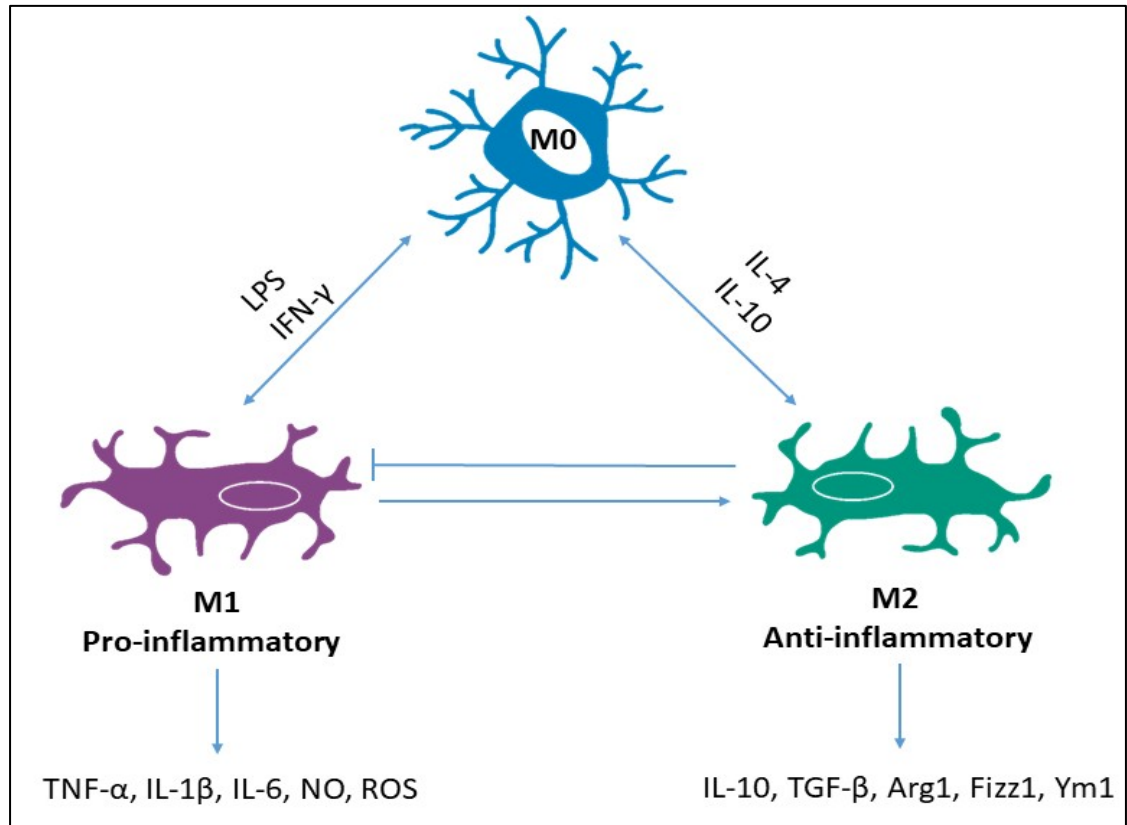
Figure 5. Microglia phenotypes. Microglia exist in three main phenotypic states; resting microglia, seen under homeostatic conditions represent the M0 phenotype. Depending on the stimulus M0 microglia can be classically activated by LPS or IFN-γ and become M1 phenotype or M2 phenotype via alternate activation from IL-4 or IL-10. M1 represent a pro-inflammatory phenotype due to the production and secretion of inflammatory cytokines and mediators like TNF-α, IL-1β, IL-6, NO, ROS; whereas M2 are anti-inflammatory due to the production of anti-inflammatory cytokines and neuroprotective agents including, IL-10, TGF-β, Arg1, Fizz1, Ym1. Furthermore, under homeostatic conditions, M1 microglia can promote M2 activity to maintain physiological levels of inflammation and M2 are able to block excess neurotoxic activity of M1. In chronic inflammation this balance and autocrine control is lost and the M1 phenotype dominates creating a neurotoxic and pro-inflammatory environment.

Astrocytes

Astrocytes constitute most the brain's glial cells. Astrocytes are involved in the maintenance of homeostasis and promote neuronal survival by regulating metabolites, secreting neurotrophic factors and regulating blood flow [179]. The roles of astrocytes depend largely on the exchange of molecules from the extracellular space [180]. Cortical astrocytes stimulated with DA show a D1/5R mediated intracellular NADH increase, via PKA [180]. Stimulation with the selective D1 agonist SKF39383 promoted the release of nerve growth factor (NGF) and glial cell-derived neurotrophic factor (GDNF), leading to the suggestion that DA activates astrocytes to promote the secretion of neuroprotective mediators [181]. Parallel studies by Shao and colleagues showed that D2R-signalling in astrocytes promotes anti-inflammatory responses that appear to be mediated by αβ-crystallin [108]. Activation of D2-like receptors has been linked to increases in brain derived neurotrophic factor (BDNF), GDNF mRNA expression and protein synthesis as well as suppression of CRYAB mediated neuroinflammation *in vivo* [182]. The role of astrocytes in neuroinflammation is often overlooked, as instead of producing neurotoxic factors like microglia, an important role of these cells is to provide neurotrophic factors that promote neuronal survival. As most strategies to reduce neuroinflammation focus on reducing microglia activity, the neurotrophic support from astrocytes is still required to help repair and promote the recovery of damaged neurons. Based on the data summarised here, we show that DA can increase the secretion of these neurotrophic factors, including GDNF and BDNF. GDNF has long been considered a potential therapy for PD, and experimental studies suggest that GDNF could protect degenerating DA-neurons in PD as well as promote the

regeneration of the nigrostriatal DA system [183]. The ability to innately stimulate astrocyte release of GDNF could prove a useful therapeutic approach to PD as the fact that GDNF cannot cross the blood brain barrier (BBB), is hindering current clinical trials with this agent. With this idea, broadening the approach to DA and neuroinflammation could provide new targets and approaches to several pathologies that are currently being overlooked.

Oligodendrocytes

Although not traditionally involved in inflammation, oligodendrocytes are another non-neuronal cell type that plays a major role in several CNS diseases like Multiple Sclerosis (MS). Interestingly, D2R and D3R mRNA and immune-reactivities have been detected in cortical oligodendrocytes [148]. Evidence also suggests that D2R and D3R agonists can protect cultured rat cortical oligodendrocytes from oxidative glutamate toxicity and combined oxygen/glucose deprivation injury [148], suggesting a protective role of these receptors. Although little is known about the role of oligodendrocytes in inflammation, recent studies have indicated key roles of these cells in several inflammatory processes, which are clearly seen in models of MS. Despite being an autoimmune disorder, the role of DA in the pathogenesis of MS has been revealed, highlighting the broad function of DA as an immune transmitter in its ability to regulate inflammation both within the brain and in the periphery.

DOPAMINE AND AUTOIMMUNITY

DA levels are altered in the brain of mouse models recapitulating two well-known autoimmune conditions: MS and systemic lupus erythematosus (SLE). The altered

expression of DRs in peripheral lymphocytes of MS and SLE patients also supports the importance of DAergic regulation in autoimmunity.

MS is a disease characterised by CD4+ T cell mediated progressive loss of neurological function, likely due to the destruction of axonal myelin sheath [184]. T cells and DCs have consistently been shown to promote disease pathogenesis in both animal models and MS patients. DCs can promote the differentiation of CD4+ T cells towards the inflammatory Th17 phenotype, corresponding to evidence previously stated showing DA derived from DCs regulating T cell phenotype [170]. Using an experimental autoimmune encephalomyelitis (EAE) model of MS, combined with MPTP administration, it was shown that MPTP-driven DA depletion in the CNS prior to MS pathology induction exacerbates the MS presentation [185]. In fact, at both the onset and peak of EAE disease, an increase in striatal DA was observed, which was accompanied by a similar increase in striatal IL-1β and TNF-α mRNA expression [169]. Although these findings require further assessment, the results obtained point to a critical role for DA in regulating the autoimmune response. In other studies, the D1R-like antagonist SCH-23390 prevented the development of EAE [149]. Patients with MS treated with interferon (IFN)-β show reductions in the elevated levels of D5Rs and TH expressed on Tregs and abolished DA-mediated inhibition of the suppressive activity of Tregs, which promotes disease progression [169]. These observations link the DAergic system with the development and progression of MS. The role of DA in MS also suggests that DA could play a role in other autoimmune diseases.

Systemic lupus erythematosus (SLE) is an autoimmune disease of variable and unpredictable disease pathology [186]. SLE is characterised by several abnormalities of the cellular immune system, including a loss of B cell tolerance

and the production of pathogenic autoantibodies [187]. Neurologic manifestations appear in between 18% and 67% of patients with SLE and are associated with inflammatory features in the brain [187]. Neurological manifestations include a range of CNS disorders, like anxiety and depressive disorders, cognitive dysfunction [188]. Jafari and colleagues have shown the abnormal expression of D2R and D4R in T cells of SLE patients [186]. They have suggested that these abnormalities contribute to SLE pathogenesis through the regulation of T cell function. They have proposed that T cell expression of D4R could provide a therapeutic target for SLE as it could be utilised to trigger T cell quiescence. The role of DA in SLE is demonstrated further in the spontaneous development of lupus-like disease in MRL-lpr mice which is accompanied by impaired DA catabolism and the degeneration of DAergic axon terminals in the midbrain [189]. Notably, DA analogues have shown therapeutic effects in animal models and patients with lupus, for example, treatment with bromocriptine (BRC), a D2R/D3R agonist, resulted in a significant reduction of mean flares/patient and serum prolactin levels in SLE patients [189].

The evidence that DA plays an important role in modulating the pathogenesis of autoimmune disorders such as MS and lupus supports its role as an immune transmitter in addition to its canonical neurotransmitter role. In addition, it exemplifies the broad functions of DA in immunity that could be utilised as novel therapeutics for a wide range of diseases, extending beyond the traditional DAergic pathologies.

DOPAMINE AND PARKINSON'S DISEASE (PD)

The most well-known DAergic pathology is Parkinson's disease (PD). PD is also the most common neurodegenerative movement disorder, characterised by the degeneration of neurons in the *SNpc*, resulting in a loss of DA availability in the striatum and associated pathways (i.e., the degeneration of the nigrostriatal pathway) [1]. The nigrostriatal pathway is responsible for the control of movement, leading to the cardinal motor symptoms of PD, which include bradykinesia, resting tremor, rigidity and postural instability [1]. PD is also associated with a myriad of non-motor symptoms such as olfactory deficits, autonomic dysfunction, pain, depression, cognitive deficits and sleep disorders, associated with the alteration of other DAergic pathways and non-DAergic signalling [1]. The aetiology of PD remains unknown; however, several factors are thought to contribute to the pathogenesis of PD including genetics, environmental factors and neuroinflammation.

The traditional PD therapeutics aim to replenish DA in the striatum either through L-DOPA (the precursor to DA) or *via* DA agonists (mainly D2 and D3). Since both the expression of DRs on the surface on microglia, astrocytes and lymphocytes have been shown [150] along with their altered expression in *post-mortem* brains of PD patients, current evidence suggests that both glial cells and lymphocytes could respond to DA-based PD therapeutics as well [20].

It has been suggested that D2Rs are the dominant receptors found in the nigrostriatal pathway (ventral tegmental area [VTA] and striatum). These receptors are thought to promote an anti-inflammatory phenotype in immune cells and glia (microglia and astrocytes) [115]. As DAergic signalling is lost during PD, the reduction of activity at D2Rs likely favours a pro-inflammatory environment, a suggestion supported by the observation that quinpirole, a D2R specific agonist,

suppressed neuroinflammation and protected against brain injury in a mouse model of PD [182].

Conversely, it has been suggested that D3Rs promote a pro-inflammatory environment, as was discussed above, pharmacologic D3R antagonism was shown to be protective against MPTP-induced neurodegeneration and motor impairments [159]. These observations are important to consider as PD therapeutics aim primarily to replace DA in the brain via administration of L-DOPA, the precursor to DA in the biosynthetic pathway (see **Figure 2**). It is therefore possible that the increased availability of DA may re-activate D2R signalling and restore the balance to DA induced inflammation. However, L-DOPA induced dyskinesia, a disabling side effect of long-term L-DOPA treatment, is often associated with a dramatic increase in striatal neuroinflammation when compared to L-DOPA treated non-dyskinetic PD patients and controls [190].

Furthermore, DA agonists commonly used in PD are D2-like agonists that act on both D2R and D3Rs. For example, common DA agonists used in PD management include:

- Pramipexole, a D3R-preferring agonist, with high selectivity for D2R
- Ropinirole, a D2R, D3R and D4R agonist
- Apomorphine, another D2R agonist [191]

As these agonists can activate both D2R and D3Rs and given that in the presence of sufficient DA levels D2R abundance is by far higher than D3R, it is possible that the mechanism of action of these drugs might primarily involve the activation of D2R-driven anti-inflammatory activities and not D3Rs. Furthermore, since DRs are ubiquitously expressed throughout the brain, it is important to target specific areas or cell types to minimise the damage to other neuronal functions. For example,

blockade of D3R can reduce sensitivity to anxiety medication, a common co-morbidity for DAergic pathologies, including PD, but also reduce ethanol related reward-associated voluntary consumption [192-194]. Therefore, it is important to determine how DRs are regulated not only in different cell types but throughout different brain regions.

Additionally, there is an association between CD4+ T cell DR expression and the degree of motor dysfunction, as assessed by Unified Parkinson's Disease Rating Scale (UPDRS) score. In fact, within the total CD4+ T cell population D1R expression decreased while in T memory cells D2R expression increased with increasing disease score [195]. This suggests the DR expression levels in T cells could be used as a useful prognostic biomarker for PD patients. The ability to monitor PD through a routine blood test would present an enormous advantage as currently clinicians are restricted to qualitative clinical scoring, neuroimaging and a comprehensive medical history.

DOPAMINE, PARKINSON'S DISEASE AND OXIDATIVE STRESS

It is well known that oxidative stress contributes to the pathogenesis of neurodegenerative disease, particularly PD. DAergic neurons are more susceptible to oxidative stress since they are long-projecting neurons with poorly myelinated axons that provide extensive synaptic innervations. In addition, DAergic neurons have autonomous pacemaker activity, resulting in high energy requirements, and DA and its metabolites containing 2-hydroxyl residues generate highly reactive DA and DOPA quinones [196]. Consequently, DA neurons require efficient mechanisms to maintain neuron functioning and pre- vent the accumulation of ROS, damaged/misfolded proteins and regenerate essential survival components

[197]. Additionally, DA quinones have been linked to mitochondrial dysfunction, inflammation and oxidative stress. This inherent highly oxidative environment means that, when there is excess DA or ineffective DA metabolism, ROS can accumulate creating oxidative stress in neurons. This in turn activates local immune cells, microglia and astrocytes, to secrete neurotrophic factors and cytokines to help reduce oxidative damage. However, in a disease like PD, we know that this sequence of events creates a vicious cycle whereby DA neurons produce more ROS, and glial cells keep secreting cytokines, leading to chronic neuroinflammation and the establishment of a self-propagating cycle that is ultimately detrimental to DAergic neurons. This cycle is also seen in other neurodegenerative diseases like Alzheimer's disease (AD).

DOPAMINE AND ALZHEIMER'S DISEASE

AD is the most common neurodegenerative disorder that is characterized by the presence of extracellular amyloid plaques, intracellular neurofibrillary tangles and hyper phosphorylated tau, neuronal loss, oxidative stress and neuroinflammation, primarily in the cortex and hippocampus [198].

The DA system has for long been associated with aging, with a decline in motor function associated with DA changes in the substantia nigra and striatum being a robust hallmark of aging [199]. One study revealed a marked increase in microglial reactivity in the SNpc in elderly humans (~81 years), which was reflected by high degree of neuronal death in these areas [199]. This is due to the higher susceptibility of DA neurons to oxidative stress, which inherently tends to increase with age.

As such, it is not surprising that there is some degree of overlap between the pathophysiology of AD and PD, as both diseases have been shown to correlate with increased levels of oxidative stress, abnormal DA regulation and evidence of neuroinflammation. This higher susceptibility to both oxidative stress and neuroinflammation may also be a contributing factor in the pathogenesis of AD, with abnormal DA signaling and expression seen in the mesolimbic pathway of AD patients, however the role of DA in AD pathogenesis remains to be elucidated [200]. The mesolimbic DAergic pathway consists of neurons arising from the ventral tegmental area which project predominantly to the prefrontal cortex, hippocampus and nucleus accumbens [201]. The degeneration of DA neurons in this pathway correlates with impairments in memory and reward performance [200]. Consistently, pharmaco- logical treatment to increase DAergic transmission improved cognitive impairment and memory deficits in AD patients and experimental models, emphasizing the critical role of DA in AD [197].

For example, it has been shown that D2R in the hippocampus correlates with memory functioning in AD [202]. Koch also demonstrated that D2R/D3R agonists may restore cortical plasticity in AD patients, which is consistent with findings in post-mortem brains of AD patients showing that there is a significant decrease in D2-like receptors in the hippocampus and prefrontal cortex [203].

Moreover, additional *ex vivo* studies in AD patients have demonstrated that lymphocytes had a low density of D2-like receptors compared to controls [204]. These results suggest that as in PD, DA modulates the immune response in AD as well. This could contribute to the neuroinflammation, and abnormal DA neurotransmission observed in AD patients.

DOPAMINE AND DRUG ABUSE

DA plays a critical role in movement, memory, cognition, and emotion [97]. Due to its role in controlling operant reinforcement, incentive salience and its ability to trigger positively-valenced emotions via the reward system, DA has been implicated in drug abuse and addiction.

As we have seen in PD and AD, DA availability influences how immune cells respond to DA, which is evident not only in neurodegenerative diseases associated with reductions in DA, but also in situations where there is an excess of DA, as seen in drug abuse. One of the most abused drugs is methamphetamine (METH), which remains a significant public health concern worldwide [205]. METH is a known powerful modulator of DA and has several effects that influence DA release, including disrupting DA reuptake and packaging through DAT and VMAT2 [206]. The mechanism of METH ultimately results in excess extracellular release of DA.

Interestingly, METH has been shown to promote neuroinflammation through DRs. Wang et al. have shown that METH exposure increased LPS induced pro-inflammatory cytokine production in the hippocampus, promoted microglia activation and increased the expression of D1-like receptors [207]. These effects were inhibited after treatment with SCH-23390 (a D1-like receptor antagonist) and minocycline (microglial inhibitor), suggesting that this response was specific to DRs expressed by microglia [207]. Furthermore, this study illustrated that D1-like receptor mediated increase in inflammation triggered by METH, involved ERK1/2 phosphorylation and activation of the CREB signalling cascade [207]. Another study that utilised a rat model of METH self-administration, revealed changes in the brain consistent with clinical findings in METH addicts [205]. Analysis of striatal brain tissue showed increased expression of genes involved in CREB signalling

and the activation of neuroinflammatory responses [205]. Kitamura and colleagues provided further support for the suggestion that METH neurotoxicity is mediated by microglia by showing that the activation of microglia accompanies METH neuro-toxicity and that inhibition of microglial activation reduced dopamine depletion and restored DAT levels [208].

The consistency of the conclusions of these studies suggests a role of DA in the pathology of drug abuse and addictive behaviour. In addition, several researchers have suggested that neuroinflammation in the striatum underlies the cognitive deficits, depression and parkinsonian symptoms reported in METH addicts. This hypothesis could form the basis of a unifying theory of DA as a major contributor to several CNS pathologies.

DOPAMINE AND HUMAN IMMUNODEFICIENCY VIRUS-1-ASSOCIATED NEUROLOGICAL DISORDERS

HIV remains a major global health concern with an estimated 35 million people living with HIV [209]. De- spite the widespread use of efficacious antiretroviral therapies to control peripheral infection more that 50% of HIV-positive individuals will suffer from neurological complications, otherwise known as HAND [210]. In HIV infected individuals, substance abuse may accelerate the development and/or increase the severity of HAND as studies have shown that altered DA signaling is a risk factor for HAND with most patients presenting with cognitive, memory, motor and behavioral deficits [209].

Typically, HIV is unable to cross the blood-brain barrier alone. However, it has been proposed that CD14+CD16+ monocytes are able to mediate the entry of HIV into the brain and that the migration of both infected and uninfected monocytes

across the blood-brain barrier contributes to the establishment and propagation of CNS HIV viral reservoirs and chronic neuroinflammation, which are essential in the development of HAND. Since drug use elevates DA, and the fact that HIV-positive people tend to fall into drug use more frequently than the healthy population, Calderon and colleagues examined the effects of DA on monocytes and HIV infection. They found that the CNS migration of the CD14+CD16+ monocyte subpopulation is increased by DA and D1-like receptor agonist SKF-38393, suggesting that the heightened migratory capacity of monocytes is mediated by D1-like receptors [211].

Additionally, Nickoloff-Bybel et al. showed that DA increases HIV entry into macrophages via a calcium-dependent mechanism, revealing that D1-like receptor activation on infected macrophages stimulated calcium and protein kinase C activation [212]. Since we know that other immune cells are also activated by DA, we can assume that high concentrations of DA can prime the CNS for further HIV viral infection, which not only increases viral reservoirs within the brain, but also contributes to HAND pathologies.

CONCLUSION

Despite strong evidence showing the expression of DA, its binding receptors and the components necessary to synthesize, store and metabolize DA in non-neuronal cells, the exact significance of these findings in the context of PD pathogenesis remains to be fully determined. Several studies have highlighted the importance of DA in regulating autoimmune diseases, such as MS and SLE, and many others have examined how DA contributes to the control of T lymphocyte functionality in disease states. Furthermore, studies in AD, drug abuse, HIV infection and HAND

emphasize the myriad of roles DA has within the brain. The evidence presented in this review calls attention to the robust and extensive ways in which DA can control immunity and the important need for a greater understanding of this novel function of DA (**Figure 6**). It is well-accepted that microglia and, to a greater extent, astrocytes, are responsible for regulating the blood brain barrier function to either promote or reduce the permeability to peripheral leukocytes. Further studies are necessary to unveil DA's regulatory activity on non-neuronal cells, especially microglia and astrocytes, as these cells are commonly altered in several CNS disease pathologies, including PD. Furthermore, the emergence of DA as an immune   transmitter may have future implications for our understanding of brain physiology, but also in the clinical management of neurological diseases, as it presents a wide array of new therapeutic and prognostic targets for CNS pathologies (**Figure 6**).
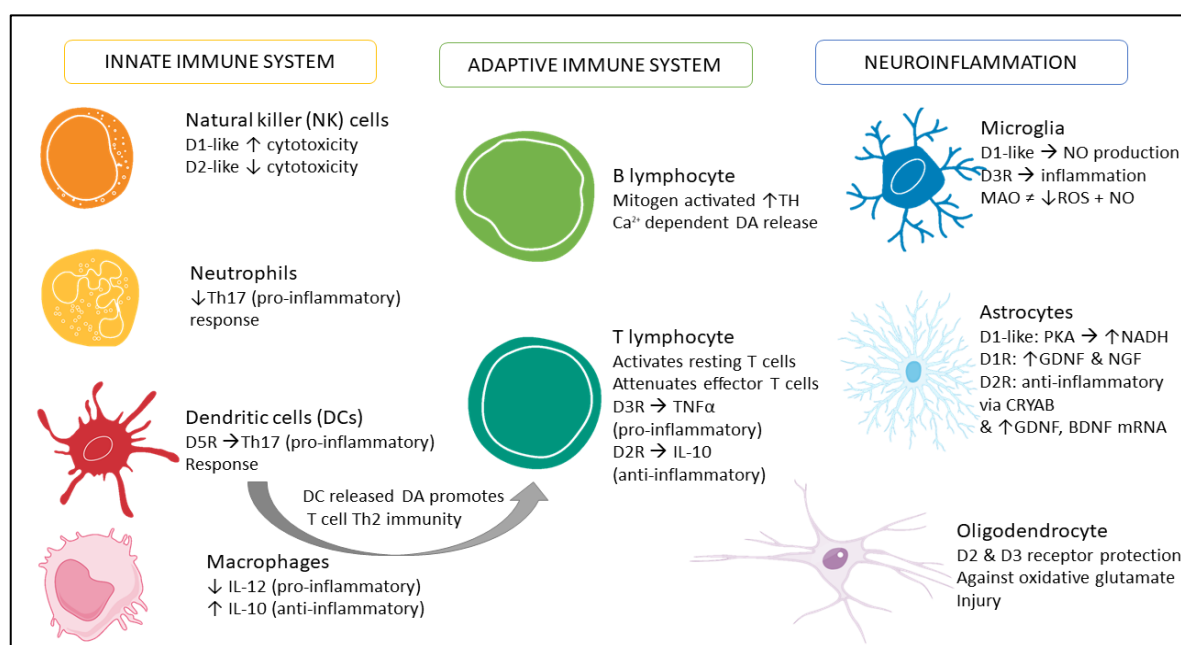

Figure 6. Summary of immune cells responses to dopamine. This figure summarises the evidence presented in this review.

1.5 Buspirone

Buspirone (Buspar®) is a Food and Drug Administration (FDA)-approved anxiolytic medicine used for the treatment of generalized anxiety disorder [213]. It exerts anxiolytic effects from its action as a selective partial agonist to the 5-hydroxytrptamine (or, serotonin, 5HT) receptor (5-HT1ar) [214].

Buspirone has become a popular anxiety medication due to its decreased side effect profile compared with other anxiolytics [214]. This safe profile is associated with high tolerability and no associated risk of physical dependence or withdrawal due to a lack of activity on GABA receptors, reducing its toxicity and potential for abuse. Moreover, it has been shown to attenuate side effects associated with PD therapy, including L-dopa induced dyskinesia [214, 215].

1.5.1 Dopamine D3 receptor antagonism

Dopamine 3 receptors (D3R) are highly expressed in the nucleus accumbens and is involved in emotion and reward systems, including mediating pleasure in the brain [22]. They have a high affinity for dopamine resulting in their function as critical modulators of dopaminergic function [216]. Recently, through computational and neuroimaging studies, it has been discovered that buspirone has a strong "off-target" function as a D3R antagonist [192, 217].

The D3R has been implicated in various aspects of PD pathophysiology [97]. One study has reported a direct correlation of the expression of D3R in peripheral blood and the degree of neuroinflammation and dopaminergic degeneration in the CNS [97]. It has also been observed that T-cells with higher D3R expression infiltrate through the BBB and induce the activation of microglia, further aggravating neuroinflammation, compared with D3R$^{-/-}$ counterparts [218]. This is validated by several studies showing the ability of the D3R to promote T-cell activation [219,

220] and astrocytes, which induces neuroinflammation [221]. One study by Franz and colleagues suggested the activation of T-cells was induced by D3R mediated reduction in cAMP levels and ERK-2 phosphorylation, however further work is needed to determine the mechanism in other cells types [96]. Similarly, D3R inhibition has been shown to attenuate parkinsonian disabilities [222] and prevent both microglial [223] and T-cell [156] activation. Additionally, D3R agonists resulted in the progressive development of dyskinesia [224], suggesting that blocking this receptor may also be a winning strategy to overcome L-dopa induced dyskinesia, the most common adverse effect of PD treatment. As such, buspirone could be considered a potential treatment in patients that no longer respond to traditional dopamine replacement therapies.

The landmark study by Elgueta and colleagues demonstrated that pharmacological blockade of the D3R reduces inflammation and consequently slows disease progression in mouse models of PD [159]. Unfortunately, this study utilised compounds that are not suitable for clinical use. The discovery that buspirone has potent D3R antagonistic activity suggests it may exert similar effects [192, 225]. If buspirone is able to demonstrate a similar disease-modifying effects in mouse models of PD, it has promise as a therapeutic in humans as a study as already confirmed, with PET imaging the occupancy of D3Rs by buspirone [225]. Altogether, evidence suggests that blocking D3R is a promising therapeutic approach in PD by reducing a major pathophysiological contributor, neuroinflammation, which may preserve dopaminergic neurons from degeneration [159, 218].

1.5.2 Good candidate for repurposing

Drug repurposing is an attractive way to discover new treatments, particularly for neurological diseases that often have only symptomatic treatments and for which there are no disease-modifying agents. It overcomes the barriers to traditional drug discovery, like long developmental timelines and high costs [226]. More importantly, it makes use of drugs that are already safe and tolerable for clinical use with known pharmacology.

As of January 2020, 34.5% of PD drugs in active clinical trials are repurposed drugs, including drugs currently used to treat Alzheimer's disease, antibiotics and GLP-1 agonists used in type 2 diabetes [227]. If we combine the percentage of drugs that target a known pathophysiological mechanism that underlies PD, including, antioxidants, mitochondria function, immunotherapy and alpha-synuclein, these only make up 12.4% of active drugs in the pipeline for PD therapies, while drugs targeting symptomatic relief make up 51.6% [227]. This emphasises the urgent need of therapies that target the underlying pathology of disease which can help to slow or stop disease progression.

One of the most challenging hurdles to overcome when developing neurological therapeutics is designing drugs that can be administered systemically and can also cross the BBB. Buspirone is known to readily cross the BBB and has therapeutic efficacy via oral tablet administration, making this a convenient and effective neurological therapy [228]. Buspirone is clinically administered orally via tablets, usually around 5-30mg [214]. However, in a pharmacological trial, healthy patients were given up to 375mg buspirone per day and developed only minor side effects like vomiting, dizziness and gastric distress [229]. This is particularly important, as Le Foll et al., demonstrated that high concentrations of buspirone are required to

achieve full D3 occupancy, although these are still within the therapeutic range [217, 230]. Additionally, anxiety is a commonly reported side effect of PD, and buspirone could help mitigate both parkinsonian and anxiety symptoms and pathology [231]. Finally, buspirone has undergone several clinical trials and longitudinal studies that have shown it is an extremely safe drug [213, 232, 233]. As such, it is possible that buspirone's D3R antagonism could reduce inflammation and therefore promote neuroprotection in neuroinflammatory diseases, like PD (**Figure 1.7**).
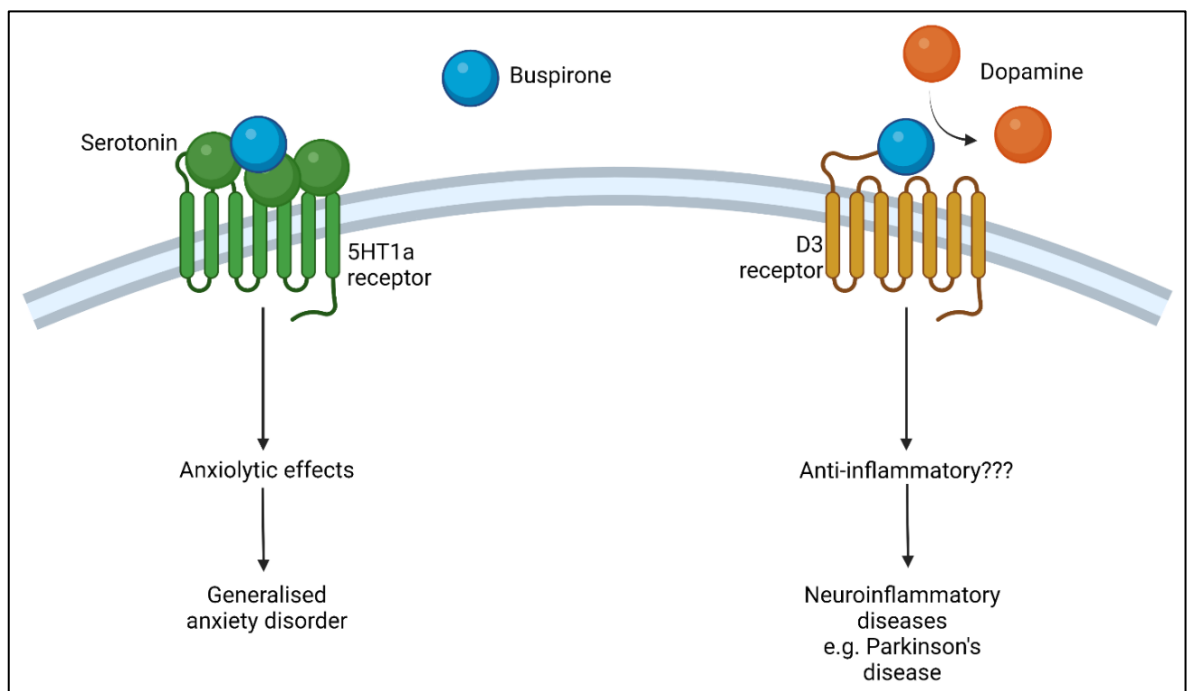
Figure 1.7. Buspirone's known pharmacological targets. Buspirone is a 5HT1a receptor partial agonist which exerts pronounced anxiolytic effects and is used to treat generalized anxiety disorder. This study proposes to investigate its novel function as a D3 receptor antagonist to determine if buspirone can elicit anti-inflammatory effects and therefore be clinically used to treat neuroinflammatory diseases like Parkinson's disease.

1.6 PACAP and VIP

The neuropeptides pituitary adenylate cyclase-activating polypeptide (PACAP) and vasoactive intestinal peptide (VIP) are widely distributed throughout the central and peripheral nervous systems and exert pleiotropic neuroprotective and immune modulatory activities [234].

The activity of these peptides is mediated by three G-protein coupled receptors, PAC1, VPAC1 and VPAC2, which appear to govern distinct and cell-type specific biological functions. In general, VPAC1 and VPAC2 are implicated in most of the immune modulatory effects, while PAC1 receptors mediate most growth factor and neuroprotective actions. This is important as although all receptors bind with high affinity to both peptides, the PAC1 receptor displays a 100-fold higher affinity for PACAP than VIP (**Figure 1.8**).
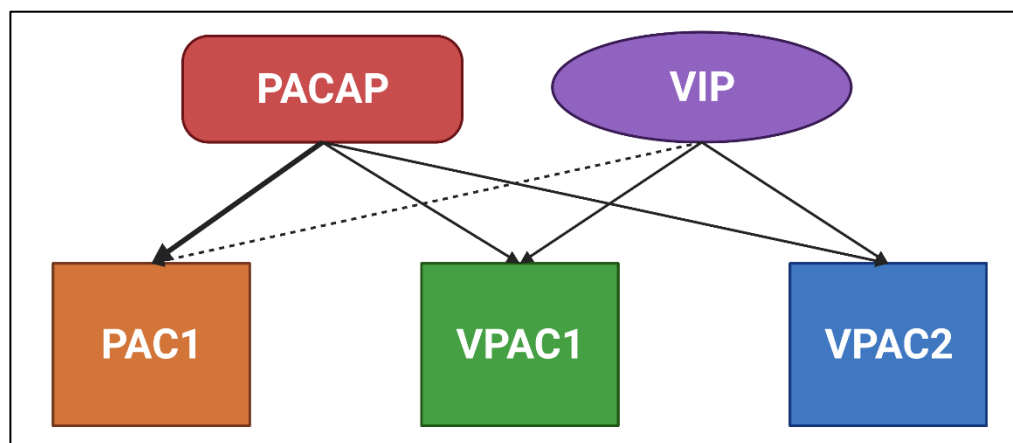
Figure 1.8. Summary of peptide interactions with receptors. PACAP (red) binds to all receptors, although it has a significantly stronger affinity (~100 fold) to PAC1 (orange), compared with VIP (purple). VIP preferentially binds to both VPAC1 (green) and VPAC2 (blue) along with PACAP.

These peptides have been linked to a range of neurodegenerative and neuroinflammatory diseases, including PD [234, 235] (**Figure 1.9**). We have previously shown that the tetracyclines, minocycline and doxycycline act as positive

allosteric modulators of the PAC1 receptor [236]. Previously we mentioned that minocycline attenuated PD progression by inhibiting microglial polarization [80]. This could be partly due to its effects on the protective PAC1 receptor. Furthermore, there are several lines of evidence that implicate PAC1 receptor activation in promoting the synthesis and release of neurotrophic factors that promote neuronal survival, such as brain-derived neurotrophic factor (BDNF) [236, 237].
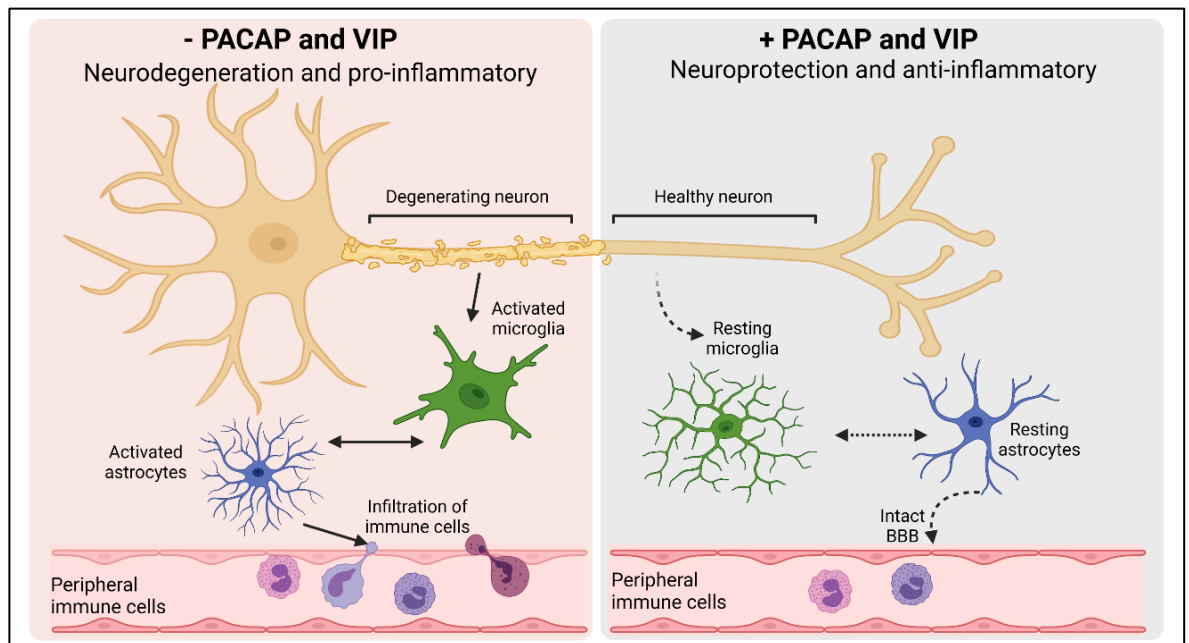
Figure 1.9. Summary of broad immunomodulatory and neuroprotective functions mediated by PACAP and VIP. The absence or disturbed function of PACAP and VIP result in neurodegeneration and acquisition of pro-inflammatory phenotype. This activates local microglia and astrocytes which can lead to the infiltration of peripheral immune cells through a leaking blood brain barrier which further aggravates inflammation. However, the maintenance or administration of PACAP and VIP promote healthy brain function including neuroprotection and anti-inflammatory activities.

PACAP knockout (KO) mice have been shown to display age-related degenerative signs earlier than wild-type animals, including increased neuronal vulnerability, systemic degeneration and increased inflammation, indicating the importance of this peptide in the maintenance of a healthy CNS [238]. Notwithstanding this, the ability of PACAP in targeting neuroinflammation is controversial. A study by Shivers and colleagues demonstrated that despite PACAP preventing behavioural deficits and attenuating dopaminergic degeneration, it failed to inhibit microglial activation in mice infused with prostaglandin J2, as an inflammatory model of PD [239]. In contrast, our study revealed that PACAP was more effective than VIP in suppressing some of the biological activities of LPS-stimulated microglia [240]. This was further validated *in vivo*, where PACAP administration restored MPTP-induced reduction in TH expression and modulated the inflammatory response [241]. Nevertheless, PACAP deficient mice are more vulnerable to damaging neurotoxic insults, suggesting that this peptide is required for neuronal survival and normal brain functioning [242].

On the other hand, VIP has more consistently been able to promote both protective and anti-inflammatory activities in PD models. VPAC2 receptor agonists have been shown to elicit potent immunomodulatory functions that led to the protection of dopaminergic neurons, including reducing microglial activation and promoting anti-inflammatory T cell response [243]. Furthermore, VIP prevented MPTP-induced dopaminergic degeneration and inflammation [244]. Moreover, systemic administration of VIP in 6-OHDA rodent model of PD exerts a variety of neuroprotective effects, including improving locomotion, promoting survival of dopaminergic neurons, reducing oxidative stress and demyelination [245].

More importantly is the strong interaction of these peptides with the dopaminergic system. Pharmacological studies show that PACAP has neurotrophic and neuroprotective actions on dopamine and serotonin neurons [246]. Previous studies in D3R KO mice revealed elevated hippocampal PACAP expression, which suggested a possible link between the PACAP neuropeptide and the dopamine system in the acquisition and retention of fear memories [114]. Moreover, the protective effect of PACAP administration correlated with increased dopamine levels [247]. The strong relationship between these neuropeptides and dopamine suggest that both PACAP and VIP hold the potential to also be considered as therapeutic targets in PD, in view of their neuroprotective and immune modulatory functions.

1.7 Aims and Hypothesis

The overarching goal of this thesis is to elucidate whether targeting the D3R can be considered an effective strategy to counteract neuroinflammation in PD. Accordingly, a complementary objective will be to test if buspirone, a drug endowed with D3R antagonism, can be repurposed for PD.

To do this, we had three main aims:

Aim 1: Determine if buspirone's anti-inflammatory activities are through dopamine D3 receptor blockade

1. Generate stable $Drd3^{-/-}$ and $Htr1a^{-/-}$ BV2 microglial cell lines using CRISPR-Cas9 technology
2. Assess cell viability of BV2 microglia following gene deletion
3. Determine the effects of buspirone and/or $Drd3^{-/-}$ after LPS challenge

Hypothesis 1: Buspirone is anti-inflammatory via its dopamine D3 receptor antagonism

Aim 2: Establish and characterise a rotenone mouse model of Parkinson's disease

1. Provide a comprehensive analysis of the neurochemical alterations triggered by systemic rotenone administration in the central nervous system of C57BL/6 mice

Hypothesis 2: Rotenone intoxication, like Parkinson's disease, causes a series of neurochemical changes throughout the central nervous system

Aim 3: Demonstrate that buspirone treatment induces neuroprotective and anti-inflammatory effects in an animal model of Parkinson's disease

1. Demonstrate that buspirone treatment improves locomotor and exploratory behaviour in the rotenone mouse model of Parkinson's disease
2. Assess the ability of buspirone to protect dopaminergic neurons from degeneration
3. Evaluate the effect of buspirone on neuroinflammation

Hypothesis 3: Buspirone will protect against rotenone-induced behavioural deficits and promote neuroprotection by reducing neuroinflammation in the central nervous system in mice

Throughout our studies we report the altered distribution of the neuropeptides PACAP and VIP. Along with previous studies identifying the upregulation of these

peptides in D3R$^{-/-}$ mice and their implication in several pathophysiological mechanisms of PD, we conducted an *in vitro* study to determine the effectiveness of PACAP and VIP in mitigating rotenone-induced BV2 microglial polarization.

Aim 4: Characterise the phenotype of PACAP and VIP treated microglial cells following exposure to rotenone

1. Assess cell viability of BV2 microglia following rotenone and PACAP and VIP co-treatment
2. Determine the ability of PACAP and VIP to prevent rotenone-induced microglial polarization

Hypothesis 4: PACAP and VIP will mitigate rotenone triggered microglial polarization

Chapter 2:

Assessing the Anti-Inflammatory

Activity of the Anxiolytic Drug

Buspirone using CRISPR-Cas9

Gene Editing in LPS-Stimulated

BV2 Microglial Cells

Chapter 2: Assessing the anti-inflammatory activity of the anxiolytic drug buspirone using CRISPR-Cas9 gene editing in LPS-stimulated BV-2 microglial cells

<u>This chapter is published as:</u>

Thomas Broome, S[*]., Fisher, T[*]., Faiz, A., Keay, K. A., Musumeci, G., Al-Badri, G., & Castorina, A. (2021). Assessing the Anti-Inflammatory Activity of the Anxiolytic Drug Buspirone Using CRISPR-Cas9 Gene Editing in LPS-Stimulated BV-2 Microglial Cells. *Cells*, 10(6), 1312. https://doi.org/10.3390/cells10061312

[*] Joint first author

<u>Contribution:</u>

- Methodology
- Data analysis
- Data curation
- Drafted manuscript

<u>Signature of co-authors:</u>

Name	Signature
Sarah Thomas Broome	Production Note: Signature removed prior to publication.
Teagan Fisher	Production Note: Signature removed prior to publication.
Alen Faiz	Production Note: Signature removed prior to publication.

Kevin A. Keay	Production Note: Signature removed prior to publication.
Giuseppe Musumeci	Production Note: Signature removed prior to publication.
Ghaith Al-Badri	Production Note: Signature removed prior to publication.
Alessandro Castorina	Production Note: Signature removed prior to publication.

The work in this manuscript addresses **Aim 1**.

Aim 1: Determine if buspirone's anti-inflammatory activities are through dopamine-3-receptor blockade

Conclusion: Buspirone and/or genetic deletion of the D3R attenuates LPS-triggered inflammation in BV-2 microglia. Additionally, we revealed a functional role of the 5HT1a receptor in regulation microglial viability and nitric oxide release.

Assessing the anti-inflammatory activity of the anxiolytic drug buspirone using CRISPR-Cas9 gene editing in LPS-stimulated BV-2 microglial cells

Sarah Thomas Broome [1, #], Teagan Fisher [1, #], Alen Faiz [2], Kevin A. Keay [3,]

Giuseppe Musumeci [4], Ghaith Al-Badri [1] and Alessandro Castorina [1, 3, *]

[1] Laboratory of Cellular and Molecular Neuroscience (LCMN), School of Life Sciences, Faculty of Science, University of Technology Sydney, 2007, NSW, Australia

[2] Respiratory Bioinformatics and Molecular Biology (RBMB) Group, School of Life Sciences, Faculty of Science, University of Technology Sydney, 2007, NSW, Australia

[3] Laboratory of Neural Structure and Function (LNSF), School of Medical Sciences (Anatomy and Histology), Faculty of Medicine and Health, University of Sydney, Sydney, NSW, 2006, Australia

[4] Section of Human Anatomy and Histology, Department of Biomedical and Biotechnological Sciences, University of Catania, via S. Sofia, 87, 95123 Catania, Italy

[#] These authors equally contributed to the work.

Abstract

Buspirone is an anxiolytic drug with robust serotonin receptor 1A (Htr1a) agonist activities. However, evidence has demonstrated that this drug also targets the dopamine D3 receptor (Drd3), where it acts as a potent antagonist. In vivo, Drd3 blockade is neuroprotective and reduces inflammation in models of Parkinson's disease. To test if buspirone also elicited anti-inflammatory activities in vitro, we generated stable Drd3$^{-/-}$ and Htr1a$^{-/-}$ BV2 microglial cell lines using CRISPR-Cas9 technology and then tested the effects of buspirone after lipopolysaccharide (LPS) challenge. We found that LPS exposure had no effect on cell viability, except in Htr1a$^{-/-}$ cells, where viability was reduced ($p < 0.001$). Drug treatment reduced viability in Drd3$^{-/-}$ cells, but not in WT or Htr1a$^{-/-}$ cells. Buspirone counteracted LPS-induced NO release, NOS2, IL-1β and TNF-A gene expression in WT cells, whereas it exerted limited effects in Drd3$^{-/-}$ or Htr1a$^{-/-}$ microglia. In summary, our findings indicate that buspirone attenuates microglial polarization after LPS challenge. These results also highlight some major effects of Drd3 or Htr1a genetic ablation on microglial biology, raising important questions on the complex role of neurotransmitters in regulating microglia functions.

Keywords: microglia; dopamine D3 receptor; 5-hydroxytryptamine 1a receptor; neuroinflammation; Parkinson's disease

1. Introduction

Buspirone (Buspar®) is a FDA-approved selective 5-hydroxytryptamine receptor (5- HT1Ar) partial agonist used in the treatment of generalised anxiety disorder [213]. It is well known that 5-hydroxytryptamine, or serotonin (5-HT) regulates both mood and sleep, and drugs that stimulate 5-HT activity are commonly used therapeutically for anxiety and depression [248, 249]. However, it has also been shown that Buspirone has a strong "off-target" function as a dopamine-3-receptor (Drd3) antagonist [192,225,229].

Drd3's are found mainly in the *striatum*, particularly within the *nucleus accumbens* where they are involved in the regulation of motor function, impulse control, memory performance, addiction and drug tolerance [111, 114, 192]. However, a novel role for dopamine receptors (DRs) in neuroinflammation has been revealed [250]. McKenna and colleagues, showed that functional DRs are expressed on the surface of multiple immune cell types including microglia [120]. Dopamine (DA) can exert its effects through interactions with any of the five DRs expressed on the membrane of target cells [115]. This is seen clearly in the ability of the Drd3 to promote inflammation [221]. For example, Elgueta et al. showed that Drd3-signalling promotes the development of PD by favoring neuroinflammation and the pathogenic CD4+ T cell response associated with Parkinson's disease (PD) [251]. Furthermore, studies using experimental compounds have shown that blocking the Drd3, significantly reduced inflammation and consequently slowed the progression of PD [159, 250]. PD is a progressive neurodegenerative disorder characterised by a loss of dopaminergic neurons in the *substantia nigra pars compacta* resulting in diminished DA availability in the *striatum* [4]. PD is also associated with chronic neuroinflammation [20]. As such, the abnormal DA

signalling observed in PD could contribute not only to the altered DA neurotransmission, but also to an altered immune response. This is particularly important as evidence from studies of LPS-mediated neurotoxicity [1] has shown that inflammatory responses from non-neuronal cells alone are sufficient to cause loss of DAergic neurons. Injection of LPS into the rodent brain results in increased levels of inflammatory mediators, including cyclooxygenase-2 (COX-2) and inducible nitric oxide synthetase (iNOS), prior to the loss of DA-ergic neurons [68]. This suggests that inflammation may precede neurodegeneration, which ultimately results in PD. Accordingly, blocking Drd3-mediated signalling presents a promising targeted therapeutic strategy for PD.

Neuroinflammation describes the local inflammatory response within the brain and is driven predominantly by microglia, the specialised scavengers of the brain [252, 253]. Normally, microglia exist in a resting state and contribute to immune surveillance [84]. In response to injury or pathological *stimuli*, microglia become activated and release cytotoxic and pro-inflammatory molecules [254], which have been shown to promote the degeneration of DA neurons [255]. This has been shown in several studies in which the chronic activation of microglia exacerbates neurodegeneration, as the excessive and sustained secretion of neurotoxic molecules such as nitric oxide (NO) and pro-inflammatory cytokines become detrimental to neighboring neuronal cells [255]. DA receptors expressed by microglia appear to modulate inflammatory responses and neuronal survival [256]. For example, it has been shown that microglial activation is prevented in Drd3-deficient mice, in the MPTP-(1- methyl-4-phenyl-1,2,3,6-tetrahydropyridine)-model of PD [159]. Furthermore, the anti-PD drug rasagiline, a brain-selective MAO inhibitor, significantly reduced both reactive oxygen species (ROS) and NO

secretion, as well as cytokine release in DA stimulated microglia [257]. Collectively, these results suggest that DA can hamper the ability of microglia to secrete cytokines and shift towards activated phenotypes.

Since microglia are the key drivers of neuroinflammation, it is crucial to determine how Drd3-mediated activity regulates these cells. For example, in PD it is well accepted that neuroinflammation drives progressive neurodegeneration. In fact, neuronal damage and uncontrolled inflammation amplify each other to induce a feed-forward vicious cycle driving the chronic progression of PD and other neurodegenerative diseases [178]. These observations underpin the substantial experimental efforts in exploring the potential utility of traditional anti-inflammatory drugs able to slow, reverse and prevent PD [250]. However, due to the peripheral effects of the long-term use of anti-inflammatory drugs, novel targets are needed specifically to counteract CNS inflammation. Studies using experimental compounds that block the Drd3 pharmacologically could help in determining whether targeting these receptors may provide a viable disease-modifying strategy to reduce chronic inflammation in PD, and perhaps for other neuroinflammatory disorders [250].

Buspirone could be one such drug. Therefore, in this study, we sought to investigate whether buspirone prevents inflammation in microglial cells exposed to the inflammatory mimetic LPS. To the best of our knowledge, no other studies have tested these effects in microglia. In the established BV-2 microglial cell line, we implemented CRISPR-Cas9 technology to generate two independent cell lines harboring a targeted Drd3 or Htr1a gene deletion, Buspirone's best known pharmacological targets. We used a combination of molecular and cellular

biological techniques to investigate: (i) the viability of these cells following gene deletion, and (ii) the functional consequences of gene deletions in response to the inflammatory mimetic, lipopolysaccharide (LPS).

2. Materials and Methods

2.1 Generation of knockout cell lines using CRISPR-Cas9 gene editing

The CRISPR-Cas9 plasmid Px458 was used to generate knockout cell lines, as previously described [28]. Guide RNA (gRNA) sequences (summarised in **Table 1**) were generated using the online design tool Benchling and synthesised by Sigma-Aldrich (Castle Hill, NSW, Australia). Plasmids were cloned in DH5-α *Escherichia coli* and, after a single colony selection from ampicillin positive (100 µg/mL) plates, extracted using the GeneJET Plasmid Miniprep Kit (ThermoFisher Scientific, North Ryde, NSW, Australia). Transfection was carried out in a 12-well plate with a seeding density of 1×10^5 cells per well.

Cells were transfected in 3 µL of Lipofectamine 3000 (Invitrogen) diluted in 62.5 µL of Opti-MEM (ThermoFisher Scientific). This was combined with a DNA mixture containing 2 µg of purified plasmid, 4 µL of P3000 reagent (Invitrogen, Carlsbad, CA, USA) and 125 µL of Opti-MEM (Thermofisher Scientific). Cells were incubated in the mixture for 4 h at 37 °C with 5% CO_2. After incubation, half of the mixture was removed and replaced with Opti-MEM and incubated for 24 h at 37 °C with 5% CO_2.

Table 1. Guide RNA (gRNA) primers used to target the mouse *Drd3* and *Htr1a* genes with the CRISPR-Cas9 plasmid.

Gene (Ref. Seq.)	(PAM) Forward Sequence 5'-3' (PAM) Reverse Sequence 3'-5'	Location	Tm (°C)
Mouse *Drd3* (NC_0.000082.6)	(AAAC) CATGCCTACTACGCCCTGTC (CACC) GACAGGGCGTAGTAGGCATG	472 491	69.7 73.9
Mouse *Htr1a* (NC_0.000079.6)	(CACC) GGTGCTCGGCAATGCCTGCG (AAAC) CGCAGGCATTGCCGAGCACC	501 520	84.2 80.0

Transfected cells were then single-cell sorted into a 96-well plate using the MoFlo© Astrios Cell Sorter, gating for green fluorescent protein (GFP) positive cells. Single-cell-derived colonies (isogenic populations) were expanded for biochemical and molecular analysis. To identify the status of genome editing, genomic DNA was extracted from the isogenic populations using ISOLATE II Genomic DNA Kit (Bioline, NSW, Australia), and end-point PCR amplification was conducted with MyTaq DNA Polymerase Kit (Bioline), using primer sets described in **Table** 2. The amplification took place in the T100 Thermal Cycler (Bio-Rad, Gladesville, NSW, Australia) under the following instrument settings: (1) 95 °C for 60 s, (2) 95 °C for 15 s, (3) 56 °C for 15 s, (4) 72 °C for 10 s, (5) repeat step 2–4 for 35 cycles.

Table 2. PCR primers used to amplify the mouse *Drd3* and *Htr1a* genes.

Gene (Ref. Seq.)	(PAM) Forward Sequence 5'-3' (PAM) Reverse Sequence 3'-5'	Location	Tm (°C)	Length (BP)
Mouse *Drd3* (NC_0.000082.6)	TTGTTGTCTGTGTTCGCCCA AGGGTCCCATCATTCATGCC	23 883	67.8 68.2	861
Mouse *Htr1a* (NC_0.000079.6)	AGTGAAATGGACAGCGCGA AATGAGCCAAGTGAGCGAGA	27 840	67 65.1	814

Following end-point PCR, we confirmed that the primers amplified the correct product by Agarose Gel Electrophoresis (AGE) (Supplementary Figure S3). Following confirmation by AGE, PCR products were purified using SureClean Plus (Bioline) and sent to Australian Genome Research Facility (AGRF) for Sanger sequencing using the primers described in **Table 3**. Sanger sequencing results

were analysed using online tools Benchling and Tracking of Indels by

Decomposition (TIDE).

Table 3. Primers used for the sequencing of the mouse *Drd3* and *Htr1a* genes.

Gene (Ref. Seq.)	(PAM) Forward Sequence 5'-3' (PAM) Reverse Sequence 3'-5'	Location	Tm (°C)	Length (BP)
Mouse *Drd3* (NC_0.000082.6)	CCAGTTCTTACAGCACTGCCT CCGGAGCAGCATGTACCATAA	209 688	63.3 66.9	480
Mouse *Htr1a* (NC_0.000079.6)	CCCTTCGAAACTCCCCAGAAA GAGCCGATGAGATAGTTGGCA	239 581	68.2 66.4	343

2.2 Cell culture

Mouse microglial BV-2 cells were used in this study. These cells share a high

transcriptome homology and response to inflammatory challenges with primary

microglia [29]. Cells were grown in full growth media containing Dulbecco's

modified eagle's medium nutrient mixture F-12 HAM (1:1 *vol*/*vol* DMEM/F12)

(Sigma-Aldrich, Castle Hill, NSW, Australia), 10% heat-inactivated fetal bovine

serum (FBS, Sigma-Aldrich, Castle Hill, NSW, Australia) and 1%

penicillin/streptomycin solution (Sigma-Aldrich, Castle Hill, NSW, Australia) and

were kept in an incubator with humidified air containing 5% CO_2 at a

temperature of 37 ^{o} C. Cells were treated with 1 µg/mL LPS (L4391, *Escherichia*

coli 0111: B4, Sigma-Aldrich) and/or 300 µM buspirone (Sigma-Aldrich) for 24 h

at 37 °C in a humidified atmosphere with 5% CO_2. LPS concentrations and

buspirone concentrations used in this study were based on preliminary

observations (data not shown).

2.3 Cell viability

To assess cell viability, we used the Cell Proliferation Kit I (MTT) (Sigma-Aldrich).

Cells were seeded at 2 x 10^4 cells per well in a 96-well plate and incubated at 37 °C with 5% CO_2 until cells reached 80% confluence. Cells were treated for 24 h with control media, 1 µg/mL LPS or both LPS and 300 µM buspirone. After 24 h, 10 µL of MTT labelling reagent was added to each well. After 4 h, 100 µL of the solubilization solution (10% SDS in 0.01 M HCl) was added to each well and incubated at 37 °C overnight. Absorbance was measured at 565 nm in the TECAN infinite M1000-PRO ELISA reader (ThermoFisher Scientific).

2.4 Nitric oxide (Griess reagent assay)

Cells were seeded at 2 x 10^4 cells per well in a 96-well plate and incubated at 37 °C with 5% CO_2 until cells reached 80% confluence. Cells were treated for 24 h with control media, 1 µg/mL LPS or both LPS and 300 µM buspirone. The supernatant was collected and placed into a new 96-well plate. A total of 100 µL of freshly prepared Griess reagent was then added to each well and incubated at room temperature for 15 min on a slow oscillation protected from light. Absorbance was measured at 540 nm using the TECAN infinite M1000-PRO ELISA reader. Optical density values from each group were recorded and reported as a percentage of control.

2.5 RNA extraction and cDNA synthesis

Total RNA was extracted using 1 mL TRI reagent (Sigma-Aldrich, Castle Hill, NSW, Australia) and 0.2 mL chloroform and precipitated with 0.5 mL 2-propanol (Sigma-Aldrich). Pellets were washed twice with 75% ethanol and air-dried. RNA concentrations were calculated using NanoDrop™ 2000 (ThermoFisher Scientific). A total of 1 µg of total RNA were loaded in each cDNA synthesis

reaction. cDNA synthesis was conducted using the T1000 thermal cycler (Bio-Rad, Gladesville, NSW, Australia) in a final volume of 20 µL. Each reaction contained 1 µg of RNA diluted in a volume of 11 µL, to which we added 9 µL of cDNA synthesis mix (Tetro cDNA synthesis kit) (Bioline, Australia). Samples were incubated at 45 °C for 40 min followed by 85 °C for 5 min. Finally, cDNA samples were stored at -20 °C until use.

2.6 Real-time quantitative polymerase chain reaction

Real-time qPCR analyses were carried out as previously reported [30,31], with minor modifications. For each gene of interest, qPCRs were performed in a final volume of 10 µL, which comprised 3 µL cDNA, 0.4 µL milliQ water, 5 µL of iTaq Universal SYBR green master mix (BioRad, Gladesville, NSW, Australia) and 0.8 µL of the corresponding forward and reverse primers (5 µM, Sigma-Aldrich, Castle Hill, NSW, Australia) to obtain a final primer concentration of 400 nM. The primers are described in **Table 4**. Reaction mixtures were loaded in Hard-Shell® 96-Well PCR Plates, and four genes of interest were tested in each run using the CFX96 Touch™ Real-Time PCR Detection System (Bio-Rad, Gladesville, NSW, Australia). Instrument settings were as follows: (1) 95 °C for 2 min, (2) 60 °C for 10 s, (3) 72 °C for 10 s, (4) plate read, (5) repeat step 2 to 4 for 45 cycles. For the melting curve analyses, settings were (1) 65 °C for 35 s, (2) plate read, (3) repeat step 1–2 for 60 times). To examine changes in expression, we analysed the mean fold change values of each sample, calculated using the ΔΔCt method, as previously described by Schmittgen and Livak [258]. PCR product specificity was evaluated by melting curve analysis, with each gene showing a single peak (data not shown).

Table 4. List of primers sets used in real-time quantitative PCR analyses.

Gene	Accession #	Primer Sequence	Length (bp)
S18	NM_011296.2	Fwd 5' CCCTGAGAAGTTCCAGCACA 3' Rev 5' GGTGAGGTCGATGTCTGCTT 3'	145
D3r	NM_007877	Fwd 5' GGGGTGACTGTCCTGGTCTA 3' Rev 5' AAGCCAGGTCTGATGCTGAT 3'	100
IL-1β	NM_008361.4	Fwd 5' GCTACCTGTGTCTTTCCCGT 3' Rev 5' CATCTCGGAGCCTGTAGTGC 3'	164
TNF-α	NM_013693.3	Fwd 5' ATGGCCTCCCTCTCATCAGT 3' Rev 5' TTTGCTACGACGTGGGCTAC 3'	97
FIZZ1	NM_020509.3	Fwd 5' AGCTGATGGTCCCAGTGAAT 3' Rev 5' AGTGGAGGGATAGTTAGCTGG 3'	98
Arg1	NM_007482.3	Fwd 5' ACAAGACAGGGCTCCTTTCAG 3' Rev 5' TTAAAGCCACTGCCGTGTTC 3'	105

2.7 Protein extraction and Western blot

Proteins were extracted using radioimmunoprecipitation assay (RIPA) buffer (Sigma- Aldrich, Castle Hill, NSW, Australia) containing 1x Protease Inhibitor cocktail (cOmplete™, Mini, EDTA-free Protease Inhibitor Cocktail, Sigma-Aldrich, Castle Hill, NSW, Australia). Protein was quantified using the Bicinchoninic-Acid (BCA) Assay Protein Assay Kit (ThermoFisher Scientific) according to manufacturer's protocol and measured using the TECAN infinite M1000-PRO ELISA reader at 562 nm.

Samples were prepared by adding 3.75 µL of Laemmli Buffer (Bio-Rad, Gladesville, NSW, Australia) containing f3-mercaptoethanol (Sigma-Aldrich, Castle Hill, NSW, Australia) mixture, (ratio 1:9 *vol*/*vol*) to 30 µg protein in a final volume of 15 µL. Samples were then heated for 10 min at 70 °C to denature proteins. Proteins were then separated by SDS-polyacrylamide gel electrophoresis (SDS-PAGE) using 4–20% mini gels (Bio-Rad, Criterion 15-well Mini-Protean SFX), alongside 5 µL of the molecular weight ladder/marker (Bio-Rad Pre-stained HyperLadder Precision Plus Protein™). Gels were transferred to a PVDF membrane using the

Trans-Blot Turbo instrument (Bio-Rad) [33]. Once terminated, membranes were immediately placed in a container filled with TBS + 0.1% Tween 20 (Sigma-Aldrich, Castle Hill, NSW, Australia) (TBST 1x) to wash out any residues during transfer. To block non-specific binding sites, membranes were blocked for 1 h in 5% dry non-fat skim milk in TBST with slow agitation (50–60 rpm).

Membranes were incubated with appropriately diluted primary antibodies in blocking buffer overnight at 4 °C with slow agitation. The following primary antibodies were used: GAPDH (VPA00187, Rb, 1:2000, BioRad, Gladesville, NSW, Australia); 5HT1ar (ab85615, Rb, 1:400, Abcam, Cambridge MA, USA). This was followed by incubation with host-specific secondary antibodies. Membranes were then placed in a container with 1 TBST and washed rapidly three times, followed by three further 5 min washes. Finally, membranes were incubated in secondary antibody (HRP-conjugated goat anti-rabbit IgG) for 1 h at room temperature, diluted in blocking buffer. The membranes were then washed once again as previously described to remove excess secondary antibody [34]. Imaging was then performed on the Bio-Rad ChemiDoc MP Imaging System (Bio-Rad). To detect bands, we utilized Clarity Western ECL Blotting Substrate (Bio-Rad). Densitometric analyses of bands was computed using NIH ImageJ (https://imagej.nih.gov/ij/download/ (accessed on 14 January 2021)). Optical densities of target proteins were normalised to those of loading controls (GAPDH).

2.8 Statistical analysis

All data are reported as mean ± S.E.M. Statistical analyses were calculated using GraphPad Prism software ver. 8.4.1 (GraphPad Software, San Diego, California, CA, USA, www.graphpad.com, accessed on 14 January 2021). Comparisons

between two groups were evaluated using the unpaired two-tailed Student's *t*-test. Differences between three or more groups were analysed using one-way ANOVA and Tukey post-hoc test. To compute statistical comparisons that involved multiple independent variables, two-way ANOVA was used followed by Tukey post-hoc test. p values ≤ 0.05 were considered statistically significant.

3. Results

3.1 Generation of stable Drd3^{-/-} and Htr1a^{-/-} cell lines

We generated stable Drd3^{-/-} *and* Htr1a^{-/-} cell lines in BV-2 microglial cells to study the pharmacological effects of buspirone following LPS challenge. BV-2 cells were transfected with one of two separate Px458 plasmids, one targeting the *Drd3* gene and the other targeting the *Htr1a* gene (please refer to **Supplementary Figure S1** for details). Sanger sequencing analysis of genomic DNA (for sequencing primers details, please refer to **Table 3**) revealed insertions/deletions (indels) in transfected cells (**Figure 1A–F**). Sanger sequencing of the alleles of *Drd3^{-/-}* BV2 cells showed the presence of deletions of either 7 base pairs (BPs) or 10 BPs (**Figure 1G**), and the alleles of *Htr1a^{-/-}* cells demonstrated an insertion of 1 BP or a deletion of 2 BPs (**Figure 1G**). Amino acid translation from the sequencing data indicated that all CRISPR-Cas9-induced mutations resulted in early stop codons (**Supplementary Figure S4**). Western blot (**Figure 1H,I**) and real-time qPCR analyses (**Figure 1J**) in Drd3^{-/-} cells further confirmed the knockout of the Drd3 protein and gene (*** $p < 0.0001$). Similarly, the absence of the 5-HT1Ar protein and gene expression in *Htr1a^{-/-}* cells was confirmed by Western blot (**Figure 1K,L**) and qPCR (Figure 1M, **** $p < 0.0001$).
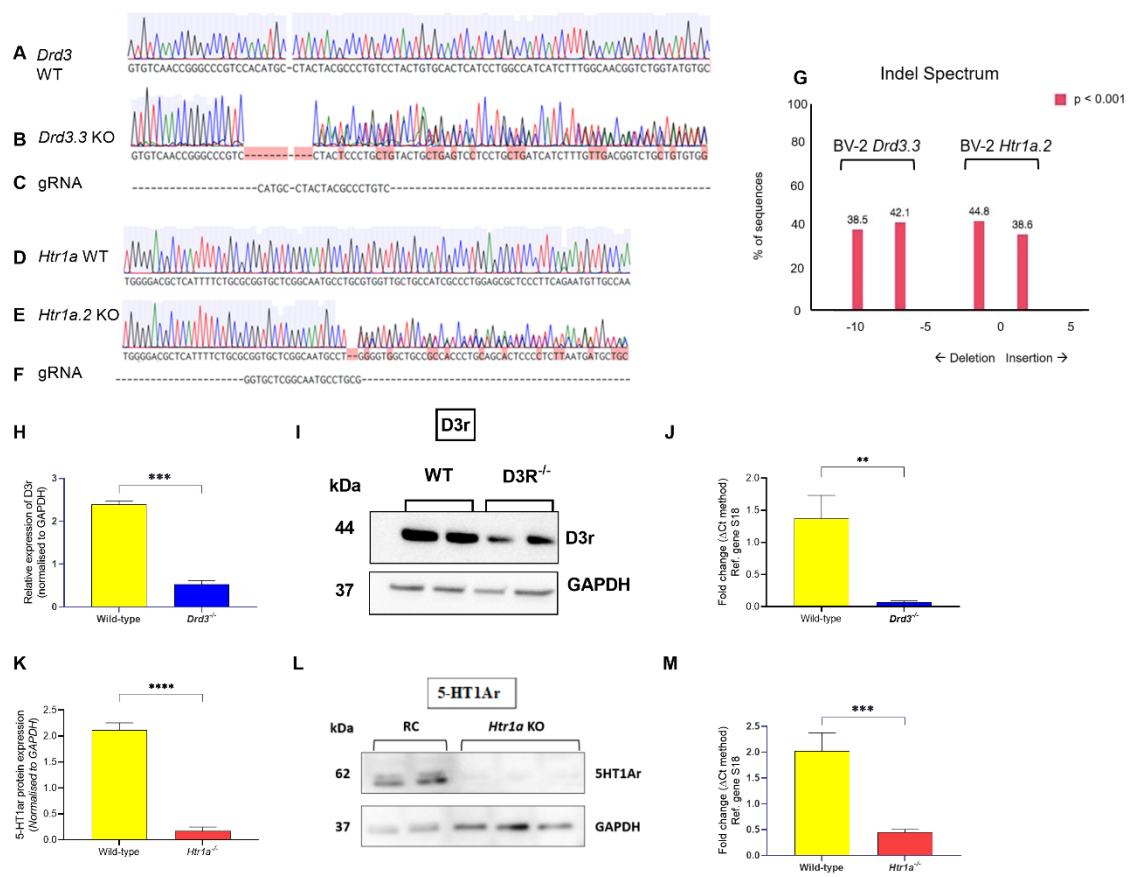
Figure 1. Confirmation of *Drd3* and *Htr1a* gene deletions in BV-2 cells.

End-point PCR products of the *Drd3* and *Htr1a* genes in the WT, Drd3$^{-/-}$ clones and Htr1a$^{-/-}$ clones were Sanger sequenced. Chromatograms of the sequences were analysed using Benchling. Green peaks indicate an Adenine base, red peaks indicate a Thymine base, blue peaks indicate a Cytosine base, and black peaks correspond to a Guanine base. Multiple peaks for one BP reveal that there are multiple sequences coming from different alleles, indicating mutation. BP mutations on the majority of sequences are shown with red boxes. (**A**) Chromatogram of the Sanger sequenced BV-2 WT *Drd3* gene. (**B**) Chromatogram of the Sanger sequenced *Drd3* gene on the Drd3$^{-/-}$ clone. (**C**) Murine *Drd3* gRNA sequence that was inserted into the Px458 plasmid is aligned with the chromatograms as a reference point for the CRISPR-Cas9 cut site. (**D**) Chromatogram of the Sanger sequenced BV-2 WT *Htr1a* gene. (**E**) Chromatogram of the Sanger sequenced

88

Htr1a gene on the Htr1a$^{-/-}$ clone. (**F**) Murine *Htr1a* gRNA sequence that was inserted into the Px458 plasmid is aligned with the chromatograms as a reference point for the CRISPR-Cas9 cut site. (**G**) Indel spectrum produced by Tracking of Indels by Decomposition: TIDE analysis shows that in the Drd3$^{-/-}$ clone, 38.5% of sequences had a deletion of 10 BPs and 42.1% of sequences had a deletion of 7 BPs. In the Htr1a$^{-/-}$ clone, there were 38.6% of sequences with an insertion of 1 BP and 44.8% of sequences with a deletion of 2 BPs. (**H**) Real-time qPCR data demonstrating differential expression of transcripts for the D3r in WT and Drd3$^{-/-}$ cells. Amplifications were performed using selected primer optimised for qPCR analyses (<155 BP length), which recognises fragments within the coding sequence of the gene of interest (for details refer to Table 2). Fold changes of each gene were obtained after normalisation to the endogenous reference gene and calculated using the comparative ΔΔCt method. (**I**) Immunoblot for 5-HT1Ar protein. (**J**) Column graph depicting protein expression levels following normalisation to the loading control GAPDH. Quantification was performed using the ImageJ software, and normalised values were calculated by dividing the mean optical density of bands over the corresponding GAPDH. Data reported as mean ± SEM, n=3-8. **$p<0.01$, ****$p0.0001$ vs WT determined by unpaired t test. Drd3: murine dopamine D3 receptor gene, 5-HT1Ar: 5-hydroxytryptamine 1A receptor, Drd3.3: murine dopamine D3 receptor gene knockout clone number 3, Htr1a.2: murine 5-hydroxytryptamine 1A receptor gene knockout clone number 2, RC: reagent control, gRNA: guide RNA, Ref: reference, S18: 40S ribosomal protein S18, GAPDH: Glyceraldehyde 3-phosphate dehydrogenase, kDa: Kilodalton, KO: knockout.

3.2 Establishing the optimal buspirone concentration and assessing the effects of Drd3 and Htr1a gene deletions and buspirone treatment on cell viability following exposure to LPS

To investigate the effects of targeted Drd3 and Htr1a gene deletions in BV2 microglial cell lines before and after LPS challenge, we first established the optimal concentration to rescue LPS-induced cell polarisation in the absence of overt toxicity. To do so, MTT and Griess reagent assays were conducted in wild-type BV-2 microglia stimulated with LPS (1 µg/mL) and increasing concentrations of buspirone (0, 100, 200, 300 and 400 µM) at 24 h. Thereafter, MTT assays were performed under the same experimental conditions in both wild-type, $Drd3^{-/-}$ and $Htr1a^{-/-}$ cells exposed to LPS or LPS + buspirone (300 µM), which was found to be the most effective concentration, devoid of toxic activity at the tested time-point.

As shown in **Figure 2A**, LPS treatment induced obvious changes in microglial morphology (i.e., flattening and swelling of the soma). Co-treatment with increasing concentrations of buspirone had no significant effect on cell viability up to 400 µM, although cell viability dropped significantly (24.73% decrease, **** $p < 0.0001$ vs. LPS and/or untreated controls, **Figure 2B**). In terms of NO release (a pro-inflammatory mediator), LPS-induced NO release was partially rescued with 200µM buspirone (*** $p < 0.001$ vs. LPS); however complete recovery was seen at concentrations >= 300 µM buspirone (**** $p < 0.0001$ vs. LPS, **Figure 2C**). When comparing the effects of LPS and buspirone across the different genotypes, we observed some genotype-specific changes in cell viability in response to the inflammatory mimetic and the drug. Specifically, LPS significantly diminished cell

viability in $Htr1a^{-/-}$ cells (** p = 0.007), but not in wild-type or $Drd3^{-/-}$ cultures

(non-significant, $p >$ 0.05) (**Figure 2D**). At the concentration tested, buspirone

was not toxic to wild-type microglial cells (p = 0.4198) and did not further reduce

viability in the $Htr1a^{-/-}$ genotype (p = 0.6758), whereas it showed significant

toxicity in LPS-treated $Drd3^{-/-}$ cells (**Figure 2D**).

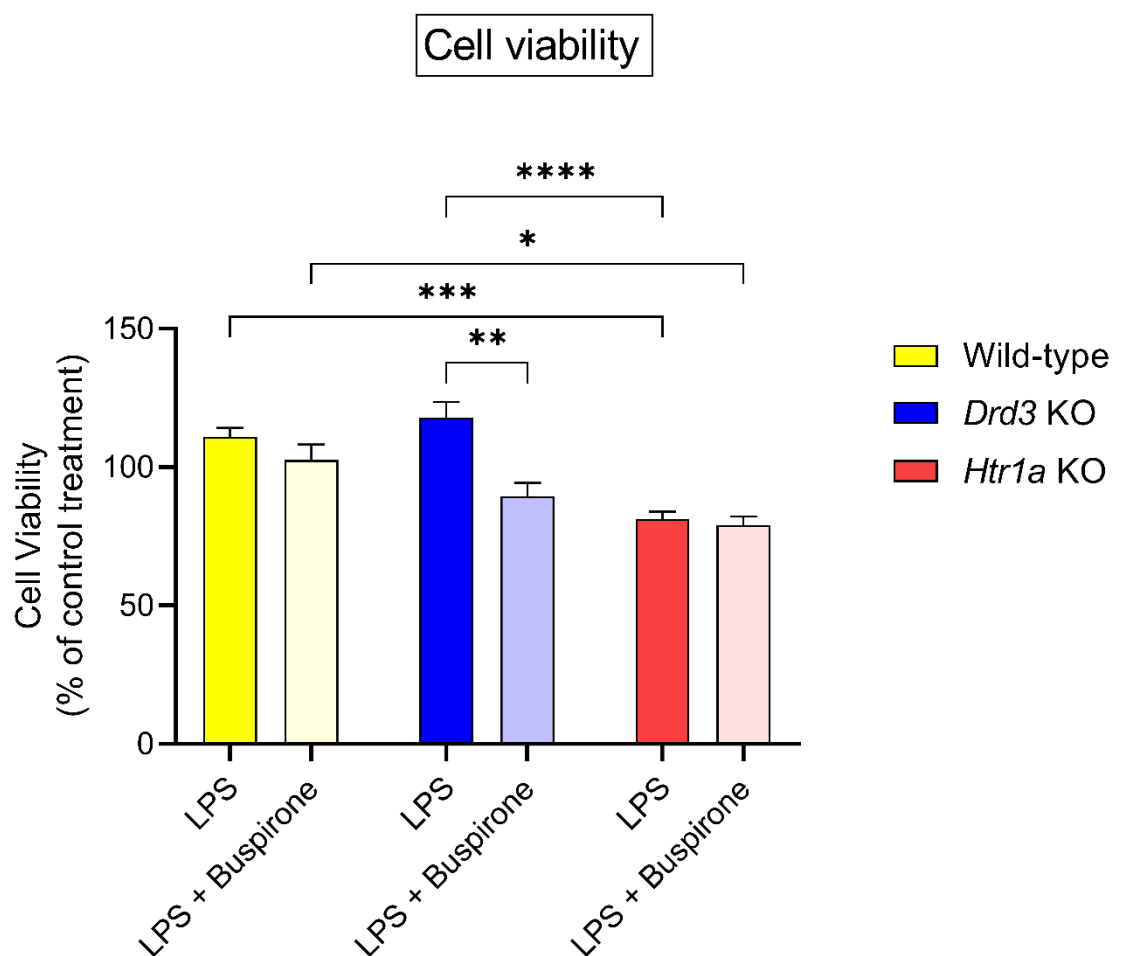**Figure 2. Cell viability of BV-2 wild type, _Drd3_ ᐟ⁻ and _Htr1a_ᐟ⁻ cells when**
treated with LPS and LPS + Buspirone. Cells were treated with either LPS

(1µg/mL) or LPS and Buspirone (300µM) for 24 hours. 10µL of MTT labelling

reagent was added to each well for 4 hours. Then 100µL of the solubilisation

solution was added overnight. Absorbance was measured at 565nm with agitation.

Data given as mean ± SEM. Statistically significant data (*p<0.05, **p<0.01, ***p<0.001, ****p<0.0001) were determined by two-way ANOVA followed by Tukey post-hoc test. n=4. WT: wild type, Drd3: murine dopamine D3 receptor gene, Htr1a: murine 5-hydroxytryptamine-1a receptor gene, KO: knockout, LPS: lipopolysaccharide.

3.3 Nitric oxide release in wild type, Drd3$^{-/-}$ and Htr1a$^{-/-}$ knockout microglial cells following LPS challenge and buspirone treatment

To determine whether genetic deletion of the Drd3 or the Htr1a genes and/or buspirone treatment altered the responsiveness of BV2 microglia to an LPS challenge, we quantified the levels of nitric oxide (NO) released in supernatants and measured relative levels using the Griess reagent assay. In WT cells, LPS significantly increased NO release (+30%, **** $p < 0.0001$, **Figure 3A**). When comparing the effects of LPS stimulation between wild-type vs. Drd3$^{-/-}$ cells, NO release was significantly reduced (**** $p < 0.0001$), reaching levels comparable to those seen in untreated wild-type controls (**Figure 3B**). Interestingly, LPS triggered an exaggerated NO release (about 5-fold that of WT cells) in the supernatant of Htr1a$^{-/-}$ cells (**** $p < 0.0001$) (**Figure 3C**).

To determine the specific involvement of the Drd3 or the Htr1a in buspirone's ability to mitigate LPS-driven NO release, we measured NO release after co-treatment with LPS and buspirone across the different genotypes. As shown in **Figure 3D**, buspirone reliably diminished the heightened NO levels in LPS-stimulated wild-type microglia (**** $p < 0.0001$). However, in Drd3$^{-/-}$ cells,

where LPS failed to induce additional NO release, buspirone was devoid of any biological activity (**Figure 3E**). Finally, Htr1a$^{-/-}$ microglial cells also responded reliably to buspirone treatment (**** $p < 0.0001$), although NO levels were still around 2.5-fold that of wild-type controls (**Figure 3F**).

Nitric oxide release
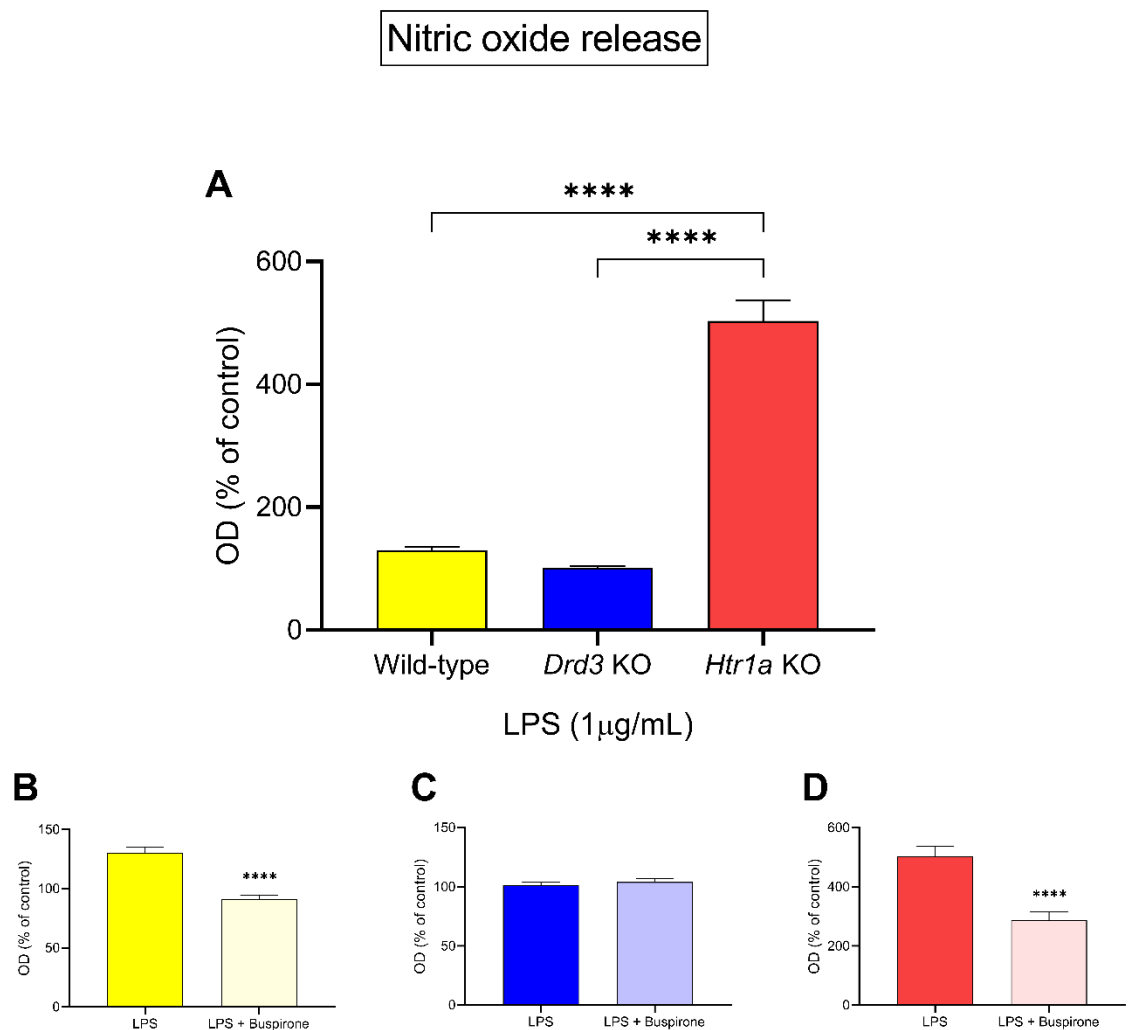
Figure 3. Nitrate levels in BV-2 wild type, *Drd3* $^{-/-}$ and *Htr1a*$^{-/-}$ cells when treated with LPS or co-treated with LPS and Buspirone. Cells were treated for 24 hours with 100μL of either control media or 1μg/mL LPS or 1μg/mL LPS and 300μM Buspirone. The supernatant was then collected and placed in a new 96-well plate and incubated with 100μL of Griess reagent for 15 minutes at room temperature, then read at 540nm. (**A**) Bar graph showing nitrate levels in BV-2 WT,

Drd3⁻ᐟ⁻ and *Htr1a⁻ᐟ⁻* cells after treatment with LPS. (**B**) Bar graph showing nitrate levels in BV-2 WT cells after treatment with either LPS-only or LPS and Buspirone. (**C**) Bar graph showing nitrate levels in BV-2 *Drd3⁻ᐟ⁻* cells after treatment with either LPS-only or LPS and Buspirone. (**D**) Bar graph showing nitrate levels in BV-2 *Htr1a⁻ᐟ⁻* cells after treatment with either LPS-only or LPS and Buspirone. Values were calculated as percentage of untreated controls. Data reported as mean ± SEM. Statistically significant data (****p<0.0001) were determined by one-way ANOVA followed by Tukey post-hoc test, n=8-19. WT: wild type, Drd3: murine dopamine D3 receptor gene, Htr1a: murine 5-hydroxytryptamine-1a receptor gene, KO: knockout, OD: optical density, LPS: lipopolysaccharide.

3.4 Effects of buspirone treatment on Inducible Nitric Oxide Synthetase (NOS2) gene expression in wild type, Drd3⁻ᐟ⁻ and Htr1a⁻ᐟ⁻ knockout microglial cells after exposure to LPS

In view of the efficacy of buspirone treatment in mitigating the NO induction triggered by LPS in BV-2 cells, we sought to determine if such beneficial effects were also associated with transcriptional changes in the mRNA expression of nitric oxide synthase 2 (*NOS2*), the gene encoding for inducible nitric oxide synthase (iNOS), an enzyme that catalyses the production of NO.

Comparative analyses of *NOS2* transcripts across the different genotypes revealed some genotype-dependent changes in gene expression in response to LPS. Specifically, LPS-induced *NOS2* mRNAs were less pronounced in *Drd3⁻ᐟ⁻* microglia compared with wild-type (~4.3-fold in *Drd3⁻ᐟ⁻* vs. ~65-fold in wild-type

cells, **Figure 4A**) although these changes were not statistically significant ($p >$ 0.05, two-way ANOVA followed by Dunnett's post-hoc test). In LPS-stimulated $Htr1a^{-/-}$ cells there was a remarkable increase in *NOS2* transcripts (**** $p <$ 0.0001 vs. wild-type, **Figure 4A).**

When assessing the effects of buspirone within each genotype, buspirone failed to reduce LPS-driven increases in *NOS2* transcripts in wild-type cells ($p >$ 0.05, **Figure 4B**). In $Drd3^{-/-}$ microglia, LPS effects on *NOS2* mRNA levels were blunted when compared to wild-type cells, but still significantly increased (* $p <$ 0.05 vs. no treatment, **Figure 4C**). Treatment with buspirone reduced gene expression, resulting in levels that did not significantly differ from those of untreated cells ($p = 0.3137$ vs. no treatment in $Drd3^{-/-}$ cells, **Figure 4C**). By contrast, *NOS2* mRNA expression in LPS-exposed $Htr1a^{-/-}$ microglial showed robust increases (~782-folds vs. no treatment in $Htr1a^{-/-}$ microglia, ** $p < 0.01$) which further increased after buspirone treatment, although not at statistically significant levels ($p = 0.07$ vs. LPS, **Figure 4D**).
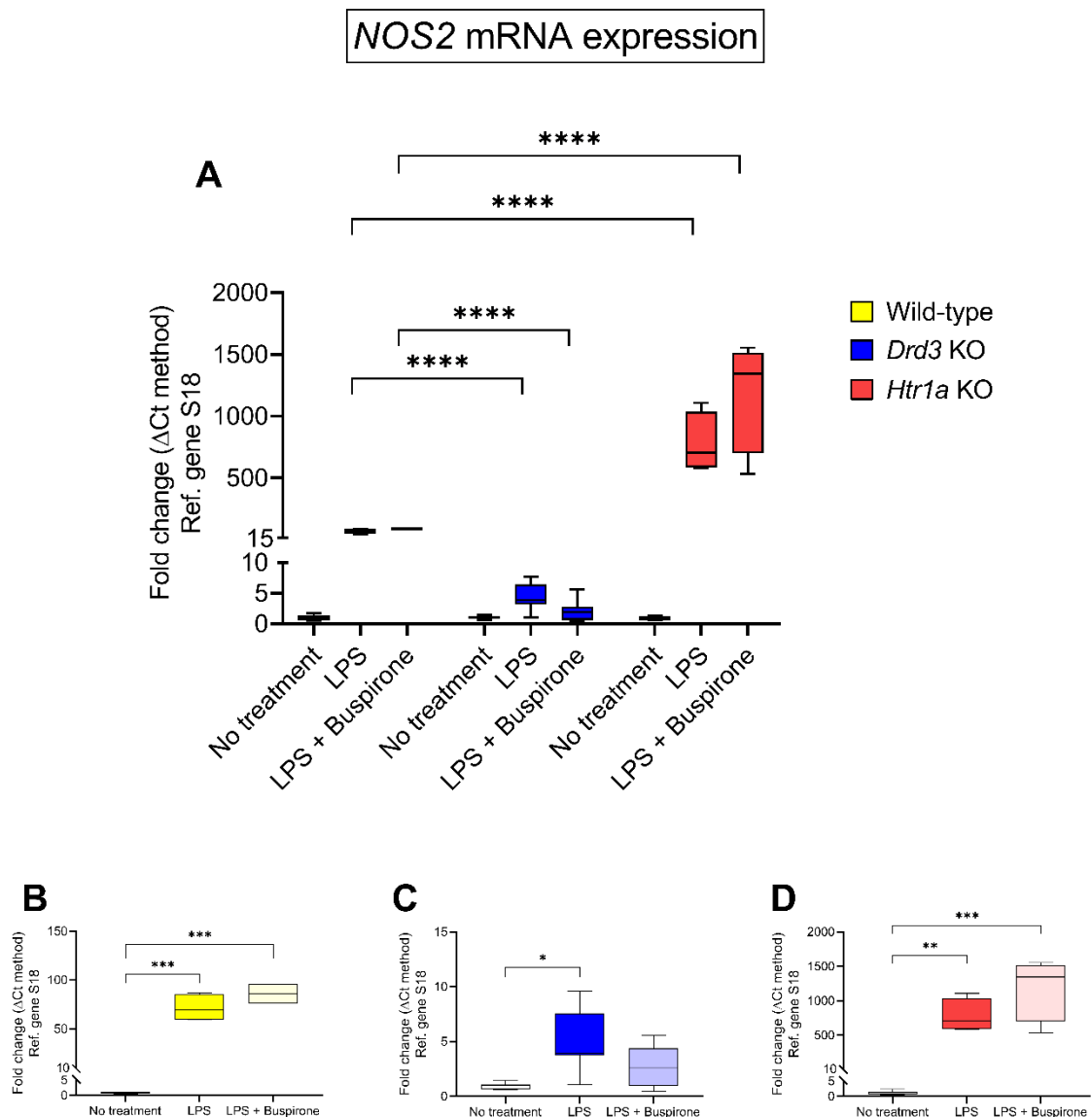
Figure 4. Gene expression profile of NOS2 following treatment with LPS and LPS and Buspirone. mRNA expression was measured using qPCR and was quantified using the ΔΔCt and normalised using the S18 gene. (**A**) Real-time qPCR data showing the differential expression of transcripts for the NOS2 gene in wild type, *Drd3*^{-/-} and *Htr1a*^{-/-} cells pertaining to indicated treatment groups. (**B**) Box and whisker plot showing mRNA expression level of NOS2 in wild type cells. (**C**) Box and whisker plot showing mRNA expression level of NOS2 in *Drd3*^{-/-} cells. (**D**) Box and whisker plot showing mRNA expression level of NOS2 in *Htr1a*^{-/-} cells. Amplifications were performed using selected primers optimised for qPCR analyses

(<155 bp length) which recognise fragments within the coding sequence of the gene of interest (for details refer to Table 4). Results are presented as mean fold changes with respect to no treatment ± SEM. Fold changes of each gene were obtained after normalisation to the endogenous reference gene and calculated using the comparative ΔΔCt method. Baseline levels of no treatment groups were set to 1. Statistically significant data (*$p<0.05$, **$p<0.01$, ***$p<0.001$, ****$p<0.0001$) were determined by one-way ANOVA followed by Tukey post-hoc test. n=4-8. WT: wild type, NOS: nitric oxide synthase, LPS: lipopolysaccharide, Ref: reference, S18: 40S ribosomal protein S18, Drd3: murine dopamine D3 receptor gene, Htr1a: murine 5-hydroxytryptamine-1a receptor gene, KO: knockout.

3.5 Effects of buspirone treatment on Interleukin-1β (IL-1β) gene expression in wild type, Drd3$^{-/-}$ and Htr1a$^{-/-}$ knockout microglial cells after exposure to LPS

We used real-time qPCR to determine whether the mRNA expression of the pro-inflammatory marker interleukin-1β (*IL-1β*) differed across genotypes in BV-2 cells stimulated with LPS (**Figure 5A**) or within each genotype after combination treatment with LPS and buspirone (**Figure 5B–D**).

IL-1β mRNA expression was notably higher than controls in wild-type cultures following LPS exposure (~1880-folds of untreated wild-type, **** $p < 0.0001$ vs. LPS wild-type, **Figure 5A**). Treatment with buspirone sharply reduced *IL-1β* mRNA expression (~380-fold of untreated wild-type, #### $p < 0.0001$ vs. LPS, **Figure 5B**), to levels that did not differ statistically to untreated wild-type controls

(p = 0.2434, **Figure 5B**). In *Drd3*$^{-/-}$ cells, drug treatment strongly reduced LPS-driven *IL-1β* gene expression. (#### p < 0.0001 vs. LPS, **Figure 5C**).

Finally, the upregulated *IL-1β* mRNAs in LPS-stimulated *Htr1a*$^{-/-}$ microglial cells were partially reversed by buspirone treatment, although they were still elevated when compared with no treatment controls (* p < 0.05, **Figure 5D**).
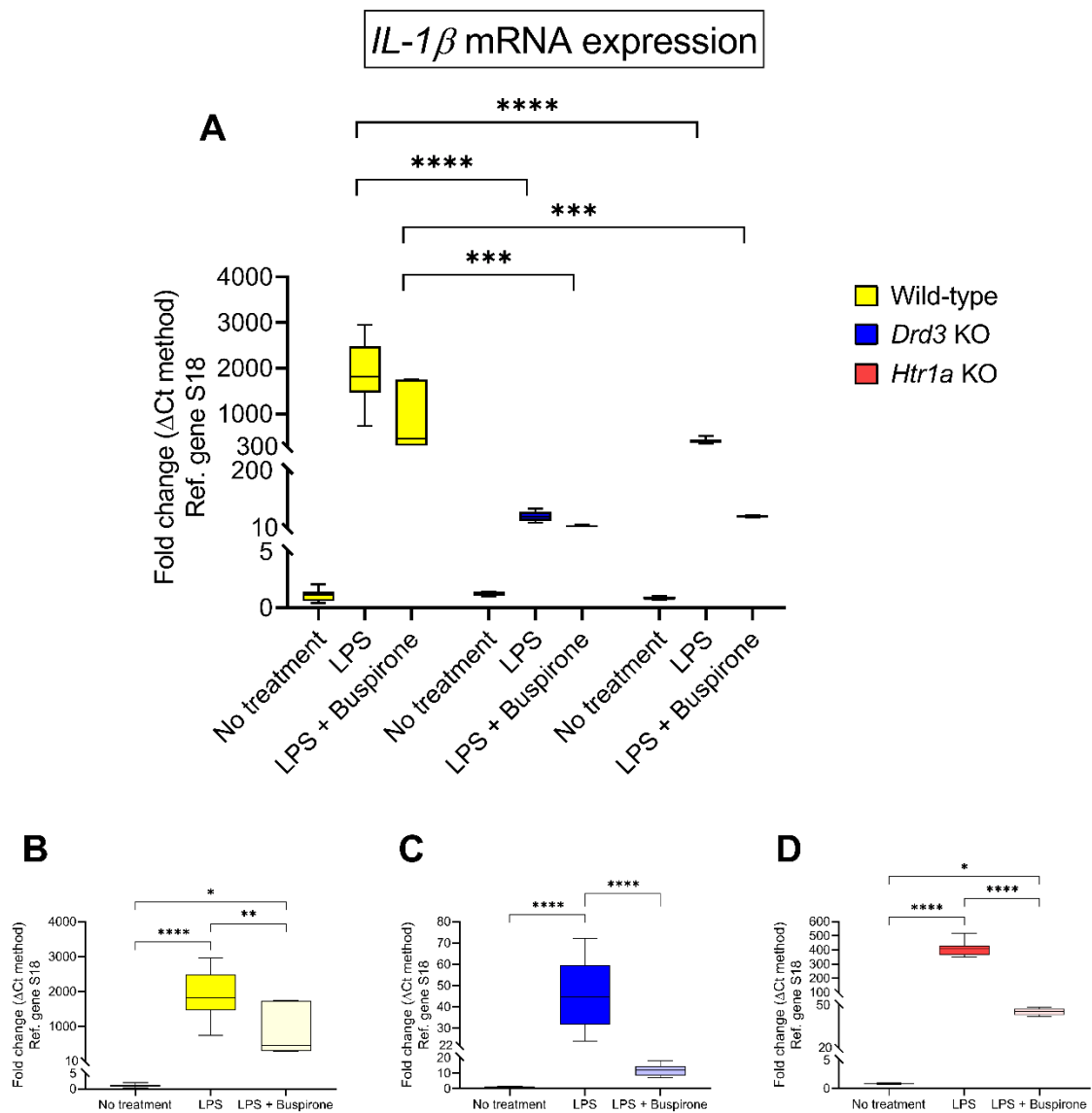

Figure 5. Gene expression profile of IL-1β following treatment with LPS and LPS and Buspirone. mRNA expression was measured using qPCR and was

quantified using the ΔΔCt and normalised using the S18 gene. (**A**) Real-time qPCR data showing the differential expression of transcripts for the IL-1β gene in wild type, *Drd3*-/- and *Htr1a*-/- cells pertaining to indicated treatment groups. (**B**) Box and whisker plot showing mRNA expression level of IL-1β in wild type cells. (**C**) Box and whisker plot showing mRNA expression level of IL-1β in *Drd3*-/- cells. (**D**) Box and whisker plot showing mRNA expression level of IL-1β in *Htr1a*-/- cells. Amplifications were performed using selected primers optimised for qPCR analyses (<155 bp length) which recognise fragments within the coding sequence of the gene of interest (for details refer to Table 4). Results are presented as mean fold changes with respect to no treatment ± SEM. Fold changes of each gene were obtained after normalisation to the endogenous reference gene and calculated using the comparative ΔΔCt method. Baseline levels of no treatment groups were set to 1. Statistically significant data (*$p<0.05$, **$p<0.01$, ***$p<0.001$, ****$p<0.0001$) were determined by one-way ANOVA followed by Tukey post-hoc test. $n=4$-8. WT: wild type, IL-1β: interleukin-1-beta, LPS: lipopolysaccharide, Ref: reference, S18: 40S ribosomal protein S18, Drd3: murine dopamine D3 receptor gene, Htr1a: murine 5-hydroxytryptamine-1a receptor gene, KO: knockout.

3.6 Effects of buspirone treatment on Tumor Necrosis Factor-α (TNF-α) gene expression in wild type, Drd3-/- and Htr1a-/- knockout microglial cells after exposure to LPS

Among LPS treated BV-2 cells, we observed a remarkable increase in *TNF-α* mRNA expression (~377-fold increase vs. no treatment), the magnitude of which was not seen in either *Drd3*-/- or *Htr1a*-/- cells (~42-fold and ~65.82-fold,

respectively), in which *TNF-α* gene expression was significantly reduced vs. wild-type (**** *p* < 0.0001 for both, **Figure 6A**).

In wild-type BV-2 cells, buspirone potently diminished *TNF-α* transcripts (~2.87-folds of no treatment, #### *p* < 0.0001 vs. LPS, **Figure 6B**). By contrast, the drug only modestly reduced *TNF-α* gene expression in the *Drd3*^{-/-} and *Htr1a*^{-/-} cell lineages (# *p* < 0.05 vs. LPS for both genotypes, **Figure 6C,D**).
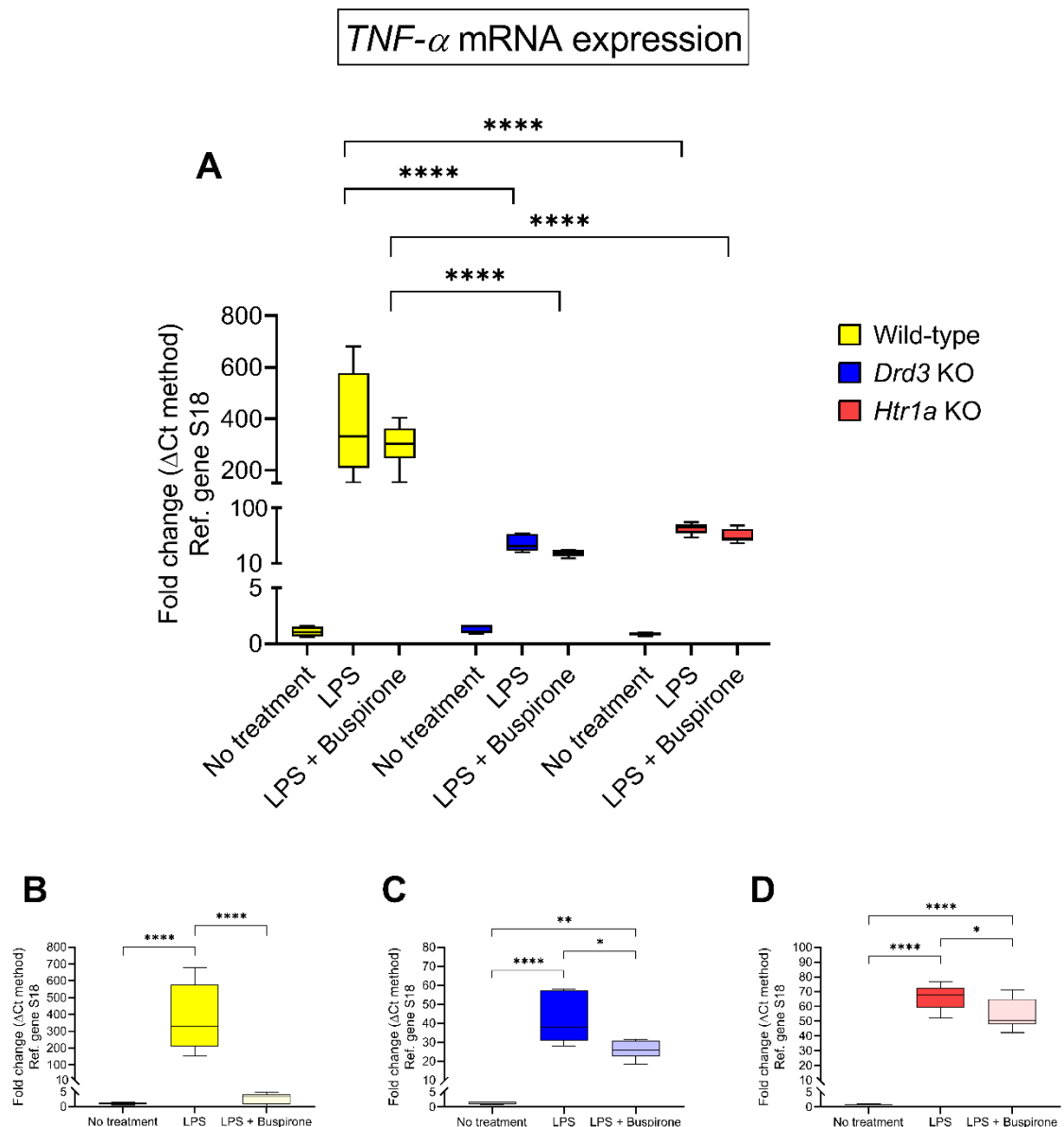
Figure 6. Gene expression profile of TNF-α following treatment with LPS and LPS and Buspirone. mRNA expression was measured using qPCR and was quantified using the ΔΔCt and normalised using the S18 gene. (**A**) Real-time qPCR data showing the differential expression of transcripts for the TNF-α gene in wild type, *Drd3*^{-/-} and *Htr1a*^{-/-} cells pertaining to indicated treatment groups. (**B**) Box and whisker plot showing mRNA expression level of TNF-α in wild type cells. (**C**) Box and whisker plot showing mRNA expression level of TNF-α in *Drd3*^{-/-} cells. (**D**) Box and whisker plot showing mRNA expression level of TNF-α in *Htr1a*^{-/-} cells. Amplifications were performed using selected primers optimised for qPCR analyses (<155 bp length) which recognise fragments within the coding sequence of the gene of interest (for details refer to Table 4). Results are presented as mean fold changes with respect to no treatment ± SEM. Fold changes of each gene were obtained after normalisation to the endogenous reference gene and calculated using the comparative ΔΔCt method. Baseline levels of no treatment groups were set to 1. Statistically significant data (*$p<0.05$, **$p<0.01$, ***$p<0.001$, ****$p<0.0001$) were determined by one-way ANOVA followed by Tukey post-hoc test. n=4-8. WT: wild type, TNF-α: tumour necrosis factor alpha, LPS: lipopolysaccharide, Ref: reference, S18: 40S ribosomal protein S18, Drd3: murine dopamine D3 receptor gene, Htr1a: murine 5-hydroxytryptamine-1a receptor gene, KO: knockout.

3.7 Effects of buspirone treatment on Arginase 1 (Arg1) gene expression in wild type, Drd3^{-/-} **and Htr1a**^{-/-} **knockout microglial cells after exposure to LPS**

Comparative analyses of *Arg1* mRNA expression (an anti-inflammatory marker) across the different genotypes revealed significant differences of gene expression

following LPS exposure (**Figure 7A**). Specifically, whereas in wild-type BV-2 cells, LPS failed to induce any significant changes in *Arg1* gene expression ($p = 0.2963$), there was a significant downregulation in *Drd3*$^{-/-}$ cells (**** $p < 0.0001$ vs. LPS-treated wild-type cells, **Figure 7A**) and, also to a lesser extent, in Htr1a$^{-/-}$ cells (**** $p < 0.0001$, **Figure 7B**). In *Drd3*$^{-/-}$ cells, buspirone did not affect *Arg1* mRNA expression ($p = 0.5993$ vs. LPS- treated cells, **Figure 7C**), whereas in *Htr1a*$^{-/-}$ cells, buspirone treatment rescued the gene downregulation caused by LPS treatment (# $p < 0.05$ vs. LPS, **Figure 7D**).
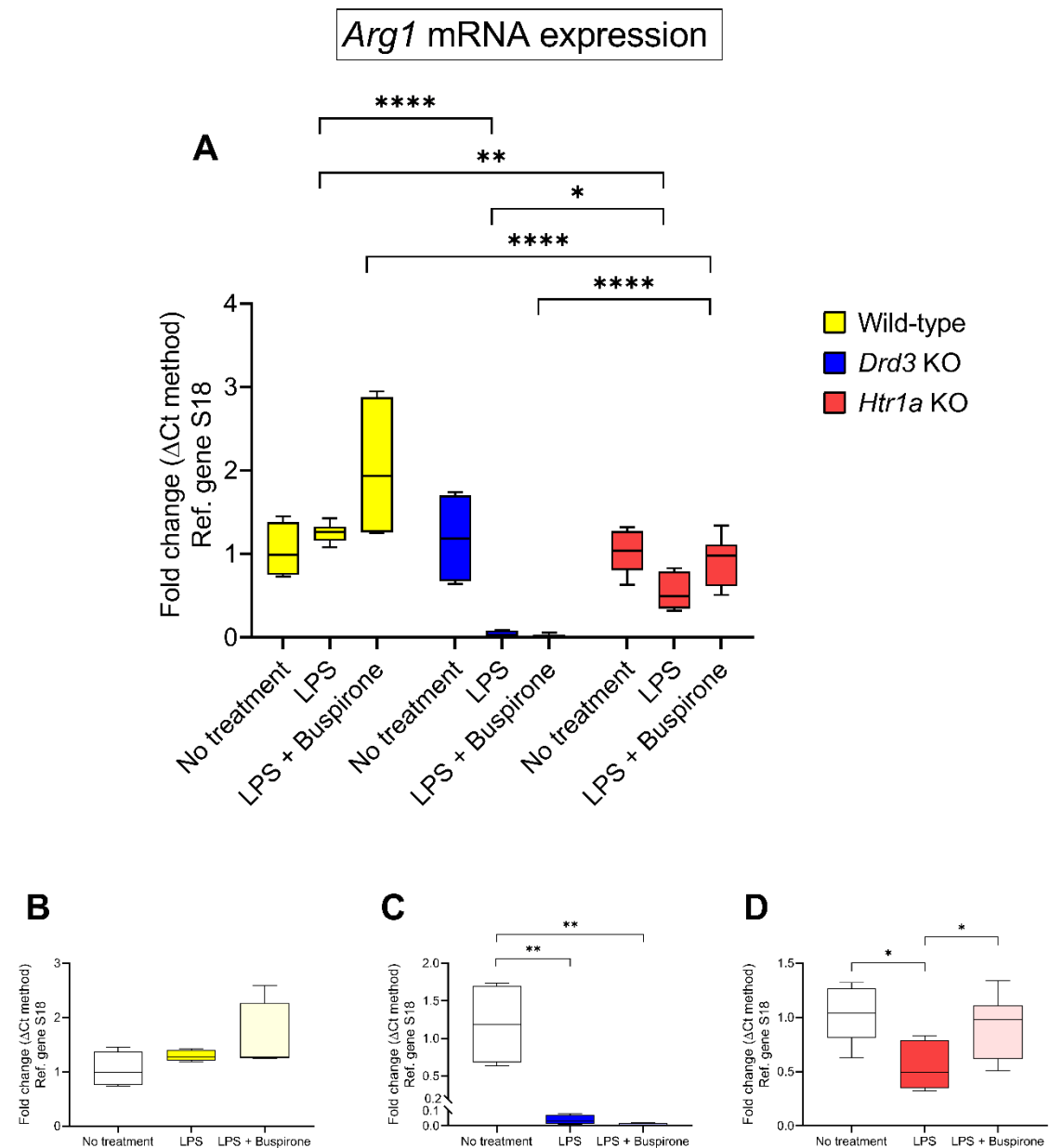
Figure 7. Gene expression profile of Arg1 following treatment with LPS and LPS and Buspirone. mRNA expression was measured using qPCR and was quantified using the ΔΔCt and normalised using the S18 gene. (**A**) Real-time qPCR data showing the differential expression of transcripts for the Arg1 gene in wild type, *Drd3*^{-/-} and *Htr1a*^{-/-} cells pertaining to indicated treatment groups. (**B**) Box and whisker plot showing mRNA expression level of Arg1 in wild type cells. (**C**) Box and whisker plot showing mRNA expression level of Arg1 in *Drd3*^{-/-} cells. (**D**) Box and whisker plot showing mRNA expression level of Arg1 in *Htr1a*^{-/-} cells. Amplifications

were performed using selected primers optimised for qPCR analyses (<155 bp

length) which recognise fragments within the coding sequence of the gene of

interest (for details refer to Table 4). Results are presented as mean fold changes

with respect to no treatment ± SEM. Fold changes of each gene were obtained

after normalisation to the endogenous reference gene and calculated using the

comparative ΔΔCt method. Baseline levels of no treatment groups were set to 1.

Statistically significant data (*p<0.05, **p<0.01, ***p<0.001, ****p<0.0001) were

determined by one-way ANOVA followed by Tukey post-hoc test. n=4-8. WT: wild

type, Arg1: arginase-1, LPS: lipopolysaccharide, Ref: reference, S18: 40S

ribosomal protein S18, Drd3: murine dopamine D3 receptor gene, Htr1a: murine 5-

hydroxytryptamine-1a receptor gene, KO: knockout.

3.8 Effects of buspirone treatment on Found in Inflammatory Zone 1 (FIZZ1) gene expression in wild type, Drd3$^{-/-}$ and Htr1a$^{-/-}$ knockout microglial cells after exposure to LPS

To provide a balanced panel of both pro- and anti-inflammatory markers in our

assessment of the activities of buspirone, we interrogated an additional microglial

anti- inflammatory marker (i.e., found in inflammatory zone 1 gene, [*FIZZ1*]) across

the different genotypes following exposure to LPS, and then within each

genotype, to assess the effect of combined treatment with LPS and buspirone.

When comparing LPS-stimulated wild-type vs. *Drd3*$^{-/-}$ cultures, there were   no

significant differences in *FIZZ1* gene expression (p = 0.7956 vs. LPS-treated wild-

type cells, **Figure 8A**). However, we found a statistically significant increase in

gene expression in *Htr1a*$^{-/-}$ cells (** p < 0.01, **Figure 8A**). Interestingly, buspirone

significantly increased *FIZZ1* mRNA expression in LPS-stimulated, wild-type microglia (## *p* < 0.01 vs. LPS-treated wild-type cells, **Figure 8B**), but had no significant effect on LPS-treated *Drd3*$^{-/-}$ cultures (*p* = 0.9734, **Figure 8C**), whilst it triggered a moderate and significant gene upregulation in *Htr1a*$^{-/-}$ cells (* *p* < 0.05 vs. no treatment group, **Figure 8D**).
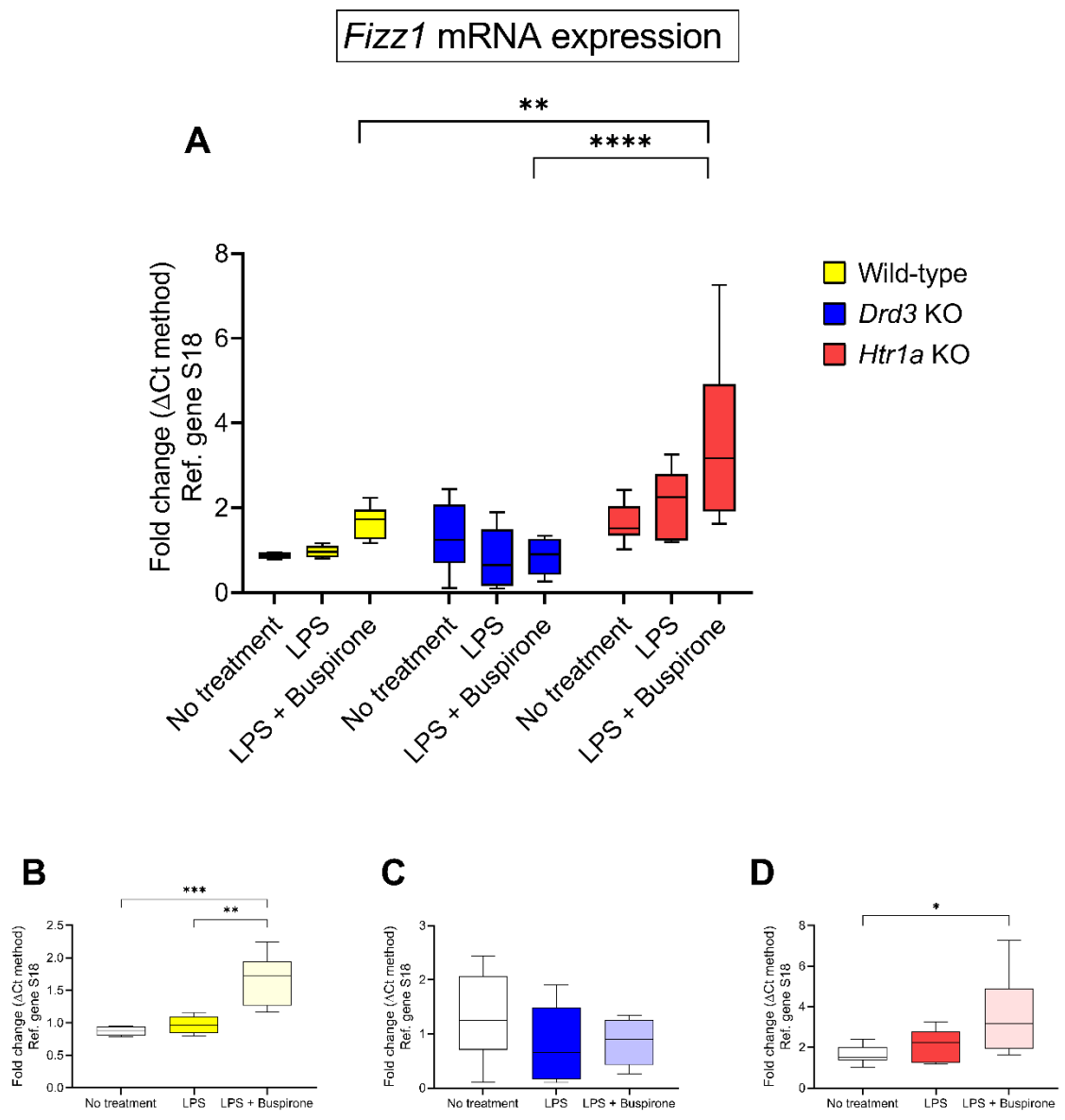

Figure 8. Gene expression profile of FIZZ1 following treatment with LPS and LPS and Buspirone. mRNA expression was measured using qPCR and was quantified using the ΔΔCt and normalised using the S18 gene. (**A**) Real-time qPCR

data showing the differential expression of transcripts for the FIZZ1 gene in wild type, *Drd3*^{-/-} and *Htr1a*^{-/-} cells pertaining to indicated treatment groups. (**B**) Box and whisker plot showing mRNA expression level of FIZZ1 in wild type cells. (**C**) Box and whisker plot showing mRNA expression level of FIZZ1 in *Drd3*^{-/-} cells. (**D**) Box and whisker plot showing mRNA expression level of FIZZ1 in *Htr1a*^{-/-} cells. Amplifications were performed using selected primers optimised for qPCR analyses (<155 bp length) which recognise fragments within the coding sequence of the gene of interest (for details refer to Table 4). Results are presented as mean fold changes with respect to no treatment ± SEM. Fold changes of each gene were obtained after normalisation to the endogenous reference gene and calculated using the comparative ΔΔCt method. Baseline levels of no treatment groups were set to 1. Statistically significant data (*$p<0.05$, **$p<0.01$, ***$p<0.001$, ****$p<0.0001$) were determined by one-way ANOVA followed by Tukey post-hoc test. n=4-8. WT: wild type, FIZZ1: found in inflammatory zone, LPS: lipopolysaccharide, Ref: reference, S18: 40S ribosomal protein S18, Drd3: murine dopamine D3 receptor gene, Htr1a: murine 5-hydroxytryptamine-1a receptor gene, KO: knockout.

4. Discussion

This is the first study, to the best of our knowledge, which describes the anti-inflammatory effects of buspirone in BV-2 microglial cells after LPS challenge and investigates the involvement of the genes for *Drd3* and *Htr1a* in mediating beneficial drug-induced effects. Buspirone has been available on the market for decades in view of its beneficial activities for the treatment of generalised anxiety disorder. Its central activity is still achieved despite low systemic bioavailability. In

fact, when administered, buspirone is extensively metabolized due to its extensive first pass metabolism, where it undergoes hepatic oxidation mediated by the CYP3A4 enzyme. Hydroxylated derivatives are produced, including a pharmacologically active metabolite 1-pyrimidinylpiperazine (1-PP), which seems to participate in the biological activity of the drug [259]. Buspirone has a relatively low solubility and there is no documented evidence of active transport mechanisms through the blood brain barrier; nonetheless, as highlighted by an [11C]-(+)-PHNO occupancy study the drug reaches Drd3-rich CNS targets, where it exerts clear Drd3 antagonist activity [230]. These results pinpoint how buspirone may display some degree of permeability in the BBB.

Using CRISPR-Cas9 technology, we selectively knocked out buspirone's best-known pharmacological targets to create a robust in vitro platform to gain novel molecular insights into the mechanism of action of buspirone and other drugs targeting these receptor types. Our findings demonstrate that buspirone treatment and the genetic deletion of *Drd3* attenuates LPS-triggered inflammation in microglia cell lines. In addition, we have identified a novel biological role of the *Htr1a* gene in controlling microglial cell viability and *NOS2*-mediated nitric oxide production after LPS insult.

4.1 Targeting Drd3 and Htr1a genes to study the effects of buspirone in microglial cells

A major reason for the generation of stable knockout BV-2 microglial cell lines using CRISPR-Cas9 gene editing technology was to develop a cellular platform that could help in unveiling the pharmacological activity of buspirone in microglial cells exposed to an inflammatory challenge with LPS. This approach was

essential to overcome any issues associated with transient reduction of gene expression using either short-interfering RNA methods, or other gene knockdown strategies, which only attenuate gene expression for a limited time, and do not always recapitulate the biological effects achieved with total gene ablation with high fidelity. We have provided supplementary data detailing the general workflow (i.e., plasmid packaging, transfection, single-cell sorting of transfected cells and confirmation of gene deletions (**Supplementary Figures S1–S4**). Analyses of the mutations induced by CRISPR-Cas9 in clonal populations revealed the presence of insertion/deletions (indels) on up to four alleles instead of two. Interestingly, this phenomenon was reported in the same cell line after CRISPR-Cas9 editing of the gene *TREM2* [260]. Although the reasons why this occurs is not known, one possibility is the aneuploidy of the target chromosome(s) (i.e., tetrasomy). This would explain why CRISPR-Cas9 gene editing was particularly challenging in BV-2 cells in comparison to what would be expected from cells harboring the traditional bi-allelic configuration, as the chances of the CRISPR-Cas9 plasmid binding to all alleles are significantly reduced with twice the number of alleles. However, despite these challenges, we succeeded in generating complete gene knockout cell lines for each of the selected gene targets, providing a reliable and potentially scalable in vitro platform at a relatively low cost. Additionally, these protocols are now optimized and can be readily adapted to create a potent pharmacological tool to gain mechanistic insights on the pharmacology of both old and new drug targets [261].

Our CRISPR-Cas9 gene knockouts were confirmed both by Western blot and real-time qPCR. Frameshift mutations within the *Drd3* and *Htr1a* coding sequences were translated as truncated and non-functional proteins, whose expression was

either strongly reduced or not detected (**Figure 1H,I,K,L**). Accordingly, *Drd3* and

Htr1a mRNA studies confirmed negligible transcript levels in the two knockout cell

lines (**Figure 1J**). It should be noted that some residual D3r protein expression

was detected in the *Drd3*$^{-/-}$ microglia (**Figure 1H,I**). This can be explained by the

fact that there are no commercially available antibodies that are specific to the

D3r, as its amino acid sequence is highly homologous with that of other D2-like

receptor subtypes, including the D2r and D4r [262], which also exhibit overlapping

molecular weights. Therefore, the residual faint bands shown in *Drd3*$^{-/-}$ cells

could be non-specific binding to any of these two receptors.

4.2 Genotype-specific and drug-related changes in BV-2 cell viability and nitric oxide release after LPS challenge

Upon exposure to LPS, wild-type BV-2 microglia displayed signs of activation.

However, buspirone dose-dependently reversed this process without significant

toxic effects at concentrations up to 300 µM, which was also accompanied by a

remarkable attenuation of nitrates in culture media (Figure 2). When comparing

the effects of LPS and buspirone across the different genotypes, we found that

exposure to LPS (1 µg/mL) slightly increased cell viability irrespective of genotype,

surpassing levels of matched untreated controls, suggesting that the inflammatory

mimetic might exert some growth-promoting effects. Similar results have

previously been reported by another in vitro study that demonstrated an increase

in the survival rate of BV-2 cells following exposure to the same concentration of

LPS used in this study after exposures of 24 and 40 h [263]. In addition, our data

are further supported by several in vivo studies that reported an increase in

microglial cell proliferation in adult mice following a single dose of LPS [264] [265].

With regards to BV-2 cell viability and nitric oxide release, our results using the

$Htr1a^{-/-}$ cell line was totally unexpected. To the best of our knowledge, there

are no reports on the effects mediated by the 5-HT1Ar on microglia. We found

that baseline cell viability in $Htr1a^{-/-}$ microglia was significantly reduced compared

with WT controls, both in LPS and cells treated with both LPS and buspirone. As

there were no changes in viability resulting from the deletion of the $Drd3$ gene,

these findings suggest that the $Htr1a$ might play a critical role in regulating the

metabolic activity of these cells. A few studies have shown that microglia express

functional serotonin receptors which are linked to distinct microglial properties and

cellular interactions [266] [267]. Our study provides unprecedented data supporting

a functional role of the 5-HT1Ar in regulating BV-2 microglia cell viability. The

degeneration of dopaminergic neurons has been linked to the robust

upregulation of inducible nitric oxide synthase (NOS2) and production of

neurotoxic levels of NO [268]. Our data show that $Htr1a$ gene ablation in BV-2 cells

exposed to LPS results in an exaggerated production of NO. These data were

confirmed by analyses of $NOS2$ mRNA expression, a gene that regulates the

production of NO through the expression of $NOS2$. This result complements an

earlier study by Zhang and collaborators, which found that the 5-HT1Ar agonist 8-

OH-DPAT downregulated the neuronal-specific nitric oxide synthase (nNOS)

expression and the 5-HT1Ar selective antagonist NAN-190 upregulated nNOS

expression [269]. Based on these results, we are tempted to believe that stimulation

of the 5-HT1Ar may hinder the activity of the NOS2/NO pathway, whilst gene

ablation may do the opposite. Importantly, buspirone itself was able to decrease

NO production in both WT and $Htr1a^{-/-}$ cells co-treated with LPS. This novel finding

suggests that the decrease in NO levels seen after buspirone treatment is most

likely due to the antagonist activity of the Drd3 and not the agonist function on 5-HT1Ar. This is further supported by the data obtained in *Drd3*[^-/-] cultures, where stimulation with LPS failed to increase NO and only marginally increased *NOS2* gene expression, in alignment with the idea that Drd3 antagonism attenuates neuroinflammation [156] [270].

4.3 Genotype-specific and drug-related changes of pro-inflammatory cytokines in LPS-stimulated BV-2 microglia

Both IL-1β and TNF-α have been implicated as main effectors of the neuroinflammatory machinery activated during neurodegeneration in models of PD [270]. Moreover, the exogenous administration of both cytokines has been shown to exacerbate 6-OHDA- induced cell death [270]. In this study, we first established whether LPS stimulation triggered the induction of IL-1β and TNF-A gene expression and then identified if there were specific differences in the expression profile of these pro-inflammatory across genotypes and in response to buspirone treatment. As expected, LPS challenge robustly increased the expression of both cytokines (in the order of about 2000-fold). In *Drd3*$^{-/-}$ and, to a lesser extent, in *Htr1a*$^{-/-}$ cells, LPS-driven IL-1β and TNF-α gene induction were much more blunted than in WT cells, providing additional evidence for a role of the *Drd3* (and perhaps the *Htr1a*) in mitigating LPS-induced inflammation. The latter consideration is in view of the effects seen after drug treatment in both genotypes, where buspirone further prevented the upregulation of both pro-inflammatory cytokines in both genotypes (*Drd3*$^{-/-}$ and *Htr1a*$^{-/-}$ BV-2 cells, respectively). This corroborates the findings in murine models, showing that either IL-1β or TNF-α induction are attenuated by xaliproden or 8-OH-DPAT, two 5-HT1Ar

agonists [271] [272]. However, the study highlights the predominant role of the

Drd3 blockage as the main route to provide an anti-inflammatory activity in BV-2

microglia, which is supported further by evidence showing that Drd3 agonists

trigger TNF-α gene upregulation [273].

4.4 Genotypic-specific and drug-related changes of anti-inflammatory cytokines in LPS stimulated BV-2 microglia

In addition to pro-inflammatory cytokines, we also analysed the expression levels

of the anti-inflammatory cytokines *Arg1* and *FIZZ1*. Our study showed that, in

untreated cells, neither of these cytokines were affected across the genotypes

(WT, *Drd3*$^{-/-}$, *Htr1a*$^{-/-}$). When cells were challenged with LPS, consistent with

previous evidence using similar experimental paradigms [274] [275] [276], *FIZZ1*

gene expression was unaffected, whereas Arg1 mRNAs were diminished in

both *Drd3*$^{-/-}$ and *Htr1a*$^{-/-}$ cells. Treatment with buspirone was unable to rescue

Arg1 gene downregulation in WT and *Drd3*$^{-/-}$ cells but was effective in restoring

gene expression in *Htr1a*$^{-/-}$ cells, suggesting a more complex interaction

between the Drd3 and 5HT1ar in regulating *Arg1* transcription. In contrast, FIZZ1

mRNA expression was strongly increased in response to buspirone treatment in

WT BV-2 cultures, but not in *Drd3*$^{-/-}$ cells and only marginally in *Htr1a*$^{-/-}$ cells.

Taken together, this evidence supports the notion that, during an LPS challenge,

the Drd3 antagonist activity of buspirone is required to convey its anti-

inflammatory response. Similar to recent reports from Pacheco and co-workers in

a PD model [158] and in a model of methamphetamine-induced intoxication [81],

our findings reveal a critical role for Drd3 in modulating the inflammatory

response. The upregulation of anti-inflammatory cytokines in microglia is

considered critical in slowing the progression of PD and other neurodegenerative conditions, as this promotes the acquisition of the M2 anti-inflammatory phenotype by microglia [277]. PG01037, a potent Drd3 antagonist, reduced microglia activity, thereby contributing to an overall anti-inflammatory and therapeutic effect in PD mouse models [256].

Despite the promising results of this study, it is important to note that microglia are not the only cells contributing to the chronic inflammatory milieu in the CNS of people afflicted by neurological disorders. Astrocytes constitute the majority of the brain's glial cell population and communicate closely with microglia to respond to neuronal damage, inflammatory and pathological stimuli. Montoya and colleagues [221] demonstrated that the Drd3s are expressed on astrocytes and that Drd3 deficiency in astrocytes attenuates microglial activation upon systemic inflammation and exacerbated the expression of the anti-inflammatory *FIZZ1* gene [221]. Furthermore, the lack of Drd3 expression in astrocytes promotes beneficial astrogliosis, which exerts anti-inflammatory and neuroprotective functions [256]. These beneficial actions of Drd3 blockade on astrocytes are particularly important in neurological diseases associated with neuroinflammation as it has been shown that, during chronic neuroinflammation, astrocytes alter the permeability of the blood brain barrier to promote the infiltration of peripheral immune cells to further promote neuroinflammation. These studies suggest that buspirone's anti-inflammatory activities may not be restricted to microglia, and that its Drd3 antagonist activity on astrocyte might elicit synergistic effects via alternative mechanisms that culminate in a robust anti-inflammatory effect that also promotes neuroprotection.

Conclusions

In conclusion, in the present manuscript, we show that either *Drd3* gene deletion or buspirone treatment reliably attenuated LPS-triggered inflammation in BV-2 microglia. Additionally, we are the first to demonstrate the functional role of the 5-HT1Ar in regulating cell viability and NO release in polarised microglia. The ability of both the *Drd3* gene deletion and buspirone treatment and, to a lesser extent, *Htr1a* gene ablation, to reduce inflammation in microglia suggests that buspirone holds the potential to be repurposed as an effective anti-inflammatory agent to treat those neurological diseases associated with chronic neuroinflammation, including Parkinson's disease. In addition, considering that there is some evidence suggesting that buspirone may also exert stimulatory activities in immune cells of the periphery, such as CD4+ T lymphocytes [278] and natural killer cells [279], in vivo work is warranted to better elucidate the full potential of this drug in the CNS.

Conflicts of Interest: The authors declare no conflict of interest.

Supplementary figures

Design of Px458 Plasmid

A

CRISPR-Cas9 Px458 plasmid 9291 BP

U6 promoter
gRNA
Ampicillin resistance
GFP
Cas9

B

Drd3 plasmid TTGTGGAAAGGACGAAACACCGAGAGGGCGTAGTAGGCATGGTTTTAGACGAGCGGATCACCAAGAC

Drd3 gRNA --------------------GACAGGGCGTAGTAGGCATG------------------------

C

Htr1a plasmid TTGTGGAAAGGACGAAACACCGGTGCTCGGCAATGCCTGCGGTTTTAGAGCTAGAAATAGCA

Htr1a gRNA --------------------GGTGCTCGGCAATGCCTGCG--------------------
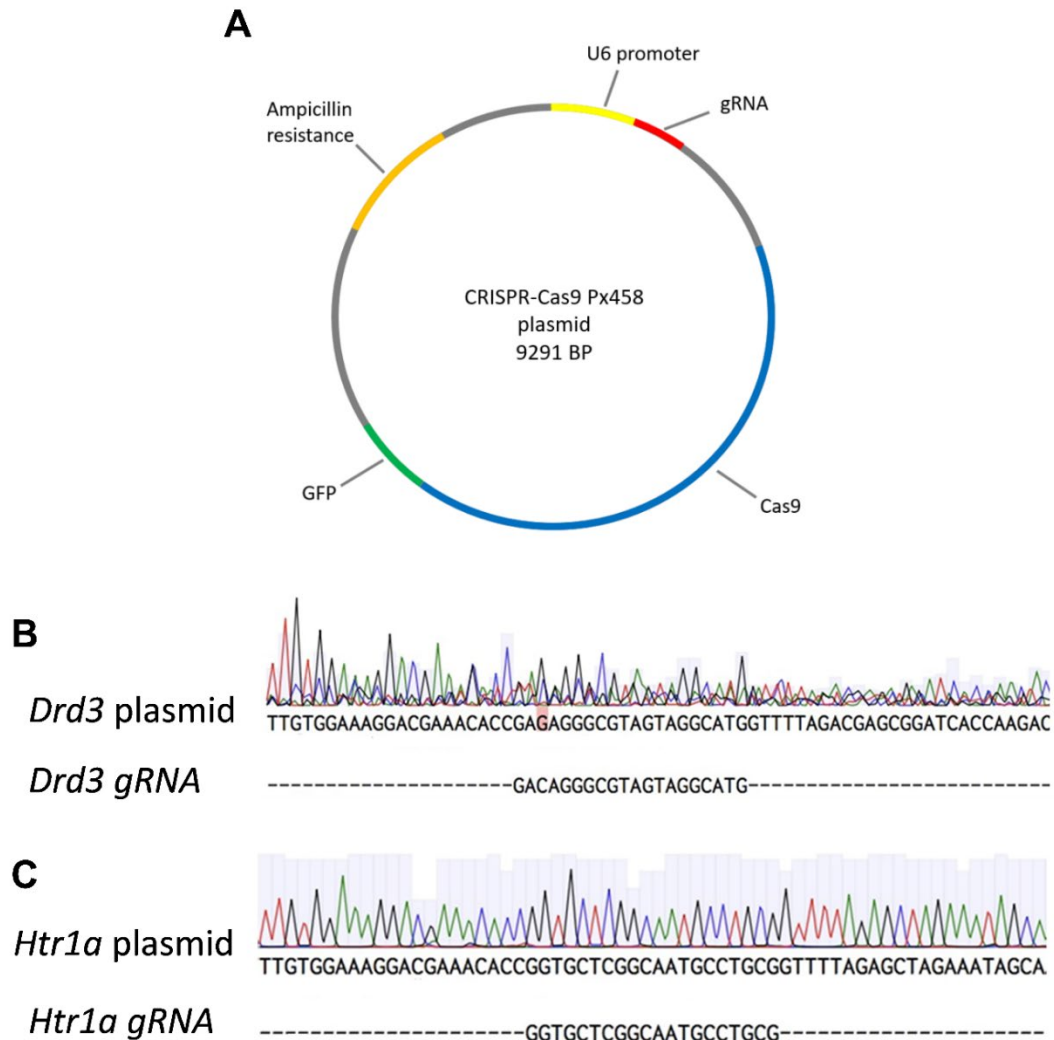
Supplementary 1. Design of the Px458 plasmid for the murine *Drd3* and *Htr1a* gene KOs and inserted their gRNA sequences. (**A**) General design of the Px458 plasmid, depicting the key features: human U6 promoter, gRNA sequences which were designed to bind specifically to the DNA of target genes, Cas9 protein, GFP, and ampicillin resistance. (**B-C**) Chromatograms created in Benchling from Sanger sequencing results and aligned gRNA sequences. Green peaks indicate an Adenine base, red peaks indicate a Thymine base, blue peaks indicate a Cytosine

base and black peaks indicate a Guanine base. (**B**) Sequencing of the *Drd3* plasmid indicates an incorrect BP of Guanine instead of Cytosine represented by the red box, however, there is still a blue peak for Cytosine, so this is likely sequencing error. (**C**) Sequencing results of the *Htr1a* plasmid shows correct alignment of the gRNA sequence. GFP: green fluorescent protein, gRNA: guide RNA, BP: base pairs, CRISPR: clustered, regularly interspaced short palindromic repeats. Drd3: murine dopamine D3 receptor gene, Htr1a: murine 5-hydroxytryptamine-1a receptor gene.

GFP positive BV-2 cells
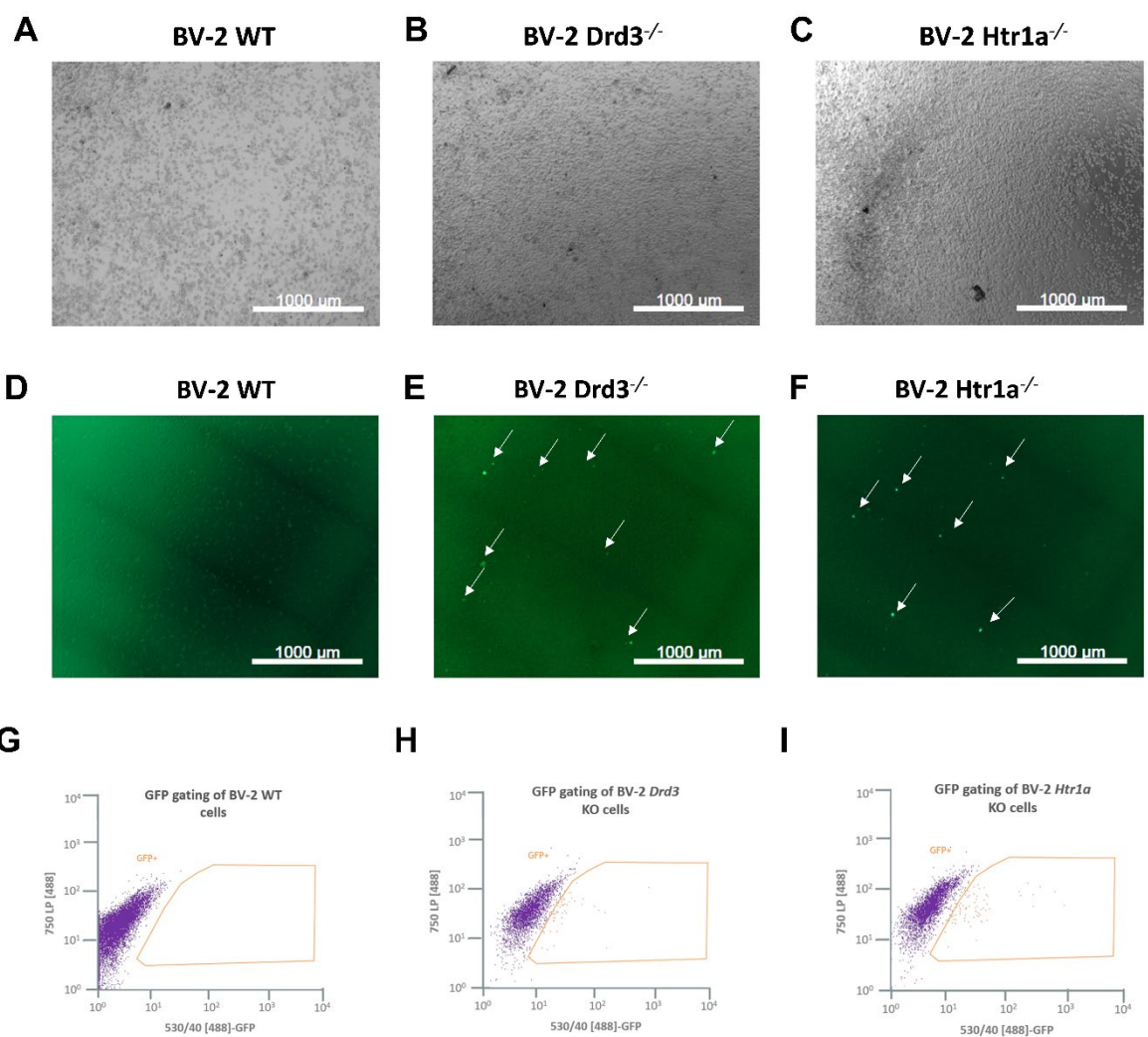
Supplementary 2. Images of transfected BV-2 cells and fluorescence scatter dot plots displaying the gating of the GFP positive cells. Cells were seeded 1 x 10^5 cells per well in 12-well plates and transfected with the appropriate plasmids. (**A-C**) Images of cells captured on a light microscope the day after transfection. (**D-F**) Images of cells under a light microscope with a GFP filter taken the day after transfection to illustrate the expression of GFP (shown by white arrow heads). (**G-I**) Each dot represents a single cell passing through the Fluorescence Activated Cell Sorting MoFlo© Astrios flow cytometer for sorting. The parameter for the horizontal axis of the dot plot is a Bandpass filter of 530/40 with a laser of 488nm. The parameter for the vertical axis is a 750 longpass (LP) filter. (**G**) Dot plot of the BV-2 WT cells illustrates the GFP negative cells and therefore acts as a guide for gating the GFP positive cells as demonstrated with the orange box. (**H**)-(**I**) Dot plots of the BV-2 cells transfected with the CRISPR-Cas9 plasmids display the GFP positive cells gated inside the orange box. GFP: green fluorescent protein, WT: Wild type, KO: knockout, *Drd3*: murine dopamine D3 receptor gene, *Htr1a*: murine 5-hydroxytryptamine-1a receptor gene.

DNA AGE

BP	Ladder	*Drd3*	*Htr1a*
1000			
800			
600			

Expected BP	861	814
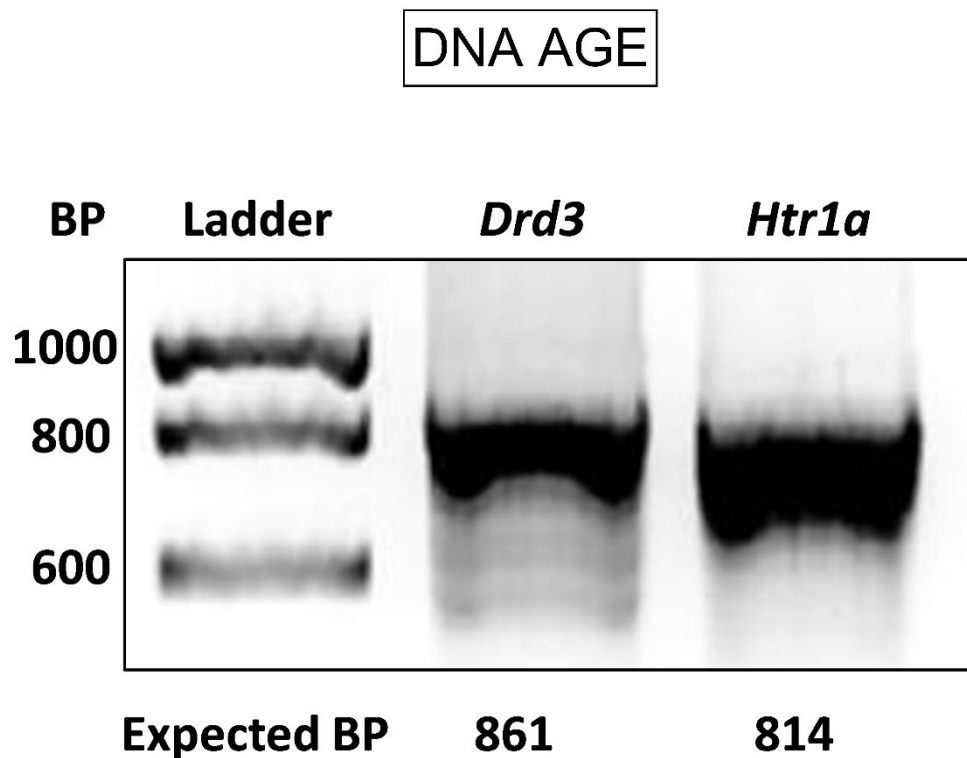
Supplementary 3. DNA agarose gel electrophoresis confirms that end-point PCR amplified *Drd3* and *Htr1a* genes correctly.

Cells were seeded 3 x 10^5 cells per well in a 6-well plate, and DNA was extracted using ISOLATE II Genomic DNA Kit (Bioline). End point PCR was conducted using primers to target the genes of interest (for details refer to Table 2), and AGE confirmed the PCR was successful. Lane 1 is the DNA ladder (Hyperladder 1KB). Lane 2 is end-point PCR product of the *Drd3* gene from BV-2 cells. Lane 3 is end-point PCR product of the *Htr1a* gene from BV-2 cells. BP: base pair, *Drd3*: murine dopamine D3 receptor gene, *Htr1a*: murine 5-hydroxytryptamine-1a receptor gene.
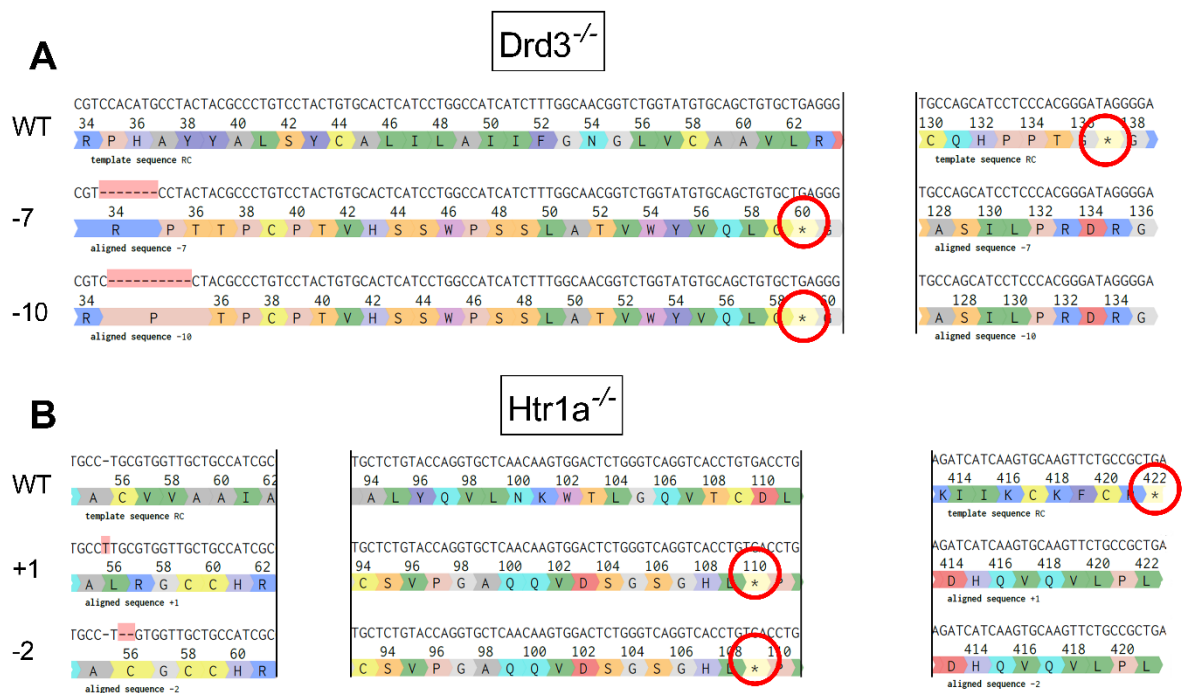
Supplementary 4. DNA sequence and amino acid translation showing early stop codons in the Drd3^{-/-} and Htr1a^{-/-}. End-point PCR products were Sanger sequenced and analysed through the program Tracking of Indels by Decomposition: TIDE. Amino acid translation was undertaken using Benchling. The corresponding amino acids for each codon are illustrated by coloured segments underneath the BPs in the DNA sequence. The number above each amino acid is indicative of the amino acid's position in the aligned sequence in Benchling. The amino acids representing the stop codons are represented by the star symbol and are surrounded by red circles. Indels are illustrated by red boxes around the affected BPs. **(A)** Amino acid translation from Sanger sequencing results of the Drd3^{-/-} indicates a deletion of 7 base pairs (BPs) and a deletion of 10 BPs. These resulted in frameshift mutations and thus a change in the codons and the corresponding amino acid sequence compared to the WT. **(B)** Amino acid translation from Sanger sequencing results of Htr1a^{-/-} reveal an insertion of 1 BP and deletion of 2 BPs, also resulting in frameshift mutations. WT: Wild type, A:

120

adenine, T: thymine, C: cytosine, G: guanine. *Drd3*: murine dopamine D3 receptor

gene, *Htr1a*: murine 5-hydroxytryptamine-1a receptor gene.

Chapter 3:

Neurotoxicity of Rotenone in the Central Nervous System of C57BL/6 Mice

Chapter 3: Neurotoxicity of rotenone in the central nervous system of C57BL/6 mice

This chapter was submitted as a manuscript to Scientific Reports on 18/11/2021.

Contribution:

- All experimental data collection and analysis

- Data analysis and curation

- Draft manuscript preparation

- Finalising manuscript

Signature of co-authors:

Name	Signature
Sarah Thomas Broome	Production Note: Signature removed prior to publication.
Alessandro Castorina	Production Note: Signature removed prior to publication.

The work in this manuscript addresses **Aim 2**.

Aim 2: Establish and characterise a rotenone mouse model of Parkinson's disease

Conclusion: Rotenone intoxication causes a series of behavioural and neurochemical changes reminiscent of Parkinson's disease, confirming its validity as a model to test the efficacy of novel compounds for Parkinson's disease

Neurotoxicity of Rotenone in the Central Nervous System of C57BL/6 Mice

Sarah Thomas Broome [1] and Alessandro Castorina [1, *]

[1] Laboratory of Cellular and Molecular Neuroscience (LCMN), School of Life Sciences, Faculty of Science, University of Technology Sydney, 2007, NSW, Australia

ABSTRACT

Systemic administration of rotenone is known to replicate several of the pathogenic and behavioural features of Parkinson's disease (PD), some of which cannot merely be explained by deficits of the nigrostriatal pathway. Unfortunately, little work has been done to characterise the neurotoxic effects of rotenone in extra-nigral structures of the central nervous system (CNS). For this purpose, the goal of this study is to provide a comprehensive analysis of several neurochemical alterations triggered by systemic rotenone administration in the CNS of C57BL/6 mice. Mice injected with either 1, 3 or 10mg/kg body weight (BW) rotenone daily via intraperitoneal route for 21 days were assessed weekly for changes in locomotor and exploratory behaviour. Results demonstrated that rotenone treatment caused significant locomotor and exploratory impairments at doses of 3 or 10mg/kg BW. Molecular analyses revealed that both TH and DAT were significantly reduced in the midbrain, striatum and spinal cord. In addition, rotenone intoxication caused a midbrain-restricted inflammatory response with heightened expression of glial markers, which, in contrast, was accompanied by reduced expression signs of inflammation and gliosis in extra-nigral CNS sites. Results also showed widespread alterations of mitochondrial function and increased signatures of oxidative stress in the midbrain, striatum, prefrontal cortex, amygdala, hippocampus and spinal cord. Rotenone also disrupted the expression of neuroprotective peptides and trophic factors such as pituitary adenylate cyclase-activating polypeptide (PACAP), vasoactive intestinal peptide (VIP), brain-derived neurotrophic factor (BDNF) and activity-dependent neuroprotective protein (ADNP) in the CNS of rotenone-treated mice. In summary, this study shows that rotenone intoxication, similarly to PD, causes a series of neurochemical alterations that extend at multiple CNS levels,

reinforcing the suitability of this pre-clinical model for the study extra-nigral CNS defects of PD.

Introduction

Parkinson's disease (PD) is a progressive neurodegenerative disorder that affects around 2% of the population over the age of 60 [1, 56]. It clinically manifests with motor impairments, including bradykinesia, tremor, rigidity and postural instability [5]. These classical parkinsonian motor symptoms are caused by the degeneration of dopamine neurons in the *substantia nigra pars compacta* (*SNpc*), resulting in a lack of dopamine in the striatum [4]. Notwithstanding these pathological hallmarks, PD patients also present with a myriad of non-motor symptoms, including depression, anxiety, cognitive deficits and autonomic dysfunction, suggesting that damage to other regions within the central nervous system (CNS) might also occur [7].

The driving force underlying the neurodegeneration observed in PD remains unknown; however, several factors are thought to contribute to disease pathogenesis, including genetics, environmental factors and neuroinflammation [25].

Rotenone, a naturally occurring compound used commercially as a pesticide and piscicide has been shown to reproduce some of the major clinical and behavioural features of PD in rats [40, 41]. Since then, rotenone has become a popular model of PD based on its high lipophilic nature, which enables it to cross biological membranes allowing systemic administration, but also due to its ability to trigger several pathological mechanisms, including oxidative stress, protein aggregation

and CNS inflammation, as well as its capability of reproducing a PD-like behavioural phenotype [49]. This ability to reproduce key pathological and phenotypic features of PD has made rotenone a valuable tool to study drug-mediated neuroprotection [59].

Rotenone administered at low doses is known to induce degeneration of the dopaminergic nigrostriatal pathway and cause motor deficits [39, 280, 281]. Rotenone-mediated dopaminergic degeneration occurs via the inhibition of the mitochondria electron transport chain complex I, which results in the formation and accumulation of reactive oxygen species, leading to oxidative stress [46]. Studies of human *post mortem* brain tissue indicate that oxidative stress and accumulation of reactive oxygen species are critical in the pathogenesis of PD [47, 48].

Chronic daily intraperitoneal injections of rotenone have been reported to induce L-DOPA responsive locomotor deficits and neurochemical abnormalities characteristic of PD in rats [52, 53], and although with some variability – depending on the route of administration, animal strain and experimental regimes – similar results have also been reported in mice [34]. However, these investigations have been focused on the analyses of neurochemical alterations in the midbrain and striatum (i.e. the nigrostriatal pathway) and have failed to provide a thorough assessment of any possible neurochemical changes in other regions of the CNS [282].

Based on the evidence indicating the existence of common clinical and pathological features shared by the rotenone toxicity model and PD patients, in the present study we aimed at characterising the range of neurochemical alterations triggered by systemic rotenone administration in the CNS of C57BL/6 mice. Once

the suitability of the model was established by behavioural assessments, we determined if rotenone toxicity disrupted the expression of dopamine, oxidative stress and inflammatory markers, as well as neuropeptides and trophic factors in at least six distinct CNS regions. Our results indicate that rotenone triggers widespread neurochemical changes that extend beyond the nigrostriatal dopaminergic system. Altogether, these findings suggest that the neurodegenerative process triggered by rotenone intoxication, similarly to PD, affects multiple central and perhaps peripheral systems, offering a viable model to investigate both nigral and extra-nigral defects triggered by PD.

Results

Rotenone intoxication impairs locomotion and exploratory behaviour in mice

To assess if rotenone induced changes in locomotor and/or exploratory behaviour, mice were subjected to the Open Field (OF) test as outlined in the experimental design (**Figure 1a**). Mice were weighed daily prior to injection (**Figure 1b**). Analyses of body weight revealed that mice receiving 3mg/kg and 10mg/kg of rotenone gained significantly less weight compared with saline-injected controls (**$p = 0.01$ and *$p = 0.0247$ Vs saline, respectively; **Figure 1c**).

MouBeAt, an ImageJ plugin, was used to track and quantify general locomotor (i.e. average speed and total distance travelled) and exploratory behaviours of mice in the OF (i.e. number of entries and total time spent in the centre quadrant)[283], which allowed us to generate representative heat maps depicting the locomotor pattern of tested mice (**Figure 1d**). Drug-induced deficits in locomotor activity were

assessed by comparing the total distance travelled ($F_{(9, 6)}$ = 2.723, ** p = 0.0099; **Figure 1e**) and average speed ($F_{(9,60)}$ = 1.631, ns p = 0.1269; **Figure 1f**) at 7, 14 and 21 days with respect to baseline-measurements prior to exposure to rotenone. To examine exploratory behaviour, we measured the number of times ($F_{(9, 60)}$ = 3.648, ** p = 0.0011; **Figure 1g**) and the total time spent by each mouse in the centre quadrant ($F_{(9, 60)}$ = 3.062, ** p = 0.0044; **Figure 1h**) of the OF. Mice display a natural aversion to open areas and preferentially stay close to the walls of the field (thigmotaxis). In contrast, they display an instinctive drive to explore a perceived threatening environment [284]. Therefore, the overall number of times a mouse enters the centre quadrant and the total time spent with respect to the periphery are indicative of the exploratory behaviour of mice (**Figure 1a**).

We report that only mice administered with 3mg/kg or 10mg/kg of rotenone developed deficits in locomotor and exploratory behaviours as compared with baseline controls. In more detail, at 3mg/kg, rotenone significantly reduced the total distance travelled in the OF on day 14 (*p = 0.0207), and this was further reduced by day 21 (**p = 0.0028) (**Figure 1e**), although this was not associated with an overall reduction in speed, except on day 7 (*p = 0.0442). In contrast, at this rotenone dosage, reductions in exploratory behaviour were only recorded on day 21 (* p = 0.0398; **Figure 1h**).

As expected, at the highest rotenone dosage tested in this study (10mg/kg), the drug severely impaired both locomotor and exploratory behaviours already after 14 days of rotenone treatment. Specifically, there was a significant reduction in the total distance travelled by these mice at both days 14 (*p = 0.0214 Vs baseline)

and 21 (*p = 0.0207 Vs baseline; *p = 0.0201 Vs Day 7) (**Figure 1e**). This was

correlated with significantly slower average speed at days 14 (*p = 0.0160 Vs

baseline) and 21 (**p = 0.0093 Vs baseline; *p = 0.0324 Vs Day 7) (**Figure 1f**).

Additionally, mice exhibited reduced exploratory behaviour, as demonstrated by the

significant reduction in the number of entries in the centre of the OF at day 21 (*p =

0.0458) (**Figure 1g**) and the reduction in the time spent in the centre Vs the

periphery, which was recorded both at day 14 (*p = 0.0317 Vs baseline; **p =

0.0094 Vs Day 7) and at day 21 (*p = 0.0342 Vs baseline; *p = 0.0111 Vs Day 7)

(**Figure 1h**).
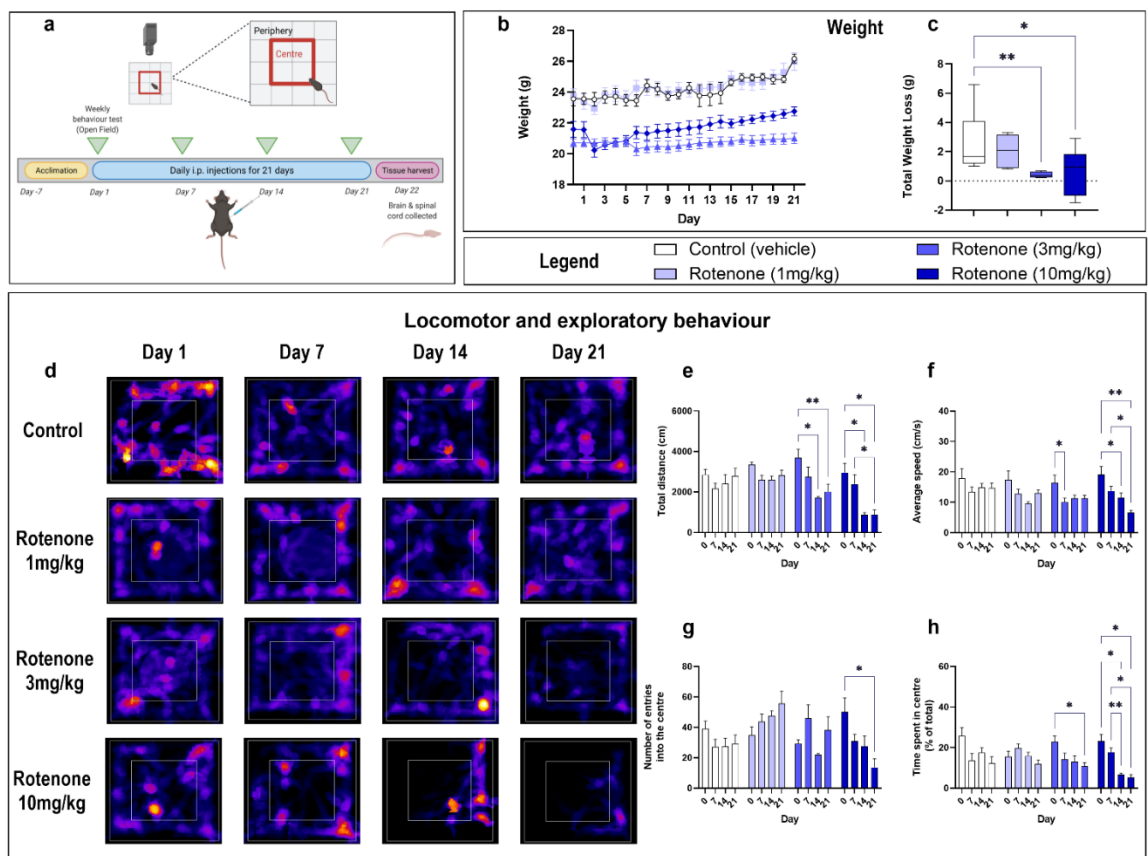
Figure 1. *Rotenone impairs locomotor and exploratory behaviours*.

Experimental timeline for injections and behavioural assessments (**a**). The Open

Field Test mice was used to assess for locomotor and exploratory behaviour in

rotenone- Vs baseline measurements every 7 days. The centre quadrant was defined as a central square with a surface area that is 25% smaller than the total area (red box), whereas the peripheral area was defined as the surface area between the centre quadrant the walls of the Open Field box. Mice received an intraperitoneal injection of indicated treatment daily for 21 days. On day 22, mice were humanely sacrificed and the brain and spinal cord was collected. Mean daily weight per treatment group (**b**) and the average weight loss/gain (**c**) was calculated using mean daily weights of day 1 versus day 22. Representative heat maps from MouBeAt Software that tracks the movement of mice during the open field (**d**). Locomotor and behaviour measurements were determined by MouBeAt software. Heat map uses colour to represent how often a mouse spent in an area. The longer a mouse spent in an area, the colour would shift from blue to red to yellow. Comparisons were made within the same treatment group compared to baseline measurements. An entry into an area was counted when at least 7% of the mouse body had completely entered the area. Total distance travelled (cm) in 5 mins (**e**). Average speed reported as cm/s (**f**). Number of entries in centre (**g**). Time spent in centre (s) (**h**). Data shown represents means of n = 4-10 mice per group. *$p < 0.05$ or **$p < 0.01$ as determined by ANOVA followed by Dunnett's *post-hoc* test or two-way repeated measures ANOVA followed by Tukey *post-hoc* test.

Rotenone reduces the expression of dopaminergic markers in the midbrain, striatum and spinal cord

PD is characterized by the loss of dopamine neurons in the midbrain, which results in a loss of dopamine availability in the *striatum* [285]. In addition, there is evidence

131

that tyrosine hydroxylase positive (TH)$^+$ and dopamine receptors'-expressing neurons are also localized in the spinal cord [286, 287], implicating a role of the spinal dopaminergic system in motor control. As such, we sought to analyse the expression of two main dopamine markers, TH and dopamine transporter (DAT), in the midbrain, striatum and spinal cord of mice to determine if rotenone caused a similar loss of dopaminergic neurons throughout the CNS (**Figure 2**).

In the midbrain, mice that received either 1mg/kg, 3mg/kg or 10mg/kg of rotenone displayed a significant reduction in TH mRNA expression (***p = 0.0002, **p = 0.0013 and ****p < 0.0001 Vs vehicle, respectively; $F_{(3,32)}$ = 11.07, ****p <0.0001; **Figure 2a**). Similarly, protein expression studies confirmed the significant reduction of TH expression, but only at 3mg/kg and 10mg/kg (**p = 0.0045 or **p = 0.0019 Vs vehicle, respectively; $F_{(3,15)}$ = 9.902, ***p = 0.0008; **Figure 2b, c**).

Striatal DAT transcript levels were significantly reduced at 3mg/kg (**p = 0.0043 Vs vehicle) and 10mg/kg rotenone (**p = 0.0049; $F_{(3, 28)}$ = 6.262, **p = 0.0022; **Figure 2d**). These results were paralleled by a decline of DAT protein expression in mice administered with 1mg/kg (***p = 0.0003 Vs vehicle) or 3mg/kg (*p = 0.0107), but surprisingly not in animals treated with 10mg/kg rotenone (p>0.05; $F_{(3,20)}$ = 8.527, **p = 0.0014; **Figure 2e, f**).

The expression of dopamine markers in the spinal cord revealed a significant reduction of TH transcripts across all treatment groups ($F_{(3,28)}$ = 41.55, ****p <0.0001; **Figure 2g**), including rotenone 1mg/kg (***p = 0.0002 Vs vehicle), with both higher doses – 3mg/kg and 10mg/kg – able to further reduce TH transcript

levels (****p < 0.0001; **Figure 2g**). These results were paralleled by similar and significant reductions of TH protein expression at all rotenone doses tested (****p<0.0001; F (3,20) = 1282, **** p<0.0001; **Figure 2h, i**). Analyses of DAT mRNAs in the spinal cord did not show changes until the highest rotenone dosage (10mg/kg), where a significant reduction was observed (****p < 0.0001 Vs vehicle; F (3, 28) = 40.88, ****p <0.0001; **Figure 2j**). Similarly, DAT protein levels were only reduced at the highest rotenone dosage (*p = 0.0172; F (3,20) = 3.566, **p = 0.325; **Figure 2i, k**).

Our rationale to test multiple dosages of the insecticide was to identify a dosage that reliably induced PD-like pathophysiology and associated behavioural deficits. Both behaviour (**Figure 1**) and dopaminergic markers (**Figure 2**) confirmed that 10mg/kg rotenone reliably reproduced the pathological and clinical features of PD. This data was further supported by immunohistochemical evidence of reduced TH[+] staining in the *SNpc* of mice exposed to rotenone 10mg/kg compared to controls (**Figure 2l-m**).
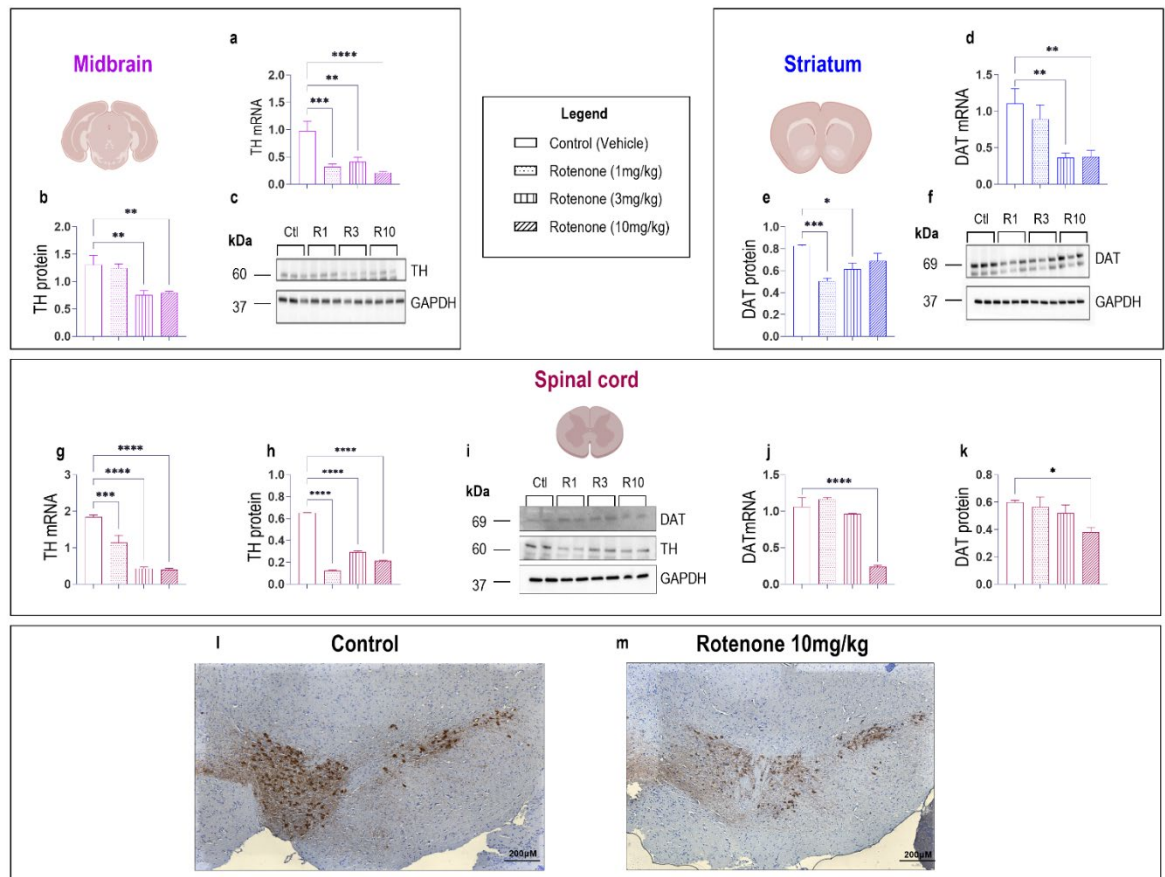
Figure 2. *Rotenone reduces the expression of dopaminergic markers in the midbrain, striatum and spinal cord*. On day 22, mice from vehicle- and rotenone-treated groups (1, 3 and 10mg/kg) were sacrificed and midbrains, striatum and spinal cords were collected for molecular analyses. TH mRNA and protein expression in the midbrain (**a-c**). DAT mRNA and protein expression in the striatum (**d-f**). TH and DAT mRNA and protein expression in the spinal cord (**g-k**). Representative photomicrographs showing TH immunoreactivity in the *SNpc* of vehicle- and 10mg/kg rotenone-treated mice (n=6 mice per group) (**l-m**). Scale bar = 200µm. Gene expression was measured using real-time qPCR and quantified using the ΔΔCt method after normalization to s18 (ribosomal protein s18 gene), the housekeeping gene. Real-time qPCR results are presented as mean fold changes with respect to vehicle-treated mice (control). In Western blots, protein expression was normalized to GAPDH, used as the loading control. Data in qPCR and

Western blots represents the means of n = 4 samples for each group. *p < 0.05,

**p < 0.01, ***p < 0.001 or ****p < 0.0001 as determined by ANOVA followed by

Dunnett's post-hoc test. Whole gel images in **Supplementary Fig. 2**.

Ctl: control; R1, 3, 10: Rotenone (1, 3, 10mg/kg); TH: tyrosine hydroxylase; DAT:

dopamine transporter; GAPDH: glyceraldehyde 3-phosphate dehydrogenase; kDa:

Kilodalton.

Rotenone triggers CNS region-specific changes in the expression of D1 and

D2 dopamine receptors

Dopamine is the main neurotransmitter affected in PD pathogenesis as a result of

the loss of dopaminergic neurons. To examine potential disturbances of the

dopaminergic system in nigral and extra-nigral regions, we analysed the mRNA

expression of the two main dopamine receptors, namely dopamine D1 and D2

receptor, in both vehicle- and 10mg/kg rotenone-treated mice. Interestingly, real-

time qPCR revealed some trends towards changes in D1 or D2 transcripts across

the brain regions analysed (**Figure 3a-l**); however no statistically significant

changes in either receptor transcript levels were observed in brain areas pertaining

to the nigro-striatal system (i.e. midbrain and striatum) (**Figure 3a-d**), prefrontal

cortex (**Figure 3e-f)** or hippocampus (**Figure 3i-j**). In the amygdala, there was a

significant reduction of D2 mRNA expression region following rotenone treatment (*

p = 0.0437; $F_{(5, 7)}$ = 5.629, *p = 0.0425; **Figure 3h**). In contrast, in the spinal cord,

rotenone treatment (10mg/kg) caused a significant reduction in D1 mRNA

expression compared to controls (** p = 0.0075; $F_{(7, 7)}$ = 2.160, p = 0.3312;

Figure 3k), whereas no significant change was seen when interrogating D2

transcripts (**Figure 3l,** p>0.05).
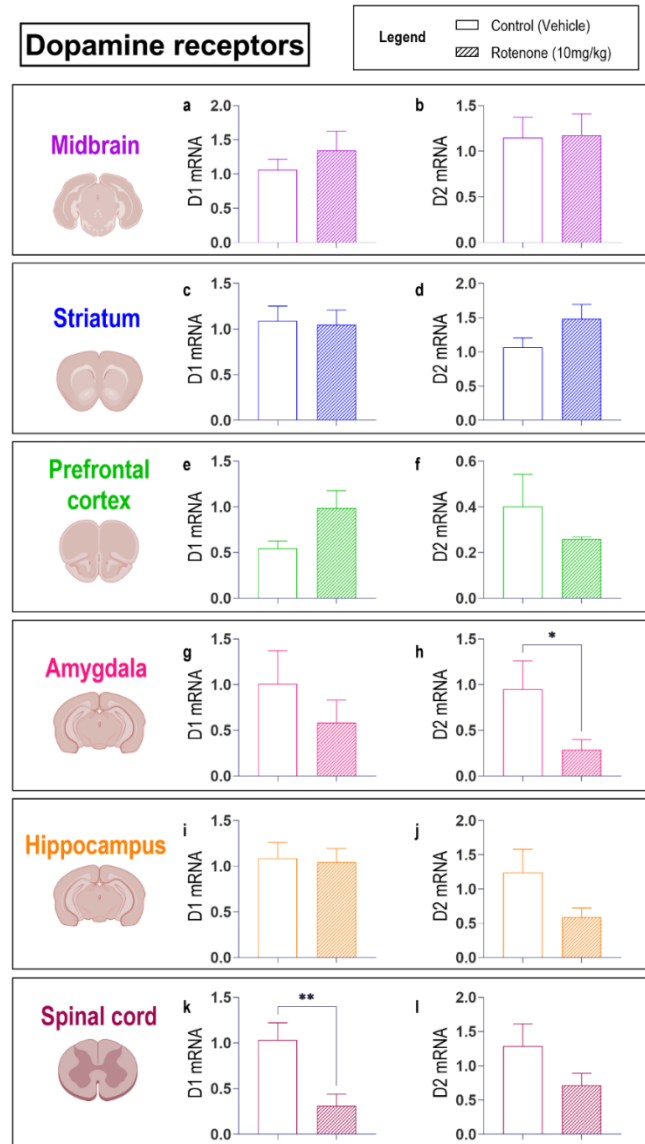
Figure 3. *Rotenone disturbs the expression of D1 and D2 dopamine receptors only in specific CNS regions*. On day 22, mice from vehicle- and rotenone-treated groups (10mg/kg) were sacrificed and midbrains, striata, prefrontal cortices, amygdala, hippocampi and spinal cords were collected for real-time qPCR analyses. D1 and D2 mRNA expression in the midbrain (**a-b**), striatum (**c-d**), prefrontal cortex (**e-f**), amygdala (**g-h**), hippocampus (**i-j**) and spinal cord (**k-l**). Gene expression was measured using real-time qPCR and quantified using the

ΔΔCt method after normalization to s18 (ribosomal protein s18 gene), the housekeeping gene. Real-time qPCR results are presented as mean fold changes with respect to vehicle-treated mice (control). Data represents the means of n = 4 samples for each group. $*p < 0.05$, $**p < 0.01$, $***p < 0.001$ or $****p < 0.0001$ as determined by unpaired Student's *t*-test.

Ctl: control; R10: Rotenone 10mg/kg; D1: dopamine D1 receptor; D2: dopamine D2 receptor

Rotenone triggers CNS region-specific changes in the expression of mitochondrial/oxidative stress markers

Rotenone is a mitochondrial complex I inhibitor [41] and prolonged treatment is thought to increase the levels of oxidative stress in the *SNpc* [57, 60]. Here, we set out to investigate if rotenone altered the expression of the mitochondrial protein, OPA1 and the antioxidant enzyme SOD1 (**Figure 4**) in the midbrain, striatum and extra-nigral regions of the CNS (i.e. prefrontal cortex, amygdala, hippocampus and spinal cord) in C57BL/6 mice after administration with increasing doses of rotenone (1, 3 and 10 mg/kg i.p.).

Analyses of OPA1 transcripts revealed that both 3mg/kg and 10mg/kg rotenone (but not the 1mg/kg dose) caused a significant down-regulation of OPA1 mRNA expression in the midbrain ($**p = 0.0033$ Vs vehicle [3mg/kg rotenone], and $****p < 0.0001$ [10mg/kg rotenone]; $F_{(3, 28)} = 9.736$, $***p = 0.0001$; **Figure 4a**) and striatum ($****p < 0.0001$, 3mg/kg and 10mg/kg rotenone, respectively; $F_{(3, 28)} = 33.67$, $****p < 0.0001$; **Figure 4f**). Most notably, all three doses of rotenone

significantly down-regulated OPA1 mRNA expression in the prefrontal cortex (****p < 0.0001; $F_{(3, 28)}$ = 44.48, ****p <0.0001; **Figure 4k**), amygdala (***p = 0.0002 [1mg/kg]; ***p = 0.0004 [3mg/kg] and ****p < 0.0001 [10mg/kg rotenone]; $F_{(3, 20)}$ = 18.66, ****p <0.0001; **Figure 4p**) and hippocampus (*p = 0.0378 [1mg/kg]; ***p = 0.0007 [3mg/kg] and ****p < 0.0001 [10mg/kg rotenone]; $F_{(3, 27)}$ = 12.17, ****p <0.0001; **Figure 4u**). In the spinal cord, moderate but significant reductions of OPA mRNA expression were observed after exposure to 1mg/kg of rotenone (*p = 0.0113 Vs vehicle; $F_{(3, 20)}$ = 4.603, *p = 0.0132; **Figure 4z**), but not with higher dosages.

Semi-quantitative analyses of OPA1 protein expression showed distinct patterns of reduction across the interrogated CNS regions. Notably, we report significantly reduced OPA1 expression in the midbrain only at 10mg/kg rotenone (**p = 0.0070; $F_{(3, 20)}$ = 4.351, *p = 0.0163; **Figure 3c, d**), whereas similar effects were seen in the hippocampus at both 3mg/kg (***p = 0.0004) and 10mg/kg (****p < 0.0001) ($F_{(3, 20)}$ = 14.40, ****p <0.0001; **Figure 4w, x**). In the prefrontal cortex, OPA1 protein expression was reduced in mice administered with 1mg/kg (*p = 0.0263) and 3mg/kg rotenone (****p < 0.0001) ($F_{(3, 20)}$ = 13.08, ****p <0.0001; **Figure 4m, n**).

Real-time qPCR analyses of SOD1 mRNA levels in the midbrain revealed significant reductions only in mice that received 10mg/kg rotenone (*p = 0.0472) ($F_{(3, 28)}$ = 8.201, ***p = 0.0005; **Figure 4b**). In contrast, lower dosages of rotenone were sufficient to induce a significant up-regulation of SOD1 transcripts in the striatum (**p = 0.0087 and **p = 0.0049, 1 and 3mg/kg rotenone respectively) ($F_{(3,}$

28) = 5.224, **p = 0.0054; **Figure 4g**) and amygdala (**p = 0.0013 and ****p < 0.0001, 1 and 3mg/kg rotenone respectively) ($F_{(3, 28)}$ = 32.29, ****p <0.0001; **Figure 4q**). The prefrontal cortex was the only region in which both 1mg/kg (*p = 0.0437), 3mg/kg (*p = 0.0387) and 10mg/kg rotenone significantly increased SOD1 mRNA expression (****p < 0.0001, $F_{(3, 28)}$ = 21.86, ****p <0.0001; **Figure 4l**). Lastly, in the hippocampus, only the highest dose of rotenone (10mg/kg) reliably up-regulated SOD1 mRNAs (* p = 0.0253) ($F_{(3, 28)}$ = 3.133, *p = 0.0412; **Figure 4v**).

Notably, at the protein level, midbrain SOD1 expression was unaffected by any rotenone dosage ($F_{(3, 32)}$ = 0.6665, p= 0.5788; **Figure 4c, e**). In contrast, SOD1 protein levels were remarkably altered by rotenone in the other CNS regions tested. Specifically, rotenone significantly increased the expression of SOD1 at all dosages both in the striatum (***p = 0.0002, **p = 0.0011 and **p = 0.0022, 1, 3 and 10mg/kg respectively. $F_{(3, 20)}$ = 10.11, ***p = 0.0003; **Figure 4h, j**) and amygdala (*p = 0.0270, *p = 0.0161 and *p = 0.0137, 1, 3 and 10mg/kg respectively) ($F_{(3, 8)}$ = 6.486, *p = 0.0155; **Figure 4r, t**). A dose-dependent increase in SOD1 protein expression was observed in the hippocampus, although levels were significantly up-regulated at 10mg/kg (*p = 0.0136, 10mg/kg rotenone) ($F_{(3, 20)}$ = 7.811, **p = 0.0012; **Figure 4w, y**) and in the spinal cord (*p = 0.0156 and **p = 0.0030 3mg/kg and 10mg/kg rotenone, respectively, ($F_{(3, 4)}$ = 25.08, **p = 0.0047; **Figure 4bb, dd**).
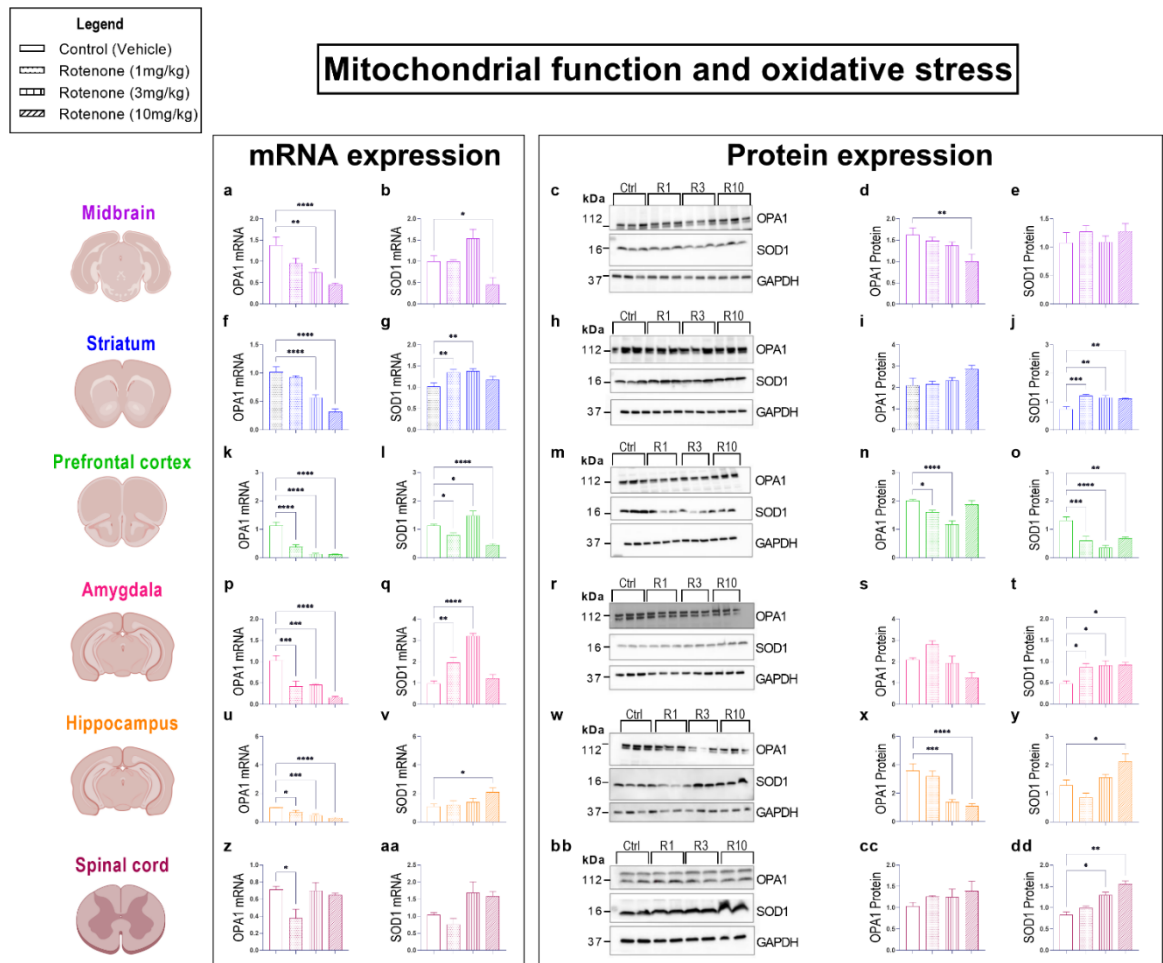
Figure 4. *Rotenone increases oxidative stress in the brain and spinal cord*.
Oxidative stress was assessed by measuring the mRNA and protein expression of
the mitochondrial marker OPA1 and the anti-oxidant enzyme SOD1. Real-time
qPCR analyses of OPA1 and SOD1 mRNA expression in the midbrain (**a, b**),
striatum (**f, g**), prefrontal cortex (**k, l**), amygdala (**p, q**), hippocampus (**u, v**) and
spinal cord (**z, aa**) of mice administered with increasing dosages of rotenone (1, 3
and 10 mg/kg BW, i.p. per 21 days). Fold-changes were calculated using the ΔΔCt
method after normalization to s18 (ribosomal protein s18 gene), the housekeeping
gene. Each data point represents the mean value from n = 4 mice per each group.
Representative Western blots and densitometry of OPA1 and SOD1 protein
expression in the midbrain (**c-e**), striatum (**h-j**), prefrontal cortex (**m-o**), amygdala

(**r-t**), hippocampus (**w-y**) and spinal cord (**bb-dd**) of mice exposed to the same treatment regimen as for mRNA studies. Protein expression was normalized to GAPDH, the loading control. Densitometric results are expressed as mean ± S.E.M from n = 4 mice per each group. *p < 0.05, **p < 0.01, ***p < 0.001 or ****p < 0.0001 as determined by ANOVA followed by Dunnett's post-hoc test. Whole gel images in **Supplementary Fig. 3.**

Ctrl: control; R1, 3, 10: Rotenone (1, 3, 10mg/kg); OPA1: Mitochondrial dynamin like GTPase; SOD1: superoxide dismutase 1; GAPDH: glyceraldehyde 3-phosphate dehydrogenase; kDa: Kilodalton.

Rotenone-induced neuroinflammation is confined to the midbrain and inhibited in extra-nigral CNS regions

In order to define whether chronic rotenone treatment caused diffuse neuroinflammation, we interrogated the gene expression of inflammatory mediators as well as the gene and protein expression of glial activation markers in the same CNS regions indicated above. To our surprise, we report that rotenone-induced neuroinflammation is restricted to the midbrain. In contrast, a global down-regulation of the expression of the pro-inflammatory cytokine IL-1β and of two distinct glial activation markers was seen in extra-nigral CNS regions. (**Figure 5**).

Real-time qPCR analyses of the pro-inflammatory cytokine IL-1β demonstrated that gene expression was significantly up-regulated in the midbrain (****p < 0.0001, $F_{(3, 19)}$ = 16.79, ****p <0.0001; **Figure 5a**) and, to a lesser extent, in the hippocampus of mice treated with the highest dose of rotenone (10mg/kg) (*p =

0.0119, F (3, 27) = 10.40, ***p = 0.0001; **Figure 5cc**). Conversely, a significant

reduction of IL-1β gene expression was observed both in the prefrontal cortex (**p

= 0.0014 and **p = 0.0036 at 1mg/kg and 3mg/kg, respectively, F (2, 28) = 6.537,

p = 0.0017; **Figure 5o) and spinal cord at the lower dosages (****p < 0.0001 at

both 1 and 3mg/kg, respectively, F (3, 19) = 26.68, ****p <0.0001; **Figure 5jj**), but

not in animals treated with 10mg/kg rotenone (p>0.05, **Figure 5o, jj**).

Gene expression of the anti-inflammatory marker Arg1 was altered in three distinct

CNS regions in response to rotenone. Notably, in the midbrain, both 1mg/kg and

3mg/kg rotenone significantly up-regulated Arg1 transcripts (*p = 0.0149 and ***p =

0.0002, respectively, F (3, 22) = 8.791, ***p = 0.0005; **Figure 5b**). Unexpectedly,

Arg1 transcripts were unchanged in mice treated with 10mg/kg rotenone. In the

prefrontal cortex, Arg1 was markedly down-regulated at all the dosages tested

(****p < 0.0001, F (3, 20), ****p <0.0001; **Figure 5p**). Lastly, rotenone up-regulated

the expression of Arg1 in the spinal cord at the lowest dosage tested (1mg/kg)

(****p < 0.0001, F (3, 12) = 38.78, ****p <0.0001; **Figure 5kk**).

Expression of CD11b, a macrophage/microglial activation marker, was measured

both at the mRNA and protein level. In the midbrain, CD11b transcripts were not

affected by any of the rotenone dosages tested (p > 0.05, F (3, 16) = 2.106, p =

0.1397; **Figure 5c**). In contrast, CD11b protein expression was significantly

increased in mice that received 1mg/kg and 10mg/kg rotenone (**p = 0.0016 and

p = 0.0011, respectively, F (3, 32) = 6.879, **p = 0.0011; **Figure 5e, f). Similarly,

to the midbrain, we report no changes in CD11b transcripts in the spinal cord (p >

0.05, F (3, 20) = 8.855, ***p = 0.0006; **Figure 5ll**); however, these were paralleled

by a significant increase in CD11b protein levels, but only at the highest dose of rotenone (*p = 0.0447, F (3, 4) = 5.433, p = 0.0678; **Figure 5nn, oo**). In the prefrontal cortex, both CD11b mRNA and protein expression was consistently down-regulated. Specifically, CD11b transcripts were significantly reduced at all the dosages tested (***p = 0.0003, ****p < 0.0001 and **p = 0.0017, 1, 3, and 10mg/kg rotenone, respectively, F (3, 28) = 11.21, ****p <0.0001; **Figure 5q**), and CD11b protein levels were reduced at both 1 and 3mg/kg rotenone (*p = 0.0329 and **p = 0.0099, F (3, 20) = 7.376, **p = 0.0016; **Figure 5s, t**). Finally, CD11b mRNA levels were robustly reduced at every dose tested both in the striatum (****p < 0.0001, F (3, 28) = 31.31, ****p <0.0001; **Figure 5j**) amygdala (***p = 0.0003 at 1mg/kg; ****p < 0.0001 at 3 and 10mg/kg, F (3, 28) = 13.38, ****p <0.0001; **Figure 5x**) and hippocampus (**** p < 0.0001, F (3, 28) = 39.28, ****p <0.0001; **Figure 5ee**). However, none of the mRNA results in these regions were corroborated by protein expression data (F (3, 32) = 4.316, *p = 0.0115; **Figure 5m,** F (3, 8) = 2.990, p= 0.0958; **Figure 5aa,** F (3, 20) = 1.601, p= 0.2207; **Figure 5hh**).

Analyses of GFAP expression, an astrocyte-specific marker, revealed a moderate but significant reduction of GFAP mRNAs in the midbrain of mice exposed 3mg/kg rotenone (**p = 0.009, F (3, 26) = 19.12, ****p <0.0001; **Figure 5d**), followed by a significant increase at the highest dosage of rotenone (***p = 0.0004, **Figure 5d**). These results were corroborated by similar changes at the protein level (*p = 0.017, F (3, 32) = 7.865, ***p = 0.0005; **Figure 5e, g**). Parallel experiments in extra-nigral regions identified a generalized down-regulation of GFAP transcripts (**Figure 5k, r, y, ff**). In the striatum, GFAP transcripts were significantly down-regulated at 3mg/kg and 10mg/kg rotenone (****p < 0.0001 and *p = 0.0443, respectively, F (3,

28) = 9.433, ***p = 0.0002; **Figure 5k**), whereas GFAP protein expression was reliably reduced at all the dosages tested (**p = 0.0069, *p = 0.02 and *p = 0.037 at 1, 3, and 10mg/kg rotenone, respectively, $F_{(3, 20)}$ = 2.652, p= 0.0766; **Figure 5l, n**). In the prefrontal cortex, GFAP mRNAs were robustly reduced by all the rotenone dosages (***p = 0.0003, ****p < 0.0001 and **p = 0.0017 at 1, 3, and 10mg/kg rotenone, respectively, $F_{(3, 28)}$ = 11.21, ****p <0.0001; **Figure 5r**). However, GFAP protein expression was significantly reduced only with 1mg/kg rotenone (**p = 0.0039), whereas it was marginally reduced at higher concentrations ($F_{(3, 20)}$ = 5.156, **p = 0.0084; **Figure 5s, u**). In the amygdala, GFAP mRNA expression was thoroughly reduced by rotenone administration at all dosages tested (****p < 0.0001, $F_{(3, 25)}$ = 33.18, ****p <0.0001; **Figure 5y**); however, these results were not supported by protein expression data ($F_{(3, 20)}$ = 1.061, p= 0.3877; **Figure 5z, bb**). On the other hand, hippocampal GFAP transcripts were significantly reduced following rotenone treatment (**p = 0.001, ****p < 0.0001 and **p = 0.0093 at 1, 3, and 10mg/kg rotenone, respectively, $F_{(3, 28)}$ = 14.15, ****p <0.0001; **Figure 5ff**). Similarly, hippocampal GFAP protein expression was reduced at different levels by rotenone (***p = 0.0001, *p = 0.0157 and ***p = 0.0005 at 1, 3, and 10mg/kg rotenone, respectively, $F_{(3, 20)}$ = 10.72, ***p = 0.0002; **Figure 5gg, ii**). In the spinal cord, GFAP mRNA expression was significantly down-regulated by all rotenone treatments (*p < 0.05 for all dosages, $F_{(3, 12)}$ = 12.22, ***p = 0.0006; **Figure 5mm**); however, these changes were not seen at the protein level (p > 0.05, $F_{(3, 4)}$ = 140.2, ***p = 0.0002; **Figure 5nn, pp**).
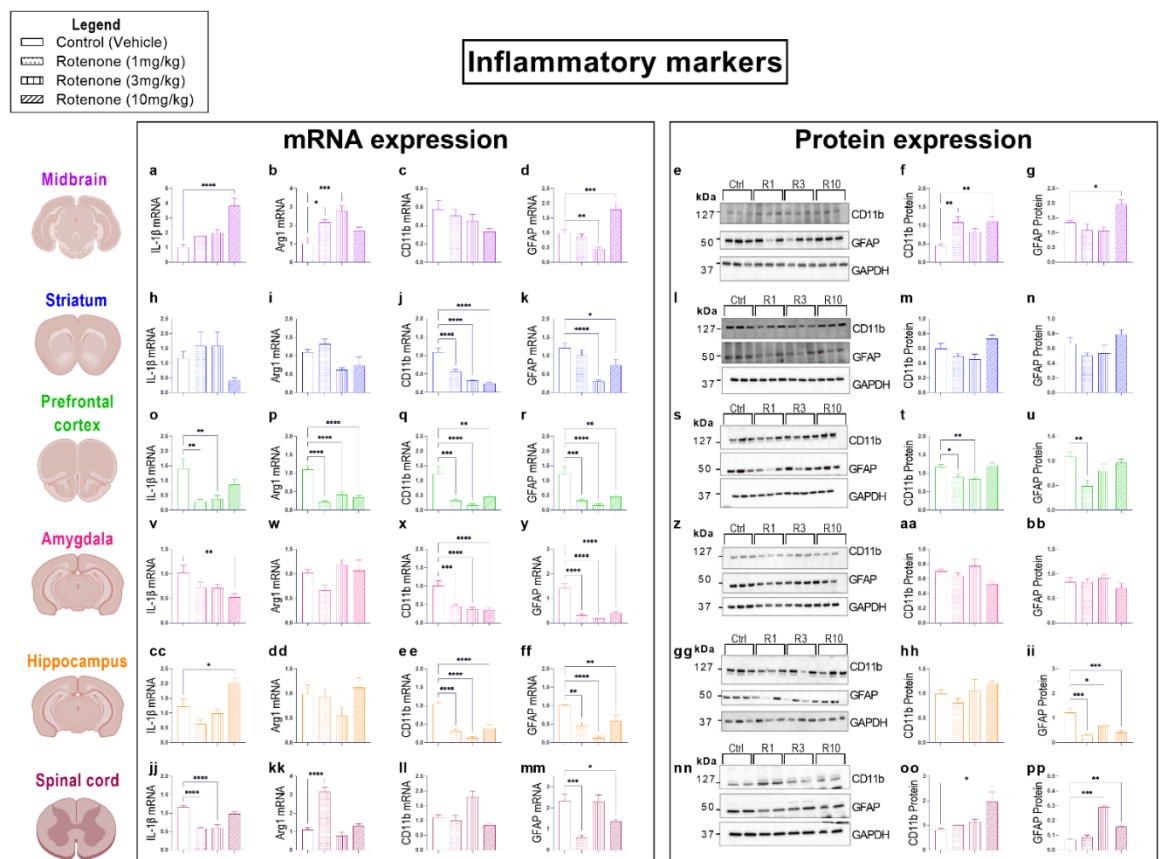
Figure 5. *Rotenone-induced neuroinflammation is restricted to the midbrain and inhibited in extra-nigral CNS regions*. Real-time qPCR analyses of IL-1β, Arg1, CD11b, GFAP mRNA expression in the midbrain (**a-d**), striatum (**h-k**), prefrontal cortex (**o-r**), amygdala (**v-y**), hippocampus (**cc-ff**) and spinal cord (**jj-mm**) of mice treated with either 1, 3 and 10mg/kg rotenone i.p. for 21 days. Fold changes were calculated using the ΔΔCt method after normalization to s18 ribosomal protein subunit gene. Data represents means of n = 4 samples for each group. Western blot and densitometric analysis of CD11b and GFAP protein expression in the midbrain (**e-g**), striatum (**l-n**), prefrontal cortex (**s-u**), amygdala (**z-bb**), hippocampus (**gg-ii**) and spinal cord (**nn-pp**). Densitometric results are expressed as mean ± S.E.M of 4-6 samples per group. *p < 0.05, **p < 0.01, ***p < 0.001 or ****p < 0.0001 as determined by ANOVA followed by Dunnett's post-hoc test. Whole gel images in **Supplementary Fig. 4.**

Ctrl: control; R1, 3, 10: Rotenone (1, 3, 10mg/kg); GFAP: Glial Fibrillary Acidic Protein; IL-1β: Interleukin-1-beta; Arg1: Arginase 1; GAPDH: Glyceraldehyde 3-phosphate Dehydrogenase; kDa: Kilodalton

Rotenone intoxication causes a global down-regulation in the expression of neuropeptides and neurotrophic factors in the CNS

In view of the protective role elicited by endogenous neuropeptides and neurotrophic factors in preventing neuronal deterioration in PD and other neurodegenerative disorders [288-290], we sought to determine if rotenone intoxication interfered with the expression of well-established neuropeptides/neurotrophic molecules. As such, we measured transcript levels of BDNF, ADNP, PACAP and VIP in the CNS of mice that received increasing dosages of rotenone. In addition, for both PACAP and VIP neuropeptides, we also measured protein expression.

Our findings demonstrate that BDNF transcripts were significantly up-regulated in response to both 3 and 10mg/kg of rotenone in the midbrain (**$p = 0.0012$ and ****$p < 0.0001$, 3mg/kg and 10mg/kg rotenone, respectively, $F_{(3, 26)} = 18.84$, ****$p < 0.0001$; **Figure 6a**) and prefrontal cortex (*$p = 0.0338$ and ***$p = 0.0004$, 3mg/kg and 10mg/kg rotenone, respectively, $F_{(3, 28)} = 7.609$, ***$p = 0.0007$; **Figure 6o**). In the striatum, the only significant increase in BDNF transcripts was seen in mice treated with 1mg/kg rotenone (** $p = 0.0075$, $F_{(3, 20)} = 4.730$, 8$p = 0.0119$; **Figure 6h**). In the amygdala, none of the rotenone dosages were able to affect BDNF transcripts ($p > 0.05$, $F_{(3, 19)} = 1.471$, $p = 0.2541$; **Figure 6v**). In

contrast, all the dosages of rotenone caused a significant down-regulation of BDNF transcripts in the hippocampus (***$p = 0.0006$, ***$p = 0.0004$ and **$p = 0.0012$, at 1, 3 and 10mg/kg rotenone, respectively, $F_{(3, 27)} = 9.228$, ***$p = 0.0002$; **Figure 6cc**). Lastly, we report a significant reduction of BDNF transcripts in the spinal cord of mice treated with 1mg/kg (**$p = 0.0073$) and 3mg/kg (**$p = 0.0037$) ($F_{(3, 12)} = 14.26$, ***$p = 0.0003$; **Figure 6jj**).

Analyses of ADNP mRNA expression in the CNS revealed a global decrease in transcript levels across the regions examined. With the exception of the midbrain, where we do not report significant changes in ADNP expression ($p>0.05$, $F_{(3, 26)} = 1.210$, $p= 0.3259$; **Figure 6b**), all rotenone treatments significantly down-regulated ADNP transcripts both in the prefrontal cortex (****$p < 0.0001$, $F_{(3, 20)} = 238.3$, ****$p <0.0001$; **Figure 6p**) and amygdala (****$p < 0.0001$, $F_{(3, 27)} = 30.65$, ****$p <0.0001$; **Figure 6w**). A similar down-regulation was observed in the spinal cord at 1mg/kg (****$p < 0.0001$), 3mg/kg (**$p = 0.003$) and 10mg/kg (***$p = 0.0003$) ($F_{(3, 12)} = 19.10$, ****$p <0.0001$; **Figure 6kk**). In the striatum, ADNP transcripts dose-dependently decreased; however, they were statistically significant only in mice that were treated with 10mg/kg of rotenone (****$p < 0.0001$, $F_{(2, 28)} = 16.67$, ****$p <0.0001$; **Figure 6i**). Conversely, only the two lowest doses of rotenone caused a significant decrease in ADNP mRNA expression in the hippocampus (***$p = 0.0004$ and ***$p = 0.0001$ at 1mg/kg and 3mg/kg rotenone, respectively, $F_{(3, 28)} = 11.52$, ****$p <0.0001$; **Figure 6dd**).

When looking at PACAP transcripts, we found significantly down-regulated mRNA levels in the midbrain, striatum, hippocampus and spinal cord (**Figure 6c, j**) ($F_{(3, }$

28) = 22.57, ****p <0.0001 **Figure 6ee**) (F (3,12) = 138.8, ****p <0.0001; **Figure 6ll**), but not in the prefrontal cortex or amygdala (F (3, 20) = 9.392, ***p = 0.0004; **Figure 6q**) (F (3, 20) = 0.1992, p= 0.8957; **Figure 6x**).In the midbrain, all dosages of rotenone reduced PACAP mRNA levels, although a significant reduction was seen only with 3mg/kg rotenone (*p = 0.0143, F (3, 21) = 3.292, *p = 0.0406; **Figure 6c**). Consistently, midbrain PACAP protein expression was significantly reduced both at 3 and 10mg/kg (*p<0.05 for both, F(3, 16) = 1.778, p =0.1918; **Figure 6e, f**). In the striatum, PACAP transcripts were robustly reduced by all rotenone dosages (****p < 0.0001, F (3, 20) = 264.4, ****p <0.0001; **Figure 6j**); however, PACAP protein levels were only slightly reduced until the highest rotenone dosage (*p = 0.0495, F (3, 20) = 2.322, p =0.1059; **Figure 6l, m**). Interestingly, whereas PACAP mRNAs were not affected by rotenone treatment in the prefrontal cortex (**Figure 6q**), protein expression was significantly reduced both at 1mg/kg (**p = 0.0039) and 3mg/kg (***p = 0.0002) and marginally at 10mg/kg (p>0.05) (F (3, 20) = 9.409, ***p =0.0004; **Figure 6s, t**). In the amygdala, consistent with PACAP mRNA measurements (**Figure 6x**), there were no significant changes in PACAP protein expression with any rotenone dosages (p>0.05, F (3, 16) = 3.778, *p = 0.0318; **Figure 6z, aa**), nor there were changes in hippocampal PACAP protein levels (p>0.05, F (3, 20) = 7.238, **p = 0.0018; **Figure 6gg, hh**).

VIP transcript levels were significantly diminished in the midbrain, hippocampus and spinal cord (**Figure 6d, ff, mm**), but not in the striatum (F (3, 20) = 2.556, p= 0.0841; **Figure 6k**), prefrontal cortex (F (3, 20) = 2.491, p= 0.0896; **Figure 6r**) or amygdala (F (3, 20) = 14.73, ****p <0.0001; **Figure 6y**). Specifically, midbrain VIP

mRNAs were down-regulated in response to the different rotenone dosages (***p = 0.0002, *p = 0.0183, ****$p < 0.0001$ at 1, 3 and 10mg/kg rotenone, respectively, $F_{(3, 22)}$ = 12.38, ****$p < 0.0001$; **Figure 6d**). In contrast, VIP protein expression was not affected by rotenone in this brain region ($p > 0.05$, $F_{(3, 18)}$ = 2.805, p= 0.0692; **Figure 6e, g**), neither it was in the striatum, amygdala or hippocampus ($p > 0.05$) ($F_{(3, 20)}$ = 6.219, **p = 0.0037; **Figure 6n**) ($F_{(3, 12)}$ = 1.435, p= 0.2811; **Figure 6bb**) ($F_{(3, 20)}$ = 16.35, ****$p < 0.0001$; **Figure 6ii**). Similarly, to PACAP, VIP expression was only reduced at the protein level in the prefrontal cortex, with significantly reduced expression at the two highest rotenone dosages tested (**p = 0.0062 and *$p < 0.05$ at 3 and 10mg/kg, respectively, $F_{(3, 20)}$ = 4.355, *p = 0.0163; **Figure 6s, u**). Hippocampal VIP expression was reduced at the transcriptional level by rotenone, with significant reductions at 1 and 3mg/kg (**p = 0.0032 and **p = 0.0015, respectively, $F_{(3, 28)}$ = 6.428, **p = 0.0019; **Figure 6ff**). Similarly, only VIP transcripts were reduced in the spinal cord by all rotenone dosages (****$p < 0.0001$ at 1 and 3mg/kg, and ***p = 0.0008 at 10mg/kg rotenone, $F_{(3, 20)}$ = 158.0, ****$p < 0.0001$; **Figure 6mm**), whereas protein levels remained unchanged ($p > 0.05$ at all dosages, $F_{(3, 12)}$ = 0.7894, p= 0.5227; **Figure 6nn-pp**).
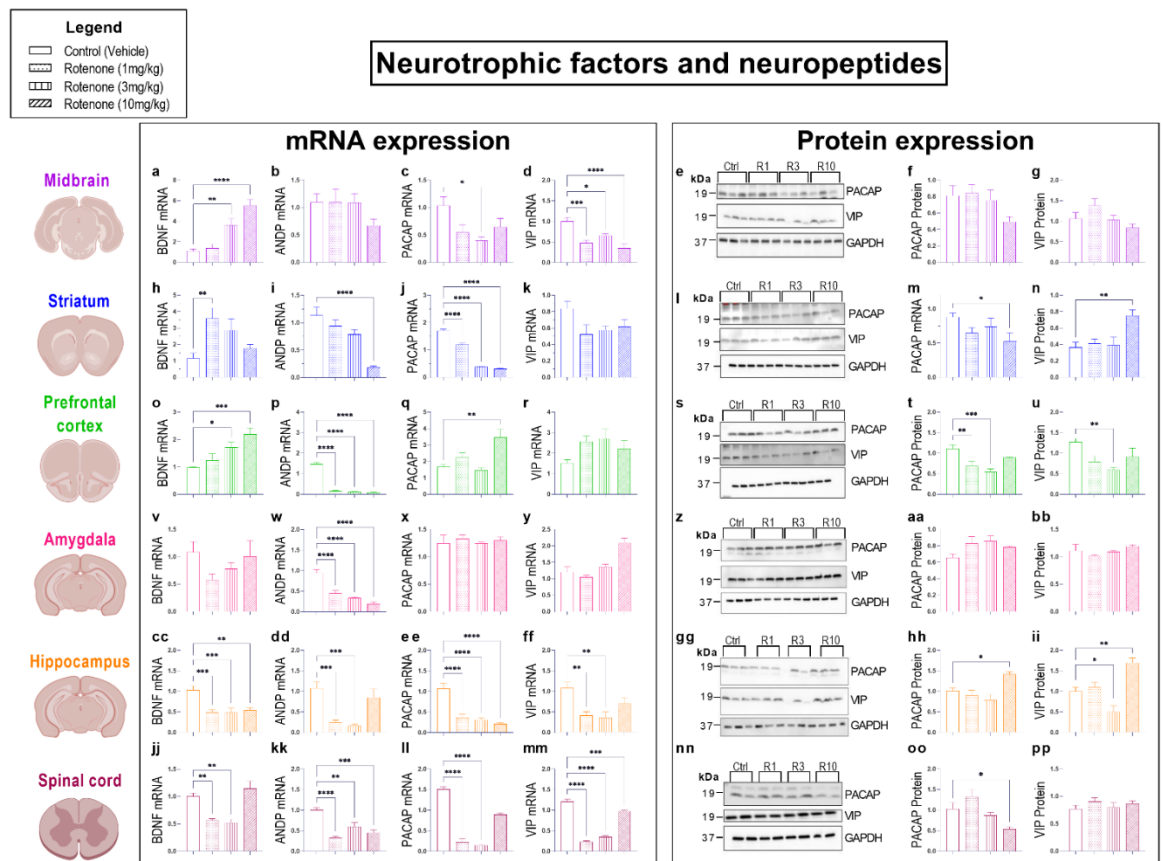
Figure 6. *Rotenone dampens the expression of neuropeptides and neurotrophic factors in the CNS*. Real-time qPCR analyses of BDNF, ADNP, PACAP and VIP mRNA expression in the midbrain (**a-d**), striatum (**h-k**), prefrontal cortex (**o-r**), amygdala (**v-y**), hippocampus (**cc-ff**) and spinal cord (**jj-mm**) of mice treated with either 1, 3 and 10mg/kg rotenone i.p. for 21 days. Fold changes were calculated using the ΔΔCt method after normalization to s18 ribosomal protein subunit gene. Data represents means of n = 4 samples for each group. Western blot and densitometric analyses of PACAP and VIP protein expression in the midbrain (**e-g**), striatum (**l-n**), prefrontal cortex (**s-u**), amygdala (**z-bb**), hippocampus (**gg-ii**) and spinal cord (**nn-pp**). Densitometric results are expressed as mean ± S.E.M of 4-6 samples per group. $*p < 0.05$, $**p < 0.01$, $***p < 0.001$ or $****p < 0.0001$ as determined by ANOVA followed by Dunnett's post-hoc test. Whole gel images in **Supplementary Fig. 5.**

Ctrl: control; R1, 3, 10: Rotenone (1, 3, 10mg/kg); PACAP: pituitary adenylate cyclase-activating peptide; VIP: vasoactive intestinal peptide; BDNF: brain-derived neurotrophic factor; ADNP: activity-dependent neurotrophic peptide; GAPDH: glyceraldehyde 3-phosphate dehydrogenase; kDa: Kilodalton

Discussion

In this study, we sought to provide a comprehensive analysis of the behavioural and neurochemical alterations caused by rotenone intoxication in C57BL/6 mice. For this purpose, animals were injected daily with rotenone at increasing dosages for a period of 21 days via intraperitoneal route. We opted to utilize this route of administration as this has been found to be the most effective to achieve a PD-like phenotype, at least in mice. In fact, whereas a large bulk of studies have demonstrated that rotenone intoxication reliably mimics human PD pathology [39, 280, 281], several discrepancies have been identified when comparing studies using different administration routes. For instance, a study reports that dopamine loss and behavioural deficits were seen in mice that were administered with 5mg/kg rotenone by oral gavage for 12 weeks [291]. Another study using the same route of administration reported that dosages as high as 30mg/kg rotenone for periods of 28 or 56 days were required to obtain similar nigrostriatal degeneration and locomotor impairments [49]. In contrast, studies in which rotenone was administered via intraperitoneal route have shown that lower dosages of rotenone (0.75 – 3mg/kg) and relatively shorter exposure periods (up to 3 weeks) were sufficient to achieve similar outcomes [54, 55]. These results suggest that, at least in mice, rotenone adsorption via the gastrointestinal tract might not be as efficient

as in rats.

A large portion of our investigations was to assess if rotenone toxicity disrupted the expression of dopamine, oxidative stress and inflammatory markers, as well as neuropeptides and trophic factors in the midbrain and in extra-nigral CNS regions known to be associated with cognition and the expression of certain affective behaviours. The reason behind these investigations was based on the ever-growing repertoire of behavioural alterations that are seen in patients with PD, which are not limited to locomotor impairment. Our data indicates that rotenone toxicity causes a broad spectrum of neurochemical alterations, such as changes in the expression of dopamine, oxidative stress and inflammatory markers, as well as neurotrophic factors/neuropeptides, some of which extend beyond the canonical nigrostriatal pathway. These results, to our knowledge, are the first to provide evidence of distinct and CNS region-specific neurochemical alterations at multiple CNS levels in rotenone intoxicated mice.

Several CNS regions are altered in PD pathogenesis; however, most PD studies focus on the nigral-striatal pathway and pay little attention to extra-nigral changes. This is surprising as non-motor symptoms of PD are known to clinically manifest much earlier than the classical motor symptoms associated with degeneration of dopaminergic neurons in the *SNpc*. For example, neuroimaging studies revealed structural and functional changes in the limbic cortico-striato-thalamocortical circuits, which correlated with the high prevalence of anxiety in PD [292]. Further imaging studies demonstrated atrophy in the gray matter, caudate, putamen, nucleus accumbens and amygdala that correlated abnormal imaging observations

with the degree of cognitive impairment observed in PD [293]. Villar-Conde and colleagues revealed changes at the level of the synapse in the hippocampus of PD patients [294], aligning with increased dementia risk in PD patients. Apathy is also one of the most common PD-associated mood changes and it has been linked to alterations in the medial and lateral prefrontal cortex and the limbic system [295]. Finally, the spinal cord, an often neglected part of the CNS in the context of PD, has been shown to exhibit alpha-synucleinopathy and could be the origin of several non-motor symptoms, including urinary, sexual, gastrointestinal and pain disturbances [13]. PD is a very heterogenous disease that presents differently in each patient. Accordingly, PD research should not be restricted to the nigro-striatal pathway, as our study reveals a unique profile of extra-nigral regions that could help inform early diagnosis and clinical management of disease.

First, we evaluated the effects of rotenone on body weight and locomotor and exploratory behaviour. Mouse rotenone models have previously shown that the toxicant does not induce significant weight loss in rats. As shown by Indel et al., they found that there was no difference in weight when comparing C57BL/6 mice that received 30 or 100mg/kg rotenone for 56 days with controls [56]. These results align with our study, as rotenone did not cause any significant weight loss; however, mice gained less weight compared to saline treated controls. Assessments of locomotor and exploratory behaviours unveiled a dose-dependent deterioration of both behavioural domains, although these were best appreciated by measures of locomotor behaviour. A similar outcome has been highlighted by several studies, in which rotenone reliably reduced the total distance travelled and number of times mice moved between areas of the OF [60, 296]. This aligns with

previous studies demonstrating that intraperitoneal injections of 3mg/kg rotenone daily for 21 days induced locomotor impairment in C57BL/6 mice [55]. Furthermore, studies report that at least a 3-week intoxication protocol is required to attain behavioural deficits [57], in agreement with our study, where the most consistent induction of locomotor and exploratory impairments was seen on day 21.

Next, we confirmed if the behavioural impairments triggered by rotenone were associated with the deterioration of dopaminergic pathway. As expected, our study reproduced the selective decline of dopaminergic neurons within the midbrain and striatum seen in other studies [55, 57]. However, rotenone dosages in our study were about ten times lower than that used in orally administered mice to achieve similar outcomes [57].Investigations were also extended to the spinal cord, another CNS region that also seem to be vulnerable to the effects of rotenone intoxication [297]. In this region, TH and DAT transcripts and protein levels were reduced, especially with the highest dosage. This result is, to some extent, similar to that reported in mutant A53T mice (a genetic model of PD), where axonal degeneration and motor neuron cell loss also extends to the spinal cord of these mice [298]. This is particularly important as some studies have already reported some degree of association between spinal cord damage and the autonomic dysfunction seen in PD [299-301]. Interestingly, we report that the extra-nigral regions of the amygdala and spinal cord were the only regions that demonstrated significant changes in the expression of the two main dopamine receptors. These receptors were analysed due to their known impairment during PD pathogenesis [302]. Both these regions had a reduction in either D1 or D2 receptor expression, which is surprising as these receptors are primarily located in nigro-striatal regions. Apparently, it can be

inferred that damage to the dopaminergic system in PD may not be limited to the nigrostriatal pathway, although more in-depth investigations are needed to understand the involvement of extra-nigral and spinal dopaminergic system damage in the development of motor and non-motor symptoms.

Rotenone is a known inhibitor of mitochondrial complex I [281, 303], which can trigger oxidative stress damage in the CNS. Here, we interrogated OPA1, a mitochondrial fusion protein and SOD1, an antioxidant enzyme as two markers of mitochondrial function and oxidative stress in the CNS [304, 305]. Our results revealed disturbances in both OPA1 and SOD1 expression in all regions tested, suggesting that rotenone toxicity causes redox dysfunctions that extend to various CNS regions. Systemic neurotoxicity of rotenone has been reported in numerous studies [49, 297, 306]. Furthermore, clinical imaging studies in PD patients have identified the coexistence of structural and functional alterations in extra-nigral regions such as the hippocampus [307], amygdala and prefrontal cortex [292]. The evidence of widespread increase in oxidative stress markers in regions outside of the nigrostriatal pathway in our PD model support the idea that such neurochemical changes might be the consequence (or cause) of structural changes. This could be clinically relevant, as there is some evidence suggesting that non-motor symptoms often precede motor symptoms in the prodromal stages of the disease [7].

Neuroinflammation has become a well-established player in PD pathogenesis [62, 250]. Rotenone has previously been shown to induce inflammation, with many studies utilizing rotenone reporting an association between oxidative stress and neuroinflammation as co-conspirators in PD pathogenesis [308]. Zhang and

colleagues provided evidence of microglial activation in hippocampal and cortical regions of mice and suggested that this contributed to the cognitive impairments seen in their rotenone-induced mouse PD model [88]. Evidence of neuroinflammation in PD patients has been found in several brain regions, including the *SNpc*, striatum, hippocampus and cerebral cortex, as well as in bodily fluids such as the cerebrospinal fluid [308]. Surprisingly, in our study we found that rotenone-induced inflammation was confined primarily to the midbrain. This is intriguing, especially given the findings reported above from other research groups. However, to make the scenario even more complex, we also found that the expression of most inflammatory and glial markers was globally down-regulated in all the other CNS structures tested. Whilst the latter could be considered as a direct effect of systemic toxicity, we cannot rule out that the stress response triggered by treatments (and behavioural tests) may have contributed to dampening the overall activity of the immune system, hence explaining why only a restricted pattern of inflammation was found in the midbrain. Other aspects to consider are the existence of conflicting data available in the literature on the ability of rotenone as an inducer of neuroinflammation. In fact, this seems to depend on several factors, including the route of administration and duration of treatment. In one study, oral administration of rotenone caused dopaminergic degeneration in the absence of marked changes in glial activation [57]. Conversely, rotenone infusion via osmotic pump strongly activated both astrocytes and microglia in the *SNpc* and striatum [50]. Altogether, these results suggest that variations to the experimental protocols used in rotenone intoxication models may produce signs of inflammation ranging from no inflammation to widespread inflammation in several CNS sites.

Lastly, we analysed the expression of neuropeptides and growth factors known to play critical roles in the modulation of neurological processes within the CNS. PACAP and VIP are two related neuropeptides that are expressed throughout the CNS that exert essential neuroprotective and immunomodulatory roles [309]. Studies using PACAP knock out mice have shown that these animals display age-related degenerative signs earlier than wild type animals, including increased neuronal vulnerability, systemic degeneration and increased inflammation [238]. These results suggest the importance of PACAP neuropeptide in maintaining a healthy and functional CNS. Similarly, VIP has been shown to prevent PD pathogenesis in several preclinical models of disease [243]. These observations provide a rationale for our analyses, as they could prompt further research to address their validity as therapeutic targets in PD, as biomarkers of a healthy CNS and/or to assess how rotenone exposure alters their expression. In a study by de Souza and collaborators, the authors describe these two peptides as neuroprotective and anti-inflammatory against experimental PD, acting mainly by reducing neuroinflammation, promoting dopaminergic neuronal survival and preserving cognitive functions [310]. Moreover, other evidence indicates that PACAP and BDNF [236] share similar neuroprotective pathways, as do VIP and ADNP [311]. Our results demonstrate these pathways are globally down-regulated in our rotenone model, suggesting that one of the modalities through which rotenone imparts damage to the CNS is via reducing the endogenous neuroprotective potential of these peptides. This correlates with studies that provide evidence on the therapeutic potential of PACAP, VIP, BDNF and ADNP in PD [235, 288, 290, 312]. However, more research is needed to elucidate the exact functions of these factors in PD pathogenesis.

Like most models of neurodegenerative diseases, it is difficult to model PD, as we still do not have a defined clinical diagnosis, with confirmation of clinical PD occurring from postmortem analyses of brain tissue. However, comparisons between genetic, neurotoxic and inflammatory models indicate that regardless of the initial trigger, what follows is a cascade of events that includes inflammation, mitochondrial dysfunction, oxidative stress and dopaminergic neuronal loss [62]. However, the neurochemical changes reported here correlate with other PD models as well as clinical studies [13, 307, 313, 314]. Altogether, our results suggest that 10mg/kg is the recommended dosage of rotenone to produce the most consistent mouse model of PD-like pathology in C57BL/6 mice. We also report that rotenone induces multiple neurochemical alterations across different CNS sites, suggesting that this disease model may be useful to study certain PD domains, thereby providing an excellent scaffold to study the efficacy of novel compounds to target non-motor and motor symptoms of PD.

Methods

Animal experiments

Twenty-four 7-week-old male C57BL/6 mice were purchased from ARC (Perth, WA, Australia). Mice were allowed to acclimate for one-week and experimental regimen commenced when mice were 8-weeks-old. Mice were housed in individually ventilated cages (4 mice per cage), under normal 12:12h light/dark cycle, with access to food and water *ad libitum.* All experiments were conducted in line with the Australian Code of Practice for the Care and Use of Animals for

Scientific Purposes, and in compliance with the ARRIVE guidelines. All animal experiments were approved by the University of Technology Sydney Animal Care and Ethics Committee (*ETH19-3322*).

Rotenone experimental protocol

Mice were randomly assigned one of four treatment groups: control, Rotenone 1mg/kg, Rotenone 3mg/kg or Rotenone 10mg/kg. Rotenone was prepared as a stock solution in 0.1% DMSO diluted in 0.1% saline. Mice underwent behaviour testing every 7 days to assess locomotor and exploratory behaviour. Mice were intraperitoneally injected with indicated treatment group daily for 21 days and monitored for 2h post injection. On day 22, mice were sacrificed and brains and spinal cord were collected. Tissue was snap frozen and used to perform molecular analysis. The brains were subsequently micro dissected into the following regions: prefrontal cortex, striatum, hippocampus, amygdala and midbrain with one hemisphere for RNA analysis and the other for protein analysis. The experimental protocol is summarized in **Figure 1**.

Open field behaviour test

The open field (OF) test was conducted every 7 days in the light cycle between 08:00h and 12:00h. Animals were acclimated in the testing rooms for 30 mins for habituation. The OF was conducted in the dark. The OF consisted of a square box (30 x 30 x 30 cm) made of grey Plexiglass plastic. Mice were placed individually in the centre of the area and allowed to freely explore for 5 min while being recorded. The OF was cleaned thoroughly between each mouse to eliminate any odour cues

with 70% ethanol. The FIJI/ImageJ Plugin MouBeAt software [283] was used to

analyse videos. MouBeAt quantifies the distance and time spent in the central and

peripheral areas, number of entries to centre region, grooming time in each area

and average speed. An entry into an area was counted when at least 70% of the

mouse body had completely entered the area.

Real-time quantitative polymerase chain reaction (RT-qPCR)

Briefly, total RNA was extracted using TRI-reagent (Sigma-Aldrich) and chloroform

and precipitated with ice-cold 2-propanol following established protocols [315, 316].

RNA concentration was determined using spectrophotometry (Nanodrop ND-1000®

spectrophotometer, Wilmington, DE, USA). Single-stranded cDNA was synthesized

using Tetro cDNA synthesis kit (Bioline, Sydney, NSW, Australia). Real-time qPCR

was performed to analyse the steady-state mRNA levels of twelve genes (**Table 1**).

The ribosomal protein 18S was used as the housekeeping gene. Each reaction

consisted of 3µL cDNA (final concentration 100ng), 5µL iTaq Universal SYBR

Green Master Mix (BioRad, VIC, Australia), 0.8µL of forward and reverse primers.

To examine changes in expression, the mean fold changes of each sample was

calculated using the ΔΔCt method as previously described [193, 258]. PCR product

specificity was evaluated by melting curve analysis, with each gene showing a

single peak (data not shown).

Accession #	Gene	Primer sequence (5'-3')	Length (bp)
NM_009377.2	Tyrosine hydroxylase (TH)	Fwd GCCCTACCAAGATCAAACCTAC Rev ATACGAGAGGCATAGTTCCTGA	93
NM_010020.3	Dopamine transporter (DAT)	Fwd ATGACATCAAGCAGATGACTGG Rev CACGACCACATACAGAAGGAAG	95
NM_010076.1	Dopamine D1 receptor (D1)	Fwd GAGCAGGACATACGCCATTT	101

		Rev GCTTCTGGGCAATCCTGTAG	
NM_010077.2	Dopamine D2 receptor (D2)	Fwd GTCAACACCAAGCGTAGCAG Rev CGGTGCAGAGTTTCATGTCC	97
NM_001131020.1	Glial fibrillary acidic protein (GFAP)	Fwd GAGATTCGCACTCAATACGAGG Rev CTGCAAACTTAGACCGATACCA	79
NM_001082960.1	CD11b	Fwd GAGCAGGGGTCATTCGCTAC Rev GCTGGCTTAGATGCGATGGT	94
NM_008361.4	Interleukin-1β (IL-1β)	Fwd GCTACCTGTGTCTTTCCCGT Rev CATCTCGGAGCCTGTAGTGC	164
NM_007482.3	Arginase-1 (Arg1)	Fwd ACAAGACAGGGCTCCTTTCAG Rev TTAAAGCCACTGCCGTGTTC	105
NM_011434.2	Superoxide dismutase (SOD1)	Fwd CAATGGTGGTCCATGAGAAACA Rev CCCAGCATTTCCAGTCTTTGTA	77
NM_001199177.1	Mitochondrial dynamin like GTPase (OPA1)	Fwd GCCCTTCTCTTGTTAGGTTCAC Rev ACACCTTCCTGTAATGCTTGTC	88
NM_007540.4	Brain-derived neurotrophic factor (BDNF)	Fwd CGAGTGGGTCACAGCGGCAG Rev GCCCCTGCAGCCTTCCTTGG	160
NM_001310086.1	Activity-dependent neuroprotective protein (ADNP)	Fwd GTGACATTGGGTTGGAATACTGT Rev AGGTTTTGTCCGATAGTCCTGA	149
NM_016989.2	Pituitary adenylate-cyclase-activating polypeptide (PACAP)	Fwd AGGCTTACGATCAGGACGGA Rev CTCCTGTCGGCTGGGTAGTA	121
NM_053991.1	Vasoactive intestinal peptide (VIP)	Fwd CCTGGCGATCCTGACACTCT Rev CTGCAGCCTGTCATCCAACC	100
NM_213557.1	18S ribosomal subunit (s18)	Fwd GGCGGAAAATAGCCTTCGCT Rev AGCCCTCTTGGTGAGGTCAA	101

Table 1. List of primer sets used in real-time qPCR analysis. Forward and

reverse primers were selected from the 5' and 3' region of each gene

mRNA. The expected length of each amplicon is indicated in the right

column.

Protein extraction and Western blot

Protein was extracted by homogenizing tissues in radioimmunoprecipitation assay

(RIPA) buffer containing a protease inhibitor to preserve protein integrity

(cOmplete^{TM}, Mini, EDTA-free Protease Inhibitor Cocktail, Sigma-Aldrich, Castle

Hill, NSW, Australia) [317]. Tissues were sonicated and then cleared by centrifugation at 12000xg for 10min. Protein quantification was determined with bicinchoninic acid assay (Pierce BCA Protein Assay Kit, ThermoFisher Scientific, VIC, Australia). Equal amounts of protein (30µg) was separated by SDS-polyacrylamide gel electrophoresis (SDS-PAGE) using 4-20% Mini-PROTEAN TGX Stain-Free Gels (15 well, BioRad, VIC, Australia). The Precision Plus Protein Prestained Standard in All Blue (BioRad, VIC, Australia) was included for comparison. Transfer to a PVDF membrane was performed using the semi-dry method (BioRad Trans-Blot Turbo Transfer System). Incubation with primary antibodies was performed overnight in 5% skim milk in TBST blocking solution at 4°C. Antibodies and dilutions are summarized in **Table 2**. Western blots were visualized using chemiluminescence BioRad Clarity Western ECL Blotting Substrate Solution. Images were acquired using the BioRad ChemiDoc MP System. Images were analysed using Fiji ImageJ and ratios normalized to GAPDH which was used as a loading control.

Antibody	Dilution	Source (Cat. #)
Tyrosine hydroxylase (TH)	1:200	Abcam (ab112)
Dopamine transporter (DAT)	1:1000	Abcam (ab128848)
Glial fibrillary acidic protein (GFAP)	1:1000	Abcam (ab68428)
CD11b	1:1000	Abcam (ab133357)
Mitochondrial dynamin like GTPase (OPA1)	1:1000	GeneTex (GTX129917)
Superoxide dismutase (SOD1)	1:1000	GeneTex (GTX100554)
Pituitary adenylate-cyclase-activating polypeptide (PACAP)	1:1000	GeneTex (GTX37576)
Vasoactive intestinal peptide (VIP)	1:1000	GeneTex (GTX129461)
Glyceraldehyde-3-phosphate dehydrogenase (GAPDH)	1:1000	BioRad (VPA00187)
Goat anti-Rabbit IgG HRP	1:10000	BioRad (STAR208P)
Goat anti-Mouse IgG (H+L)-HRP	1:10000	BioRad (1706516)

Table 2. List of primary and secondary antibodies used in Western blot.

Immunohistochemistry

Brains were fixed in 4% paraformaldehyde for 48 h before dehydration and embedding in paraffin. 5 µM thick coronal sections were cut using a microtome and mounted on glass slides. The sections were deparaffinized in xylene and rehydrated through decreasing concentrations of ethanol. Dopaminergic neurons were labeled with tyrosine hydroxylase (TH) (1:500, ab112, Abcam). The immunoreactivity of the antibody was revealed using the Rabbit specific HRP/DAB (ABC) Detection IHC Kit (ab64261, Abcam, VIC, Australia) according to manufacturer's protocol. Hematoxylin was used to counterstain nuclei and to appreciate the gross architecture of the *SNpc*. Sections were dehydrated in increasing concentrations of ethanol and xylene before being mounted. Images were taken on a ZEISS AxioScan.Z1 at ×20 magnification.

Statistical analysis

All data is reported as mean ± S.E.M. Statistical analyses were performed using GraphPad Prism software ver. 9.0.2. (GraphPad Software, La Jolla, CA). For behavioural analysis two-way repeated measures ANOVA followed by Tukey *post-hoc* test was performed. Comparisons between two or more groups were analyzed by one-way ANOVA followed by Dunnett's post-hoc test. To compute statistical comparisons that involved multiple independent variables, two-way ANOVA was used followed by Tukey post-hoc test. p-values ≤ 0.05 were considered statistically significant.

Acknowledgements

Author contributions statement

S.T.B. and A.C. conceived the experiments, S.T.B. conducted the experiments. S.T.B. and A.C. analysed the results. S.T.B. drafted the manuscript. A.C. reviewed the manuscript.

Competing interests

The authors do not declare any competing interests.

Data availability statement

The datasets generated and/or analysed during the current study are available upon reasonable request.

Chapter 4:

The anxiolytic drug buspirone prevents rotenone-induced toxicity in a mouse model of Parkinson's disease

Chapter 4: The anxiolytic drug buspirone prevents rotenone-induced toxicity in a mouse model of Parkinson's disease

This chapter has been published in The International Journal of Molecular Science on . 06/02/2022.

Contribution:

- All experimental data collection and analysis

- Data analysis and curation

- Draft manuscript preparation

Signature of co-authors:

Name	Signature
Sarah Thomas Broome	Production Note: Signature removed prior to publication.
Alessandro Castorina	Production Note: Signature removed prior to publication.

The work in this manuscript addresses **Aim 3**.

Aim 3: Demonstrate the buspirone treatment induces neuroprotective and anti-inflammatory effects in an animal model of Parkinson's disease

Conclusion: Buspirone was able to prevent rotenone-induced behavioural deficits and dose-dependently protect dopaminergic neurons. Buspirone mitigated

rotenone intoxication throughout the brain by alleviating mitochondrial dysfunction, reducing inflammation and promoting the expression of neuroprotective factors, including anti-inflammatory cytokines, neurotrophic and growth factors and neuropeptides. Overall, this suggests the potential of buspirone as an anti-inflammatory and neuroprotective agent in neurodegenerative and neuroinflammatory diseases.

The anxiolytic drug buspirone prevents rotenone-induced toxicity in a mouse model of Parkinson's disease

Sarah Thomas Broome [1] and Alessandro Castorina [1, *]

[1] Laboratory of Cellular and Molecular Neuroscience (LCMN), School of Life Sciences, Faculty of Science, University of Technology Sydney, 2007, NSW, Australia

Abstract

Pharmacological and genetic blockade of the dopamine D3 receptor (D3R) has shown to be neuroprotective in models of Parkinson's disease (PD). The anxiolytic drug buspirone, a serotonin receptor 1A agonist, also functions as a potent D3R antagonist. To test if buspirone elicited neuroprotective activities, C57BL/6 mice were subjected to rotenone treatment (10mg/kg i.p for 21 days) to induce PD-like pathology and were co-treated with increasing dosages of buspirone (1, 3 or 10mg/kg) to determine if the drug could prevent rotenone-induced damage to the central nervous system (CNS). We found that high dosages of buspirone prevented the behavioural deficits caused by rotenone in the open field test. Molecular and histological analyses confirmed that 10mg/kg buspirone prevented the degeneration of TH-positive cells. Buspirone attenuated the induction of interleukin-1β and interleukin-6 expression by rotenone, and this was paralleled by the up-regulation of arginase-1, brain-derived neurotrophic factor (BDNF) and activity-dependent neuroprotective protein (ADNP) in the midbrain, striatum, prefrontal cortex, amygdala and hippocampus. Buspirone treatment also improved mitochondrial function and antioxidant activities. Lastly, the drug prevented the disruptions in the expression of two neuroprotective peptides, pituitary adenylate cyclase-activating polypeptide (PACAP) and vasoactive intestinal peptide (VIP). These results pinpoint the neuroprotective efficacy of buspirone against rotenone toxicity, suggesting its potential use as a therapeutic agent in neurodegenerative and neuroinflammatory diseases, like PD.

1. Introduction

Parkinson's disease (PD) is the most common neurodegenerative movement disorder, characterised by the progressive loss of dopaminergic neurons in the *substantia nigra pars compacta* (SNpc) and resulting in a deficit of dopamine (DA) in the *striatum* [4]. PD is a multi-factorial disease that arises from a complex interplay between several environmental factors, genetic predisposition and defective cellular processes [36, 68]. Many attempts have been made to reproduce in rodents some of the pathological domains of PD. For example, the environmental toxin, rotenone, is a popular PD-mimetic due to its ability to reproduce the major clinical and behavioural features of PD in rodents, including motor deficits, dopaminergic degeneration, mitochondrial impairment and neuroinflammation [40, 41].

Neuroinflammation describes the local immune response within the central nervous system (CNS), and is predominantly driven by resident microglia [20, 63]. It is a major contributor to PD pathology and is consistently linked to disease progression and clinical severity [44]. Furthermore, it has been shown that neuroinflammation alone is sufficient to promote the death of dopaminergic neurons, as shown in a study involving an injection of the inflammatory mimetic, LPS, into the rodent brain, resulting in increased levels of inflammatory mediators prior to the loss of dopaminergic neurons [44]. Adding complexity to PD pathogenesis, is the discovery that DA itself can control inflammation [250].

The discovery of functional dopamine receptors expressed on the surface of multiple immune cell subtypes, including microglia [120] suggests that DA itself can modulate at least certain immune responses [250]. This is clearly seen in the ability of the dopamine 3 receptor (D3R) to promote inflammation. It has been shown that D3R-signalling promotes disease progression by favouring neuroinflammation and promoting the pathogenic CD4+ T cell response associated with PD [156, 159]. Additionally, microglial activation is repressed in D3R-deficient mice [159]. Most importantly, compounds able to block the D3R reduced CNS inflammation and consequently slowed the progression of PD [97, 159].

Computational and neuroimaging studies have revealed that the anxiolytic drug Buspirone (Buspar®), a partial 5-hydroxytryptamine receptor (5-HT1Ar) agonist, has a strong "off-target" function as a D3R antagonist [192, 225, 229]. In recent work, we have demonstrated that either genetic deletion of D3R or buspirone treatment reliably attenuated LPS-triggered inflammation in BV2 microglia [315]. It is well accepted that blocking microglial induced inflammation reduces neurodegeneration and slows disease progression [318, 319].

The emerging evidence extending the pharmacological properties of buspirone, together with the neuroprotective effects seen in response to D3R blockade, prompted us to investigate if buspirone protects dopaminergic degeneration by attenuating neuroinflammation in a rotenone mouse model of PD. We focused on the ability of buspirone to protect against rotenone-induced behavioural deficits,

dopaminergic degeneration, mitochondrial dysfunction and inflammation. To the best of our knowledge, this is the first study to characterise the neurochemical changes triggered by buspirone as an anti-inflammatory agent in several CNS structures. Our results indicate that, at high dosages, buspirone is able to prevent rotenone-induced deficits in locomotor and exploratory behaviour, protect dopaminergic neurons from degeneration, and reduce the expression of inflammatory mediators, whilst heightening the expression of neurotrophic factors and protective neuropeptides in several CNS regions. Collectively, these findings support the idea that buspirone protects the CNS against rotenone intoxication in a mouse model of PD.

2. Results

2.1 Buspirone prevents rotenone-induced deficits in locomotor and exploratory behaviour

Buspirone is clinically used as an anxiolytic and has been utilised as a positive control in assessing the exploratory behaviour of C57BL/6 mice in the open field (OF) [80] (**Supplementary Figure 1**). Rotenone (10mg/kg) induced significant deficits in exploratory behaviour of mice, as determined by a reduction in the number of entries and time spent in the centre quadrant of the OF (Inner white box on representative heat maps; **Figure 1A**). Notably, at day 21 there was a significant reduction in the number of entries in the centre of the OF (* $p < 0.05$; **Figure 1B**), which correlated with a reduction in the time spent in the centre at both day 14 (* $p < 0.05$) and day 21 (* $p < 0.05$) (**Figure 1C**). As expected, buspirone

was able to prevent rotenone-induced deficits in exploratory behaviour (**Figure 1B-C**).

Drug-induced effects on locomotor behaviour were also appraised by comparing the total distance travelled (**Figure 1D**) and average speed (**Figure 1E**). Rotenone significantly impaired locomotion after only 14 days of treatment. There was a significant reduction in the total distance travelled at day 14 (* $p < 0.05$ Vs baseline) and day 21 (* $p < 0.05$) (**Figure 1D**), concurrent with a reduction in average speed at both day 14 (* $p < 0.05$) and 21 (* $p < 0.05$) (**Figure 1E**). In rotenone-treated mice, 1mg/kg buspirone was unable to prevent deficits in locomotor behaviour. In fact, mice still displayed a significant reduction in total distance travelled at both day 14 (* $p < 0.05$ Vs baseline) and day 21 (* $p < 0.05$ Vs baseline) (**Figure 1D**), which correlated with a slower average speed at day 21 (*** $p < 0.001$ Vs baseline; **Figure 1E**), compared to baseline measurements. However, higher concentrations of buspirone (3 and 10mg/kg) prevented these locomotor deficits (**Figure 1D-E**).
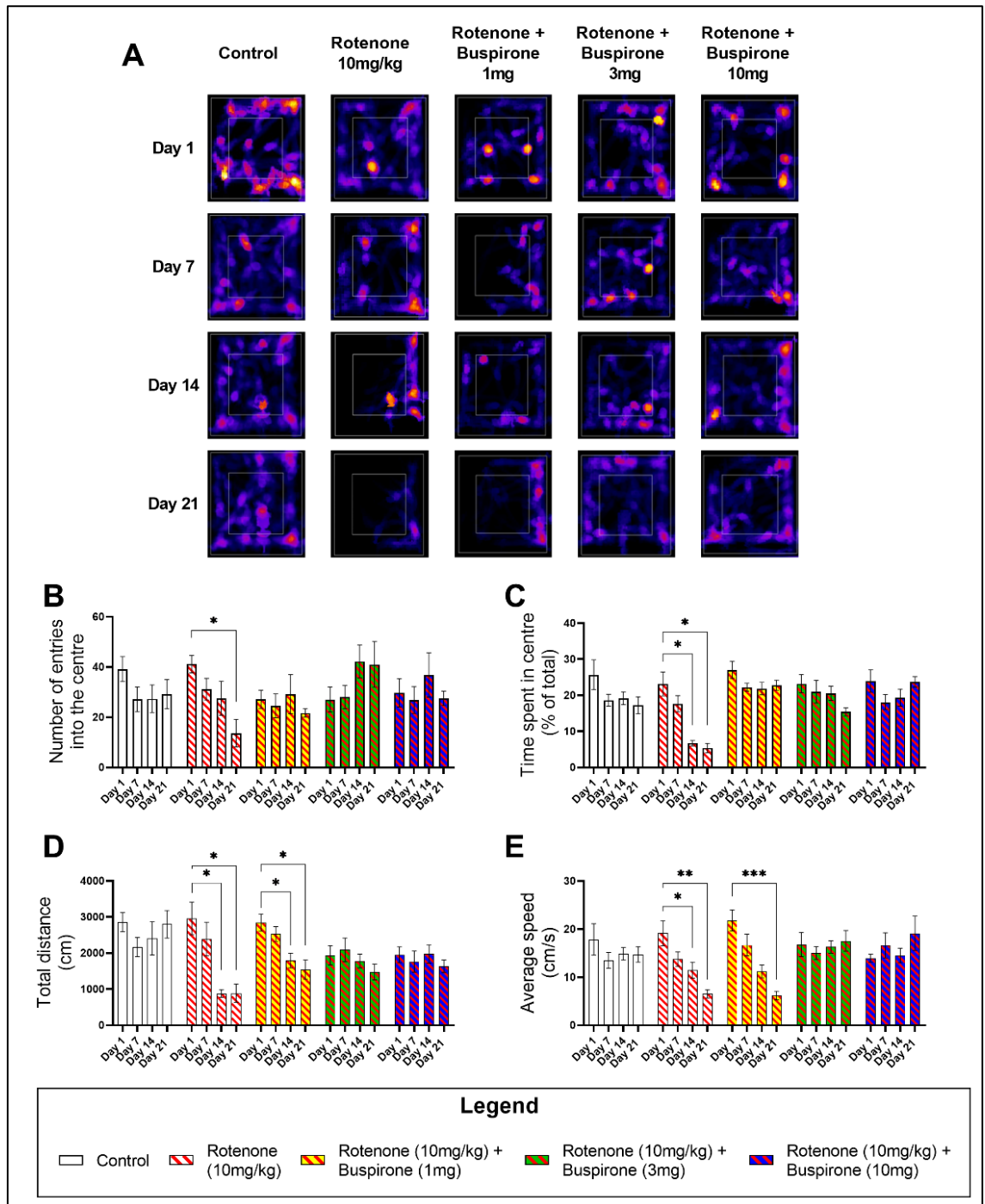
Figure 1. Buspirone prevents rotenone induced locomotor and exploratory behavioural deficits. The open field (OF) test was used to assess locomotor and exploratory behaviours of mice on a weekly basis for a total of 21 days. Representative heat maps generated from MouBeAt Software illustrate the locomotor pattern of mice during 5 min spent in the OF (**A**). Exploratory behaviour

was determined by measuring the number of entries (**B**) and the total time (**C**) each mouse spent in the centre quadrant. Locomotor activity was assessed by comparing the total distance travelled (**D**) and average speed (**E**) of mice. Comparisons were made within the same treatment group compared to baseline measurements. Data shown represents 8-12 mice per group. *$p < 0.05$, **$p < 0.01$ or *** $p < 0.001$ as determined by one-way ANOVA followed by Dunnett's post-hoc test.

2.2 Buspirone prevents the loss of dopaminergic neurons in rotenone-treated mice

To assess if buspirone protected dopaminergic neurons from the detrimental effects of rotenone, we analysed the expression two dopaminergic markers, tyrosine hydroxylase (TH) and dopamine transporter (DAT), in the midbrain and striatum, respectively (**Figure 2**). As expected, rotenone administration resulted in a significant reduction of TH mRNA (**** $p < 0.0001$ Vs vehicle; **Figure 2A**) and protein expression (**** $p < 0.0001$ Vs vehicle; **Figure 2B-C**) in the midbrain. Buspirone treatment up-regulated the expression of TH transcripts in the midbrain, at all doses, compared to rotenone treated mice (**** $p < 0.0001$; **Figure 2A**). These results were associated with a dose-dependent increase in TH expression at the protein level, which was statistically significant at the highest dosage of buspirone (### $p < 0.001$ Vs rotenone-treated mice; **Figure 2B**). Immunohistochemical data corroborated these findings, as the significant reduction in the number of TH-positive cells in the SNpc (** $p < 0.01$ Vs vehicle) was prevented by buspirone in a dose-dependent manner, although results were significant only at the highest dosage tested (### $p < 0.001$, buspirone 10mg/kg Vs rotenone-treated mice; **Figure 2D-E**).
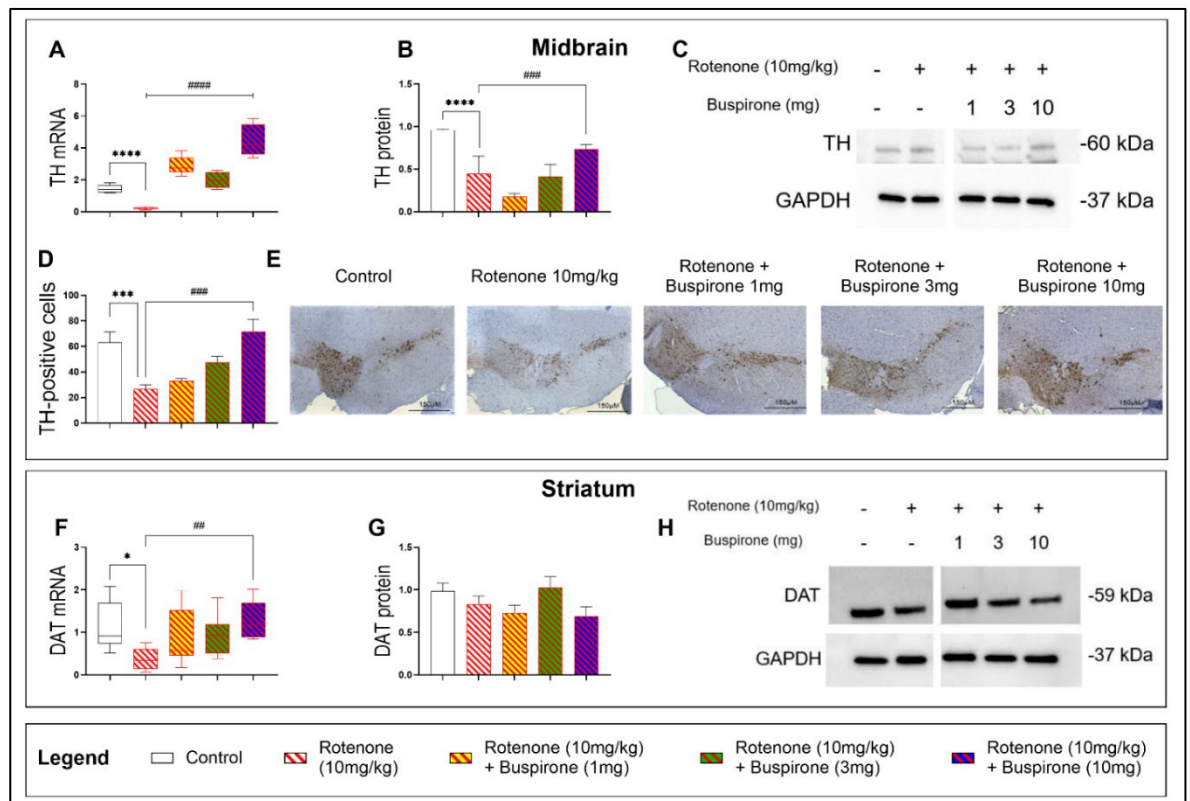
Figure 2. Buspirone at high dosages protects nigro-striatal dopaminergic neurons from degeneration. TH mRNA (**A**) and protein expression in the midbrain (**B-C**). Representative photomicrographs depicting TH immunoreactivity and semi-quantitative measurement of staining intensity in the *SNpc*, scale bar = 150μM (**D-E**). Striatal DAT mRNA (**F**) and protein expression (**G-H**). Gene expression was measured by qRT-PCR and quantified using the ΔΔCt method after normalization to s18 (the housekeeping gene). qRT-PCR results are reported as mean fold changes with respect to vehicle-treated control mice. Protein expression was determined by Western blot and normalized to GAPDH (the loading control). Western blots are cropped and removed lanes are included in Supplementary file 2. Densitometry results presented as mean ± S.E.M. TH-

positive cells reported as percent of TH-positive cells normalized to the total number of nuclei ± S.E.M. Data represents 3-4 mice per group. *p < 0.05, **p < 0.01, *** p < 0.001 or **** p < 0.0001, as determined by ANOVA followed by Dunnett's post-hoc test. TH: tyrosine hydroxylase; DAT: dopamine transporter; GAPDH: glyceraldehyde 3-phosphate dehydrogenase; kDa: Kilodalton; s18: ribosomal protein s18 gene.

2.3 Buspirone triggers brain region-specific changes in the expression of glial activation markers

To determine if buspirone treatment prevented rotenone-induced activation of astrocytes and microglia, we measured the relative mRNA and protein expression of GFAP (astrocytic activation marker) and CD11b or Iba1 (microglial activation markers) in several brain regions (i.e. midbrain, striatum, prefrontal cortex, amygdala and hippocampus). To our surprise, glial activation followed a region-specific pattern and was more pronounced in extra-nigral regions (**Figure 3**).

In the midbrain, GFAP mRNA and protein expression were increased in rotenone-treated mice (* p < 0.05 Vs vehicle; **Figures 3A, C & D**); however, co-treatment with buspirone failed to prevent GFAP gene and protein induction at all the dosages tested (p > 0.05 Vs rotenone). Striatal GFAP transcripts and proteins were not significantly affected by rotenone exposure or buspirone co-treatment, although expression levels were slightly increased when compared with controls (p > 0.05 Vs vehicle; **Figures 3F, H & I**). In the prefrontal cortex, GFAP transcripts were significantly down-regulated in response to rotenone administration (** p < 0.01 Vs

vehicle; **Figure 3K**), but not in animals that were co-treated with buspirone, where levels were comparable to controls ($p > 0.05$ Vs vehicle). In contrast, GFAP protein levels were not diminished by rotenone and were significantly increased in animals that received 10mg/kg buspirone (# $p < 0.05$; **Figure 3M & N**). In the amygdala, GFAP mRNA expression was slightly reduced by rotenone exposure ($p > 0.05$ Vs vehicle). Surprisingly, buspirone co-treatment caused a strong increase in GFAP transcripts at all dosages (#### $p < 0.0001$ Vs rotenone; **Figure 3P**). Conversely, GFAP protein expression was remarkably increased in the amygdala or rotenone-intoxicated mice (**** $p < 0.0001$ Vs vehicle) and significantly reduced by buspirone co-administration (#### $p < 0.0001$ Vs rotenone; **Figure 3R & S**). Hippocampal GFAP transcripts were not affected by rotenone ($p > 0.05$ Vs vehicle); however, mRNA levels were significantly increased when animals were co-administered with the two highest dosages of buspirone (## $p < 0.01$ and ### $p < 0.0001$ Vs rotenone, respectively; **Figure 3U**). GFAP protein expression in the hippocampus did not match mRNA data. In fact, GFAP protein levels were significantly reduced upon rotenone treatment (** $p < 0.01$ Vs vehicle) and increased in response to the highest dosage of buspirone (### $p < 0.001$ Vs rotenone; **Figure 3W & X**).

Gene expression studies of the microglial marker CD11b across the different brain regions did not show any major effects of rotenone ($p > 0.05$ Vs vehicle; **Figures 3B, G, L, Q & V**), although some trends towards a reduction were seen in the striatum and prefrontal cortex. In contrast, buspirone co-treatment induced significant CD11b gene up-regulation in the striatum (#### $p < 0.0001$ Vs rotenone at 3 and 10mg/kg; **Figure 3G**), prefrontal cortex (#### $p < 0.0001$ Vs rotenone at 1, 3 and 10mg/kg: **Figure 3L**), amygdala (#### $p < 0.0001$ Vs rotenone at 1, 3 and

10mg/kg: **Figure 3Q**) and, to some extent, in the hippocampus, although not significantly (p > 0.05 Vs rotenone at 1, 3 and 10mg/kg: **Figure 3V**).

Protein expression of the microglial marker Iba1 showed a robust induction in the CNS following rotenone exposure, and levels were in great part prevented upon buspirone co-administration (**Figures E, J, O, T & Y**). More in detail, rotenone significantly increased Iba1 protein expression in the midbrain (**** p < 0.0001 Vs vehicle; **Figure 3C & E**), striatum (**** p < 0.0001 Vs vehicle; **Figure 3H & J**), prefrontal cortex (**** p < 0.0001 Vs vehicle, **Figure 3M & O**), amygdala (** p < 0.01 Vs vehicle; **Figure 3R & T**) and, to a minor extent, in the hippocampus, despite not significantly (p > 0.05 Vs vehicle; **Figure W & Y**).

In the midbrain, all doses of buspirone prevented rotenone-induced Iba1 up-regulations (#### p < 0.0001 Vs rotenone; **Figure 3E**). Within the striatum, Iba1 expression was not affected neither by buspirone at 1 mg/kg nor at 10 mg/kg; however, it was significantly increased at 3 mg/kg (# p < 0.05 Vs rotenone; **Figure 3H & I**). Buspirone also reduced Iba1 expression in the amygdala (# p < 0.05 at 1 and 3 mg/kg and #### p < 0.0001 at 10mg/kg buspirone Vs rotenone; **Figure 3R & T**) and in the hippocampus, but only at 10mg buspirone (# p < 0.05 Vs rotenone; **Figure 3Y**).
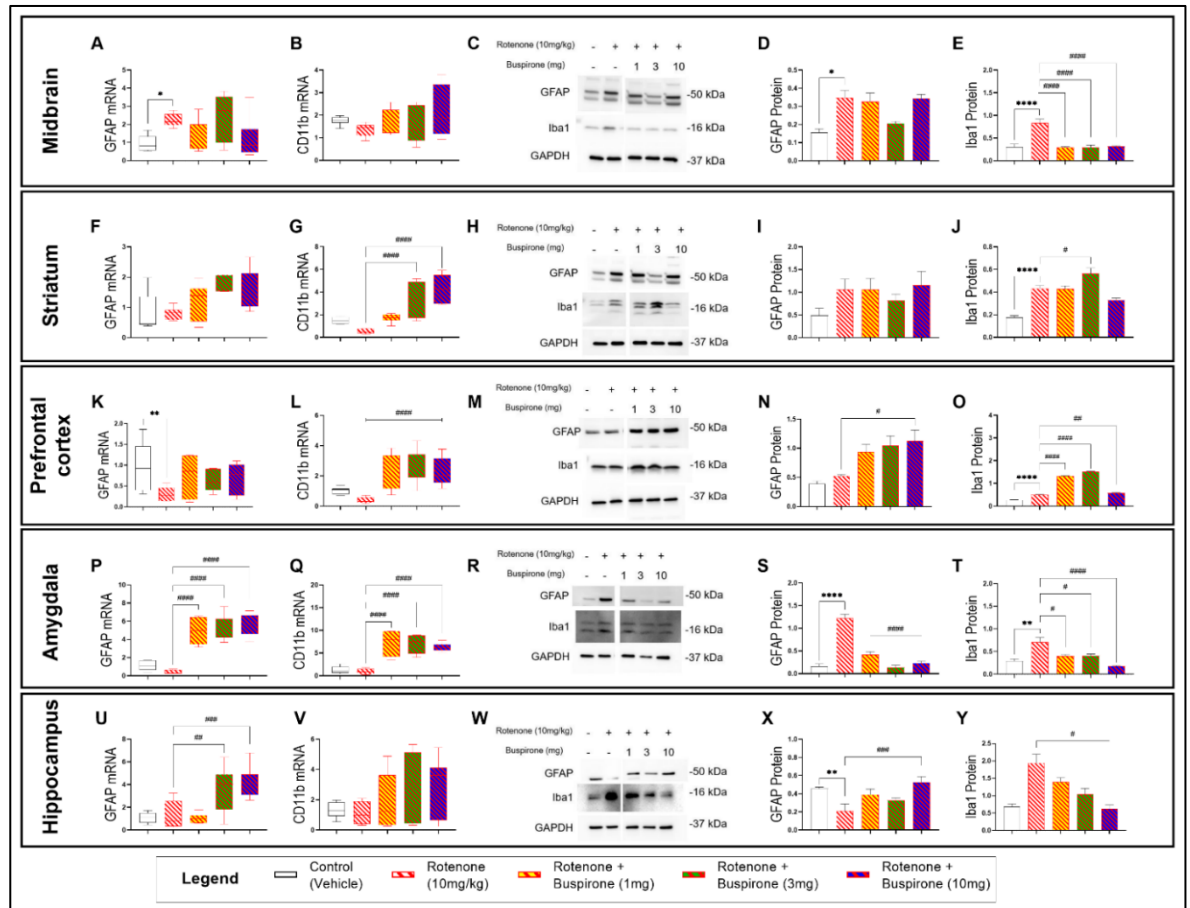
Figure 3. Buspirone triggers region-specific changes in the expression of glial activation markers. Real-time qPCR analyses of GFAP and CD11b in the midbrain (**A-B**), striatum (**F-G**), prefrontal cortex (**K-L**), amygdala (**P-Q**) and hippocampus (**U-V**), reported as mean fold changes calculated with the ΔΔCt method after normalization to s18 (the housekeeping gene). Western blot and densitometric analysis of GFAP and Iba1 in the midbrain (**C-E**), striatum (**H-J**), prefrontal cortex (**M-O**), amygdala (**R-T**) and hippocampus (**W-Y**). Western blots are cropped and removed lanes are included in supplementary 3. Densitometric

results are expressed as mean ± S.E.M. All data represents 4-6 samples per treatment group. *$p < 0.05$, **$p < 0.01$ or ****$p < 0.0001$, compared to vehicle-treated controls; or # $p < 0.05$, ## $p < 0.01$, ### $p < 0.001$ or ####$p < 0.0001$, compared to rotenone (10mg/kg) treated mice, as determined by ANOVA followed by Dunnett's post-hoc test. GFAP: Glial Fibrillary Acidic Protein; Iba1: ionized calcium binding adapter molecule 1; s18: ribosomal protein s18 gene; GAPDH: Glyceraldehyde 3-phosphate Dehydrogenase; kDa: Kilodalton.

2.4 Buspirone reduces neuroinflammation and promotes the expression of neurotrophic factors

In view of the effects of buspirone in the glial compartment, we sought to interrogate the mRNA expression of the pro-inflammatory cytokines (IL-1β and IL-6) and the anti-inflammatory marker (Arg1), as well as that of two neurotrophic factors (BDNF and ADNP) after 21-days of systemic rotenone administration with or without buspirone co-administration by qRT-PCR (**Figure 4**). Systemic administration of rotenone (10mg/kg) significantly induced the expression of IL-1β in the midbrain (**** $p < 0.0001$; **Figure 4A**), and hippocampus (**** $p < 0.0001$; **Figure 4E**), but not in the striatum, prefrontal cortex or amygdala ($p > 0.05$ Vs vehicle; **Figures 4B – D**). Similarly, the expression of IL-6 was significantly up-regulated in the midbrain (**** $p < 0.0001$; **Figure 4F**), striatum (**** $p < 0.0001$; **Figure 4G**), amygdala (**** $p < 0.0001$; **Figure 4I**) and hippocampus (**** $p < 0.0001$; **Figure 4J**), but not in the prefrontal cortex ($p > 0.05$; **Figure 4C**).

Gene expression of the pro-inflammatory cytokines IL-1β and IL-6 were globally down-regulated in response to buspirone co-treatment (**Figures 4A – J**). Both IL-1β (#### $p < 0.0001$; **Figure 4A**) and IL-6 (#### $p < 0.0001$; **Figure 4F**) were robustly down-regulated in the midbrain, compared with rotenone-treated mice. In the striatum, all buspirone concentrations were able to reduce IL-6 expression (#### $p < 0.0001$; **Figure 4G**), but only 10mg buspirone was able to reduce IL-1β mRNA expression in the striatum (## $p < 0.01$ Vs rotenone-treated mice; **Figure 4B**). Similarly, in the hippocampus, 10 mg/kg buspirone was required to fully prevent rotenone-driven up-regulation of IL-6 expression (#### $p < 0.0001$; **Figure 4J**), whilst all buspirone dosages reliably attenuated rotenone-increases IL-1β levels within the same region (#### $p < 0.0001$; **Figure 4E**). Both 3 and 10 mg/kg buspirone significantly down-regulated IL-6 expression in the amygdala (## $p < 0.01$ and #### $p < 0.0001$, respectively; **Figure 4I**). Buspirone treatment had no effects on IL-1β in the amygdala or on either pro-inflammatory cytokine in the prefrontal cortex ($p > 0.05$; **Figure 4C-D, H**).

Real-time qPCR analyses revealed that rotenone administration did not alter the expression of the anti-inflammatory marker Arg1 in the brain (**Figures 4K – O**). Conversely, both 3 and 10 mg/kg buspirone significantly increased Arg1 mRNAs in the midbrain (#### $p < 0.0001$ and ## $p < 0.01$ Vs rotenone, respectively; **Figure 4K**) and hippocampus (## $p < 0.01$ and # $p < 0.05$, respectively; **Figure 4O**). In the amygdala, all buspirone treatment groups demonstrated an increase in Arg1 mRNA expression in response to drug co-treatment (### $p < 0.001$, ## $p < 0.01$ and # $p < 0.05$ at 1, 3 and 10 mg/kg, respectively; **Figure 4N**), whereas it had no

ameliorative effects in the striatum and prefrontal cortex (p > 0.05 Vs rotenone; **Figures 4L & M**).

The mRNA expression of the neurotrophic factors BDNF and ADNP was assessed in the CNS of mice exposed to rotenone and/or co-treated with buspirone. As shown, rotenone significantly increased BDNF transcripts in the midbrain and prefrontal cortex (*** p < 0.001 and ** p < 0.01 Vs vehicle, respectively; **Figures 4P & R**), but not in the striatum, amygdala and hippocampus, where transcripts were marginally decreased (p > 0.05 Vs vehicle; **Figures 4Q, S & T**). Co-administration of buspirone to rotenone-treated mice partly reversed the effects of the toxicant on gene expression. In the midbrain, it significantly reversed BDNF gene induction at all the dosages tested (## p < 0.01 at 1 and 3 mg/kg and # p < 0.05 at 10 mg/kg; **Figure 4P**). Striatal BDNF mRNA were significantly increased when buspirone was used at 3 and 10 mg/kg (### p < 0.001 and #### p < 0.0001 Vs rotenone; **Figure 4Q**), an effect that was seen at all dosages in the hippocampus (## p < 0.01 at 1 mg/kg and #### p < 0.0001 Vs rotenone at 3 and 10 mg/kg; **Figure 4T**). In the prefrontal cortex, drug co-treatment reliably reduced BDNF gene expression (### p < 0.001 at 1 mg/kg and # p < 0.05 at 10 mg/kg, respectively; **Figure 4R**). In the amygdala, BDNF gene expression was not affected by rotenone or buspirone co-administration (p > 0.05; **Figure 4S**).

A global trend towards a reduction of ADNP transcripts was observed in the CNS of animals treated with rotenone, although this was significant only in the striatum (* p < 0.05 Vs vehicle; **Figures 4U – Y**). In contrast, buspirone robustly increased

ADNP mRNAs in the CNS regions tested. In the midbrain, buspirone increased ADNP (### $p < 0.001$, ## $p < 0.01$ and #### $p < 0.0001$ Vs rotenone at 1, 3 and 10 mg/kg; **Figure 4U**). Similarly, in the striatum, both 1, 3 and 10 mg/kg of buspirone significantly increased the expression of ADNP (# $p < 0.05$, ## $p < 0.01$ and #### $p < 0.0001$, respectively; **Figure 4V**). Additionally, all buspirone treatments promoted the up-regulation of ADNP in the prefrontal cortex (#### $p < 0.0001$, #### $p < 0.0001$ and ### $p < 0.001$ at 1, 3 and 10 mg/kg buspirone, respectively; **Figure 4W**) and hippocampus (#### $p < 0.0001$; 1, 3 and 10 mg/kg buspirone, respectively; **Figure 4Y**), whereas only a trend was seen in the amygdala ($p > 0.05$ Vs rotenone; **Figure 4X**).
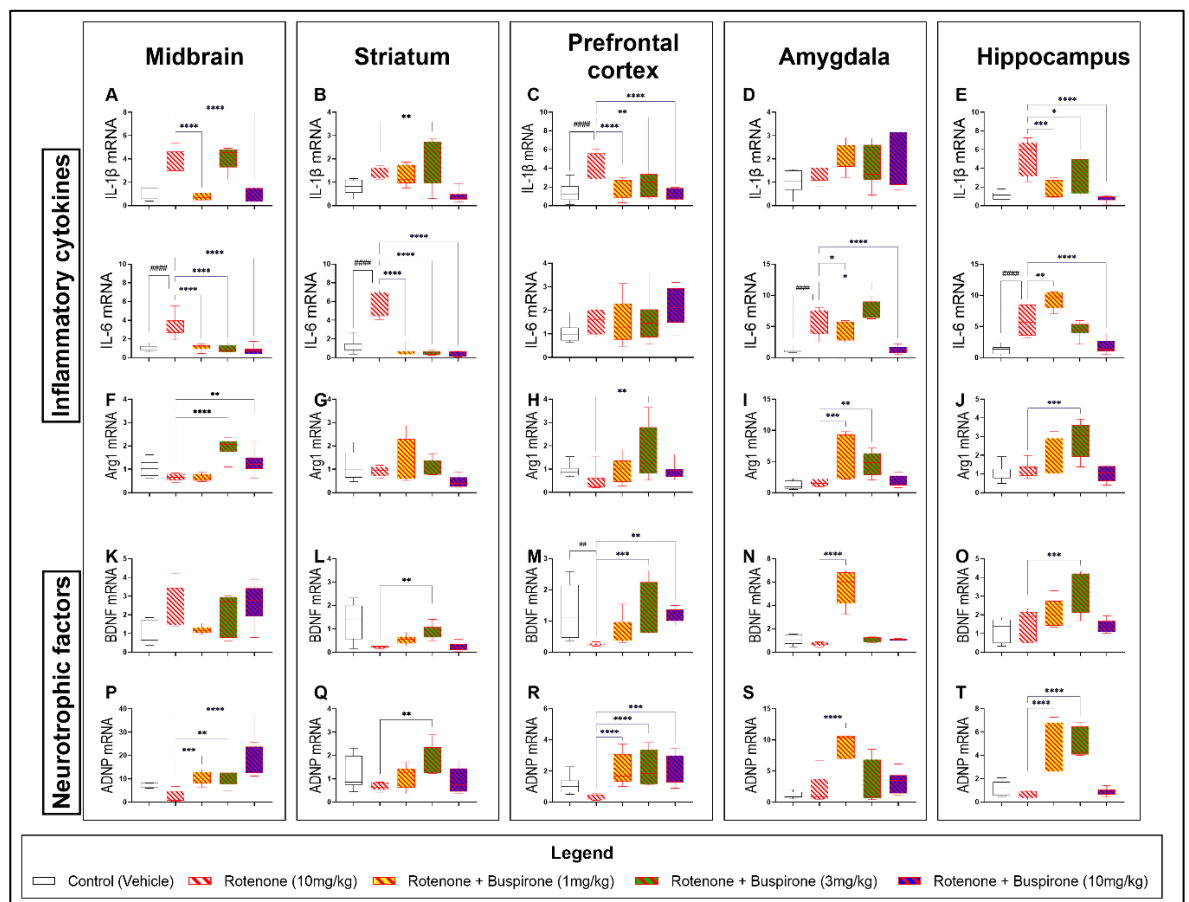
Figure 4. Buspirone reduces expression of inflammatory cytokines and up-regulates the expression of neurotrophic factors. Real-time qPCR analyses of the pro-inflammatory cytokines IL-1β (**A-E**) and IL-6 (**F-J**), the anti-inflammatory cytokine Arg1 (**K-O**) and neurotrophic factors BDNF (**P-T**) and ADNP (**U-Y**) in the midbrain (box 1), striatum (box 2), prefrontal cortex (box 3), amygdala (box 4) and hippocampus (box 5), reported as mean fold changes calculated with the ΔΔCt method after normalization to s18 (the housekeeping gene. All data represents 5-8 samples per treatment group. $*p < 0.05$, $**p < 0.01$, $***p < 0.001$ or $****p < 0.0001$, compared to vehicle-treated controls; or # $p < 0.05$, ## $p < 0.01$, ### $p < 0.001$ or ####$p < 0.0001$, compared to rotenone (10mg/kg) treated mice, as determined by ANOVA followed by Sidak's post-hoc test. IL-1β: interleukin-1beta: IL-6: interleukin-6; Arg1: arginase 1; BDNF: brain-derived neurotrophic factor; ADNP: activity-dependent neuroprotective protein; s18: ribosomal protein s18 gene; GAPDH: Glyceraldehyde 3-phosphate Dehydrogenase; kDa: Kilodalton.

2.5 Buspirone dampens rotenone-induced oxidative stress in distinct brain regions

Rotenone is a known mitochondrial complex I inhibitor able to increase the levels of reactive oxygen species, promoting oxidative stress and mitochondrial damage. To determine if buspirone could prevent mitochondrial damage, we assessed mitochondrial function by analysing OPA1 mRNA expression and the expression of the antioxidant enzyme SOD1, as an indirect measure of oxidative stress, throughout the brain (**Figure 5**).

Analyses of OPA1 transcripts revealed that rotenone attenuated gene expression throughout the CNS, but not significantly ($p > 0.05$; **Figures 5A, E, I, M & Q**). Buspirone treatments promoted the expression of OPA1 mRNA, specifically in the midbrain (# $p < 0.05$ Vs rotenone at 1 and 10 mg/kg, **Figure 5A**), striatum (#### $p < 0.0001$; **Figure 5E**), prefrontal cortex (#### $p < 0.0001$; **Figure 5I**), amygdala (#### $p < 0.0001$; **Figure 5M**) and hippocampus (# $p < 0.05$ and ## $p < 0.01$ at 3 and 10 mg/kg; **Figure 5Q**).

Real-time qPCR analysis of SOD1 mRNA levels did not show any changes in the midbrain and striatum after treatment with rotenone and/or co-treatment with buspirone (**Figure 5B & F**). However, Western blots to measure SOD1 protein levels in these same brain regions showed significant increases following rotenone exposure (** $p < 0.01$ and * $p < 0.05$ Vs vehicle, respectively), which were prevented using buspirone (midbrain: ## $p < 0.01$ and #### $p < 0.0001$ Vs rotenone at 3 and 10 mg/kg; striatum: # $p < 0.05$ Vs rotenone; **Figures 5C, D, G & H**). In the prefrontal cortex, SOD1 mRNA expression was significantly reduced by rotenone (** $p < 0.01$ Vs vehicle) and rescued by 3 and 10 mg/kg buspirone (# $p < 0.05$ for both; **Figure 5J**). However, results in this brain region were not corroborated by protein expression analyses. Prefrontal SOD1 protein expression was slightly increased by rotenone ($p > 0.05$) and diminished following buspirone treatment (## $p < 0.01$ at both 1 and 10 mg/kg; **Figures 5K & L**). Similar to the midbrain and striatum, SOD1 mRNAs were not affected by rotenone and/or buspirone treatments in the amygdala (**Figure 5N**). However, at the protein level we observed a significant increase of SOD1 expression after rotenone exposure (**** $p < 0.0001$ Vs vehicle), which was prevented by co-treatment with the highest

dosage of buspirone (#### p < 0.0001 Vs rotenone; **Figure 5O & P**). Lastly, hippocampal SOD1 mRNA levels were significantly increased by rotenone (**** p < 0.0001 Vs vehicle) and fully prevented by co-administration with buspirone at all dosages (#### p < 0.0001 Vs rotenone; **Figures 5R**). Transcript results were corroborated by protein findings, as SOD1 protein expression was induced by rotenone (* p < 0.05 Vs vehicle) and mitigated by buspirone (# p < 0.05 Vs rotenone at 1 and 3 mg/kg, ## p < 0.01 Vs rotenone at 10 mg/kg; **Figures 5S & T**).
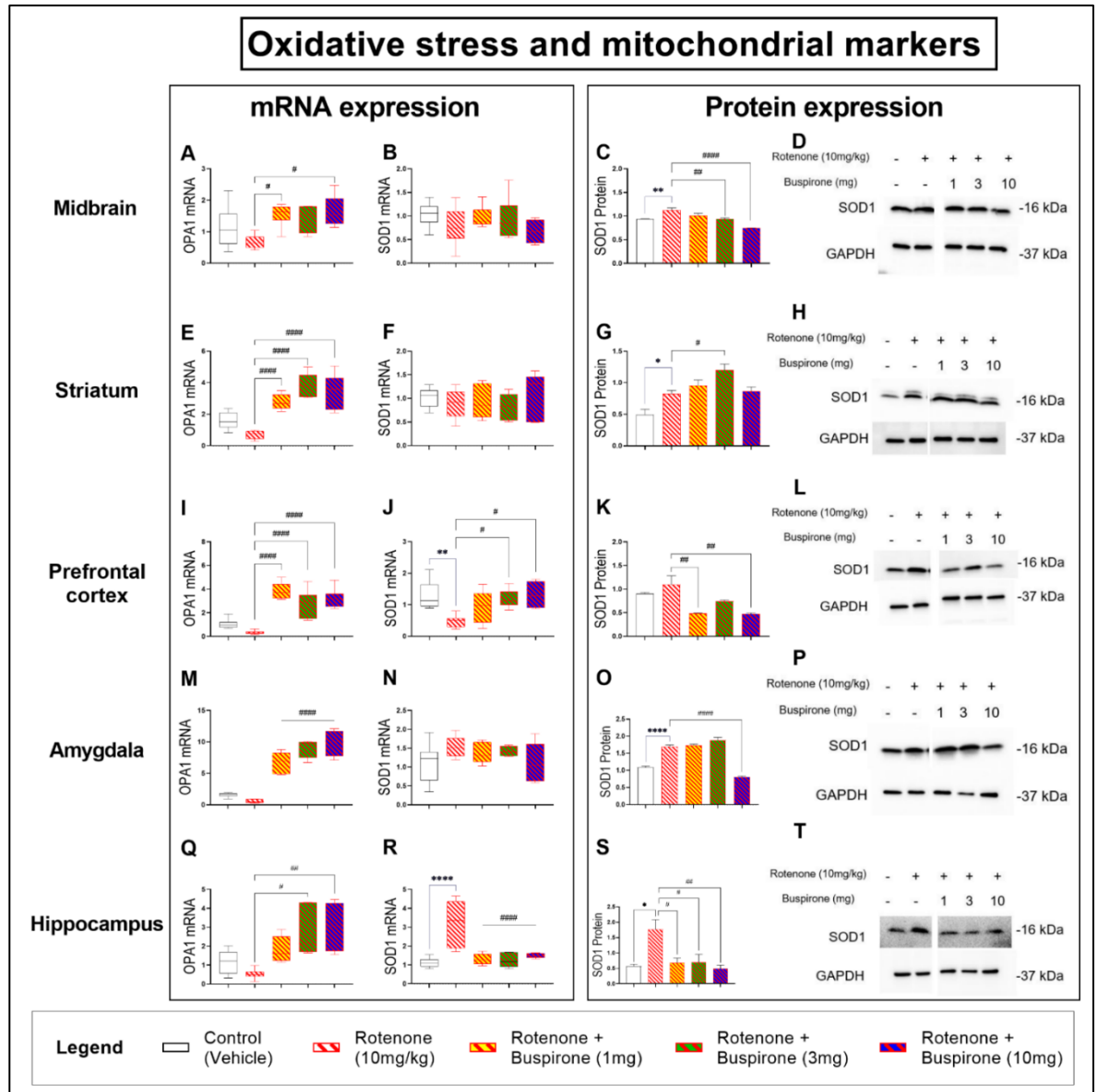
Figure 5. Buspirone dampens rotenone-induced oxidative stress in the brain.

The mitochondrial marker, OPA1, was analysed to determine rotenone-induced mitochondrial damage and the antioxidant enzyme SOD1 was investigated as an indirect measure of oxidative stress. Real-time qPCR analyses of OPA1 and SOD1 mRNA expression in the midbrain (**A-B**), striatum (**E-F**), prefrontal cortex (**I-J**), amygdala (**M-N**) and hippocampus (**Q-R**) following administration of rotenone (10mg/kg) and/or buspirone (1, 3 or 10mg) daily for 21 days. Fold-changes were

calculated using the ΔΔCt method after normalization to s18 (ribosomal protein s18 gene), the housekeeping gene. Each data point represents the mean value from n = 5-8 mice per each group. Representative Western blots and densitometry of SOD1 protein expression in the midbrain (**C-D**), striatum (**G-H**), prefrontal cortex (**K-L**), amygdala (**O-P**) and hippocampus (**S-T**). Protein expression was normalized to GAPDH, the loading control. Western blots are cropped and removed lanes are included in supplementary 5. Densitometric results are expressed as mean ± S.E.M from n = 5-8 mice per each group. *$p < 0.05$, **$p < 0.01$, ***$p < 0.001$ or ****$p < 0.0001$, compared to vehicle-treated controls; or # $p < 0.05$, ## $p < 0.01$, ### $p < 0.001$ or ####$p < 0.0001$, compared to rotenone (10mg/kg) treated mice, as determined by ANOVA followed by Dunnett's post-hoc test. OPA1: Mitochondrial dynamin like GTPase; SOD1: superoxide dismutase 1; s18: ribosomal protein s18 gene; GAPDH: glyceraldehyde 3-phosphate dehydrogenase; kDa: Kilodalton.

2.6 Buspirone prevents PACAP and VIP neuropeptides dysregulations in the brain of rotenone-treated mice

The neuropeptides PACAP and VIP are involved in a range of neuroprotective and immune modulatory functions in the CNS [234]. We have previously shown that genetic blockade of the D3R promotes the expression of PACAP [114]. To determine if buspirone, a D3R antagonist, altered the expression of these peptides during rotenone intoxication, we analysed their gene and protein expression throughout the brain (**Figure 6**).

In the midbrain, rotenone exposure alone had no effects on PACAP mRNAs ($p >$ 0.05 Vs vehicle); however, the highest dosage of buspirone reduced gene expression (# $p < 0.05$ Vs rotenone; **Figure 6A**). Protein analyses did not show significant changes in PACAP protein expression in response to rotenone and/or buspirone co-treatment ($p > 0.05$; **Figures 6C & D**). In the striatum, PACAP mRNAs were slightly reduced and co-treatment with buspirone prevented these effects, although not significantly ($p > 0.05$ Vs rotenone; **Figure 6F**). In contrast, PACAP protein expression was robustly increased by rotenone in the striatum (**** $p < 0.0001$ Vs vehicle) and buspirone reduced the expression at 3 and 10 mg/kg (# $p < 0.05$ and #### $p < 0.0001$ Vs rotenone; **Figures 6H & I**). In the prefrontal cortex, PACAP transcripts were down-regulated in response to rotenone (* $p < 0.05$ Vs vehicle). Co-treatment with buspirone significantly increased gene expression (# $p < 0.05$ Vs rotenone; **Figure 6K**). At the protein level, PACAP showed no changes after rotenone exposure; however, buspirone co-treatment significantly reduced PACAP protein expression (#### $p < 0.0001$ Vs rotenone; **Figures 6M & N**). In the amygdala, rotenone did not modify the mRNA expression of PACAP ($p > 0.05$ Vs vehicle), however, a significant induction was seen after 1 mg/kg buspirone co-administration (## $p < 0.01$ Vs rotenone; **Figure 6P**). In contrast, PACAP protein analyses showed that rotenone strongly increased protein expression (**** $p < 0.0001$ Vs vehicle), and levels were remarkably diminished in the amygdala of mice co-treated with both rotenone and buspirone (# $p < 0.05$ at 1 mg/kg and #### $p < 0.0001$ Vs rotenone at 3 and 10 mg/kg, respectively; **Figures 6R & S**). Hippocampal PACAP transcripts were only modestly reduced by rotenone ($p > 0.05$ Vs vehicle) and significantly increased in response to 3 mg/kg buspirone (## $p < 0.01$ Vs rotenone; **Figure 6U**). At the protein level, PACAP was significantly

reduced by rotenone (* $p < 0.05$ Vs vehicle) and reliably increased by buspirone (#### $p < 0.0001$ at 1 and 3 mg/kg, ## $p < 0.01$ Vs rotenone at 10 mg/kg; **Figures 6W & X**).

Analyses of VIP transcripts in the midbrain revealed a significant reduction in gene expression after rotenone exposure (** $p < 0.01$ Vs vehicle), which was not ameliorated by buspirone co-treatment ($p > 0.05$ Vs rotenone; **Figure 6B**). However, Western blot did not support these results, as VIP expression was up-regulated by rotenone (* $p < 0.05$ Vs vehicle) and not further affected by buspirone ($p > 0.05$ Vs rotenone; **Figures 6C & E**). We did not observe any significant transcript changes in the striatum ($p > 0.05$; **Figure 6G**), whereas protein results showed that buspirone significantly reduced VIP expression (### $p < 0.001$ at 1 mg/kg, #### $p < 0.0001$ Vs rotenone at 3 and 10 mg/kg; **Figures 6H & J**). In the prefrontal cortex, VIP mRNAs were reduced by rotenone (** $p < 0.01$ Vs vehicle) and returned to control levels upon buspirone co-treatment (## $p < 0.01$ and ### $p < 0.001$ at 3 and 10 mg/kg, respectively; **Figure 6L**). However, these results were not confirmed by Western blots, as VIP expression was unchanged in response to treatments ($p > 0.05$; **Figures 6M & O**). In the amygdala, VIP mRNA expression was not affected by rotenone treatment ($p > 0.05$ Vs vehicle); however, transcripts were up-regulated by buspirone (### $p < 0.001$ Vs rotenone; **Figure 6Q**). Instead, VIP protein expression was up-regulated by rotenone (*** $p < 0.001$ Vs vehicle) and robustly reduced upon buspirone co-administration (#### $p < 0.0001$ Vs rotenone at all dosages; **Figures 6R & T**). Finally, hippocampal VIP mRNA levels were unchanged after rotenone and/or buspirone co-treatment ($p > 0.05$; **Figure 6V**). However, VIP protein expression was reduced in the hippocampus of mice co-

191

treated with rotenone and buspirone (### $p < 0.001$ at 1 mg/kg, ## $p < 0.01$ at 3 mg/kg and #### $p < 0.0001$ Vs rotenone at 10 mg/kg; **Figures 6W & Y**).
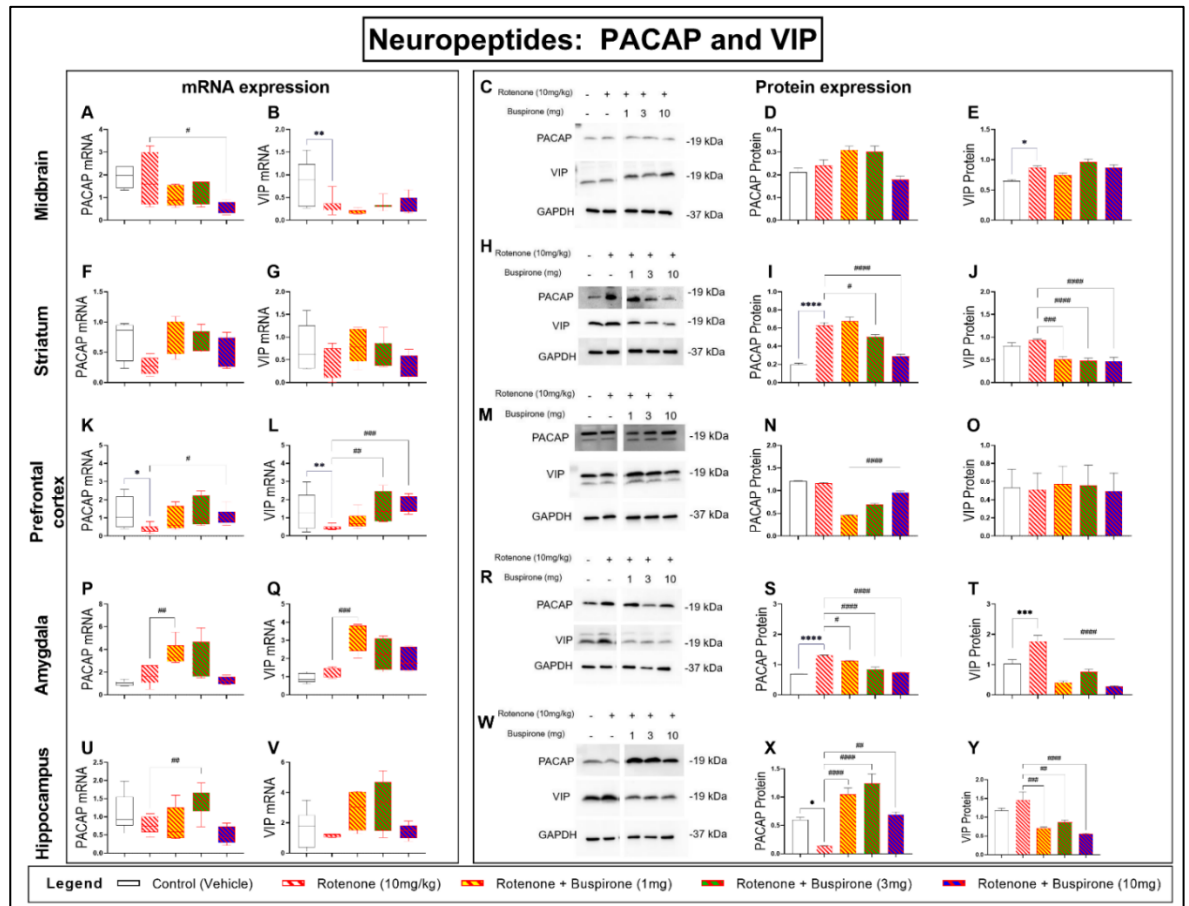
Figure 6. Buspirone prevents PACAP and VIP neuropeptides dysregulations in the brain of rotenone-treated mice. Real-time qPCR analyses of PACAP and VIP mRNA expression in the midbrain (**A-B**), striatum (**F-G**), prefrontal cortex (**K-L**), amygdala (**P-Q**) and hippocampus (**U-V**) following administration of rotenone (10mg/kg) and/or buspirone (1, 3 or 10mg) daily for 21 days. Fold-changes were calculated using the ΔΔCt method after normalization to s18 (ribosomal protein s18 gene), the housekeeping gene. Each data point represents the mean value from n = 5-8 mice per each group. Representative Western blots and densitometry of PACAP

and VIP protein expression in the midbrain (**C-E**), striatum (**H-J**), prefrontal cortex (**M-O**), amygdala (**R-T**) and hippocampus (**W-Y**). Protein expression was normalized to GAPDH, the loading control. Western blots are cropped and removed lanes are included in supplementary 6. Densitometric results are expressed as mean ± S.E.M from n = 5-8 mice per each group. $*p < 0.05$, $**p < 0.01$, $***p < 0.001$ or $****p < 0.0001$, compared to vehicle-treated controls; or # $p < 0.05$, ## $p < 0.01$, ### $p < 0.001$ or ####$p < 0.0001$, compared to rotenone (10mg/kg) treated mice, as determined by ANOVA followed by Sidak's post-hoc test. PACAP: pituitary adenylate cyclase-activating peptide; VIP: vasoactive intestinal peptide; s18: ribosomal protein s18 gene; GAPDH: glyceraldehyde 3-phosphate dehydrogenase; kDa: Kilodalton.

3. Discussion

Pharmacological blockade of the D3R has previously been shown to reduce inflammation and consequently slow disease progression in animal models of PD [159]. Interestingly, computational analyses have identified buspirone as a drug with strong off-target function as a D3R antagonist [192]. In addition, we previously demonstrated that either genetic deletion or buspirone treatment reliably attenuated LPS-triggered microglial polarization in BV2 cells, an effect that was not seen in D3R knockout (D3R$^{-/-}$) microglia [315]. This led us to test the efficacy of buspirone to reduce inflammation and promote neuroprotection in a rotenone mouse model of PD.

To our knowledge, this is the first study to investigate the ability of buspirone to prevent inflammation and promote neuroprotection in a model of PD. We report that buspirone prevented rotenone-induced deficits in locomotor and exploratory behaviour and dose-dependently rescued dopaminergic degeneration in the *substantia nigra pars compacta,* midbrain and striatum. Interestingly, buspirone also prevented glial activation in a brain region-specific pattern. Concurrently, the drug robustly prevented rotenone-induced up-regulations of pro-inflammatory cytokines and increased the expression of neurotrophic and anti-inflammatory factors, suggesting that buspirone is able to afford some of its beneficial effects by modulating the immune response and promoting the release of protective factors. Additionally, buspirone restored levels of the mitochondrial marker OPA1 and of the antioxidant enzyme SOD1, and prevented the disruptions to the two neuroprotective and immune modulatory peptides PACAP and VIP throughout the brain.

Several studies have described behavioural deficits in mice resulting from systemic administration or rotenone [55, 57, 60, 298]. These studies, consistent with current findings using 10 mg/kg rotenone, indicate that a three-week induction regime using this dosage of pesticide is sufficient to attain locomotor impairments consistent with a PD-like pathology. Previous studies on D3R^{-/-} mice revealed that this dopamine receptor subtype mediates inhibitory effects on aversive learning [113] and both spontaneous and forced ethanol consumption in mice [192]. However, in this study we did not observe any specific changes in general locomotor and exploratory behaviour, nor in the dopaminergic activities of mice treated with buspirone alone (**Supplementary Figures 1 & 2**), in contrast to

194

previous reports from other laboratories using rats [320]. However, when the drug was co-administered with rotenone at the highest dosages (3 and 10 mg/kg), it successfully prevented the behavioural impairments caused by the pesticide. As such, it is conceivable that any preventative effect of buspirone on rotenone-induced behavioural impairments was likely to be attributed to its widespread restorative capacity in the CNS. Interestingly, similar anxiolytic and motor effects have been previously reported in mice treated with minocycline, a tetracycline antibiotic endowed with anti-inflammatory functions, further suggesting that agents able to attenuate inflammation may also be effective in preventing behavioural deficits [80]. These effects are likely to be attributed to buspirone-mediated D3R antagonistic activity, as our results corroborate prior evidence of reduced anxiety-like behaviour in D3R$^{-/-}$ mice [193]. Unfortunately, buspirone's ameliorative effects on locomotor activity in rodents were not translated into a clinical setting, as PD patients subjected to buspirone drug regime showed a poor response in terms of anxiolytic response [321]. However, this study was designed to assess buspirone's anxiolytic effect in PD patients, and an overall efficacy was reported with poor translation related to concomitant anxiolytics and PD therapy, with the authors suggesting buspirone monotherapy should be considered. This species-specific diversity in drug response could be due to the different D3R Vs D2R distribution in the CNS between mice and humans. Additionally, given that buspirone also binds to D2R (with much lower affinity than D3R) to antagonize receptor activation [321], it is also possible that drug-induced D2R blockade in humans (but not in rodents) may elicit some anti-psychotic effects that, however, are not accompanied by improvements on motor function, as shown in other studies [216]. It is the high homology between D2R and D3R that renders the development of specific D3R

antagonists challenging and often results in mixed effects. Further refining of the drug to enhance receptor selectivity may be a viable strategy to overcome this unwanted effect. However, it should be noted that the lack of motor improvements in PD patients is not necessarily paralleled by the lack of other critical disease-modifying effects of the drug, such as the reduced neuroinflammation and increased trophic support reported in this study. In addition, we cannot exclude that some of buspirone's inherent activities may be related to the ability of the drug in promoting glial activation and trophic factor expression in certain CNS regions (**Supplementary Figures 3 – 6**), whose significance warrants additional investigations. Furthermore, the neuroprotective effects can also be attributed to its canonical 5HT1a agonist activity, which may act synergistically to the D3R to improve the neurochemical disbalances seen in PD.

The landmark study by Elgueta et al. [159] demonstrated that pharmacological antagonism of the D3R reduced the extent of dopaminergic degeneration in an MPTP model of PD [159]. We report a similar dose-dependent protection of dopaminergic neurons in response to 10mg/kg buspirone. This finding corroborates the hypothesis that high dosages of buspirone are required to achieve enough D3R occupancy [230]. The protection of dopaminergic neurons is suggested to be secondary to buspirone's ability to reduce neuroinflammation. Accordingly, we analysed the expression of glial activation markers, inflammatory cytokines and neurotrophic factors in distinct brain regions to determine how buspirone modulates the immune response in the brain.

Gao and colleagues [318] revealed that the presence of microglia greatly enhanced the neurodegenerative and neurotoxic effects of rotenone by increasing the susceptibility of neuron-enriched cultures to the toxin. In line with this study, we show that rotenone treatment induced the up-regulation of microglial activation markers and pro-inflammatory cytokines. Previously, our laboratory has shown that D3R gene deletion and/or buspirone treatment prevented LPS-triggered microglial activation [315]. Here, we sought to determine if buspirone could exert similar effects *in vivo*. Therefore, we interrogated the expression of glial activation markers along with that of pro-inflammatory cytokines and neurotrophic factors. In contrast to our *in vitro* study, here we observed a drug-induced reduction of Iba1 expression in the midbrain and amygdala, and an increase in the prefrontal cortex compared with mice treated receiving rotenone-alone. Unexpectedly, these results were accompanied by a global increase in CD11b transcripts, which contrasts with Iba1 response to the anxiolytic drug. These differences in the expression of glial activation markers could be due to the acquisition of differing microglial phenotypes during the course of PD. It is known that activated microglia exist in two main phenotypes, M1, considered pro-inflammatory and M2 considered anti-inflammatory [322]. Depending on disease severity and the local CNS inflammatory state, microglia may present as heterogeneous subpopulations that may or may not benefit from the anti-inflammatory effects of the drug, although this remains to be ascertained. This theory would explain why we saw a region-specific variability in the expression of glial activation markers.

Buspirone also produced a robust down-regulation of the pro-inflammatory cytokines IL-1β and IL-6. This was accompanied by a global up-regulation of the

anti-inflammatory marker Arg1, as well as a remarkable increase in the expression of neuroprotective and neurotrophic/growth factors, all known to exert a range of protective effects in the CNS [309]. Rotenone is known to reduce the expression of BDNF in vulnerable CNS regions [323]. This was partly seen in the hippocampus and amygdala, whereas levels were increased in the midbrain and prefrontal cortex. Irrespective of how BDNF transcript were regulated by rotenone in the different CNS sites, buspirone prevented these changes. These results suggest that the drug is able to promote neuroplasticity, cell survival and perhaps axonal growth during rotenone toxicity [324]. This is corroborated by significant and robust induction of ADNP in all the brain regions we studied. ADNP is also essential in neuronal survival and brain formation and is dysregulated in neurodegenerative and neuroinflammatory diseases [325]. The combined cytokine and neurotrophic profiles reported in this study indicate that buspirone favours the adoption of the M2 phenotype that promotes the dampening of neuroinflammation, CNS repair and neuroprotection [79]. This agrees with our *in vitro* study that showed that D3R$^{-/-}$ and/or buspirone treatment inhibited M1 markers, including NO, NOS2, IL-1β and TNF-α [315]. However, microglia are not the only glial cell type mediating the immune response. They work closely with astrocytes, however more studies are needed to elucidate the role of buspirone on astrocytes. We report minimal changes in the expression of the astrocytic marker, GFAP. This correlates with analysis of GFAP-positive cells and morphology in D3R$^{-/-}$ mice that did not differ to wild-type animals [223] suggesting the anti-inflammatory effect observed is primarily the result of buspirone's activity on microglia and perhaps, other immune cells. This contrasts another study that reported D3R antagonism reduces neuroinflammation response of astrocytes [326]. To determine the role of

buspirone on astrocytes, primary astrocytic cultures could be used, or isolating astrocytes from mouse brains could extrapolate the phenotype of astrocytes in this model. However, it has been shown that the neuroprotective effects of 5HT1a agonism are mediated by astrocytes, which prevent dopaminergic degeneration in parkinsonian mice [327]. This suggests that the 5HT1a agonist activity of buspirone may also contribute to the neuroprotective effects reported in this study. 5HT1a agonists, including buspirone, have been reported as effective neuroprotective agents in traumatic brain injury [233]. The role of the serotonin system in PD is being revealed with some studies suggesting 5HT1a receptor could be a target alone for improving both motor function [328] and microglial responses [266].

Rotenone toxicity is mediated by its inhibitory action on mitochondria which ultimately results in oxidative stress [49]. To determine if the effects of buspirone were due to rotenone intoxication, we analysed the expression of OPA1, a mitochondrial marker, and SOD1, an antioxidant enzyme as indirect evidence of oxidative stress. As expected, rotenone significantly reduced the expression of OPA1, indicating mitochondrial dysfunction. This was also verified by the up-regulation of SOD1 throughout the various CNS regions. The widespread distribution of rotenone intoxication suggests this model may be capturing additional prodromal dysfunctions of the disease, as changes in extra-nigral regions correlated with changes in CNS regions that are associated with some of the non-motor symptoms that usually remain silent or do not clinically manifest until motor symptoms appear [7, 292, 307]. This could also explain the lack of glial activation, which is commonly observed in the late stages of the disease due to a chronic neuroinflammation.

PACAP and VIP have both been shown to promote neuroprotection and reduce inflammation in several models of PD [329]. Notably, in primary rat mesencephalic neuron-glia cultures, PACAP prevented microglial polarization and protected against LPS-induced DAergic neurotoxicity [330]. This aligns with our recent study demonstrating the ability of these peptides to reduce LPS-induced inflammation and promote unique microglial phenotypes *in vitro* [240]. We have previously shown that D3R deletion enhances the expression of theses peptides [114]. The upregulation of neuroprotective growth factors and peptides by buspirone provides additional evidence of its neuroprotective activity and therapeutic potential in neurodegenerative diseases; however, further investigations on the exact role exerted by these protective agents with respect to the specific brain regions remains a topic of further investigation.

4. Materials and Methods

4.1. Animal experiments

Seventy-two 7-week-old C57BL/6 male mice were purchased from ARC (Perth, WA, Australia). Mice were housed in individually ventilated cages (4 mice per cage), under normal 12:12 h light/dark cycle, with access to food and water ad libitum. All experiments were conducted in line with the Australian Code of Practice for the Care and Use of Animals for Scientific Purposes. All animal experiments were approved by the University of Technology Sydney Animal Care and Ethics Committee (ETH19-3322).

Table 1. Summary of treatment groups of study.

Group	Parkinson's disease	Buspirone
1	Saline (vehicle)	Saline (vehicle)
2	Rotenone 10mg/kg	Saline (vehicle)
3[1]	Saline (vehicle)	Buspirone 1mg/kg
4[1]	Saline (vehicle)	Buspirone 3mg/kg
5[1]	Saline (vehicle)	Buspirone 10mg/kg
6	Rotenone 10mg/kg	Buspirone 1mg/kg
7	Rotenone 10mg/kg	Buspirone 3mg/kg
8	Rotenone 10mg/kg	Buspirone 10mg/kg

[1] Buspirone control groups (groups 3-5) are included as supplementary data.

4.2 Experimental protocol

Rotenone was prepared as a stock solution in 0.1% DMSO diluted in 0.1% saline. 0.1% DMSO was added to Parkinson's disease saline treatment groups (Groups 1, 3-5) as a control. Buspirone was prepared as a stock solution in 0.1% saline. The experimental regime (**Figure 7**) lasted for 21 days, and involved daily intraperitoneal injections (i.p) of rotenone or saline, followed 2h later by buspirone

or saline, also administered by intraperitoneal injection. Mice were weighed daily and were subjected to the open field test every 7 days to assess locomotor and exploratory behaviour. On day 22, mice were sacrificed and brains were collected. Brains were either snap frozen for molecular analysis or fixed in 4% paraformaldehyde for immunohistochemical analysis. Brains for molecular analysis were micro dissected into the following regions: prefrontal cortex, striatum, amygdala, hippocampus and midbrain.
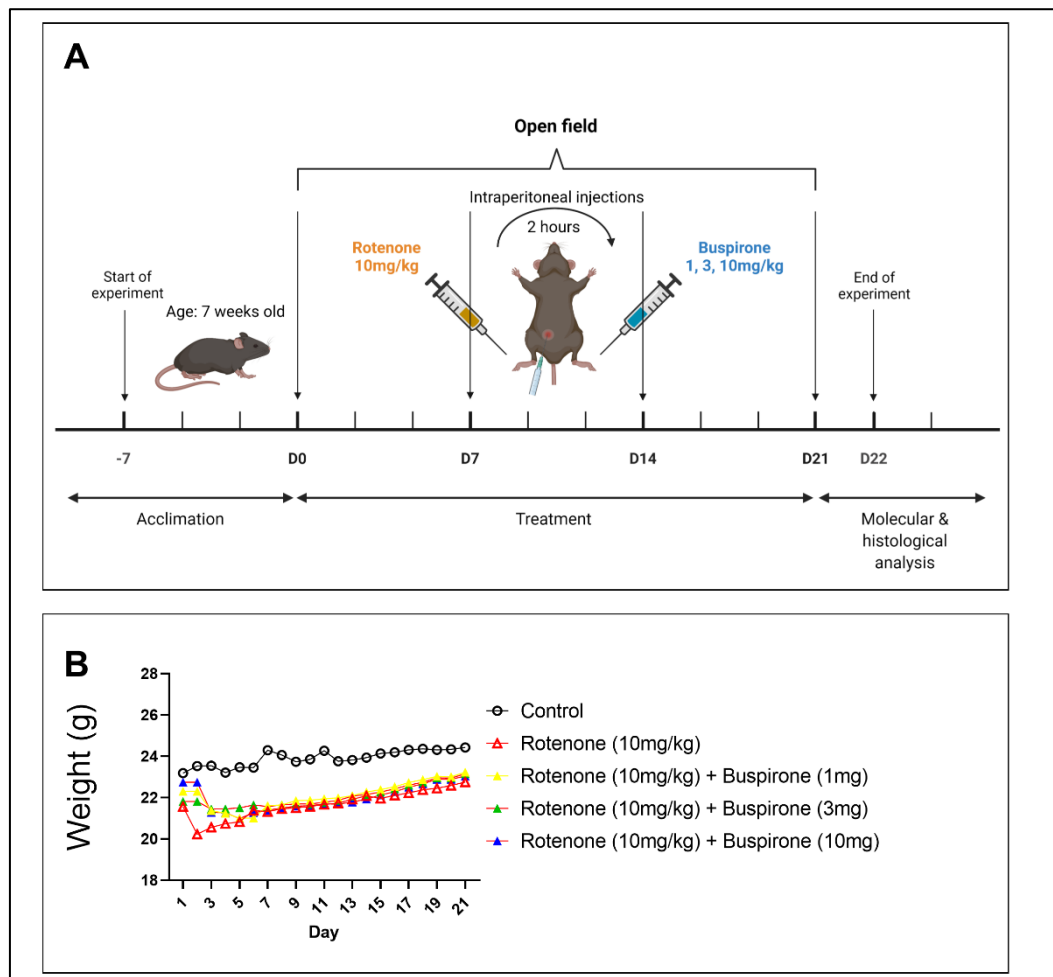

Figure 7. Experimental timeline. (**A**) Schematic of experimental timeline of injection regimen. 7-week-old C57BL/6 male mice were allowed to acclimate for

one-week. Mice were exposed to daily intraperitoneal injections of rotenone 10mg/kg followed 2h later by 1, 3, or 10mg buspirone for 21 days. At baseline, mice were subjected to the open field for locomotor and exploratory behavioural assessment, and again on days 7, 14 and 21. On day 22, mice were euthanised and brains were collected for molecular and histological analysis. (**B**) Mice were weighed daily to monitor health and well-being. Data represented as daily average. N = 8-12 mice per group.

4.3 Open field

The open field (OF) test was performed every 7 days. Baseline measurements were performed prior to any intervention. Animals were acclimated in the testing room for 30 mins for habituation. The OF was conducted in the dark using a square box made of grey Plexiglass plastic (30 x 30 x 30 cm). Individually, mice were placed in the centre of the OF and allowed to freely explore for 5 min while being recorded. The OF was cleaned thoroughly between each mouse to eliminate excretions and any odour cues using 70% ethanol and allowed to air dry. The FIJI/ImageJ Plugin MouBeAt software [283] was used to analyse videos. Locomotor activity was determined by the total distance travelled and average speed of the mice, as calculated by MouBeAt. Exploratory behaviour was defined as the number of times a mouse entered the centre of the OF and the time spent in the centre.

4.4 Real-time quantitative polymerase chain reaction (RT-qPCR)

Total RNA was extracted using TRI-reagent and precipitated with 2-propanol following established protocols [331]. Single-stranded cDNA was synthesized using

the Tetro cDNA synthesis kit (Bioline, Sydney, NSW, Australia) as per

manufacturer's instructions. Real-time qPCR was performed to analyse the mRNA

levels of 12 genes (**Table 2**). The ribosomal protein 18S was used as the

housekeeping gene. Each reaction consisted of 3μL cDNA (final concentration

100ng), 5μL iTaq Universal SYBR Green Master Mix (BioRad), 0.8μL of forward

and reverse primers. To examine changes in expression, the mean fold changes of

each sample was calculated using the ΔΔCt method as previously described [315].

PCR product specificity was evaluated by melting curve analysis, with each gene

showing a single peak (data not shown).

Table 2. List of primer sets used in real-time qPCR analysis. Forward and reverse primers were selected from the 5' and 3' region of each gene. The expected length of each amplicon is indicated in the right column.

Accession #	Gene	Primer sequence (5'-3')	Length (bp)
NM_009377.3	Tyrosine hydroxylase (TH)	Fwd GCCCTACCAAGATCAAACCTAC Rev ATACGAGAGGCATAGTTCCTGA	93
NM_010020.3	Dopamine transporter (DAT)	Fwd ATGACATCAAGCAGATGACTGG Rev CACGACCACATACAGAAGGAAG	95
NM_001131020.1	Glial fibrillary acidic protein (GFAP)	Fwd GAGATTCGCACTCAATACGAGG Rev CTGCAAACTTAGACCGATACCA	79
NM_001082960.1	CD11b	Fwd GAGCAGGGGTCATTCGCTAC Rev GCTGGCTTAGATGCGATGGT	94
NM_008361.4	Interleukin-1β (IL-1β)	Fwd GCTACCTGTGTCTTTCCCGT Rev CATCTCGGAGCCTGTAGTGC	164
NM_007482.3	Arginase-1 (Arg1)	Fwd ACAAGACAGGGCTCCTTTCAG Rev TTAAAGCCACTGCCGTGTTC	105
NM_011434.2	Superoxidase dismutase (SOD1)	Fwd CAATGGTGGTCCATGAGAAACA Rev CCCAGCATTTCCAGTCTTTGTA	77
NM_001199177.1	Mitochondrial dynamin like GTPase (OPA1)	Fwd GCCCTTCTCTTGTTAGGTTCAC Rev ACACCTTCCTGTAATGCTTGTC	88
NM_007540.4	Brain derived neurotrophic factor (BDNF)	Fwd CGAGTGGGTCACAGCGGCAG Rev GCCCCTGCAGCCTTCCTTGG	160
NM_001310086.1	Activity-dependent neuroprotective protein (ADNP)	Fwd GTGACATTGGGTTGGAATACTGT Rev AGGTTTTGTCCGATAGTCCTGA	149
NM_016989.2	Pituitary adenylate cyclase-activating polypeptide (PACAP)	Fwd AGGCTTACGATCAGGACGGA Rev CTCCTGTCGGCTGGGTAGTA	121
NM_053991.1	Vasoactive intestinal peptide (VIP)	Fwd CCTGGCGATCCTGACACTCT Rev CTGCAGCCTGTCATCCAACC	100
NM_213557.1	18S ribosomal subunit (s18)	Fwd GGCGGAAAATAGCCTTCGCT Rev AGCCCTCTTGGTGAGGTCAA	101

4.5 Western blot

Protein was extracted by homogenizing tissues in radioimmunoprecipitation assay (RIPA) buffer as previously described and quantified using the bicinchoninic acid assay (Pierce BCA Protein Assay Kit, ThermoFisher Scientific, VIC, Australia). 30 µg of protein was separated by SDS-polyacrylamide gel electrophoresis (SDS-PAGE) using 4-20% Mini-PROTEAN TGX Stain-Free Gels (15 well, BioRad, VIC, Australia). The Precision Plus Protein Prestained Standard in All Blue (BioRad, VIC, Australia) was included for comparison. Transfer to a PVDF membrane was performed using the semi-dry method (BioRad Trans-Blot Turbo Transfer System). Primary antibodies were incubated overnight in 5% skim milk in TBST blocking solution at 4°C. Antibodies and dilutions are summarized in **Table 3**. Membranes were incubated in secondary antibody 1 hr at RT. Western blots were visualized using chemiluminescence BioRad Clarity Western ECL Blotting Substrate Solution. Images were acquired using the BioRad ChemiDoc MP System. Images were analysed using Fiji ImageJ and ratios normalized to GAPDH which was used as a loading control.

Table 3. Antibodies used in western blot and immunohistochemistry.

Antibody	Dilution	Source (Cat. #)
Tyrosine hydroxylase (TH)	1:200 (WB) 1:500 (IHC-P)	Abcam (ab112)
Dopamine transporter (DAT)	1:1000	Abcam (ab128848)
Glial fibrillary acidic protein (GFAP)	1:1000	Abcam (ab68428)
Ionized calcium binding protein (Iba1)	1:1000	Sigma Aldrich (SAB2702364)
Mitochondrial dynamin like GTPase (OPA1)	1:1000	GeneTex (GTX129917)
Superoxidase dismutase (SOD1)	1:1000	GeneTex (GTX100554)
Pituitary adenylate cyclase-activating polypeptide (PACAP)	1:1000	GeneTex (GTX37576)

Vasoactive intestinal peptide (VIP)	1:1000	GeneTex (GTX129461)
Glyceraldehyde-3-phosphate dehydrogenase (GAPDH)	1:1000	BioRad (VPA00187)
Goat anti-Rabbit IgG HRP	1:10 000	BioRad (STAR208P)
Goat anti-Mouse IgG (H+L)-HRP	1:10 000	BioRad (1706516)

WB: western blot; IHC-P: immunohistochemistry on paraffin embedded tissue.

4.6 Immunohistochemistry

Brains were fixed in 4% paraformaldehyde at 4°C for 48 h before dehydration and embedding in paraffin. 5 µM thick coronal sections were cut with a microtome and mounted on glass slides. The sections were deparaffinised in xylene and rehydrated through decreasing concentrations of ethanol. Dopaminergic neurons were labelled with TH. The immunoreactivity of TH was visualized using the Rabbit specific HRP/DAB (ABC) Detection IHC Kit (ab64261, Abcam, VIC, Australia) according to manufacturer's protocol. Negative controls were created for all regions analysed by not incubating with the primary antibody. Hematoxylin was used as a counterstain to visualize nuclei. Sections were dehydrated in increasing concentrations of ethanol and xylene before being mounted. Images were taken on a ZEISS AxioScan.Z1 at x20 magnification. Fiji ImageJ was used for the semi-quantification of DAB-positive cells normalized to nuclei (hematoxylin stain) [332].

4.7 Statistical analysis

All data is reported as mean ± SEM. Statistical analyses were calculated using GraphPad Prism software ver. 9.0.2. (GraphPad Software, La Jolla, CA). Comparisons between two or more groups were analysed by ANOVA followed by

Dunnett's or Sidak's post-hoc tests. p-values ≤ 0.05 were considered statistically significant.

5. Conclusions

In conclusion, our results corroborate the idea that D3R receptor blockage may serve as a neuroprotective and anti-inflammatory mechanism to attenuate PD burden. Buspirone effectively prevented rotenone-induced behavioural deficits and dose-dependently protected dopaminergic neurons from the detrimental effects of rotenone intoxication. Buspirone mitigated rotenone toxicity throughout the brain, mainly by alleviating mitochondrial dysfunction, reducing inflammation and promoting the expression of neuroprotective factors, including anti-inflammatory cytokines, neurotrophic and growth factors and neuropeptides. Overall, this evidence suggests that buspirone may be a viable candidate for drug repurposing, as its anti-inflammatory and neuroprotective effects may prevent disease severity and progression in patients with neurodegenerative/neuroinflammatory conditions such as PD.

Supplementary Materials: The following are available online at www.mdpi.com/xxx/s1, Figure S1: Locomotor and exploratory behaviour of treatment controls, Figure S2: Buspirone alone did not disturb the expression of nigro-striatal dopamine markers, Figure S3: Buspirone treatment activated glial cells, Figure S4: Buspirone treatment alone reduced basal levels of inflammatory cytokines and up-regulated neurotrophic factors, Figure S5: Buspirone promoted mitochondrial function and upregulated the expression of anti-oxidant enzymes, Figure S6: Buspirone alters the expression profile of the neuropeptides PACAP and VIP.

Supplementary Figures (1-6) and Figure Legends

Supplementary Figure 1. Locomotor and exploratory behaviour of locomotor controls. Mice were weighed daily to monitor health and well-being (**A**). The open field (OF) test was used to assess for locomotor and exploratory behaviour in mice overtime. Representative heat maps generated from MouBeAt Software illustrating movement of mice during 5 min in OF (**B**). Exploratory behaviour was examined by the number of times (**C**) and the total time (**D**) a mouse spent in the entre quadrant (inner white square on heat maps). Locomotor activity was assessed by comparing the total distance travelled (**E**) and average speed (**F**). Comparisons were made

within the same treatment group compared to baseline measurements. Data shown

represents 7-12 mice per group. p ≤ 0.05 was considered statistically significant, as

determined by one-way ANOVA followed by Dunnett's post-hoc test.
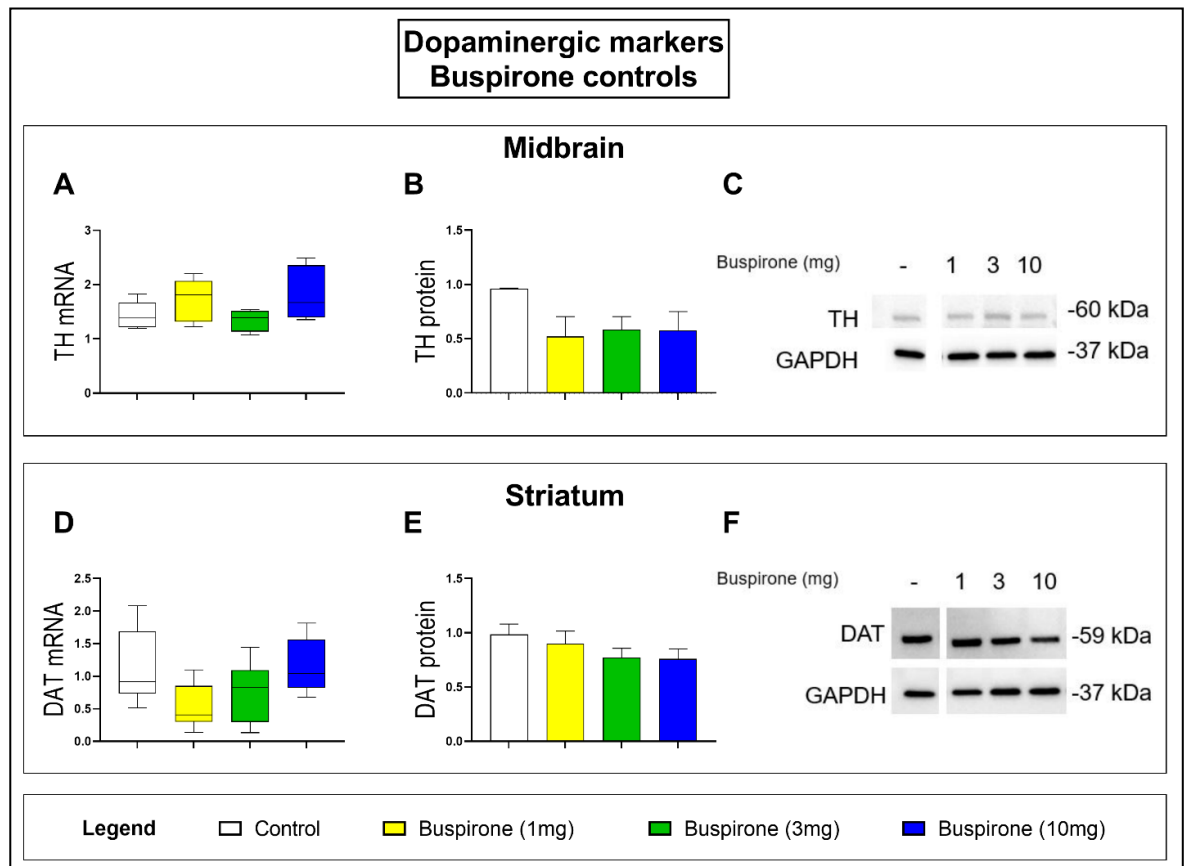
Supplementary Figure 2. Buspirone alone did not disturb the expression of

nigro-striatal dopaminergic markers. TH mRNA (**A**) and protein expression (**B-**

C) in the midbrain. Striatal DAT mRNA (**D**) and protein expression (**E-F**). Gene

expression was measured by qRT-PCR and quantified using the ΔΔCt method

after normalization to s18 (the housekeeping gene). qRT-PCR results are reported

as mean fold changes with respect to vehicle-treated control mice. Protein

expression was determined by western blot and normalized to GAPDH (the loading

control). Western blots show lanes removed from in text figure 2. Densitometry

results presented as mean ± S.E.M. Data represents 3-4 mice per group. p ≤ 0.05

was considered statistically significant, as determined by one-way ANOVA followed by Dunnett's post-hoc test. TH: tyrosine hydroxylase; DAT: dopamine transporter; GAPDH: glyceraldehyde 3-phosphate dehydrogenase; kDa: Kilodalton; s18: ribosomal protein s18 gene.
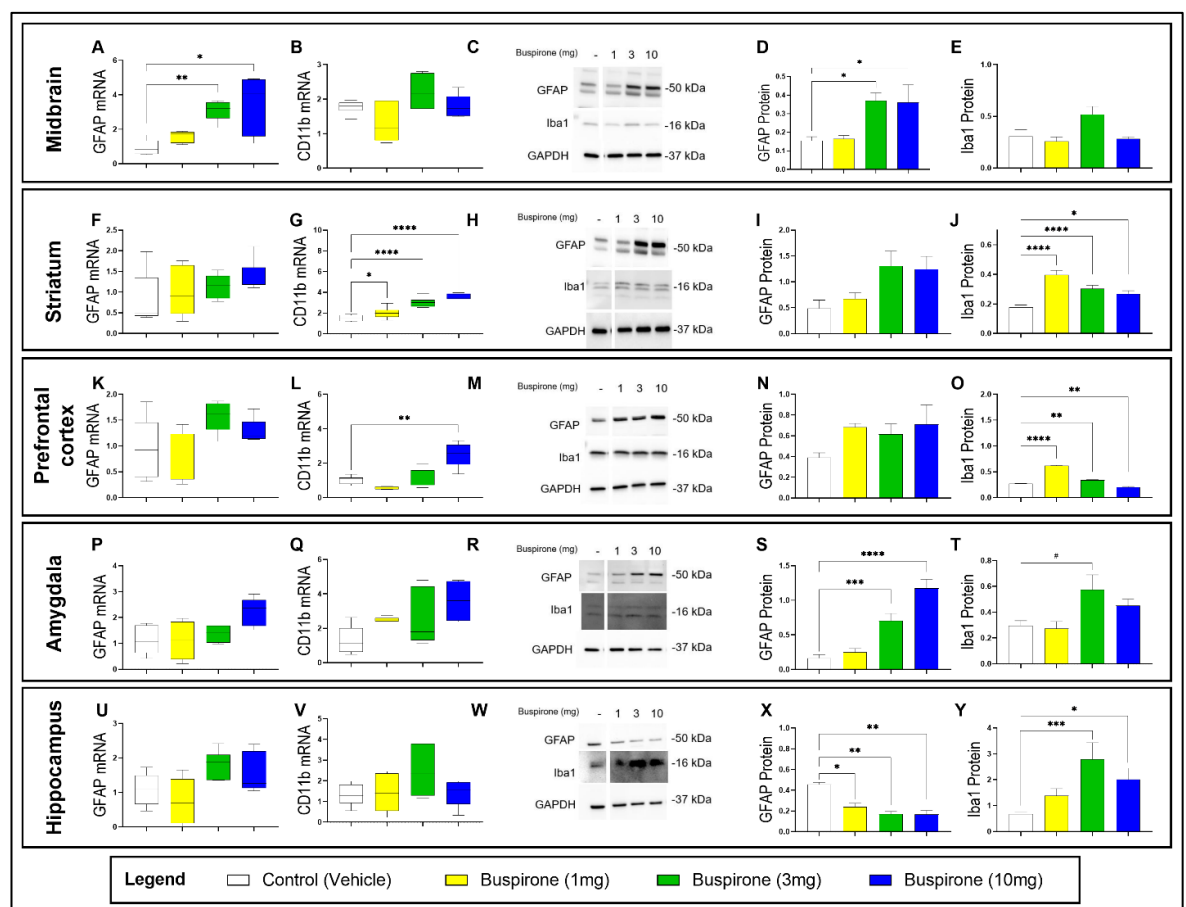
Supplementary Figure 3. Effect of buspirone treatment alone on the expression of glial cells markers. GFAP was used as an activation marker of astrocytes and CD11b and Iba1 were used collectively as markers of microglial activation. Real-time qPCR analyses of GFAP and CD11b in the midbrain (**A-B**), striatum (**F-G**), prefrontal cortex (**K-L**), amygdala (**P-Q**) and hippocampus (**U-V**),

reported as mean fold changes calculated with the ΔΔCt method after normalization to s18 (the housekeeping gene). Western blot and densitometric analysis of GFAP and Iba1 in the midbrain (**C-E**), striatum (**H-J**), prefrontal cortex (**M-O**), amygdala (**R-T**) and hippocampus (**W-Y**). Densitometric results are expressed as mean ± S.E.M. Western blots show lanes removed from in text figure 3. All data represents 4-6 samples per treatment group. *p < 0.05, **p < 0.01, ***p < 0.001 or ****p < 0.0001 as determined by ANOVA followed by Dunnett's post-hoc test. GFAP: Glial Fibrillary Acidic Protein; Iba1: ionized calcium binding adapter molecule 1; s18: ribosomal protein s18 gene; GAPDH: Glyceraldehyde 3-phosphate Dehydrogenase; kDa: Kilodalton.
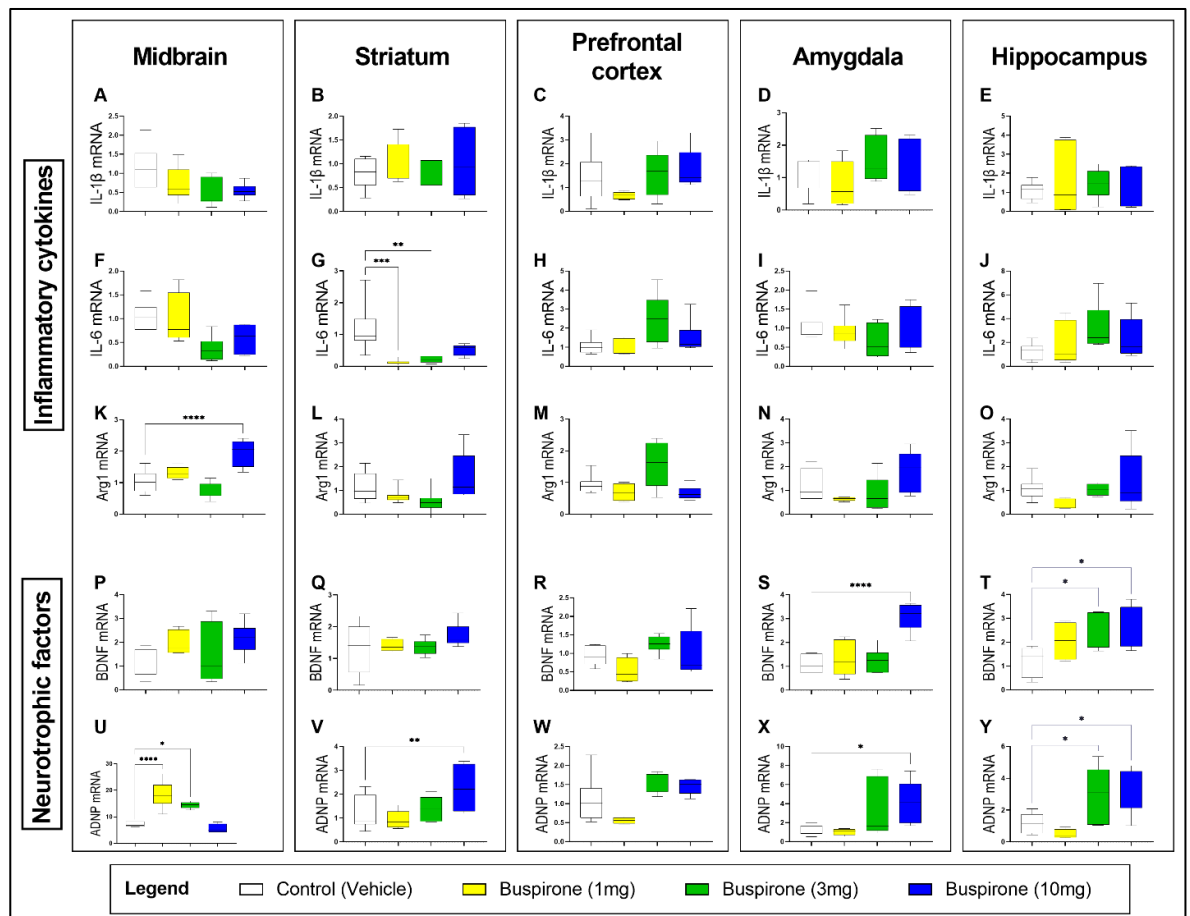
Supplementary Figure 4. Buspirone treatment alone, reduced basal levels of inflammatory cytokines and up-regulates the expression of neurotrophic factors in the brain. Real-time qPCR analyses of the pro-inflammatory cytokines IL-1β (**A-E**) and IL-6 (**F-J**), the anti-inflammatory cytokine Arg1 (**K-O**) and neurotrophic factors BDNF (**P-T**) and ADNP (**U-Y**) in the midbrain (box 1), striatum (box 2), prefrontal cortex (box 3), amygdala (box 4) and hippocampus (box 5), reported as mean fold changes calculated with the ΔΔCt method after normalization to s18 (the housekeeping gene. All data represents 5-8 samples per treatment group. *$p < 0.05$, **$p < 0.01$, ***$p < 0.001$ or ****$p < 0.0001$, compared to vehicle-treated controls, as determined by ANOVA followed by Dunnett's post-hoc test. IL-1β: interleukin-1beta: IL-6: interleukin-6; Arg1: arginase 1; BDNF: brain-derived neurotrophic factor; ADNP: activity-dependent neuroprotective protein; s18: ribosomal protein s18 gene; GAPDH: Glyceraldehyde 3-phosphate Dehydrogenase; kDa: Kilodalton.

Supplementary Figure 5. Buspirone improves mitochondrial function and stimulates the expression of anti-oxidant enzymes. The mitochondrial marker, OPA1, was analysed to determine rotenone-induced mitochondrial damage and the antioxidant enzyme SOD1 was investigated as an indirect measure of oxidative stress. Real-time qPCR analyses of OPA1 and SOD1 mRNA expression in the midbrain (**A-B**), striatum **(E-F)**, prefrontal cortex (**I-J**), amygdala (**M-N**) and hippocampus (**Q-R**) following administration of rotenone (10mg/kg) and/or buspirone (1, 3 or 10mg) daily for 21 days. Fold-changes were calculated using the

ΔΔCt method after normalization to s18 (ribosomal protein s18 gene), the housekeeping gene. Each data point represents the mean value from n = 5-8 mice per each group. Representative Western blots and densitometry of SOD1 protein expression in the midbrain (**C-D**), striatum (**G-H**), prefrontal cortex (**K-L**), amygdala (**O-P**) and hippocampus (**S-T**). Protein expression was normalized to GAPDH, the loading control. Western blots show lanes removed from in text figure 5. Densitometric results are expressed as mean ± S.E.M from n = 5-8 mice per each group. *$p < 0.05$, **$p < 0.01$, ***$p < 0.001$ or ****$p < 0.0001$, compared to vehicle-treated controls, as determined by ANOVA followed by Dunnett's post-hoc test. OPA1: Mitochondrial dynamin like GTPase; SOD1: superoxide dismutase 1; s18: ribosomal protein s18 gene; GAPDH: glyceraldehyde 3-phosphate dehydrogenase; kDa: Kilodalton.
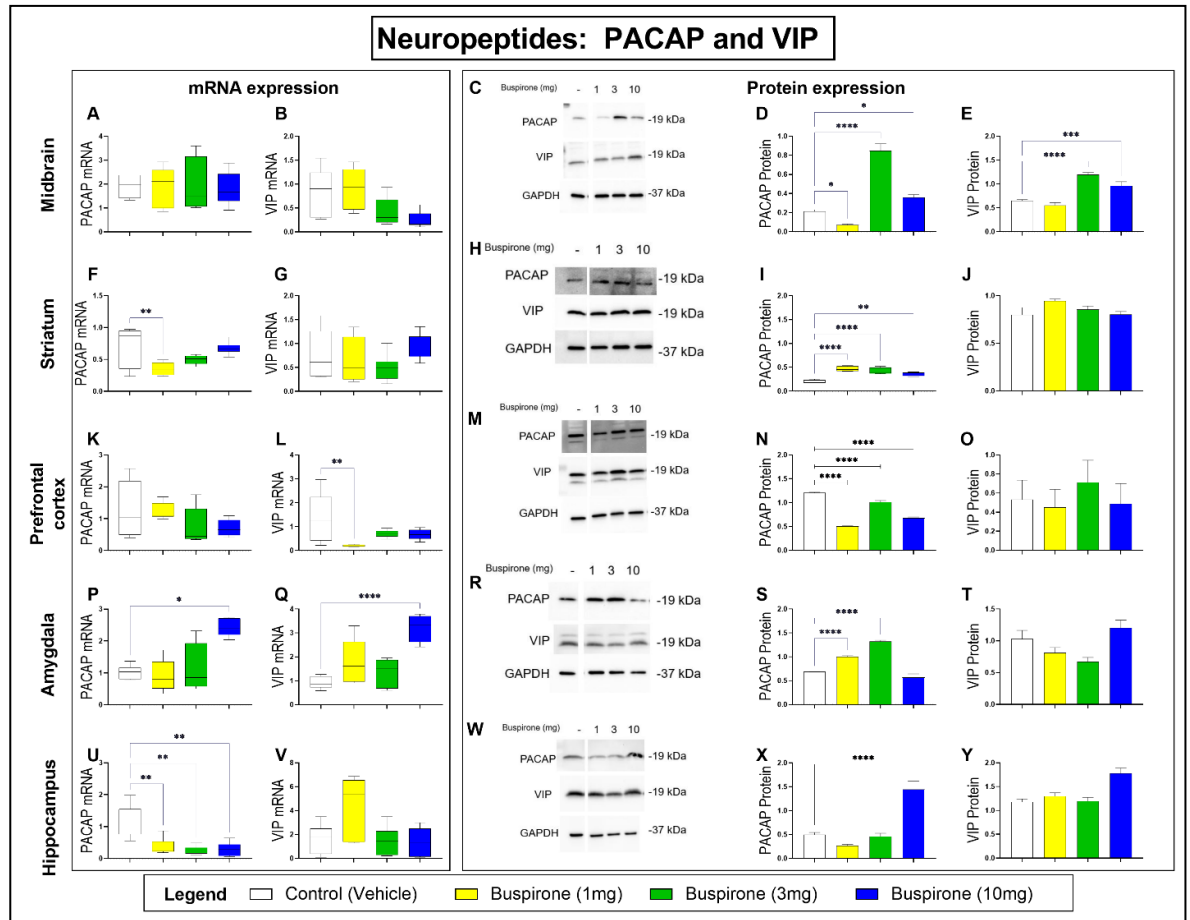
Supplementary Figure 6. Buspirone alters the endogenous expression of the neuropeptides PACAP and VIP. Real-time qPCR analyses of PACAP and VIP mRNA expression in the midbrain (**A-B**), striatum (**F-G**), prefrontal cortex (**K-L**), amygdala (**P-Q**) and hippocampus (**U-V**) following administration of rotenone (10mg/kg) and/or buspirone (1, 3 or 10mg) daily for 21 days. Fold-changes were calculated using the ΔΔCt method after normalization to s18 (ribosomal protein s18 gene), the housekeeping gene. Each data point represents the mean value from n = 5-8 mice per each group. Representative Western blots and densitometry of PACAP and VIP protein expression in the midbrain (**C-E**), striatum (**H-J**), prefrontal cortex (**M-O**), amygdala (**R-T**) and hippocampus (**W-Y**). Protein expression was normalized to GAPDH, the loading control. Western blots show lanes removed

from in text figure 6. Densitometric results are expressed as mean ± S.E.M from n

= 5-8 mice per each group. *p < 0.05, **p < 0.01, ***p < 0.001 or ****p < 0.0001,

compared to vehicle-treated controls, as determined by ANOVA followed by

Dunnett's post-hoc test. PACAP: pituitary adenylate cyclase-activating peptide;

VIP: vasoactive intestinal peptide; s18: ribosomal protein s18 gene; GAPDH:

glyceraldehyde 3-phosphate dehydrogenase; kDa: Kilodalton.

Chapter 5:

PACAP and VIP mitigate rotenone-induced inflammation in BV2 microglial cells

Chapter 5: PACAP and VIP mitigate rotenone-induced inflammation in BV-2 microglial cells

This chapter has been published in the Journal of Molecular Neuroscience on 06/01/2022.

Contribution:

- All experimental data collection and analysis

- Data analysis and curation

- Draft manuscript preparation

Signature of co-authors:

Name	Signature
Sarah Thomas Broome	Production Note: Signature removed prior to publication.
Giuseppe Musumeci	Production Note: Signature removed prior to publication.
Alessandro Castorina	Production Note: Signature removed prior to publication.

The work in this manuscript addresses **Aim 4.**

Aim 4: Characterise the phenotype of PACAP and VIP treated microglial cells following exposure to rotenone

Conclusions: PACAP and VIP attenuated rotenone triggered microglial polarization, suggesting their efficacy as anti-inflammatory agents in neuroinflammatory diseases like Parkinson's disease.

PACAP and VIP mitigate rotenone-induced inflammation in BV-2 microglial cells

Sarah Thomas Broome[1], Giuseppe Musumeci[2], Alessandro Castorina[1, *]

[1] *Laboratory of Cellular and Molecular Neuroscience (LCMN), School of Life Sciences, Faculty of Science, University of Technology Sydney, 2007, NSW, Australia*

[2] *Section of Human Anatomy, Histology and Movement Science, Department of Biomedical and Biotechnological Sciences, University of Catania, via S. Sofia, 87, 95123 Catania, Italy*

Abstract

Rotenone is a commercial pesticide commonly used to model Parkinson's disease (PD) due to its ability to induce dopaminergic degeneration. Studies have confirmed that rotenone causes microglial activation, which seems to contribute to the toxic effects seen in rodent models. Pituitary adenylate cyclase-activating polypeptide (PACAP) and vasoactive intestinal peptide (VIP) are two structurally related neuropeptides that have robust neuroprotective and anti-inflammatory properties. However, their ability to regulate microglial activity in response to rotenone is not fully understood. Using rotenone as an inflammatory stimulus, we tested whether PACAP or VIP could mitigate microglial activation in BV2 microglial cells. Rotenone dose-dependently reduced cell viability and the percentage of apoptotic cells. It also increased the release of nitric oxide (NO) in culture media, the expression of microglial activation markers and pro-inflammatory markers, including CD11b, MMP-9 and IL-6, and heightened the endogenous levels of PACAP and its preferring receptor PAC1. Co-treatment with PACAP or VIP prevented rotenone-induced increase of NO, CD11b, MMP-9 and IL-6. These results indicate that both PACAP and VIP are able to prevent the pro-inflammatory effects of rotenone in BV2 cells, supporting the idea that these molecules can have therapeutic value in slowing down PD progression.

Keywords: pituitary adenylate cyclase-activating peptide (PACAP), vasoactive intestinal peptide (VIP), rotenone, microglia, neuroinflammation.
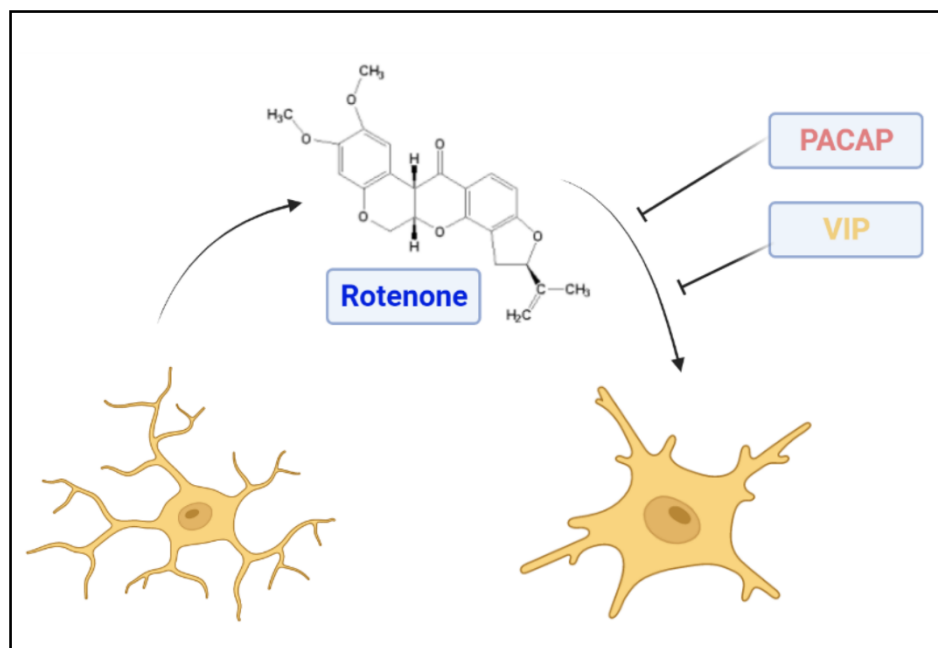
Graphical abstract. Rotenone induces microglial polarisation which is prevented by treatment with PACAP or VIP. Image created on Biorender.

Introduction

Parkinson's disease (PD) is a progressive neurodegenerative disease that is characterised by the degeneration of dopaminergic neurons in the *substantia nigra pars compacta*, resulting in a deficit of dopamine in the striatum [1, 7]. The consequent nigro-striatal depletion of dopamine is responsible for a myriad of symptoms, including bradykinesia, postural instability, resting tremor, but also cognitive and mood disorders and autonomic dysfunctions [4, 5]. Unfortunately, the cause of PD remains unknown; however, a range of risk factors have been identified, including genetics, age and environmental exposure to toxicants [25].

Rotenone is a commercial pesticide and piscicide that is used to model PD due to its ability to selectively damage dopaminergic neurons [40, 52]. Rotenone has

become a popular model as it can mimic several key pathological features of the disease, including dopaminergic degeneration, mitochondrial dysfunction, α-synuclein aggregation and neuroinflammation [41, 49].

Neuroinflammation is considered one of the main pathological mechanisms of PD, with inflammation alone being able to induce dopaminergic cell death [44, 68]. Microglia are the predominant cell types regulating neuroinflammation in the central nervous system (CNS), and these cells produce most of the pro-inflammatory and neurotoxic mediators [85, 86]. Factors that can mitigate microglial activation might display neuroprotective effects in PD [75, 315]. For example, it has been shown that rotenone induces microglial activation in mice and suppression of rotenone induced microglial activation renders mice more resistant to degeneration in models of PD [54]. Furthermore, studies have shown that rotenone-induced microglial activation contributes to neurodegeneration [280] and cognitive impairments [88]. Notably, it has been shown that rotenone causes microglial activation before anatomical evidence of dopaminergic degeneration was observed in a rodent model of PD [333].

Pituitary adenylate cyclase-activating polypeptide (PACAP) and vasoactive intestinal peptide (VIP) are neuropeptides that are associated with a range of neuroprotective and immunomodulatory functions [234, 311, 334, 335]. Both PACAP and VIP have been shown to exert neuroprotective effects in dopamine-rich regions of the CNS [336, 337]. Additionally, PACAP protects extra-nigral regions including the hippocampus, prefrontal cortex, amygdala [114, 331]. Furthermore, they both demonstrated to possess potent anti-inflammatory activities both in the CNS and periphery [338-341]. At the cellular level, PACAP and VIP

have shown to be able to reduce the polarisation of microglia driven by several inflammatory mimetics [240, 342].

In the context of PD, the administration of either peptide has shown to be neuroprotective. For example, PACAP administration protected against MPTP dopaminergic degeneration [241] and VIP treatment modulated inflammation to prevent MPTP and 6-OHDA induced degeneration [243, 343]. Of note, PACAP has shown to be neuroprotective against rotenone induced toxicity in both PC12 cells and snail models of PD [344, 345]. However, it is still unclear if these peptides can also prevent inflammation in microglial cells exposed to the PD-mimetic rotenone.

In the present work, we tested this hypothesis using morphological, biochemical and molecular analyses. Results demonstrated that these peptides prevented microglial polarization, nitric oxide release as well as the induction of a range of pro-inflammatory markers in response to rotenone-induced inflammation, hence supporting the theory that PACAP and VIP are effective anti-inflammatory agents.

Materials & methods

Cell cultures

Mouse microglial BV-2 cells were grown in full growth media containing Dulbecco's modified eagles medium nutrient mixture F-12 HAM (1:1 *vol/vol* DMEM/F12) (Sigma-Aldrich, Castle Hill, NSW, Australia), 10% heat-inactivated foetal bovine serum (FBS, Scientifix Australia, Clayton, VIC, Australia) and 1% penicillin/streptomycin solution (Sigma-Aldrich, Castle Hill, NSW, Australia) and were stored in an incubator with humidified air containing 5% CO_2 at a temperature

of 37 °C. Cells were serum-starved in 1% FBS 24 prior to treatment. When cells reached 80-85% confluence they were treated as indicated for 24 h.

Cell viability (MTT assay)

To assess cell viability, we used the Cell proliferation kit I (Sigma-Aldrich, NSW, Australia). Cells were treated with increasing doses of rotenone (0.0001-1µM) and/or PACAP or VIP (0.0001-1µM, respectively) for 24 h. Supernatant was removed and used for Griess reagent assay (please see below). 10 µL of MTT labelling reagent was added to each well of a 96-well plate for 4 h. Cells were incubated overnight in 100 µL of solubilization solution. Absorbance was measured at 656 nm in the TECAN infinite M1000-PRO ELISA reader (ThermoFisher Scientific, Victoria, Australia). Optical density values were recorded and reported as a percentage of control.

Relative Nitric Oxide measurements (Griess reagent assay)

Cells were treated with indicated treatments for 24 h before supernatant was transferred to a new 96-well plate. 100 µL of Griess reagent (Sigma-Aldrich, NSW, Australia) was added for 15 min on a slow oscillation at room temperature. Absorbance was measured at 540 nm using the TECAN infinite M1000-PRO ELISA reader (ThermoFisher Scientific, Victoria, Australia). Optical density values were recorded and reported as a percentage of control.

Morphological analysis

BV2 cells were seeded in 96 well plates for cell viability analysis and treated with indicated treatments for 24 h. Images were then captured using a Nikon Eclipse TS2 inverted microscope (using the embossing filter settings) and subjected to morphological assessment (magnification ×20). Images were de-identified for analysis. Gross morphology was assessed based on the following three categories: 1) resting cells (rounded cells, with or without thin processes), 2) activated (flattened cell body, swollen somata and/or thick retracted processes) or 3) apoptotic (smaller and/or fragmented cells [apoptotic bodies]), as summarised in **Figure 1**. Analyses of microscope images were performed using Fiji Image J, where cells were labelled into individual categories, counted, and expressed as a percentage of total cells.
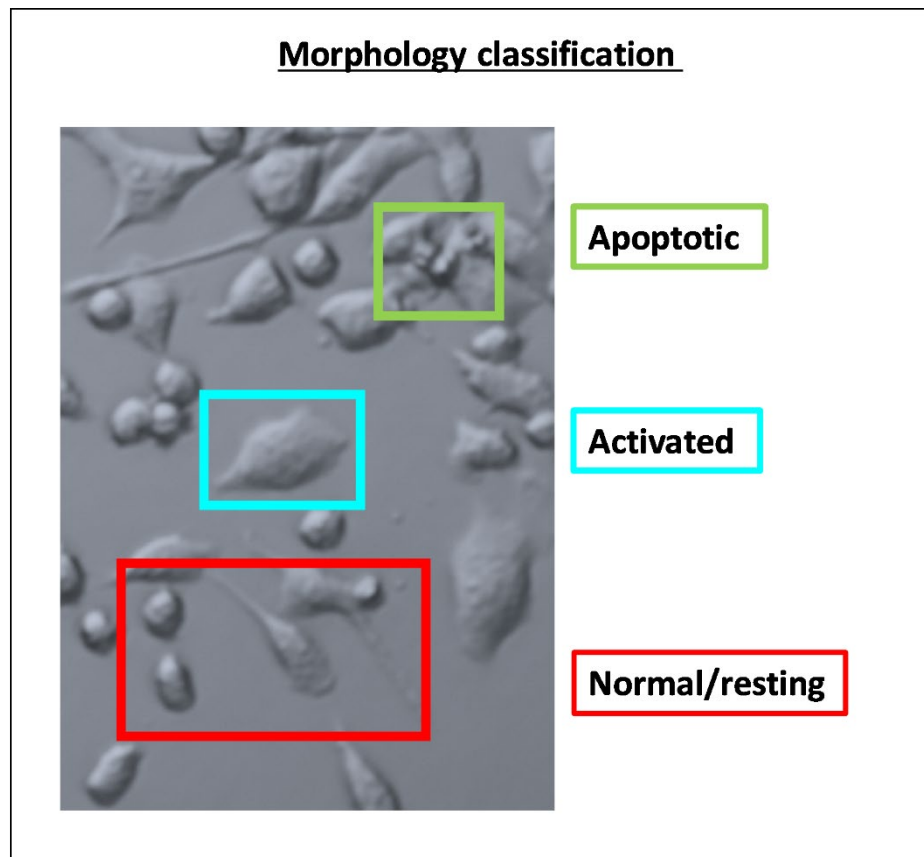
Figure 1. Morphological classification of microglial phenotypes. BV2 microglial cells were grossly classified into three categories: 1) normal/resting based on their rounded appearance with or without processes (red); 2) activated based on flattened and swollen appearance with no processes (blue); or 3) apoptotic based on shrinkage and fragmentation (green).

Real-time quantitative polymerase chain reaction (RT-qPCR)

Total RNA was extracted using TRI reagent (Sigma-Aldrich, NSW, Australia) and precipitated with ice-cold 2-propanol (Sigma-Aldrich). Pellets were washed twice with 75% ethanol and air-dried. RNA concentrations were calculated using NanoDrop™ 2000 (ThermoFisher Scientific). A total of 1 μg of total RNA was used

to synthesised cDNA using the Tetro cDNA synthesis kit (Bioline, Australia). Real-time qPCR analyses were performed as previously reported [193, 315]. Briefly, for each gene of interest 3 µL cDNA, 0.4 µL milliQ water, 5 µL iTaq Universal SYBR green master mix (BioRad) and 0.8 µL corresponding forward and reverse primers (5 µM) for the gene of interest (detailed in **Table 1**) were combined and detected using the CFX96 Touch TM Real-Time PCR Detection System (BioRad, NSW, Australia). Instrument settings were as follows: (1) 95 °C for 2 min, (2) 60 °C for 10 s, (3) 72 °C for 10 s, (4) plate read, (5) repeat step 2 to 4 for 45 cycles. For the melting curve analyses, settings were (1) 65 °C for 35 s, (2) plate read, (3) repeat step 1–2 for 60 times). To examine changes in gene expression, we analysed the mean fold change values of each sample, calculated using the ΔΔCt method, as previously described by Schmittgen and Livak [258]. PCR product specificity was evaluated by melting curve analysis, with each gene showing a single peak (data not shown).

Accession #	Gene	Primer sequence (5'-3')	Length (bp)
NM_000600.4	Interleukin-6 (IL-6)	Fwd TGACCCAACCACAAATGCCA Rev ATTTGCCGAAGAGCCCTCAG	135
NM_001082960.1	CD11b	Fwd GAGCAGGGGTCATTCGCTAC Rev GCTGGCTTAGATGCGATGGT	94
NM_013599.4	Matrix metallopeptidase 9 (MMP-9)	Fwd ATCATAGAGGAAGCCCATTACAG Rev TTTGACGTCCAGAGAAGAAGAAA	129
NM_010927.4	Nitric oxide synthetase 2 (NOS2)	Fwd TACCAAAGTGACCTGAAAGAGG Rev TCATCTTGTATTGTTGGGCTGA	89
NM_007482.3	Arginase-1 (Arg1)	Fwd ACAAGACAGGGCTCCTTTCAG Rev TTAAAGCCACTGCCGTGTTC	105
NM_010548.2	Interleukin-10	Fwd GCATGGCCCAGAAATCAAGG	91

	(IL-10)	Rev GAGAAATCGATGACAGCGCC	
NM_016989.2	Pituitary adenylate-cyclase-activating polypeptide (PACAP)	Fwd AGGCTTACGATCAGGACGGA Rev CTCCTGTCGGCTGGGTAGTA	121
NM_053991.1	Vasoactive intestinal peptide (VIP)	Fwd CCTGGCGATCCTGACACTCT Rev CTGCAGCCTGTCATCCAACC	100
NM_007407.3	PAC1 receptor	Fwd CAGTCCCCAGACATGGGAGGCA Rev AGCGGGCCAGCCGTAGAGTA	139
NM_011703.4	VPAC1 receptor	Fwd TCAATGGCGAGGTGCAGGCAG Rev TGTGTGCTGCACGAGACGCC	127
NM_009511.2	VPAC2 receptor	Fwd GCGTCGGTGGTGCTGACCTG Rev ACACCGCTGCAGGCTCTCTGAT	155
NM_213557.1	18S ribosomal subunit (s18)	Fwd GGCGGAAAATAGCCTTCGCT Rev AGCCCTCTTGGTGAGGTCAA	101

Table 1. List of primer sets used in real-time qPCR analysis. Forward and reverse primers were selected from the 5' and 3' region of each gene mRNA. The expected length of each amplicon is indicated in the right column.

Western blots

Protein was extracted using a radioimmunoprecipitation assay (RIPA) buffer containing protease inhibitors to preserve protein integrity (cOmplete, Mini, EDTA-free Protease Inhibitor Cocktail, Sigma-Aldrich, Castle Hill, NSW, Australia) as previously reported [236]. Protein quantification was determined using the bicinchoninic acid assay (Pierce BCA Protein Assay Kit, ThermoFisher Scientific, VIC, Australia). 30 μg of protein lysates were separated by sodium dodecyl sulphate-polyacrylamide gel electrophoresis (SDS-PAGE) using 4-20% Mini-PROTEAN TGX Stain-Free Gels (15 well, BioRad, VIC, Australia). Precision Plus Protein Prestained Standard in All Blue (BioRad, VIC, Australia) was included to determine the molecular weight of bands of interest. Transfer to a PVDF membrane was performed using the semi-dry method (BioRad, Trans-Blot Turbo

Transfer System). Incubation with primary antibodies was performed overnight in

5% skim milk in TBST blocking solution at 4°C on a slow oscillation.

Primary/Secondary antibodies and related working dilutions are summarized in

Table 2. Membranes were incubated with secondary antibody for 1 hr at RT before

being visualized with chemiluminescence BioRad Clarity Western ECL Blotting

Substrate Solution. Images were acquired using the BioRad ChemiDoc MP

System. Densitometry of bands was conducted using Fiji ImageJ and ratios were

normalized to GAPDH, which was used as a loading control [114].

Antibody	Dilution	Source (Cat. #)
Ionised calcium binding adaptor molecule 1 (Iba1)	1:1000	Abcam (ab133357)
Arginase 1 (Arg1)	1:1000	GeneTex (GTX109242)
Pituitary adenylate-cyclase-activating polypeptide (PACAP)	1:1000	GeneTex (GTX37576)
PAC1 receptor	1:1000	GeneTex (GTX30026)
Glyceraldehyde-3-phosphate dehydrogenase (GAPDH)	1:1000	BioRad (VPA00187)
Goat anti-Rabbit IgG HRP	1:10000	BioRad (STAR208P)

Table 2. List of primary and secondary antibodies used in Western blot.

Statistical analysis

Statistical analyses were performed using GraphPad Prism version 9.02 for

Windows (GraphPad Software, San Diego California, USA). All experimental data

are reported as mean ± S.E.M. To assess for statistical differences between two

groups (i.e. untreated Vs rotenone-treated cells), we utilised the unpaired Student's *t*-test. Analyses of three or more groups were conducted using One-Way ANOVA followed by Sidak's or Dunnett's *post-hoc* tests, as appropriate. P values ≤ 0.05 were considered statistically significant.

Results

Rotenone induces polarization in BV2 microglial cells

To establish which concentration of rotenone produced sub-toxic but strong inflammatory effects, to use in subsequent experiments, we determined the effects of increasing concentrations of rotenone (0.0001 μM to 1 μM) on cell viability and nitric oxide (NO) secretion, an indicator of microglial activation [346].

Representative photomicrographs demonstrate the morphological effect of increasing rotenone concentration on microglial cells (**Figure 2a**). Gross morphological analysis revealed a dose-dependent reduction in the percentage of resting cells (from 49% down to 4%) and a steady percentage of activated cells (ranging from 48 – 64%), as identified by flattened and swollen cell somata (**Figure 2b**). At the highest concentrations tested (1 μM), rotenone dramatically increased the proportion of apoptotic cells (51%), as opposed to 0.1 μM rotenone, whose percentage was only 24%. These results correlated with a dose-dependent loss of cell viability ($F_{5,87}$ = 52.63, **** $p < 0.0001$) (**Figure 2c**).

Accordingly, a dose-dependent increase in NO levels was also seen in rotenone-treated BV2 microglial cells (**Figure 2d**). Of note, 0.01 μM was the first dose to record a significant increase in NO compared to untreated controls ($F_{5,78}$ = 10.48, *

p = 0.0476). Both 0.1 µM and 1 µM rotenone significantly increased NO levels, compared to untreated controls (**** p < 0.0001, respectively) (**Figure 2d**).

Based on the above results, we chose 0.1 µM rotenone as the sub-toxic concentration (<50% apoptotic, **Figure 2a-c**) able to trigger significant NO release (**Figure 2d**). At this concentration, rotenone also caused significant increase in the protein expression of microglial activation and pro-inflammatory markers, CD11b (* p = 0.0493, **Figure 2e**), IL-17a (*** p = 0.0002; **Figure 2f**), MMP-9 (**** p < 0.0001; **Figure 2g**) and Iba1 (**** p < 0.0001; **Figure 2h**).
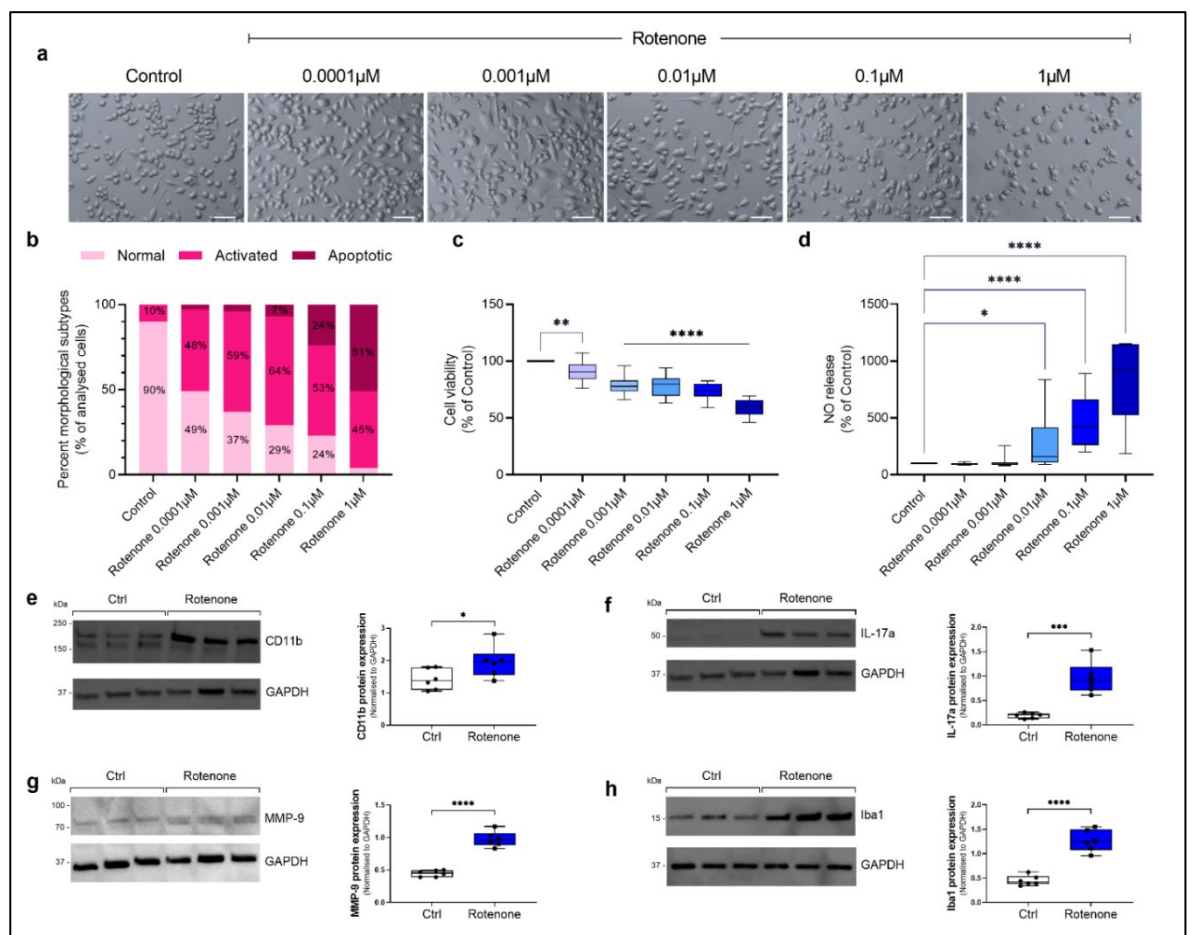
Figure 2. Effects of rotenone on cell viability, nitrate release and expression of microglial activation markers. (**a**) BV2 microglial cells were treated with

increasing concentrations of rotenone (0.0001 – 1 µM) for 24 h and representative photomicrographs (using embossing filter settings) were taken (scale bar = 60 µm). (**b**) Morphological assessment was determined by assigning cells into three gross categories (normal, activated or apoptotic [please refer to **Figure 1**]) and by calculating the percentage of cells in each category. For these analyses, at least eight representative micrographs per condition were appraised (n = 8). (**c**) Cell viability and (**d**) nitric oxide release were assessed under the same experimental conditions. Representative Western blots and densitometry of (**e**) CD11b, (**f**) IL-17a, (**g**) MMP-9 and (**h**) Iba1 protein expression in BV2 cells exposed to 0.1 µM rotenone for 24 h. Results are expressed as mean ± SEM. Western blot data represent the mean of two independent experiments, each run in triplicate (n = 6). Bands were normalised to GAPDH, the loading control. * $p < 0.05$, ** $p < 0.01$, *** $p < 0.001$ or **** $p < 0.0001$ vs untreated controls, as determined by one-way ANOVA followed by Dunnett's post hoc test (**a-d**) or unpaired Student *t*-test (**e-h**). NO: nitric oxide; IL-17a: interleukin 17a; MMP-9: matrix metalloproteinase-9; Iba1: ionised calcium binding adaptor molecule 1; GAPDH: Glyceraldehyde 3-phosphate dehydrogenase.

PACAP prevents rotenone-induced nitric oxide release but not cytotoxicity

To determine if PACAP prevents rotenone-induced toxicity, BV2 cells were exposed to 0.1 µM rotenone and treated with increasing concentrations (0.0001 µM to 1 µM) of the peptide PACAP (**Figure 3**).

Results from morphological assessments demonstrated that co-treatment with PACAP dose-dependently reduced the % of apoptotic cells, increased resting/normal appearing cells but had no apparent effects on the subpopulation of cells exhibiting polarised/activated morphology (**Figure 3a – b**).

Interestingly, biochemical analyses of cell viability (MTT) revealed that PACAP treatment was not associated with improved viability in BV2 cells at any of the concentrations tested ($F_{6, 105}$ = 4.654, *** p = 0.0004; **Figure 3c**).

However, in line with the phenotypic changes, we observed a sharp reduction in nitric oxide levels in the supernatant in response to all concentrations of PACAP tested (#### p < 0.0001, compared to rotenone-treated cells; **Figure 3d**). Of note, PACAP concentrations of 0.01 µM and above fully prevented nitric oxide release, with levels comparable to untreated controls ($F_{6,101}$ = 31.13, **** p < 0.0001, **Figure 3d**).

Figure 3. Dose-response effects of PACAP on rotenone-treated microglia.

PACAP titration experiments showing dose-dependent changes in morphology, cell viability and nitric oxide release. (**a**) BV2 cells were either treated with rotenone alone (0.1 µM) or with increasing concentrations of PACAP (0.0001 – 1 µM) for 24 h and representative photomicrographs (using the embossing filter settings) were taken (scale bar = 60 µm). (**b**) Morphological assessment was determined by assigning cells into three gross categories (normal, activated or apoptotic) and by calculating the percentage of cells in each category. For these analyses, at least eight representative micrographs per condition were appraised (n = 8). (**c**) Cell viability and (**d**) nitric oxide release were assessed under the same experimental conditions. Data reported as mean ± SEM from at least three independent experiments run using eight biological replicates per group (n = 24). **** p < 0.0001 vs untreated controls or #### p < 0.0001 vs rotenone-treated cells, as determined by one-way ANOVA followed by Sidak's post hoc test. PACAP: pituitary adenylate cyclase-activating polypeptide; NO: nitric oxide.

VIP prevents rotenone-induced nitric oxide release but not cytotoxicity

Similar analyses were performed using increasing concentrations (0.0001 µM to 1 µM) of VIP on rotenone-treated cells (**Figure 4**).

We observed a more pronounced anti-inflammatory effect of VIP in comparison with PACAP, as co-treatment with VIP largely prevented the shift of cells towards an activated phenotype and resulted in reduced apoptotic cells (**Figure 4a – b**). In contrast, MTT data showed that none of the concentrations of VIP tested reliably

prevented rotenone-induced reduction of cell viability (**** p < 0.0001, compared to untreated controls; **Figure 4c**).

Nevertheless, a significant reduction in nitric oxide secretion was observed in response to VIP treatment, at all doses (#### p < 0.0001, compared to rotenone treated cells; **Figure 4d**). Similarly, to PACAP treatment, cells exposed to 0.01 µM and above of VIP reduced nitric oxide levels comparable to untreated controls ($F_{6,96}$ = 20.30, **** p < 0.0001; **Figure 4d**).

Our results align with other studies in similar experimental paradigms whereby nanomolar concentrations of each peptide are sufficient to produce anti-inflammatory and protective effects [240]. Accordingly, we proceeded using 0.01 µM as the preferred peptide concentration for the remainder of this study.
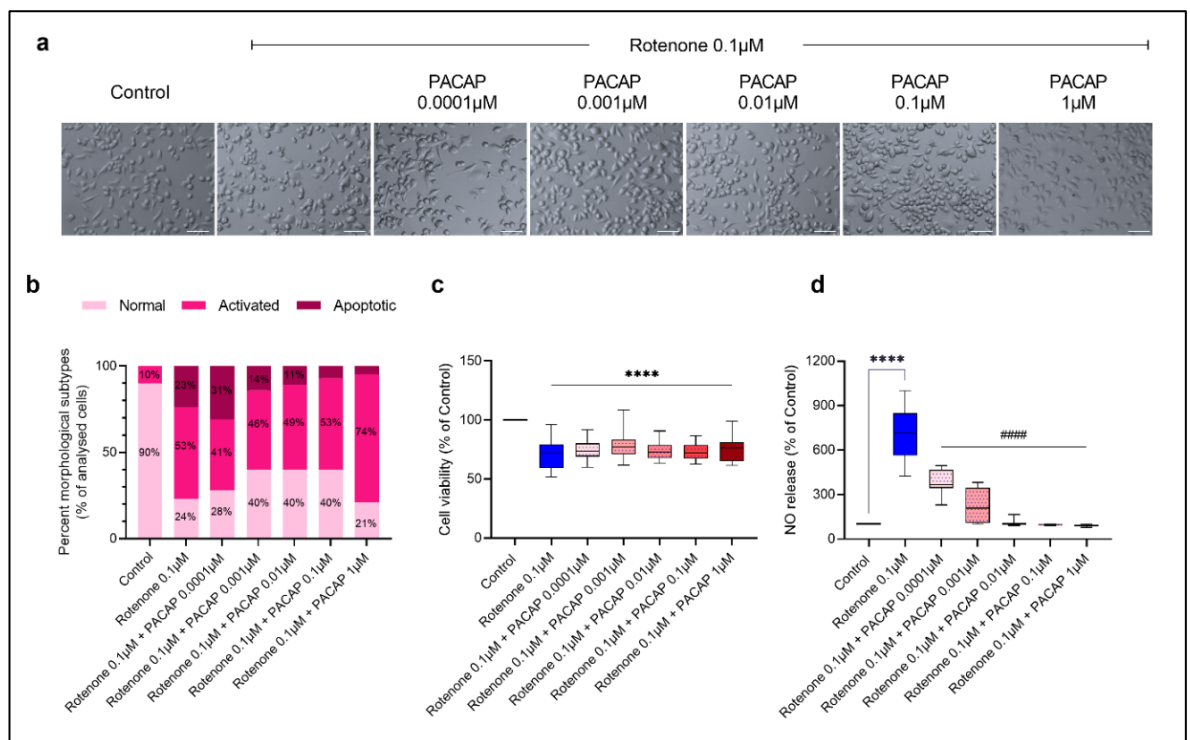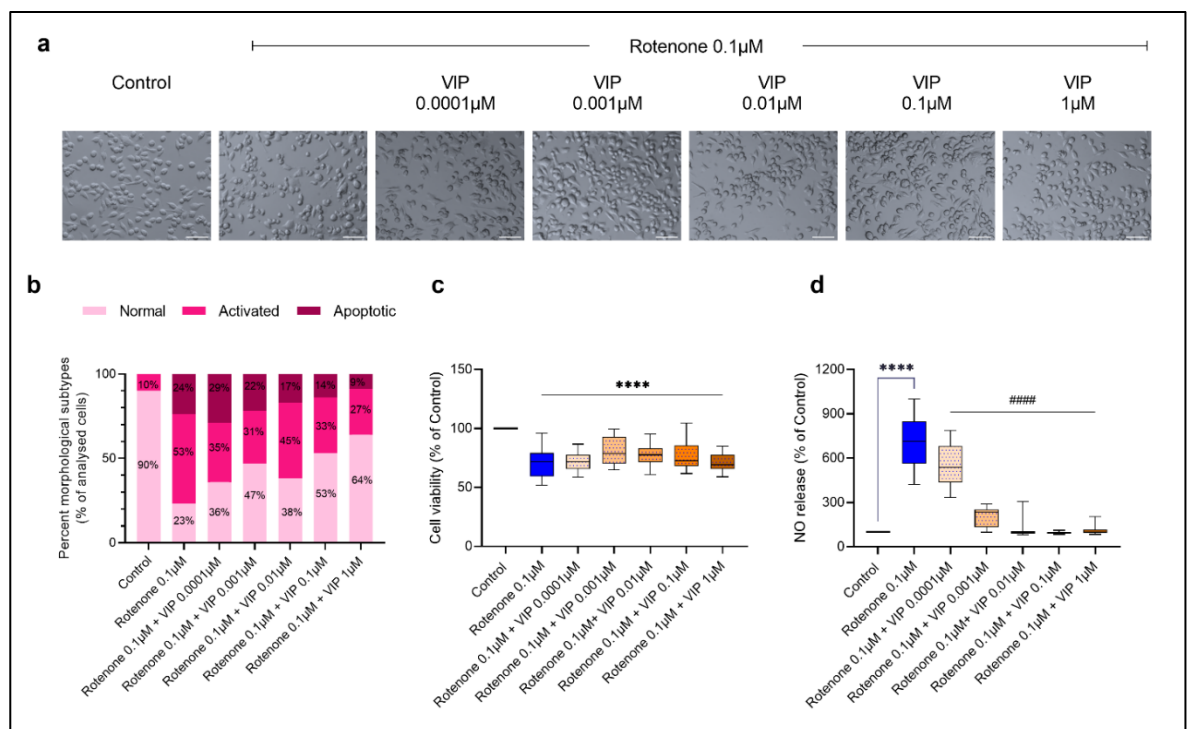
Figure 4. Dose-response effects of VIP on rotenone-treated microglia. VIP titration experiments showing dose-dependent changes in morphology, cell viability and nitric oxide release. (**a**) BV2 cells were either treated with rotenone alone (0.1 µM) or increasing concentrations of VIP (0.0001 – 1 µM) for 24 h and representative photomicrographs (using the embossing filter settings) were taken (scale bar = 60 µm). (**b**) Morphological assessment was determined by assigning cells into three gross categories (normal, activated or apoptotic) and by calculating the percentage of cells in each category. For these analyses, at least eight representative micrographs per condition were appraised (n = 8). (**c**) Cell viability and (**d**) nitric oxide release were assessed under the same experimental conditions. Data reported as mean ± SEM from at least three independent experiments run using eight biological replicates per group (n = 24). **** $p < 0.0001$ vs untreated controls or #### $p < 0.0001$ vs rotenone-treated cells, as determined by one-way ANOVA followed by Sidak's post hoc test. VIP: vasoactive intestinal peptide; NO: nitric oxide.

PACAP and VIP prevent rotenone-induced microglial polarization

To evaluate if PACAP or VIP co-treatment prevented rotenone-induced microglial polarization we measured the expression levels of pro- and anti-inflammatory genes. BV2 cells were exposed to rotenone (0.1 µM) and/or PACAP (0.01 µM) and VIP (0.001 µM) for 24 h. As shown in **Figures 5a – d**, rotenone treatment strongly increased the gene expression of IL-6 (**** $p < 0.0001$), NOS2 (* $p = 0.0120$), CD11b (**** $p < 0.0001$) and MMP-9 (** $p = 0.0051$), compared to untreated

controls. Similarly, Iba1 protein expression was increased in response to rotenone (** p = 0.0065). The mRNA expression of the anti-inflammatory cytokine, IL-10 was also significantly increased in response to rotenone treatment (** p = 0.0019; **Figure 5e**), but Arg1 levels remained unchanged ($F_{5,42}$ = 2.613, * p =0.0382; **Figure 5f**).

Co-treatment with PACAP significantly decreased the expression of IL-6 (#### p < 0.0001; **Figures 5a**), NOS2 (#### p < 0.0001; **Figures 5b**), CD11b (#### p < 0.0001; **Figures 5c**) and MMP-9 (#### p < 0.0001; **Figures 5d**), compared to rotenone-treated cells. However, PACAP was unable to prevent IL-10 induction by rotenone (**Figure 5e**) and had no effects on Arg1 mRNA expression (**Figure 5f**) mRNA expression levels compared to rotenone-treated cells. PACAP was the only peptide to significantly reduce the protein expression of Iba1 in response to rotenone-induced inflammation (# p = 0.0258) (**Figure 5g – h**).

With regards to VIP, peptide co-treatment also reliably decreased the expression of IL-6 (#### p < 0.0001, **Figure 5a**), NOS2 (#### p < 0.0001, **Figure 5b**), CD11b (#### p < 0.0001, **Figure 5c**) and MMP-9 (## p = 0.011; **Figure 5d**) as compared to rotenone-treated cells.

Notably, in contrast to PACAP, VIP co-treatment prevented the increase of IL-10 gene expression caused by rotenone (## p = 0.0051, **Figure 5e**).
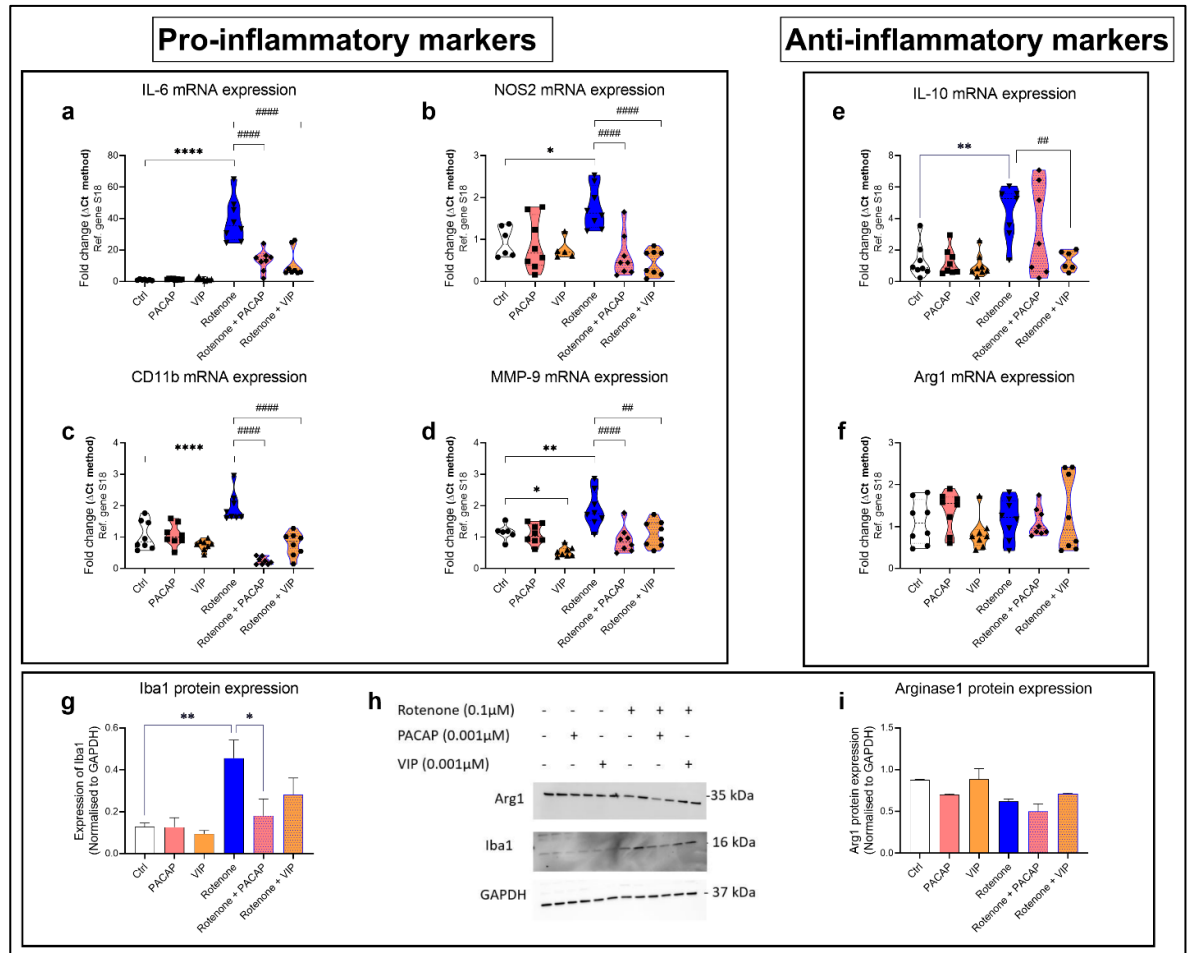
Figure 5. Effects of PACAP or VIP treatment on BV2 microglia inflammatory profile after exposure to rotenone. Real-time qPCR and Western blot analyses of microglial activation markers, pro- and anti-inflammatory cytokines in cells exposed to rotenone alone (0.1 μM), PACAP alone (0.001 μM), VIP alone (0.001 μM) or in combination for 24 h. Gene expression changes of (**a**) IL-6, (**b**) NOS2, (**c**) CD11b, (**d**) MMP-9, (**e**) IL-10 and (**f**) Arg1 in response to treatments are shown. Relative changes in mRNA levels were determined using the ΔCT method and normalized to the ribosomal protein subunit S18, used as the housekeeping gene. (**g – i**) Western blot analyses and densitometry of (**g**) Iba1 and (**i**) Arg1 protein expression. Quantifications were performed using the ImageJ software, and bands densities were normalised to GAPDH, the loading control. Data represent the mean

of 3–6 biological replicates for each group. Results are expressed as mean ± SEM. * $p < 0.05$, ** $p < 0.01$ or **** $p < 0.0001$ compared to untreated controls. ## $p < 0.01$ or #### $p < 0.0001$ compared to rotenone treated cells as determined by one-way ANOVA followed by Sidak's post hoc test. PACAP: pituitary adenylate cyclase-activating polypeptide; VIP: vasoactive intestinal peptide; s18: ribosomal protein s18; GAPDH: Glyceraldehyde 3-phosphate dehydrogenase; kDa: kilodalton; n.s.: not significant; Ctl: untreated controls. IL-6: interleukin-6; NOS2: nitric oxide synthase 2; MMP-9: matrix metallopeptidase 9; IL-10: interleukin-10; Arg1: arginase-1; Iba1: ionised calcium binding adaptor molecule 1.

Rotenone alters the expression of PACAP, VIP and related receptors

To determine whether rotenone perturbed the endogenous expression of PACAP, VIP and/or their receptors in BV2 cells challenged with rotenone, real-time qPCR and Western blots were conducted. In the absence of rotenone, PACAP supplementation increased the endogenous mRNA levels of both PACAP and VIP (** $p = 0.0014$, PACAP gene expression; **Figure 6a**; * $p = 0.0160$, VIP expression; **Figure 6b**). Almost overlapping effects were observed with VIP supplementation (** $p = 0.0074$, PACAP gene expression; **Figure 6a**; * $p = 0.0121$, VIP gene expression; **Figure 6b**). However, exogenous stimulation with either peptides did not alter the expression of genes encoding PACAP/VIP receptors ($p > 0.05$, **Figure 6c – e**).

Exposure to rotenone significantly up-regulated PACAP transcripts (**** $p < 0.0001$ vs Ctrl; **Figure 6a**) and, although not significantly PAC1 gene expression (**Figure**

6c). Rotenone also down-regulated both VPAC1 (*** $p < 0.001$; **Figure 6d**) and VPAC2 mRNAs (** $p = 0.0038$; **Figure 6e**).

Co-treatment with PACAP or VIP in cells exposed to rotenone resulted in a significant reduction of PACAP (# $p < 0.05$ and #### $p < 0.0001$ vs rotenone, respectively; **Figure 6a**) but not VIP gene expression ($p > 0.05$ vs rotenone; **Figure 6b**). Similarly, PACAP, PAC1 gene expression levels were also reduced by exogenous peptide treatments, although reductions in gene levels were statistically significant only for VIP (# $p < 0.05$) and not PACAP ($p = 0.08$; **Figure 6c**). Neither of rotenone-induced effects on VPAC1 and VPAC2 gene expression were prevented by PACAP or VIP co-treatment ($p > 0.05$ for both genes, respectively; **Figures 6d – e**).

To confirm if the preventative activities of PACAP or VIP on rotenone-induced changes in PACAP and PAC1 genes could also be seen at the protein level, we performed Western blots. As shown, PACAP or VIP co-treatment resulted in a significant down-regulation of PACAP (# $p = 0.0396$ in rotenone + PACAP; $p = 0.0828$ in rotenone + VIP) and PAC1 protein expression (# $p = 0.0321$ in rotenone + PACAP; $p = 0.0938$ in rotenone + VIP; **Figures f – h**).
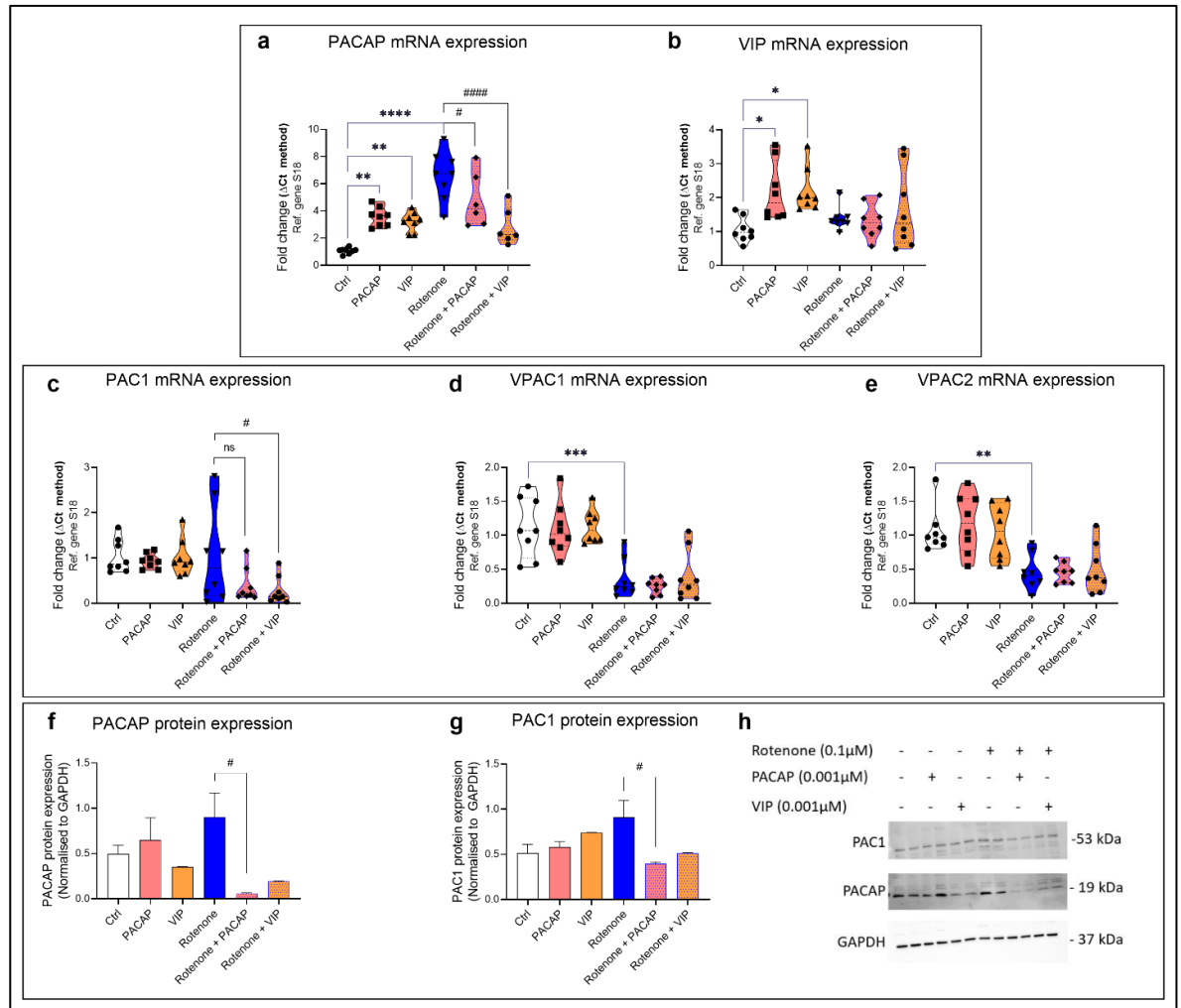
Figure 6. Expression of PACAP, VIP and their receptors in BV2 microglia exposed to rotenone. PACAP, VIP and receptor gene expression after treatment with 0.1 µM rotenone in the presence or not of exogenous PACAP (0.001 µM) or VIP (0.001 µM) for 24 h. Real-time qPCR analyses of (**a**) PACAP, (**b**) VIP, (**c**) PAC1, (**d**) VPAC1 and (**e**) VPAC2 gene expression. Relative changes in mRNA levels were determined using the ΔCT method and normalized to the ribosomal protein subunit S18, here used as the housekeeping gene. (**f – h**) Western blot analysis and densitometry of (**f**) PACAP and (**g**) PAC1 protein expression. Quantifications were performed using the ImageJ software, and normalised values were calculated by dividing the mean optical density of bands over the

corresponding GAPDH. Data represent the mean of 3–6 biological replicates for each group. Results are expressed as mean ± SEM. * $p < 0.05$, ** $p < 0.01$, *** $p < 0.001$ or **** $p < 0.0001$ compared to untreated controls. # $p < 0.05$ or #### $p < 0.0001$ compared to rotenone treated cells as determined by one-way ANOVA followed by Sidak's post hoc test. PACAP: pituitary adenylate cyclase-activating polypeptide; VIP: vasoactive intestinal peptide; s18: ribosomal protein s18; GAPDH: Glyceraldehyde 3-phosphate dehydrogenase; kDa: kilodalton; n.s.: not significant; Ctrl: untreated controls.

Discussion

In this study, we tested whether rotenone, a well-known PD-mimetic, could induce microglial polarization and see whether PACAP or VIP co-treatment could prevent it. For this purpose, we utilized murine BV2 microglial cells, as these cells share several biological and biochemical properties with primary microglial cultures [347]. Our data indicates that rotenone reduces viability and causes microglial polarization of BV2 microglial cells. Interestingly, neither peptide was able to prevent cell death caused by rotenone toxicity; however, both prevented microglial activation, expression of pro-inflammatory factors and release of nitric oxide. Additionally, we demonstrated that rotenone treatment perturbs the endogenous gene expression levels of both peptides and their related receptors, and this is partly prevented by PACAP or VIP supplementation.

The progressive degeneration of dopaminergic neurons and inflammatory processes are closely related in PD [54, 68] It has been shown that LPS-induced

inflammation promotes the degeneration of dopaminergic neurons, which did not reverse 21 days post lesion [44]. Rotenone has become a popular mimetic utilized to induce PD-like pathology, including dopaminergic degeneration and neuroinflammation in several pre-clinical models of PD [35, 36, 314]. Furthermore, studies have determined that reduction in microglial activation is crucial in promoting neuroprotection in rotenone models of PD [54, 348]. Along with the evidence of microglial activation in *post-mortem* PD brains [83], these studies suggest that microglia polarization and the consequent accumulation of pro-inflammatory factors may be critical in promoting PD pathogenesis. Vice versa, inhibition of microglia activities has been indicated as a viable strategy to attenuate neurodegeneration, relieve motor symptoms and slow disease progression [75].

In animal studies, recent evidence has shown that rotenone-induced microglial activation precedes neurodegeneration [88]. Therefore, the identification of treatments that can inhibit inflammation represent an attractive strategy to prevent the ongoing neurodegeneration seen in PD and other neurodegenerative conditions.

In line with other studies, we demonstrated that rotenone induced the expression of microglial activation and the pro-inflammatory markers Iba1 and IL-1β in BV2 microglial cells [61, 349]. We also report that both PACAP and VIP are able to mitigate rotenone-induced inflammation and microglial activation in BV2 cells. These observations align with our previous data indicating that these peptides exert immunosuppressive effects in LPS-treated BV2 cells [240]. Furthermore, it corroborates previous evidence demonstrating that PACAP provides protection against MPP+ neurotoxicity to primary rat mesencephalic neuron-glia cultures only in the presence of microglia, suggesting that an essential component of PACAP

neuroprotective function is achieved via microglial inactivation [330]. This is strengthened by studies demonstrating neuroprotective effects PACAP administration against rotenone toxicity [344, 345]. Similarly, to PACAP, the neuroprotective effect of VIP has also been associated with its ability to block/prevent microglial activation and reduce the expression of pro-inflammatory mediators in a MPTP mouse model of PD [244]. Some studies have enhanced the activity of VIP through TAT-tagging which allowed for positive allosteric modulation of the PAC1 receptor, which was shown to be more protective against MPTP neurotoxicity than PACAP alone [329]. The present findings further strengthen such *in vivo* evidence in a controlled monoculture, thereby excluding the potential influence of other glial cells.

Previous reports have demonstrated that PACAP and VIP reduced the inhibition of cytokine production by lipopolysaccharide in primary microglia [336], an effect that was mediated by the VPAC1 receptor. In contrast, our results pinpoint the PAC1 receptor as the main player of PACAP and VIP modulatory activities in BV2 microglial cells exposed to rotenone. This is not surprising, as the nature of the insult causing inflammation in the two studies is different. In addition, despite the similarities with primary microglia, we cannot exclude that some differences might exist in the way BV2 vs. primary microglia regulate the expression of this class of receptors in response to a toxic stimulus. Mechanistic gain and loss-of-function studies are warranted to dissect the specific contribution of PACAP/VIP receptors in regulating inflammatory responses. However, it should be noted that studies in PAC1 receptor knockout mice proposed that the PACAP/PAC1 axis is at the forefront of the anti-inflammatory signalling in mice [350] [351], supporting the notion that the expression and activity of the PACAP/VIP protective/anti-

inflammatory system may be influenced by several factors, including the response of neighbouring glia or neurons to an inflammatory microenvironment. In fact, microglia are in constant communication with astrocytes to regulate the immune response within the CNS [352], and both PACAP and VIP play an important role in mediating the activity of astrocytes [339].

In conclusion, our study has demonstrated that stimulation with PACAP or VIP reliably prevented the induction of NO release, microglial activation markers and pro-inflammatory cytokines in BV2 microglia exposed to rotenone. In addition, our findings reveal that the toxicant perturbs the endogenous expression of PACAP/VIP peptides and receptors in a way that differs from that seen with other inflammatory mimetics. This raises the possibility that upon rotenone exposure, microglial cells need to re-adjust the expression of peptides and receptors to enable the activation of both protective and anti-inflammatory pathways, rendering cells able to cope with the detrimental effects of this toxicant. Nonetheless, whilst no in vitro model can recapitulate all the pathogenic features of PD, these results bring us a step closer into our understanding of the potent immune modulatory role elicited by these peptides and suggest their consideration as potential targets to relieve the chronic inflammation and microglial activation observed in several neurodegenerative disorders of the CNS, where an inflammatory component is present.

Abbreviations:

Parkinson's disease (PD); central nervous system (CNS); Pituitary adenylate cyclase-activating peptide (PACAP); Vasoactive intestinal peptide (VIP); Lipopolysaccharide (LPS); Nitric oxide (NO); Interleukin-17a (IL-17a); Matrix metallopeptidase 9 (MMP-9); Ionised calcium-binding adapter molecule 1 (Iba1); Interleukin-6 (IL-6); Nitric oxide synthase 2 (NOS2); Interleukin-10 (IL-10); Arginase-1 (Arg1).

Data Availability Statement

The authors declare that [the/all other] data supporting the findings of this study are available within the article [and its supplementary information files]

Statements and declarations

Chapter 6:

General discussion and future perspectives

6.1 Summary of main findings
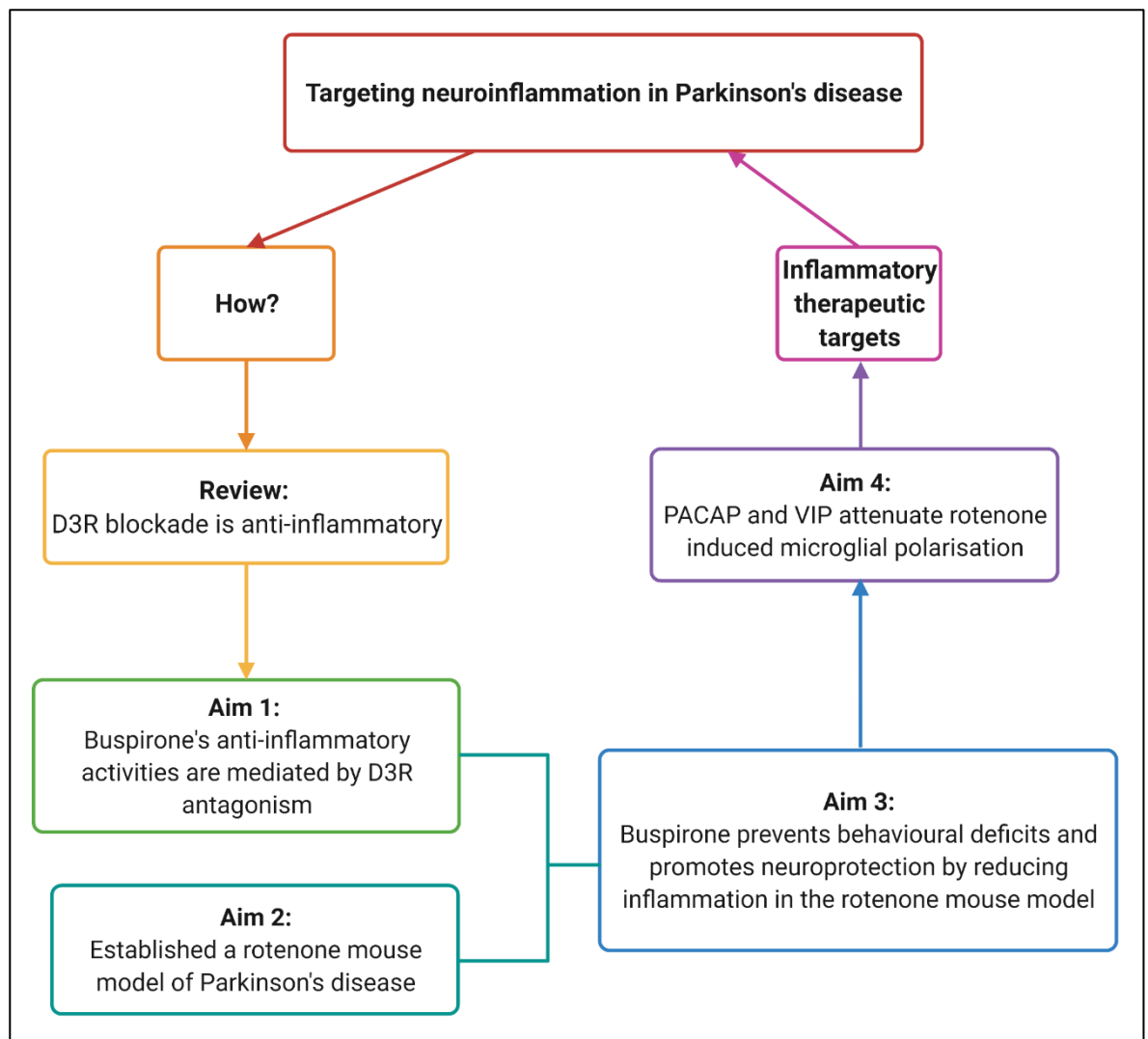
Figure 6.1. Summary of main findings of thesis.

Neurodegenerative disorders threaten our society with a substantial health, social and economic burden. There is an urgent need to develop novel therapeutic strategies that address the underlying disease pathogenesis in order to slow down or halt disease progression. Neuroinflammation is a major contributor to the pathophysiology of PD and is associated with both promoting disease progression

and clinical severity. Therefore, inhibiting or reducing inflammation is a promising therapeutic strategy for PD.

But how do you target neuroinflammation? As previously discussed, several attempts have been made to target inflammation with traditional anti-inflammatory agents like NSAIDs; however, these were not successful in clinical practice. We took a different approach and reviewed the emerging role of dopamine as an *immune transmitter* (Chapter 1.4). Through this review, we found that nearly all immune cell types express the components required to both synthesise, transport and metabolise dopamine, as well as functional dopamine receptors. We provided evidence that dopamine can control the behaviour of these immune cells in a dopamine-receptor-subtype and cell-specific manner. Most notably was the strong evidence that implicated the D3R as a promoter of inflammation across several cell types and in various neurological pathologies, including PD. Previous studies had revealed a strong "off-target" function of the anxiolytic drug buspirone as a D3R antagonist. Due to the lack of clinically available D3R antagonists and the safety profile of buspirone as a neurological therapeutic, we sought to investigate if buspirone could be a neuroprotective agent in PD by targeting neuroinflammation.

First, we developed a cellular model of neuroinflammation, in which we selectively knocked out the D3R and the 5HT1a receptors, buspirone's best known pharmacological targets, with CRISPR-Cas9 gene editing in BV2 microglial cells. The functional consequence of gene deletion and/or buspirone treatment in response to the inflammatory mimetic LPS was determined by cellular and molecular analysis. This study confirmed that antagonistic activity or gene deletion of the D3R prevented microglial polarization and inflammation *in vitro* (Chapter 2).

To test if this anti-inflammatory effect translated *in vivo*, we first established our own rotenone mouse model of PD (Chapter 3). Through behavioural and neurochemical analyses, we revealed that systemic administration of rotenone (10mg/kg BW) can cause exploratory and locomotor behavioural deficits that correlated with a myriad of neurochemical changes that extended beyond the nigro-striatal pathway into regions like the prefrontal cortex, amygdala and hippocampus. The changes reported were reminiscent of those seen in clinical PD patients and *post-mortem* brains. Therefore, we created a valid preclinical model to determine the efficacy of buspirone in preventing behavioural deficits, dopaminergic degeneration and neuroinflammation associated with PD.

Buspirone treatment was able to prevent rotenone-induced deficits in both locomotor and exploratory behaviour as observed in the open field test. Additionally, we report that high doses of buspirone (10mg/kg BW) were able to protect midbrain and *SNpc* dopaminergic neurons from degeneration. Importantly, buspirone treatment resulted in significant modulation of neuroinflammation. This included a global downregulation of pro-inflammatory mediators (IL-1β and IL-6), which correlated with an upregulation of both anti-inflammatory markers (Arg1) and neurotrophic factors (BDNF and ADNP). This evidence suggests that buspirone holds potential as a neuroprotective agent in PD in view of its ability to reduce neuroinflammation in distinct brain regions (Chapter 4).

Interestingly, throughout both *in vivo* studies (Chapters 3 and 4) we identified pronounced disruptions in the expression of the neuropeptides PACAP and VIP in several of the CNS regions studied. For instance, we found that rotenone dampens the expression of neuropeptides in Chapter 3. In contrast, buspirone treatment in great part prevented rotenone-induced disruptions to both PACAP and VIP

expression throughout the brain (Chapter 4). Based on these findings, and due to their well-established neuroprotective and immunomodulatory functions, we decided to complement this project with a further study aimed at determining if these peptides could attenuate rotenone driven microglial polarization *in vitro*. We found that both neuropeptides significantly reduced the expression of a range of pro-inflammatory and microglial activation markers in BV2 cells exposed to rotenone (Chapter 5). As such, this thesis identified three potential therapeutic targets that reduce neuroinflammation in preclinical models of PD.

6.2 Challenges modeling Parkinson's disease

Developing an accurate model of PD remains extremely difficult for several reasons, including the fact that the aetiology of disease remains unknown. Adding further complexity to this scenario is the sporadic nature of the disease and the fact that clinical diagnosis of PD occurs when over half of dopaminergic neurons are already compromised. This means that we are still in the dark about what pathophysiological processes occur early in the disease that cause irreversible damage and chronic pathology. This gives us limited information to work with to develop preclinical models that accurately recapitulate disease pathogenesis and progression in a similar way as it occurs in humans.

Unsurprisingly, the gold standard preclinical models that exist, play off this limited information and were developed based on their ability to promote the degeneration of dopaminergic neurons. Using these models, we have come to understand more

about the pathology of disease, including the contribution of neuroinflammation. However, the translational efficacy of these models has come under constant fire due to the large number of clinical trials that have failed, despite the great success in preclinical studies.

Therefore, it is important to consider the limitations of the models used to draw out accurate and impartial results regarding the efficacy of treatments. For example, this study utilised BV2 microglial cells to assess the ability of buspirone, PACAP and VIP in preventing microglia-induced inflammation. BV2 cells are an accepted *in vitro* model to study microglial biology, as they share 90% of the transcriptional profile of primary microglia, along with several biochemical, functional and morphological similarities [353, 354]. BV2 cells are an immortalized cell line allowing for higher throughput and sub-culturing, resulting in a cost and time effective cellular model to study microglial inflammation [355]. However, despite these technical advantages, further investigations in primary microglia will shed more light on the ability of these compounds to prevent microglial activation and the consequent inflammation. However, it may be worth pointing out that some studies using both BV2 and primary microglia [356], and *in vivo* studies complemented with BV2 experiments [357], have revealed consistent findings in the effects of novel compounds on microglia.

Furthermore, advances in induced pluripotent stem cells (iPSCs) have allowed for their differentiation into glial cells, including microglia, from patient-derived samples [358]. These cells carry disease specific phenotypes that would provide us with essential information on how microglia are behaving in PD. Moreover, the ability to manipulate these cells with CRISPR and create "brain-in-a-dish" co-culture experiments has dramatically enhanced the translational efficacy of iPSCs. These

organoid-like cultures can re-create endothelial cells and pericytes to develop a BBB structures, astrocytes, microglia and neurons [358]. This has enabled the recapitulation of neuropathology specific to patient's disease and an environment that mimics the human condition, allowing for a more precise and valid method to devise and assess novel treatments for neurodegenerative disorders [359].

Neurotoxin models of PD, like rotenone, are the current gold standard models to study neurodegeneration and the efficacy of novel therapeutics because they recapitulate several pathophysiological features of PD, including locomotor and exploratory deficits, dopaminergic degeneration, mitochondrial impairment, oxidative stress and neuroinflammation [360]. However, these models do not capture the whole spectrum of PD pathology and the choice of the model depends on the research question being investigated. In this project, we used rotenone for several reasons, including its ability to be administered systemically and the low dosage required to trigger PD-like pathology, making it technically simple to use and allowing us to create a reproducible model that was devoid of damage to the CNS arising from the administration procedure (i.e. stereotaxic injection), and with low associated mortality.

The focus of the project was to investigate the neuroinflammatory component of the disease and other associated neurochemical changes. However, we did not investigate all aspects of PD-like pathology rotenone can induce. For example, rotenone is known to induce α-synuclein pathology and the appearance of eosin positive inclusions resembling Lewy bodies, although this was beyond the scope of our study [281]. However, α-synuclein accumulation is thought to link the central and peripheral nervous systems in PD. For example, inflammation and α-synuclein observed in the gastrointestinal tract are reflective of each other and contribute to

the progressive severity of disease [361]. Further studies are required to understand the role of the buspirone, PACAP and VIP in counteracting α-synuclein pathology and toxicity, especially since α-synuclein contributes to neuroinflammation [362].

In addition to the expected PD-related motor symptoms, which are attributed to dopamine depletion caused by the degeneration of the nigro-striatal pathway, we identified a broader set of aberrant neurochemical changes in CNS regions that control mood, cognition and memory also known to be affected in PD. Specifically, we found disturbed expression of a myriad of markers associated with neurotoxicity in the prefrontal cortex, amygdala and hippocampus (Chapter 3). Interestingly, similar alterations have been seen in other neurological disorders like Alzheimer's disease [363, 364], depression [365, 366] and psychiatric disorders [367, 368]. Of note, depression, anxiety, apathy and cognitive dysfunction are thought to occur prior to the diagnosis of PD [369], with studies identifying these cognitive impairments are not attributed to dopamine depletion, highlighting the need to characterise extranigral sources of cognitive deficits observed in PD [370]. More recently, functional magnetic resonance imaging has been assessed as a tool to predict the risk of developing PD by investigating changes in brain regions associated with cognitive impairment and depression [371]. Functional and neurochemical disturbances in extra-nigral brain regions have been the focus of why current PD therapeutics aggravate non-motor symptoms in PD. This has been shown in studies investigating adverse effects of deep brain stimulation (DBS) in PD patients by revealing the importance of the location of neurostimulation, with evidence of worsened cognition and depression following DBS [32, 372]. Moreover, these studies highlight the need for a holistic approach to PD management,

treatment and research in acknowledging the role of extra-nigral brain region in pathogenesis and therapeutic response. Recent reviews have suggested that buspirone's pharmacological targets as a 5HT1a agonist and D3R antagonist could be beneficial across a range of neurodegenerative and neuroinflammatory diseases [216, 373]. This is strengthened by our study investigating the therapeutic potential of buspirone, which demonstrated that the drug prevents, to a large extent, the development of these neurochemical changes and perhaps, the associated behavioural dysfunctions, although this warrants further studies to be confirmed (Chapter 4).

6.3 Limitations of repurposing buspirone for Parkinson's disease

One of the major limitations of this study was that it failed to discern the exact contribution of one or both of buspirone's pharmacological targets to the neuroprotective activity observed. For example, blocking the D3R has been shown to prevent CD4+ T cell and microglial activation [156, 159]. By contrast, stimulation of 5HT1a receptors has been linked to a reduction in TNF-α expression and the number of Iba1-positive cells [374]. Further studies to dissect the specific neuroprotective properties elicited by buspirone's pharmacological targets would allow for the development of more targeted therapies for PD. This could be achieved using conditional knockout and/or knock-in mice (**Figure 6.2**).

Figure 6.2 Inducible and conditional knockout models to isolate neuronal and glial functions of the D3 receptor.

From the data generated, we did not appreciate many changes in GFAP expression in response to buspirone. This contradicts a study by Miyazaki and colleagues that demonstrated that targeting 5HT1a receptors on astrocytes enhances striatal astrocyte proliferation and increases TH expression in a 6-OHDA PD model [327]. Overexpressing 5HT1a in GFAP-positive cells (astrocytes) or deleting 5HT1a in this cell population would reveal the functional relevance of this receptor in both PD disease pathogenesis and buspirone treatment. Additionally, deleting the D3R in Cx3Cr1-positive cells (microglia) *in vivo* could determine if reducing microglial polarization represents one of buspirone's main mechanisms of neuroprotection, as shown in Chapter 2. These mechanistic studies could also aid in revealing the possible existence of a synergistic interaction between the D3R and 5HT1a receptors, where each receptor mediates distinct functions that contribute to the overall beneficial effect elicited by buspirone. Alternatively, these studies could help to explain certain unexpected responses of microglial cells, such as the exacerbated nitric oxide response when the 5HT1a receptor was genetically

ablated, as observed in Chapter 2. Specifically, a well-planned approach using genetically modified mice and/or cells could prove the theory in which, the crosstalk between distinct neurotransmitter systems may be fundamental for the homeostatic response of resident immune/glial cells to inflammatory triggers. In addition, use of conditional and/or cell-specific deletions of the D3R would also control for any impact buspirone's antagonistic activity may have on neuronal function.

The interplay between dopaminergic and serotonergic systems is receiving a lot of attention due to the potential therapeutic efficacy of 5HT1a agonism in counteracting dyskinesias [375, 376]. Buspirone has been suggested as a potential therapeutic over more specific 5HT1a agonists, like 8-OH-DPAT, perhaps due to its high therapeutic index and reduced risk of 5HT syndrome [377]. This could explain why we did not observe any adverse effects resulting from an over-stimulation of the serotonin system. Indeed, buspirone, via its partial 5HT1a agonist activity, may have prevented any negative effects associated with excess serotonin activity, even when administered at high doses. It is worth mentioning that several other neurotransmitters have been reported to modulate the immune response. This is not surprising given the overlap of receptors, signalling molecules and anatomy shared by the nervous and immune systems. Additionally, disturbed activity of several neurotransmitters has been reported in PD pathogenesis, suggesting targeting their immunomodulatory effects could be another therapeutic approach to reduce neuroinflammation [10]. In fact, modulating glutamate receptor 1 has shown to revert PD phenotype in MPTP and 6-OHDA models via ceftriaxone treatment [378]. Additionally, GABA acts as a negative regulator of macrophage and microglial production of pro-inflammatory molecules [105]. Interestingly, 5HT appears to exert both pro and anti-inflammatory functions. Some studies suggest

that 5HT is pro-inflammatory as studies have shown that depletion of 5HT reduces animal models of inflammation such as adjuvant-induced arthritis [379]. While others have reported that 5HT2a agonism suppresses TNF-α induced inflammation [380]. Furthermore, 5HT has been shown to enhance the chemotactic response of microglia [266] while PACAP-PAC1 signalling can regulate 5HT2a internalisation suggesting a potential interaction between both 5HT, dopamine and the neuropeptide [381]. It would also be important to investigate regions with high density of 5HT1a receptors, like the raphe nucleus, which imaging studies have shown to be disrupted during PD [382]. Like dopamine, conflicting data has been reported about the role of serotonin in neuroinflammation, and it is likely that this response is also subtype dependent [383]. As such, it is highly plausible that the beneficial effects of buspirone treatment is also due to 5HT1a agonism exerting anti-inflammatory and neuroprotective effects, although further studies would be needed to prove this. Neurotransmitter regulation of neuroinflammation is an emerging field which requires further investigation.

This is evident in the conflicting role of the D3R in neuroinflammation. The emergence of dopamine as an *immune transmitter* is novel. As such, we still do not know the complete story of dopamine's function on each cell type and under a range of diverse neurological insults. Furthermore, it is still hard to find a DR drug that specifically targets one DR subtype. The highly conserved transmembrane sequences of D2-like receptors (D2R, D3R and D4R) result in therapeutics targeting all three subtypes [384]. Buspirone has been shown to act on both the D2R and D3R receptors, although with much lower affinity for the former [230]. This can still produce conflicting results, with drugs acting on more than one receptor subtype simultaneously. Current evidence suggests that low-affinity

dopamine receptors (D2R) induce anti-inflammatory actions, whereas high affinity receptors (D3R) promote inflammation [158]. However, buspirone has been shown to have an affinity for D3R that is 70-fold higher than D2R and 11-fold higher than 5HT1a [230] suggesting that the neuroprotective effects observed are most likely driven by buspirone antagonist activity on the D3R. Furthermore, the unique distribution and low brain abundance of neuronal D3 receptors make them an attractive therapeutic target for the development of drugs with limited adverse effects on motor function [216]. Additionally, D3Rs are found in areas important in the control of psychotic symptoms making them a valuable target to treat non-motor PD symptoms, like depression, anxiety, emotion and cognition. We show that buspirone treatment alone, even at high doses (10mg/kg B/W) did not alter motor function compared to saline-injected controls (**Chapter 4 Supplementary Figure 1**) in the open field test. It is possible that blocking the D3R will not significantly impact motor function and other neuronal functions mediated by D3Rs, although further studies are required to determine this. In fact, other studies using D3R antagonists have revealed blocking D3R does not impact motor function but improves cognition, psychotic behaviours and substance abuse [385].

Furthermore, the model could be adapted to determine if buspirone can rescue both behavioural and neurochemical changes induced by rotenone intoxication. This could be achieved with a delayed treatment regimen by first inducing PD-like pathology with rotenone administration, then after a washout period, exposing animals to buspirone. This approach usually occurs after a preliminary of co-administration such as this one. Co-administration allows you to determine if the therapeutic can mitigate the effects of the disease-inducing agent. If successful, the delayed treatment regime, allows you to first induce disease then determine if the

therapeutic can reduce symptoms and/or delay disease progression, in the context of neurodegenerative disease. This is particularly important for translational efficacy as this would more closely resemble the clinical management of PD. Additionally, the ability to provide symptomatic and/or pathological relief is a much harder feat than during co-administration. The delayed treatment regimen is a more stringent and clinically relevant test for the potential efficacy of a therapeutic and is a logical next step for this work. However, it should be noted that this type of experiment applies to neuropathological conditions that can be reversed. Current understanding is that neurodegeneration is partially irreversible process and as such therapeutics are deemed successful when they prevent or halt neuron loss, not reverse it [386]. As such, the co-administration design of our study is suitable for assessing the ability of buspirone to attenuate neuron loss.

Lastly, transcriptomic and/or proteomic analyses are required to determine the downstream intracellular pathways, genes and protein targets activated by buspirone to dampen inflammation and perhaps, regulate other essential microglial functions. Chapter 2 did not investigate any morphological or functional changes of BV2 microglia in response to either gene deletion or buspirone treatment. In other studies, we have shown that PACAP and VIP treatments, despite exhibiting overlapping anti-inflammatory effects, induced distinct morphological phenotypes and differing migratory capacity in cells exposed to LPS [240]. A similar approach could be instrumental in unveiling if each of buspirone's receptor targets distinctively regulate critical biological activities of microglia that are essential to provide an effective anti-inflammatory response. Additionally, in chapters 3 and 4, more in-depth analyses to determine how glial cells responded to rotenone and buspirone are required. The use of conditional knockouts targeting specific glial

populations (i.e. astrocytes or microglia), as mentioned above, would aid in this analysis. However, additional localization studies using immunohistochemistry combined with stereological assessments would allow the acquisition of relevant information such as changes in cell morphology, number and distribution in CNS structures. These additional findings could provide a clearer indication of any phenotypic shift of cells, otherwise not identifiable by measuring the expression of certain molecular markers. Furthermore, flow cytometry to isolate distinct cellular populations could reveal any changes in the number and phenotype of glial subtypes, from classically (M1 and A1) and alternatively (M2 and A2) activated microglia and astrocytes, respectively [79, 84, 91]. Several studies that aim to target neuroinflammation in PD have suggested that the disease is characterised by a lack of M2 and A2 response and have put forward the theory stating that PD therapeutics should aim to promote M2/A2 responses to drive neuroprotective and anti-inflammatory activities that ultimately provide growth and trophic support to degenerating dopamine neurons [86].

6.4 Potential of PACAP and VIP as therapeutic targets

Due to the promising results of PACAP and VIP in attenuating microglial polarization *in vitro*, the logical next step would be to administer these peptides to rotenone-treated mice to assess their ability to protect against rotenone intoxication. Several studies of these peptides in preclinical models suggest their effectiveness as immune modulatory and therefore neuroprotective agents in PD

[243, 245, 342, 387]. For example, PACAP treatment prevented dopamine loss in 6-OHDA exposed rats [247]. Additionally, both PACAP and VIP, through the VPAC1 receptor, inhibited microglial chemokine production [336]. Moreover, VIP administration could protect neurons, which was able to reverse 6-OHDA induced motor deficits in parkinsonian rats [343].

Despite their success in several preclinical models of neurological diseases, these peptides and/or synthetic analogues able to target PACAP/VIP receptors have not yet entered the clinic. This is due to a variety of reasons, namely, the efficiency of compounds to cross the BBB and the preferential activation of second messengers for biased signalling [388]. In addition, both peptides show limited bioavailability, with a half-life of only a few minutes once thee enter the bloodstream [389, 390]. Moreover, we did not investigate how the expression of PACAP/VIP receptors was affected by rotenone and/or buspirone administration *in vivo*. This would shed more light on the functional consequences and downstream signalling pathways activated by the observed changes in peptide expression, as the PAC1 receptor is associated with neuroprotection and cell survival [391], whereas VPAC receptors [392] have a stronger effect on regulating immune responses [244, 393, 394]. Current advances in developing PACAP and VIP therapeutics suggest that we are closer to seeing a therapeutic targeting these peptides in the clinic. TAT-tagging VIP improved the neuroprotective effects of VIP in cellular and animal models of PD [329]. Additionally, studies in other neuroinflammatory and neurodegenerative diseases have shown the utility of PAC1 activation in protecting neurons during neuroinflammation [395].

6.5 Conclusion

In summary, using both cellular and animal models of PD, we have demonstrated the ability of the anxiolytic drug, buspirone, to attenuate microglial polarization, prevent locomotor/exploratory deficits, protect dopaminergic neurons from degeneration, dampen the expression of inflammatory mediators, promote the expression of neuropeptides and neurotrophic factors. Additionally, we provide preliminary evidence of the ability of PACAP and VIP to inhibit microglial mediated neuroinflammation. Overall, this thesis provides novel insights into the potential of buspirone, PACAP and VIP as anti-inflammatory agents that may find application for the treatment of PD and perhaps, other neuroinflammatory and/or neurodegenerative conditions.
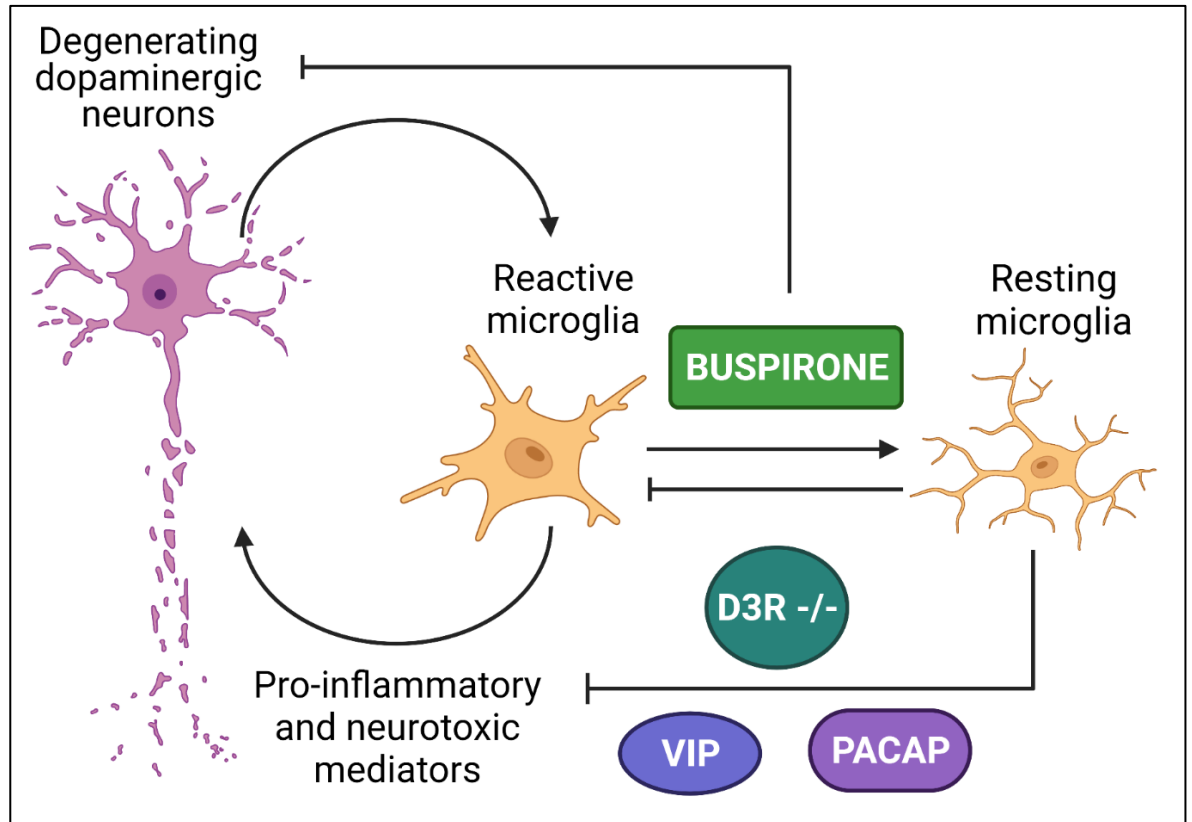
Figure 6.3. Schematic diagram illustrating the main findings. Buspirone (Chapters 2 & 4), D3R knockout (Chapter 2), VIP and PACAP (Chapter 5) prevent microglial activation which inhibits the release of pro-inflammatory and neurotoxic mediators. Buspirone also protects dopaminergic neurons from degeneration (Chapter 4).

Bibliography

References:

1. Glass, C.K., et al., *Mechanisms underlying inflammation in neurodegeneration.* Cell, 2010. **140**(6): p. 918-34.
2. Reeve, A., E. Simcox, and D. Turnbull, *Ageing and Parkinson's disease: why is advancing age the biggest risk factor?* Ageing Res Rev, 2014. **14**: p. 19-30.
3. Wyss-Coray, T., *Ageing, neurodegeneration and brain rejuvenation.* Nature, 2016. **539**(7628): p. 180-186.
4. Braak, H., et al., *Stages in the development of Parkinson's disease-related pathology.* Cell Tissue Res, 2004. **318**(1): p. 121-34.
5. Sveinbjornsdottir, S., *The clinical symptoms of Parkinson's disease.* J Neurochem, 2016. **139 Suppl 1**: p. 318-324.
6. Kobylecki, C., *Update on the diagnosis and management of Parkinson's disease.* Clin Med (Lond), 2020. **20**(4): p. 393-398.
7. Schapira, A.H.V., K.R. Chaudhuri, and P. Jenner, *Non-motor features of Parkinson disease.* Nat Rev Neurosci, 2017. **18**(7): p. 435-450.
8. Stogbauer, J., et al., *Striatal dopamine transporters and cognitive function in Parkinson's disease.* Acta Neurol Scand, 2020. **142**(4): p. 385-391.
9. Nakajima, S., et al., *The potential role of dopamine D(3) receptor neurotransmission in cognition.* Eur Neuropsychopharmacol, 2013. **23**(8): p. 799-813.
10. Sanjari Moghaddam, H., et al., *Neurotransmission systems in Parkinson's disease.* Rev Neurosci, 2017. **28**(5): p. 509-536.
11. Rietdijk, C.D., et al., *Exploring Braak's Hypothesis of Parkinson's Disease.* Front Neurol, 2017. **8**: p. 37.
12. Poewe, W., *Non-motor symptoms in Parkinson's disease.* Eur J Neurol, 2008. **15 Suppl 1**: p. 14-20.
13. Raudino, F. and S. Leva, *Involvement of the spinal cord in Parkinson's disease.* Int J Neurosci, 2012. **122**(1): p. 1-8.
14. Anderson, J.P., et al., *Phosphorylation of Ser-129 is the dominant pathological modification of alpha-synuclein in familial and sporadic Lewy body disease.* J Biol Chem, 2006. **281**(40): p. 29739-52.
15. Natale, G., et al., *Parallel manifestations of neuropathologies in the enteric and central nervous systems.* Neurogastroenterol Motil, 2011. **23**(12): p. 1056-65.
16. Atik, A., T. Stewart, and J. Zhang, *Alpha-Synuclein as a Biomarker for Parkinson's Disease.* Brain Pathol, 2016. **26**(3): p. 410-8.
17. Friedman, L.G., et al., *Disrupted autophagy leads to dopaminergic axon and dendrite degeneration and promotes presynaptic accumulation of α-synuclein and LRRK2 in the brain.* 2012. **32**(22): p. 7585-7593.
18. Zhang, S., R. Wang, and G. Wang, *Impact of Dopamine Oxidation on Dopaminergic Neurodegeneration.* ACS Chem Neurosci, 2019. **10**(2): p. 945-953.
19. Dorszewska, J., et al., *Oxidative stress factors in Parkinson's disease.* Neural Regen Res, 2021. **16**(7): p. 1383-1391.
20. Gelders, G., V. Baekelandt, and A. Van der Perren, *Linking Neuroinflammation and Neurodegeneration in Parkinson's Disease.* J Immunol Res, 2018. **2018**: p. 4784268.
21. LeWitt, P.A., *Levodopa therapy for Parkinson's disease: Pharmacokinetics and pharmacodynamics.* Mov Disord, 2015. **30**(1): p. 64-72.
22. Ayano, G., *Dopamine: Receptors, Functions, Synthesis, Pathways, Locations and Mental Disorders: Review of Literatures.* Journal of Mental Disorders and Treatment, 2016. **2**(2).
23. Chao, O.Y., et al., *Intranasally applied L-DOPA alleviates parkinsonian symptoms in rats with unilateral nigro-striatal 6-OHDA lesions.* Brain Res Bull, 2012. **87**(2-3): p. 340-5.

24. Warren Olanow, C., et al., *Factors predictive of the development of Levodopa-induced dyskinesia and wearing-off in Parkinson's disease.* Mov Disord, 2013. **28**(8): p. 1064-71.

25. Cacabelos, R., *Parkinson's Disease: From Pathogenesis to Pharmacogenomics.* Int J Mol Sci, 2017. **18**(3).

26. Zhang, Z., et al., *Roles of Glutamate Receptors in Parkinson's Disease.* Int J Mol Sci, 2019. **20**(18).

27. Beaulieu, J.M. and R.R. Gainetdinov, *The physiology, signaling, and pharmacology of dopamine receptors.* Pharmacol Rev, 2011. **63**(1): p. 182-217.

28. Bostwick, J.M., et al., *Frequency of New-Onset Pathologic Compulsive Gambling or Hypersexuality After Drug Treatment of Idiopathic Parkinson Disease.* Mayo Clinic Proceedings, 2009. **84**(4): p. 310-316.

29. Seeman, P. and H.B. Niznik, *Dopamine receptors and transporters in Parkinson's disease and schizophrenia.* FASEB J, 1990. **4**(10): p. 2737-44.

30. Thobois, S., et al., *Role of dopaminergic treatment in dopamine receptor down-regulation in advanced Parkinson disease: a positron emission tomographic study.* Arch Neurol, 2004. **61**(11): p. 1705-9.

31. Pahwa, R., et al., *Practice Parameter: treatment of Parkinson disease with motor fluctuations and dyskinesia (an evidence-based review): report of the Quality Standards Subcommittee of the American Academy of Neurology.* Neurology, 2006. **66**(7): p. 983-95.

32. Combs, H.L., et al., *Cognition and Depression Following Deep Brain Stimulation of the Subthalamic Nucleus and Globus Pallidus Pars Internus in Parkinson's Disease: A Meta-Analysis.* Neuropsychol Rev, 2015. **25**(4): p. 439-54.

33. Pang, S.Y., et al., *The interplay of aging, genetics and environmental factors in the pathogenesis of Parkinson's disease.* Transl Neurodegener, 2019. **8**: p. 23.

34. Bhurtel, S., et al., *Mechanistic comparison between MPTP and rotenone neurotoxicity in mice.* Neurotoxicology, 2019. **71**: p. 113-121.

35. Dawson, T.M., T.E. Golde, and C. Lagier-Tourenne, *Animal models of neurodegenerative diseases.* Nat Neurosci, 2018. **21**(10): p. 1370-1379.

36. Gamber, K.M., *Animal Models of Parkinson's Disease: New models provide greater translational and predictive value.* BioTechniques, 2016. **61**(4): p. 210-211.

37. Salari, S. and M. Bagheri, *In vivo, in vitro and pharmacologic models of Parkinson's disease.* Physiol Res, 2019. **68**(1): p. 17-24.

38. Tanner, C.M., et al., *Rotenone, paraquat, and Parkinson's disease.* Environ Health Perspect, 2011. **119**(6): p. 866-72.

39. Chia, S.J., E.K. Tan, and Y.X. Chao, *Historical Perspective: Models of Parkinson's Disease.* Int J Mol Sci, 2020. **21**(7).

40. Radad, K., et al., *Rotenone: from modelling to implication in Parkinson's disease.* Folia Neuropathol, 2019. **57**(4): p. 317-326.

41. Betarbet, R., et al., *Chronic systemic pesticide exposure reproduces features of Parkinson's disease.* Nat Neurosci, 2000. **3**(12): p. 1301-6.

42. Sherer, T.B., et al., *Mechanism of toxicity of pesticides acting at complex I: relevance to environmental etiologies of Parkinson's disease.* J Neurochem, 2007. **100**(6): p. 1469-79.

43. Giguere, N., S. Burke Nanni, and L.E. Trudeau, *On Cell Loss and Selective Vulnerability of Neuronal Populations in Parkinson's Disease.* Front Neurol, 2018. **9**: p. 455.

44. Castano, A., et al., *Lipopolysaccharide intranigral injection induces inflammatory reaction and damage in nigrostriatal dopaminergic system.* J Neurochem, 1998. **70**(4): p. 1584-92.

45. Mosharov, E.V., et al., *Interplay between cytosolic dopamine, calcium, and alpha-synuclein causes selective death of substantia nigra neurons.* Neuron, 2009. **62**(2): p. 218-29.

46. Ramalingam, M., S. Jang, and H.S. Jeong, *Neural-Induced Human Adipose Tissue-Derived Stem Cells Conditioned Medium Ameliorates Rotenone-Induced Toxicity in SH-SY5Y Cells.* Int J Mol Sci, 2021. **22**(5).

47. Elstner, M., et al., *Expression analysis of dopaminergic neurons in Parkinson's disease and aging links transcriptional dysregulation of energy metabolism to cell death.* Acta Neuropathol, 2011. **122**(1): p. 75-86.

48. Schapira, A.H.V., et al., *Mitochondrial Complex I Deficiency in Parkinson's Disease.* The Lancet, 1989. **333**(8649).

49. Miyazaki, I., et al., *Chronic Systemic Exposure to Low-Dose Rotenone Induced Central and Peripheral Neuropathology and Motor Deficits in Mice: Reproducible Animal Model of Parkinson's Disease.* Int J Mol Sci, 2020. **21**(9).

50. Murakami, S., et al., *Long-Term Systemic Exposure to Rotenone Induces Central and Peripheral Pathology of Parkinson's Disease in Mice.* Neurochem Res, 2015. **40**(6): p. 1165-78.

51. Pan-Montojo, F., et al., *Progression of Parkinson's disease pathology is reproduced by intragastric administration of rotenone in mice.* PLoS One, 2010. **5**(1): p. e8762.

52. Alam, M. and W.J. Schmidt, *Rotenone destroys dopaminergic neurons and induces parkinsonian symptoms in rats.* Behavioural Brain Research, 2002. **136**(1): p. 317-324.

53. Alam, M. and W.J. Schmidt, *L-DOPA reverses the hypokinetic behaviour and rigidity in rotenone-treated rats.* Behav Brain Res, 2004. **153**(2): p. 439-46.

54. Jing, L., et al., *Microglial Activation Mediates Noradrenergic Locus Coeruleus Neurodegeneration via Complement Receptor 3 in a Rotenone-Induced Parkinson's Disease Mouse Model.* J Inflamm Res, 2021. **14**: p. 1341-1356.

55. Zhang, Y., et al., *Involvement of Akt/mTOR in the Neurotoxicity of Rotenone-Induced Parkinson's Disease Models.* Int J Environ Res Public Health, 2019. **16**(20).

56. Inden, M., et al., *Parkinsonian rotenone mouse model: reevaluation of long-term administration of rotenone in C57BL/6 mice.* Biol Pharm Bull, 2011. **34**(1): p. 92-6.

57. Inden, M., et al., *Neurodegeneration of mouse nigrostriatal dopaminergic system induced by repeated oral administration of rotenone is prevented by 4-phenylbutyrate, a chemical chaperone.* J Neurochem, 2007. **101**(6): p. 1491-1504.

58. Liu, H.F., et al., *Combined LRRK2 mutation, aging and chronic low dose oral rotenone as a model of Parkinson's disease.* Sci Rep, 2017. **7**: p. 40887.

59. Abdel-Salam, O.M.E., et al., *The effect of low dose amphetamine in rotenone-induced toxicity in a mice model of Parkinson's disease.* Iran J Basic Med Sci, 2020. **23**(9): p. 1207-1217.

60. Dhanalakshmi, C., et al., *Vanillin Attenuated Behavioural Impairments, Neurochemical Deficts, Oxidative Stress and Apoptosis Against Rotenone Induced Rat Model of Parkinson's Disease.* Neurochem Res, 2016. **41**(8): p. 1899-910.

61. Li, H., et al., *Resveratrol attenuates rotenone-induced inflammation and oxidative stress via STAT1 and Nrf2/Keap1/SLC7A11 pathway in a microglia cell line.* Pathol Res Pract, 2021. **225**: p. 153576.

62. Hoban, D.B., et al., *Further characterisation of the LPS model of Parkinson's disease: a comparison of intra-nigral and intra-striatal lipopolysaccharide administration on motor function, microgliosis and nigrostriatal neurodegeneration in the rat.* Brain Behav Immun, 2013. **27**(1): p. 91-100.

63. DiSabato, D.J., N. Quan, and J.P. Godbout, *Neuroinflammation: the devil is in the details.* J Neurochem, 2016. **139 Suppl 2**: p. 136-153.

64. Hirsch, E.C. and S. Hunot, *Neuroinflammation in Parkinson's disease: a target for neuroprotection?* The Lancet Neurology, 2009. **8**(4): p. 382-397.

65. Ghosh, P., et al., *Cellular and molecular influencers of neuroinflammation in Alzheimer's disease: Recent concepts & roles.* Neurochem Int, 2021. **151**: p. 105212.

66. Stuckey, S.M., et al., *Neuroinflammation as a Key Driver of Secondary Neurodegeneration Following Stroke?* Int J Mol Sci, 2021. **22**(23).

67. Zelic, M., et al., *RIPK1 activation mediates neuroinflammation and disease progression in multiple sclerosis.* Cell Rep, 2021. **35**(6): p. 109112.
68. Hunter, R.L., et al., *Inflammation induces mitochondrial dysfunction and dopaminergic neurodegeneration in the nigrostriatal system.* J Neurochem, 2007. **100**(5): p. 1375-86.
69. Gerhard, A., et al., *In vivo imaging of microglial activation with [11C](R)-PK11195 PET in idiopathic Parkinson's disease.* Neurobiol Dis, 2006. **21**(2): p. 404-12.
70. Brodacki, B., et al., *Serum interleukin (IL-2, IL-10, IL-6, IL-4), TNFalpha, and INFgamma concentrations are elevated in patients with atypical and idiopathic parkinsonism.* Neurosci Lett, 2008. **441**(2): p. 158-62.
71. McGeer, P.L., et al., *Reactive microglia are positive for HLA-DR in the substantia nigra of Parkinson's and Alzheimer's disease brains.* Neurology, 1988. **38**(8): p. 1285-91.
72. Inden, M., et al., *Neuroprotective effect of the antiparkinsonian drug pramipexole against nigrostriatal dopaminergic degeneration in rotenone-treated mice.* Neurochem Int, 2009. **55**(8): p. 760-7.
73. Mogi, M., et al., *Interleukin (IL)-1β, IL-2, IL-4, IL-6 and transforming growth factor-α levels are elevated in ventricular cerebrospinal fluid in juvenile parkinsonism and Parkinson's disease.* Neuroscience Letters, 1996. **211**(1): p. 13-16.
74. Blum-Degena, D., et al., *Interleukin-1β and interleukin-6 are elevated in the cerebrospinal fluid of Alzheimer's and de novo Parkinson's disease patients.* Neuroscience Letters, 1995. **202**(1-2): p. 17-20.
75. Gupta, N., et al., *Recent progress in therapeutic strategies for microglia-mediated neuroinflammation in neuropathologies.* Expert Opin Ther Targets, 2018. **22**(9): p. 765-781.
76. Santiago, J.A., V. Bottero, and J.A. Potashkin, *Biological and Clinical Implications of Comorbidities in Parkinson's Disease.* Front Aging Neurosci, 2017. **9**: p. 394.
77. Leng, F. and P. Edison, *Neuroinflammation and microglial activation in Alzheimer disease: where do we go from here?* Nat Rev Neurol, 2021. **17**(3): p. 157-172.
78. Shi, K., et al., *Global brain inflammation in stroke.* The Lancet Neurology, 2019. **18**(11): p. 1058-1066.
79. Burke, N.N., et al., *Minocycline modulates neuropathic pain behaviour and cortical M1-M2 microglial gene expression in a rat model of depression.* Brain Behav Immun, 2014. **42**: p. 147-56.
80. Liu, H.Y., et al., *Chronic minocycline treatment reduces the anxiety-like behaviors induced by repeated restraint stress through modulating neuroinflammation.* Brain Res Bull, 2018. **143**: p. 19-26.
81. Li, X., et al., *Methamphetamine causes neurotoxicity by promoting polarization of macrophages and inflammatory response.* Hum Exp Toxicol, 2018. **37**(5): p. 486-495.
82. McLean, G., et al., *Co-morbidity and polypharmacy in Parkinson's disease: insights from a large Scottish primary care database.* BMC Neurol, 2017. **17**(1): p. 126.
83. Badanjak, K., et al., *The Contribution of Microglia to Neuroinflammation in Parkinson's Disease.* Int J Mol Sci, 2021. **22**(9).
84. Zhang, L., J. Zhang, and Z. You, *Switching of the Microglial Activation Phenotype Is a Possible Treatment for Depression Disorder.* Front Cell Neurosci, 2018. **12**: p. 306.
85. Janda, E., L. Boi, and A.R. Carta, *Microglial Phagocytosis and Its Regulation: A Therapeutic Target in Parkinson's Disease?* Front Mol Neurosci, 2018. **11**: p. 144.
86. Cherry, J.D., J.A. Olschowka, and M.K. O'Banion, *Neuroinflammation and M2 microglia: the good, the bad, and the inflamed.* J Neuroinflammation, 2014. **11**: p. 98.
87. Cao, J.J., K.S. Li, and Y.Q. Shen, *Activated immune cells in Parkinson's disease.* J Neuroimmune Pharmacol, 2011. **6**(3): p. 323-9.
88. Zhang, D., et al., *Microglial activation contributes to cognitive impairments in rotenone-induced mouse Parkinson's disease model.* J Neuroinflammation, 2021. **18**(1): p. 4.

89.   Li, K., et al., *Reactive Astrocytes in Neurodegenerative Diseases.* Aging Dis, 2019. **10**(3): p. 664-675.

90.   Liddelow, S.A., et al., *Neurotoxic reactive astrocytes are induced by activated microglia.* Nature, 2017. **541**(7638): p. 481-487.

91.   Kwon, H.S. and S.H. Koh, *Neuroinflammation in neurodegenerative disorders: the roles of microglia and astrocytes.* Transl Neurodegener, 2020. **9**(1): p. 42.

92.   Brochard, V., et al., *Infiltration of CD4+ lymphocytes into the brain contributes to neurodegeneration in a mouse model of Parkinson disease.* J Clin Invest, 2009. **119**(1): p. 182-92.

93.   Kannarkat, G.T., J.M. Boss, and M.G. Tansey, *The role of innate and adaptive immunity in Parkinson's disease.* J Parkinsons Dis, 2013. **3**(4): p. 493-514.

94.   Bhatia, D., et al., *T-cell dysregulation is associated with disease severity in Parkinson's Disease.* J Neuroinflammation, 2021. **18**(1): p. 250.

95.   Ahn, J.J., M. Abu-Rub, and R.H. Miller, *B Cells in Neuroinflammation: New Perspectives and Mechanistic Insights.* Cells, 2021. **10**(7).

96.   Li, R., et al., *Abnormal B-Cell and Tfh-Cell Profiles in Patients With Parkinson Disease: A Cross-sectional Study.* Neurol Neuroimmunol Neuroinflamm, 2022. **9**(2).

97.   Yang, P., et al., *Dopamine D3 receptor: A neglected participant in Parkinson Disease pathogenesis and treatment?* Ageing Res Rev, 2020. **57**: p. 100994.

98.   Wexler, M. *NSAIDs May Lower LRRK2 Parkinson's Risk, Study Asserts*. 2020 [cited 2021 31/12/2021]; Available from: https://parkinsonsnewstoday.com/2020/07/30/nsaids-may-lower-lrrk2-parkinsons-risk-study-asserts/.

99.   Schonhoff, A.M., et al., *Innate and adaptive immune responses in Parkinson's disease.* Prog Brain Res, 2020. **252**: p. 169-216.

100.   Thomas, M. and W.D. Le, *Minocycline: neuroprotective mechanisms in Parkinson's disease.* Curr Pharm Des, 2004. **10**(6): p. 679-86.

101.   Du, Y., et al., *Minocycline prevents nigrostriatal dopaminergic neurodegeneration in the MPTP model of Parkinson's disease.* Proc Natl Acad Sci U S A, 2001. **98**(25): p. 14669-74.

102.   D'Antonio, M., et al., *Gene profiling and bioinformatic analysis of Schwann cell embryonic development and myelination.* Glia, 2006. **53**(5): p. 501-15.

103.   Bassett, B., et al., *Minocycline alleviates depression-like symptoms by rescuing decrease in neurogenesis in dorsal hippocampus via blocking microglia activation/phagocytosis.* Brain Behav Immun, 2021. **91**: p. 519-530.

104.   Vijiaratnam, N. and T. Foltynie, *Disease modifying therapies III: Novel targets.* Neuropharmacology, 2021. **201**: p. 108839.

105.   Hodo, T.W., et al., *Critical Neurotransmitters in the Neuroimmune Network.* Front Immunol, 2020. **11**: p. 1869.

106.   Asanuma, M. and I. Miyazaki, *3-O-Methyldopa inhibits astrocyte-mediated dopaminergic neuroprotective effects of L-DOPA.* BMC Neurosci, 2016. **17**(1): p. 52.

107.   Mastroeni, D., et al., *Microglial responses to dopamine in a cell culture model of Parkinson's disease.* Neurobiol Aging, 2009. **30**(11): p. 1805-17.

108.   Shao, W., et al., *Suppression of neuroinflammation by astrocytic dopamine D2 receptors via alphaB-crystallin.* Nature, 2013. **494**(7435): p. 90-4.

109.   Fan, Y., et al., *Differential Regulation of Adhesion and Phagocytosis of Resting and Activated Microglia by Dopamine.* Front Cell Neurosci, 2018. **12**: p. 309.

110.   Pinoli, M., F. Marino, and M. Cosentino, *Dopaminergic Regulation of Innate Immunity: a Review.* J Neuroimmune Pharmacol, 2017. **12**(4): p. 602-623.

111.   Castorina, A., et al., *Dopamine D3 receptor deletion increases tissue plasminogen activator (tPA) activity in prefrontal cortex and hippocampus.* Neuroscience, 2013. **250**: p. 546-56.

112. D'Amico, A.G., et al., *Hippocampal neurofibromin and amyloid precursor protein expression in dopamine D3 receptor knock-out mice following passive avoidance conditioning.* Neurochem Res, 2013. **38**(3): p. 564-72.

113. D'Amico, A.G., et al., *Increased hippocampal CREB phosphorylation in dopamine D3 receptor knockout mice following passive avoidance conditioning.* Neurochem Res, 2013. **38**(12): p. 2516-23.

114. Marzagalli, R., et al., *Genetic blockade of the dopamine D3 receptor enhances hippocampal expression of PACAP and receptors and alters their cortical distribution.* Neuroscience, 2016. **316**: p. 279-95.

115. Rangel-Barajas, C., I. Coronel, and B. Floran, *Dopamine Receptors and Neurodegeneration.* Aging Dis, 2015. **6**(5): p. 349-68.

116. Gaskill, P.J., et al., *Characterization and function of the human macrophage dopaminergic system: implications for CNS disease and drug abuse.* J Neuroinflammation, 2012. **9**: p. 203.

117. Mackie, P., et al., *The dopamine transporter: An unrecognized nexus for dysfunctional peripheral immunity and signaling in Parkinson's Disease.* Brain Behav Immun, 2018. **70**: p. 21-35.

118. Rönnberg, E., G. Calounova, and G. Pejler, *Mast cells express tyrosine hydroxylase and store dopamine in a serglycin-dependent manner.* Biol Chem, 2012. **393**(1-2): p. 107-12.

119. Matt, S.M. and P.J. Gaskill, *Where Is Dopamine and how do Immune Cells See it?: Dopamine-Mediated Immune Cell Function in Health and Disease.* J Neuroimmune Pharmacol, 2019.

120. McKenna, F., et al., *Dopamine receptor expression on human T- and B-lymphocytes, monocytes, neutrophils, eosinophils and NK cells: a flow cytometric study.* Journal of Neuroimmunology, 2002. **132**(1-2): p. 34-40.

121. Wang, Q., Y. Liu, and J. Zhou, *Neuroinflammation in Parkinson's disease and its potential as therapeutic target.* Transl Neurodegener, 2015. **4**: p. 19.

122. Miyazaki, I., et al., *Direct evidence for expression of dopamine receptors in astrocytes from basal ganglia.* Brain Res, 2004. **1029**(1): p. 120-3.

123. Levite, M., *Dopamine and T cells: dopamine receptors and potent effects on T cells, dopamine production in T cells, and abnormalities in the dopaminergic system in T cells in autoimmune, neurological and psychiatric diseases.* Acta Physiol (Oxf), 2016. **216**(1): p. 42-89.

124. Qiu, Y.H., et al., *Effect of endogenous catecholamines in lymphocytes on lymphocyte function.* J Neuroimmunol, 2005. **167**(1-2): p. 45-52.

125. Pacheco, R., et al., *Role of dopamine in the physiology of T-cells and dendritic cells.* J Neuroimmunol, 2009. **216**(1-2): p. 8-19.

126. Musso, N.R., et al., *Catecholamine content and in vitro catecholamine synthesis in peripheral human lymphocytes.* J Clin Endocrinol Metab, 1996. **81**(10): p. 3553-7.

127. Redell, J.B. and P.K. Dash, *Traumatic brain injury stimulates hippocampal catechol-O-methyl transferase expression in microglia.* Neurosci Lett, 2007. **413**(1): p. 36-41.

128. Bisaglia, M., et al., *Dysfunction of dopamine homeostasis: clues in the hunt for novel Parkinson's disease therapies.* Faseb j, 2013. **27**(6): p. 2101-10.

129. Morales, I., et al., *Striatal astrocytes engulf dopaminergic debris in Parkinson's disease: A study in an animal model.* PLoS One, 2017. **12**(10): p. e0185989.

130. Schain, M. and W.C. Kreisl, *Neuroinflammation in Neurodegenerative Disorders-a Review.* Curr Neurol Neurosci Rep, 2017. **17**(3): p. 25.

131. Winner, B.M., et al., *Metabolism of Dopamine in Nucleus Accumbens Astrocytes Is Preserved in Aged Mice Exposed to MPTP.* Front Aging Neurosci, 2017. **9**: p. 410.

132. Petrelli, F., et al., *Dysfunction of homeostatic control of dopamine by astrocytes in the developing prefrontal cortex leads to cognitive impairments.* Mol Psychiatry, 2020. **25**(4): p. 732-749.

133. Asanuma, M., et al., *Striatal astrocytes act as a reservoir for L-DOPA.* PLoS One, 2014. **9**(9): p. e106362.

134. Lohr, K.M., et al., *Vesicular Monoamine Transporter 2 (VMAT2) Level Regulates MPTP Vulnerability and Clearance of Excess Dopamine in Mouse Striatal Terminals.* Toxicol Sci, 2016. **153**(1): p. 79-88.

135. Cosentino, M., et al., *HPLC-ED measurement of endogenous catecholamines in human immune cells and hematopoietic cell lines.* Life Sci, 2000. **68**(3): p. 283-95.

136. Amenta, F., et al., *Identification of dopamine plasma membrane and vesicular transporters in human peripheral blood lymphocytes.* Journal of Neuroimmunology, 2001. **117**(1-2): p. 133-142.

137. Meiser, J., D. Weindl, and K. Hiller, *Complexity of dopamine metabolism.* Cell Communication and Signaling, 2013. **11**(1): p. 34.

138. Meiser, J., D. Weindl, and K. Hiller, *Complexity of dopamine metabolism.* Cell Commun Signal, 2013. **11**(1): p. 34.

139. Tong, J., et al., *Brain monoamine oxidase B and A in human parkinsonian dopamine deficiency disorders.* Brain, 2017. **140**(9): p. 2460-2474.

140. Bidart, J.M., et al., *Catechol-O-methyltransferase activity and aminergic binding sites distribution in human peripheral blood lymphocyte subpopulations.* Clinical Immunology and Immunopathology, 1983. **26**(1): p. 1-9.

141. Balsa, M.D., N. Gómez, and M. Unzeta, *Characterization of monoamine oxidase activity present in human granulocytes and lymphocytes.* Biochimica et Biophysica Acta (BBA) - General Subjects, 1989. **992**(2): p. 140-144.

142. Cosentino, M., et al., *Endogenous catecholamine synthesis, metabolism, storage and uptake in human neutrophils.* Life Sci, 1999. **64**(11): p. 975-81.

143. Anlauf, M., et al., *Vesicular monoamine transporter 2 (VMAT2) expression in hematopoietic cells and in patients with systemic mastocytosis.* J Histochem Cytochem, 2006. **54**(2): p. 201-13.

144. Wang, X.Q., et al., *Expression of tyrosine hydroxylase in CD4(+) T cells contributes to alleviation of Th17/Treg imbalance in collagen-induced arthritis.* Exp Biol Med (Maywood), 2016. **241**(18): p. 2094-2103.

145. Gopinath, A., et al., *A novel approach to study markers of dopamine signaling in peripheral immune cells.* J Immunol Methods, 2020. **476**: p. 112686.

146. Boyd, K.N. and R.B. Mailman, *Dopamine receptor signaling and current and future antipsychotic drugs.* Handb Exp Pharmacol, 2012(212): p. 53-86.

147. Felger, J.C., *The Role of Dopamine in Inflammation-Associated Depression: Mechanisms and Therapeutic Implications.* Curr Top Behav Neurosci, 2017. **31**: p. 199-219.

148. Rosin, C., et al., *Dopamine D2 and D3 receptor agonists limit oligodendrocyte injury caused by glutamate oxidative stress and oxygen/glucose deprivation.* Glia, 2005. **52**(4): p. 336-43.

149. Nakano, K., et al., *Antagonizing dopamine D1-like receptor inhibits Th17 cell differentiation: preventive and therapeutic effects on experimental autoimmune encephalomyelitis.* Biochem Biophys Res Commun, 2008. **373**(2): p. 286-91.

150. Arce-Sillas, A., et al., *Expression of Dopamine Receptors in Immune Regulatory Cells.* Neuroimmunomodulation, 2019. **26**(3): p. 159-166.

151. Matt, S.M. and P.J. Gaskill, *Where Is Dopamine and how do Immune Cells See it?: Dopamine-Mediated Immune Cell Function in Health and Disease.* J Neuroimmune Pharmacol, 2020. **15**(1): p. 114-164.

152. Klein, M.O., et al., *Dopamine: Functions, Signaling, and Association with Neurological Diseases.* Cell Mol Neurobiol, 2019. **39**(1): p. 31-59.

153. Wang, H., et al., *cAMP Response Element-Binding Protein (CREB): A Possible Signaling Molecule Link in the Pathophysiology of Schizophrenia.* Front Mol Neurosci, 2018. **11**: p. 255.

154. Maggio, R., et al., *Heterodimerization of dopamine receptors: new insights into functional and therapeutic significance.* Parkinsonism Relat Disord. , 2009. **15**: p. 2-7.
155. Talhada, D., M. Rabenstein, and K. Ruscher, *The role of dopaminergic immune cell signalling in poststroke inflammation.* Ther Adv Neurol Disord, 2018. **11**: p. 1756286418774225.
156. Elgueta, D., et al., *Dopamine Receptor D3 Expression Is Altered in CD4(+) T-Cells From Parkinson's Disease Patients and Its Pharmacologic Inhibition Attenuates the Motor Impairment in a Mouse Model.* Front Immunol, 2019. **10**: p. 981.
157. Brito-Melo, G.E., et al., *Increase in dopaminergic, but not serotoninergic, receptors in T-cells as a marker for schizophrenia severity.* J Psychiatr Res, 2012. **46**(6): p. 738-42.
158. Pacheco, R., *Targeting dopamine receptor D3 signalling in inflammation.* Oncotarget, 2017. **8**(5): p. 7224-7225.
159. Elgueta, D., et al., *Pharmacologic antagonism of dopamine receptor D3 attenuates neurodegeneration and motor impairment in a mouse model of Parkinson's disease.* Neuropharmacology, 2017. **113**(Pt A): p. 110-123.
160. Contreras, F., et al., *Dopamine Receptor D3 Signaling on CD4+ T Cells Favors Th1- and Th17-Mediated Immunity.* J Immunol, 2016. **196**(10): p. 4143-9.
161. Contreras, F., et al., *Dopamine Receptor D3 Signaling on CD4+ T Cells Favors Th1- and Th17-Mediated Immunity.* J Immunol, 2016. **196**(10): p. 4143-9.
162. Yan, Y., et al., *Dopamine controls systemic inflammation through inhibition of NLRP3 inflammasome.* Cell, 2015. **160**(1-2): p. 62-73.
163. Vidal, P.M. and R. Pacheco, *Targeting the Dopaminergic System in Autoimmunity.* J Neuroimmune Pharmacol, 2019.
164. Sarkar, C., et al., *The immunoregulatory role of dopamine: an update.* Brain Behav Immun, 2010. **24**(4): p. 525-8.
165. Vermeren, S., U. Karmakar, and A.G. Rossi, *Immune complex-induced neutrophil functions: A focus on cell death.* Eur J Clin Invest, 2018. **48 Suppl 2**: p. e12948.
166. Nagatomo, K., et al., *Dopamine D1 Receptor Immunoreactivity on Fine Processes of GFAP-Positive Astrocytes in the Substantia Nigra Pars Reticulata of Adult Mouse.* Front Neuroanat, 2017. **11**: p. 3.
167. Gaskill, P.J., et al., *Dopamine receptor activation increases HIV entry into primary human macrophages.* PLoS One, 2014. **9**(9): p. e108232.
168. Gaskill, P.J., et al., *Drug induced increases in CNS dopamine alter monocyte, macrophage and T cell functions: implications for HAND.* J Neuroimmune Pharmacol, 2013. **8**(3): p. 621-42.
169. Pacheco, R., F. Contreras, and M. Zouali, *The dopaminergic system in autoimmune diseases.* Front Immunol, 2014. **5**: p. 117.
170. Prado, C., et al., *Stimulation of dopamine receptor D5 expressed on dendritic cells potentiates Th17-mediated immunity.* J Immunol, 2012. **188**(7): p. 3062-70.
171. Nakano, K., et al., *Dopamine induces IL-6-dependent IL-17 production via D1-like receptor on CD4 naive T cells and D1-like receptor antagonist SCH-23390 inhibits cartilage destruction in a human rheumatoid arthritis/SCID mouse chimera model.* J Immunol, 2011. **186**(6): p. 3745-52.
172. Kempuraj, D., et al., *Brain and Peripheral Atypical Inflammatory Mediators Potentiate Neuroinflammation and Neurodegeneration.* Front Cell Neurosci, 2017. **11**: p. 216.
173. DiSabato, D.J., N. Quan, and J.P. Godbout, *Neuroinflammation: the devil is in the details.* Journal of Neurochemistry, 2016. **139**: p. 136-153.
174. Fernandez-Egea, E., et al., *Peripheral Immune Cell Populations Associated with Cognitive Deficits and Negative Symptoms of Treatment-Resistant Schizophrenia.* PLoS One, 2016. **11**(5): p. e0155631.

175. Teismann, P. and J.B. Schulz, *Cellular pathology of Parkinson's disease: astrocytes, microglia and inflammation.* Cell Tissue Res, 2004. **318**(1): p. 149-61.

176. Janda, E., L. Boi, and A.R. Carta, *Microglial Phagocytosis and Its Regulation: A Therapeutic Target in Parkinson's Disease?* 2018. **11**(144).

177. Wang, B., et al., *Dopamine Alters Lipopolysaccharide-Induced Nitric Oxide Production in Microglial Cells via Activation of D1-Like Receptors.* Neurochem Res, 2019. **44**(4): p. 947-958.

178. Gao, H.M. and J.S. Hong, *Why neurodegenerative diseases are progressive: uncontrolled inflammation drives disease progression.* Trends Immunol, 2008. **29**(8): p. 357-65.

179. Guttenplan, K.A. and S.A. Liddelow, *Astrocytes and microglia: Models and tools.* J Exp Med, 2019. **216**(1): p. 71-83.

180. Jennings, A., et al., *Dopamine elevates and lowers astroglial Ca2+ through distinct pathways depending on local synaptic circuitry.* Glia, 2017. **65**: p. 447-459.

181. Jennings, A. and D.A. Rusakov, *Do Astrocytes Respond to Dopamine? .* OM&P, 2016. **2**(1): p. 34-43.

182. Zhang, Y., et al., *Activation of Dopamine D2 Receptor Suppresses Neuroinflammation Through alphaB-Crystalline by Inhibition of NF-kappaB Nuclear Translocation in Experimental ICH Mice Model.* Stroke, 2015. **46**(9): p. 2637-46.

183. Hong, M., K. Mukhida, and I. Mendez, *GDNF therapy for Parkinson's disease.* Expert Rev Neurother, 2008. **8**(7): p. 1125-39.

184. Ferreira, T.B., et al., *Dopamine favors expansion of glucocorticoid-resistant IL-17-producing T cells in multiple sclerosis.* Brain Behav Immun, 2014. **41**: p. 182-90.

185. Balkowiec-Iskra, E., et al., *MPTP-induced central dopamine depletion exacerbates experimental autoimmune encephalomyelitis (EAE) in C57BL mice.* Inflamm Res, 2007. **56**(8): p. 311-7.

186. Jafari, M., et al., *Distorted expression of dopamine receptor genes in systemic lupus erythematosus.* Immunobiology, 2013. **218**(7): p. 979-83.

187. Ikenouchi-Sugita, A., et al., *Continuous decrease in serum brain-derived neurotrophic factor (BDNF) levels in a neuropsychiatric syndrome of systemic lupus erythematosus patient with organic brain changes.* Neuropsychiatr Dis Treat, 2008. **4**(6): p. 1277-81.

188. Muscal, E. and R.L. Brey, *Neurologic manifestations of systemic lupus erythematosus in children and adults.* Neurol Clin, 2010. **28**(1): p. 61-73.

189. Jara, L.J., et al., *Prolactin has a pathogenic role in systemic lupus erythematosus.* 2017. **65**(2): p. 512-523.

190. Carta, A.R., et al., *l-DOPA-induced dyskinesia and neuroinflammation: do microglia and astrocytes play a role?* Eur J Neurosci, 2017. **45**(1): p. 73-91.

191. Borovac, J., *Side effects of a dopamine agonist therapy for Parkinson's disease: a mini-review of clinical pharmacology.* The Yale journal of biology and medicine, 2016. **89**: p. 37-47

192. Leggio, G.M., et al., *Dopamine D3 receptor is necessary for ethanol consumption: an approach with buspirone.* Neuropsychopharmacology, 2014. **39**(8): p. 2017-28.

193. Leggio, G.M., et al., *Dopamine D3 receptor-dependent changes in alpha6 GABAA subunit expression in striatum modulate anxiety-like behaviour: Responsiveness and tolerance to diazepam.* Eur Neuropsychopharmacol, 2015. **25**(9): p. 1427-36.

194. Leggio, G.M., et al., *Dopaminergic-GABAergic interplay and alcohol binge drinking.* Pharmacol Res, 2019. **141**: p. 384-391.

195. Kustrimovic, N., et al., *Dopaminergic Receptors on CD4+ T Naive and Memory Lymphocytes Correlate with Motor Impairment in Patients with Parkinson's Disease.* Sci Rep, 2016. **6**: p. 33738.

196. Miyazaki, I. and M. Asanuma, *Dopaminergic neuron-specific oxidative stress caused by dopamine itself.* Acta Med Okayama, 2008. **62**(3): p. 141-50.

197.   Krashia, P., A. Nobili, and M. D'Amelio, *Unifying Hypothesis of Dopamine Neuron Loss in Neurodegenerative Diseases: Focusing on Alzheimer's Disease.* Front Mol Neurosci, 2019. **12**: p. 123.

198.   Serrano-Pozo, A., et al., *Neuropathological alterations in Alzheimer disease.* Cold Spring Harb Perspect Med, 2011. **1**(1): p. a006189.

199.   Rollo, C.D., *Dopamine and aging: intersecting facets.* Neurochem Res, 2009. **34**(4): p. 601-29.

200.   Nobili, A., et al., *Dopamine neuronal loss contributes to memory and reward dysfunction in a model of Alzheimer's disease.* Nat Commun, 2017. **8**: p. 14727.

201.   Adinoff, B., *Neurobiologic processes in drug reward and addiction.* Harv Rev Psychiatry, 2004. **12**(6): p. 305-20.

202.   Donthamsetti, P., et al., *Arrestin recruitment to dopamine D2 receptor mediates locomotion but not incentive motivation.* Mol Psychiatry, 2020. **25**(9): p. 2086-2100.

203.   Koch, G., et al., *Dopaminergic modulation of cortical plasticity in Alzheimer's disease patients.* Neuropsychopharmacology, 2014. **39**(11): p. 2654-61.

204.   Arreola, R., et al., *Immunomodulatory Effects Mediated by Dopamine.* J Immunol Res, 2016. **2016**: p. 3160486.

205.   Krasnova, I.N., Z. Justinova, and J.L. Cadet, *Methamphetamine addiction: involvement of CREB and neuroinflammatory signaling pathways.* Psychopharmacology (Berl), 2016. **233**(10): p. 1945-62.

206.   Hedges, D.M., et al., *Methamphetamine Induces Dopamine Release in the Nucleus Accumbens Through a Sigma Receptor-Mediated Pathway.* Neuropsychopharmacology, 2018. **43**(6): p. 1405-1414.

207.   Wang, B., et al., *Methamphetamine exacerbates neuroinflammatory response to lipopolysaccharide by activating dopamine D1-like receptors.* Int Immunopharmacol, 2019. **73**: p. 1-9.

208.   Kitamura, O., et al., *Microglial and astrocytic changes in the striatum of methamphetamine abusers.* Leg Med (Tokyo), 2010. **12**(2): p. 57-62.

209.   Zhu, J., S. Ananthan, and C.G. Zhan, *The role of human dopamine transporter in NeuroAIDS.* Pharmacol Ther, 2018. **183**: p. 78-89.

210.   McArthur, J. and B. Smith, *Neurologic Complications and Considerations in HIV-Infected Persons.* Curr Infect Dis Rep, 2013. **15**(1): p. 61-6.

211.   Calderon, T.M., et al., *Dopamine Increases CD14(+)CD16(+) Monocyte Transmigration across the Blood Brain Barrier: Implications for Substance Abuse and HIV Neuropathogenesis.* J Neuroimmune Pharmacol, 2017. **12**(2): p. 353-370.

212.   Nickoloff-Bybel, E.A., et al., *Dopamine increases HIV entry into macrophages by increasing calcium release via an alternative signaling pathway.* Brain Behav Immun, 2019. **82**: p. 239-252.

213.   Honorato, J. and M. Catalan, *La buspirona: un nuevo fármaco ansiolítico no benzodiacepínico [Buspirone: a new non-benzodiazepine anxiolytic drug].* Rev Clin Esp., 1990. **186**(6): p. 286-91.

214.   TK, W. and T. J. *Buspirone*. 2021 12 Aug 2021 [cited 2021; Available from: https://www.ncbi.nlm.nih.gov/books/NBK531477/.

215.   Loane, C. and M. Politis, *Buspirone: what is it all about?* Brain Res, 2012. **1461**: p. 111-8.

216.   Maramai, S., et al., *Dopamine D3 Receptor Antagonists as Potential Therapeutics for the Treatment of Neurological Diseases.* Front Neurosci, 2016. **10**: p. 451.

217.   Kim, S.W., et al., *Therapeutic doses of buspirone block D3 receptors in the living primate brain.* Int J Neuropsychopharmacol, 2014. **17**(8): p. 1257-67.

218.   Gonzalez, H., et al., *Dopamine receptor D3 expressed on CD4+ T cells favors neurodegeneration of dopaminergic neurons during Parkinson's disease.* J Immunol, 2013. **190**(10): p. 5048-56.

219.	Franz, D., et al., *Dopamine receptors D3 and D5 regulate CD4(+)T-cell activation and differentiation by modulating ERK activation and cAMP production.* J Neuroimmunol, 2015. **284**: p. 18-29.

220.	Ilani, T., R.D. Strous, and S. Fuchs, *Dopaminergic regulation of immune cells via D3 dopamine receptor: a pathway mediated by activated T cells.* FASEB J, 2004. **18**(13): p. 1600-2.

221.	Montoya, A., et al., *Dopamine receptor D3 signalling in astrocytes promotes neuroinflammation.* J Neuroinflammation, 2019. **16**(1): p. 258.

222.	Mela, F., et al., *The selective D(3) receptor antagonist, S33084, improves parkinsonian-like motor dysfunction but does not affect L-DOPA-induced dyskinesia in 6-hydroxydopamine hemi-lesioned rats.* Neuropharmacology, 2010. **58**(2): p. 528-36.

223.	Wang, J., et al., *Microglial activation contributes to depressive-like behavior in dopamine D3 receptor knockout mice.* Brain Behav Immun, 2020. **83**: p. 226-238.

224.	Lanza, K., et al., *Reciprocal cross-sensitization of D1 and D3 receptors following pharmacological stimulation in the hemiparkinsonian rat.* Psychopharmacology (Berl), 2020. **237**(1): p. 155-165.

225.	Kim, S.W., et al., *Therapeutic doses of buspirone block D3 receptors in the living primate brain – CORRIGENDUM.* The International Journal of Neuropsychopharmacology, 2014. **17**(08).

226.	Ragot, H. and A. Hovnanian, *Drug Repurposing Reveals mTOR Inhibition as a Promising Strategy for Epidermolysis Bullosa Simplex.* J Invest Dermatol, 2021.

227.	McFarthing, K., et al., *Parkinson's Disease Drug Therapies in the Clinical Trial Pipeline: 2020.* J Parkinsons Dis, 2020. **10**(3): p. 757-774.

228.	Marathe, P.H., et al., *Pharmacokinetics of buspirone following oral administration to rhesus monkeys.* J Pharm Pharmacol, 1999. **51**(5): p. 601-7.

229.	Raber, J., R.A. Wienclaw., and L.J. Cataldo., *Buspirone* The Gale Encyclopedia of Mental Health, 2012. **Gale: Detroit, MI.**: p. p. 264-267.

230.	Le Foll, B., et al., *Occupancy of Dopamine D3 and D2 Receptors by Buspirone: A [11C]-(+)-PHNO PET Study in Humans.* Neuropsychopharmacology, 2016. **41**(2): p. 529-37.

231.	Foley, J.A. and L. Cipolotti, *Apathy in Parkinson's Disease: A Retrospective Study of Its Prevalence and Relationship With Mood, Anxiety, and Cognitive Function.* Front Psychol, 2021. **12**: p. 749624.

232.	Mahmood, I. and C. Sahajwalla, *Clinical pharmacokinetics and pharmacodynamics of buspirone, an anxiolytic drug.* Clin Pharmacokinet, 1999. **36**(4): p. 277-87.

233.	Cheng, J.P., et al., *5-hydroxytryptamine1A (5-HT1A) receptor agonists: A decade of empirical evidence supports their use as an efficacious therapeutic strategy for brain trauma.* Brain Res, 2016. **1640**(Pt A): p. 5-14.

234.	Waschek, J.A., *VIP and PACAP: neuropeptide modulators of CNS inflammation, injury, and repair.* Br J Pharmacol, 2013. **169**(3): p. 512-23.

235.	de Souza, F.R., F.M. Ribeiro, and P.M.d.A.J.C.m.c. Lima, *Implications of VIP and PACAP in Parkinson's Disease: What do we Know So Far?* 2021. **28**(9): p. 1703-1715.

236.	Thomas Broome, S., G. Musumeci, and A. Castorina, *Doxycycline and Minocycline Act as Positive Allosteric Modulators of the PAC1 Receptor and Induce Plasminogen Activators in RT4 Schwann Cells.* Applied Sciences, 2021. **11**(16).

237.	Tabikh, M., et al., *Parkinson disease: protective role and function of neuropeptides.* Peptides, 2021: p. 170713.

238.	Reglodi, D., et al., *PACAP deficiency as a model of aging.* Geroscience, 2018. **40**(5-6): p. 437-452.

239.	Shivers, K.Y., et al., *PACAP27 prevents Parkinson-like neuronal loss and motor deficits but not microglia activation induced by prostaglandin J2.* Biochim Biophys Acta, 2014. **1842**(9): p. 1707-19.

240. Karunia, J., et al., *PACAP and VIP Modulate LPS-Induced Microglial Activation and Trigger Distinct Phenotypic Changes in Murine BV2 Microglial Cells.* Int J Mol Sci, 2021. **22**(20).

241. Lamine, A., et al., *Characterizations of a synthetic pituitary adenylate cyclase-activating polypeptide analog displaying potent neuroprotective activity and reduced in vivo cardiovascular side effects in a Parkinson's disease model.* Neuropharmacology, 2016. **108**: p. 440-50.

242. Brown, D., et al., *PACAP protects against salsolinol-induced toxicity in dopaminergic SH-SY5Y cells: implication for Parkinson's disease.* J Mol Neurosci, 2013. **50**(3): p. 600-7.

243. Olson, K.E., et al., *Selective VIP Receptor Agonists Facilitate Immune Transformation for Dopaminergic Neuroprotection in MPTP-Intoxicated Mice.* J Neurosci, 2015. **35**(50): p. 16463-78.

244. Delgado, M. and D. Ganea, *Neuroprotective effect of vasoactive intestinal peptide (VIP) in a mouse model of Parkinson's disease by blocking microglial activation.* FASEB J, 2003. **17**(8): p. 944-6.

245. Korkmaz, O.T. and N. Tuncel, *Advantages of Vasoactive Intestinal Peptide for the Future Treatment of Parkinson's Disease.* Curr Pharm Des, 2018. **24**(39): p. 4693-4701.

246. Hashimoto, H., et al., *Altered psychomotor behaviors in mice lacking pituitary adenylate cyclase-activating polypeptide (PACAP).* Proc Natl Acad Sci U S A, 2001. **98**(23): p. 13355-60.

247. Jungling, A., et al., *Alterations of Nigral Dopamine Levels in Parkinson's Disease after Environmental Enrichment and PACAP Treatment in Aging Rats.* Life (Basel), 2021. **11**(1).

248. Caliendo, G., et al., *Derivatives as 5HT1A receptor ligands--past and present.* Curr Med Chem, 2005. **12**(15): p. 1721-53.

249. Garcia-Garcia, A.L., A. Newman-Tancredi, and E.D. Leonardo, *5-HT(1A) [corrected] receptors in mood and anxiety: recent insights into autoreceptor versus heteroreceptor function.* Psychopharmacology (Berl), 2014. **231**(4): p. 623-36.

250. Thomas Broome, S., et al., *Dopamine: an immune transmitter.* Neural Regen Res, 2020. **15**(12): p. 2173-2185.

251. Elgueta, D., et al., *Pharmacologic antagonism of dopamine receptor D3 attenuates neurodegeneration and motor impairment in a mouse model of Parkinson's disease.* Neuropharmacology, 2017. **113**(Pt A): p. 110-123.

252. Ginhoux, F. and S. Garel, *The mysterious origins of microglia.* Nat Neurosci, 2018. **21**(7): p. 897-899.

253. Yang, B., et al., *Unveiling anti-oxidative and anti-inflammatory effects of docosahexaenoic acid and its lipid peroxidation product on lipopolysaccharide-stimulated BV-2 microglial cells.* J Neuroinflammation, 2018. **15**(1): p. 202.

254. Sun, G.Y., et al., *Quercetin Potentiates Docosahexaenoic Acid to Suppress Lipopolysaccharide-induced Oxidative/Inflammatory Responses, Alter Lipid Peroxidation Products, and Enhance the Adaptive Stress Pathways in BV-2 Microglial Cells.* Int J Mol Sci, 2019. **20**(4).

255. Tansey, M.G. and M.S. Goldberg, *Neuroinflammation in Parkinson's disease: its role in neuronal death and implications for therapeutic intervention.* Neurobiol Dis, 2010. **37**(3): p. 510-8.

256. Xia, Q.P., Z.Y. Cheng, and L. He, *The modulatory role of dopamine receptors in brain neuroinflammation.* Int Immunopharmacol, 2019. **76**: p. 105908.

257. Trudler, D., et al., *DJ-1 deficiency triggers microglia sensitivity to dopamine toward a pro-inflammatory phenotype that is attenuated by rasagiline.* J Neurochem, 2014. **129**(3): p. 434-47.

258. Schmittgen, T.D. and K.J. Livak, *Analyzing real-time PCR data by the comparative C(T) method.* Nat Protoc, 2008. **3**(6): p. 1101-8.

259. Tollefson, G.D., S.P. Lancaster, and J. Montague-Clouse, *The association of buspirone and its metabolite 1-pyrimidinylpiperazine in the remission of comorbid anxiety with depressive features and alcohol dependency.* Psychopharmacol Bull, 1991. **27**(2): p. 163-70.

260. Lim, Y.M., et al., *[P1-208]: Crispr/Cas9-Mediated Gene Editing of Trem2 in Monocytic and Microglial Cell Lines.* Alzheimer's & Dementia, 2017. **13**(7S_Part_6): p. P322-P322.

261. Hanger, B., et al., *Emerging Developments in Human Induced Pluripotent Stem Cell-Derived Microglia: Implications for Modelling Psychiatric Disorders With a Neurodevelopmental Origin.* Front Psychiatry, 2020. **11**: p. 789.

262. Prante, O., M. Dörfler, and P.J.D.R.S.-S.D.D.-L.R.H.P. Gmeiner, Totowa, NJ, *The Dopamine Receptors.* 2010: p. 101-135.

263. Twayana, K.S., N. Chaudhari, and P. Ravanan, *Prolonged lipopolysaccharide exposure induces transient immunosuppression in BV2 microglia.* Journal of Cellular Physiology, 2019. **234**(2): p. 1889-1903.

264. McGuiness, B., et al., *Exaggerated Increases in Microglia Proliferation, Brain Inflammatory Response and Sickness Behaviour upon Lipopolysaccharide Stimulation in Non-Obese Diabetic Mice.* Neuroimmunomodulation, 2016. **23**(3): p. 137-150.

265. Fukushima, S., et al., *Robust increase of microglia proliferation in the fornix of hippocampal axonal pathway after a single LPS stimulation.* J Neuroimmunol, 2015. **285**: p. 31-40.

266. Krabbe, G., et al., *Activation of serotonin receptors promotes microglial injury-induced motility but attenuates phagocytic activity.* Brain Behav Immun, 2012. **26**(3): p. 419-28.

267. Stojakovic, A., et al., *Role of the IL-1 Pathway in Dopaminergic Neurodegeneration and Decreased Voluntary Movement.* Mol Neurobiol, 2017. **54**(6): p. 4486-4495.

268. Schwenkgrub, J., et al., *Effect of human interleukin-10 on the expression of nitric oxide synthases in the MPTP-based model of Parkinson's disease.* Pharmacol Rep, 2013. **65**(1): p. 44-9.

269. Zhang, J., et al., *Neuronal nitric oxide synthase alteration accounts for the role of 5-HT1A receptor in modulating anxiety-related behaviors.* J Neurosci, 2010. **30**(7): p. 2433-41.

270. Leal, M.C., et al., *Interleukin-1beta and tumor necrosis factor-alpha: reliable targets for protective therapies in Parkinson's Disease?* Front Cell Neurosci, 2013. **7**: p. 53.

271. Lewin, A.S., et al., *The 5HT1a Agonist Xaliproden Exhibits Anti-oxidant and Anti-inflammatory Properties and Protects the Retina in a Mouse Model of Geographic Atrophy.* Investigative Ophthalmology & Visual Science, 2016. **57**(12): p. 4428-4428.

272. Besser, M.J., Y. Ganor, and M. Levite, *Dopamine by itself activates either D2, D3 or D1/D5 dopaminergic receptors in normal human T-cells and triggers the selective secretion of either IL-10, TNFalpha or both.* J Neuroimmunol, 2005. **169**(1-2): p. 161-71.

273. Sharifi, H., A. Mohajjel Nayebi, and S. Farajnia, *8-OH-DPAT (5-HT1A agonist) Attenuates 6-Hydroxy- dopamine-induced catalepsy and Modulates Inflammatory Cytokines in Rats.* Iranian journal of basic medical sciences, 2013. **16**(12): p. 1270–1275.

274. Cunha, C., et al., *Exploring New Inflammatory Biomarkers and Pathways during LPS-Induced M1 Polarization.* Mediators of Inflammation, 2016. **2016**: p. 1-17.

275. Menzies, F.M., et al., *Sequential expression of macrophage anti-microbial/inflammatory and wound healing markers following innate, alternative and classical activation.* Clin Exp Immunol, 2010. **160**(3): p. 369-79.

276. Zanin, R.F., et al., *Differential macrophage activation alters the expression profile of NTPDase and ecto-5'-nucleotidase.* PLoS One, 2012. **7**(2): p. e31205.

277. Chourbaji, S., et al., *Dopamine receptor 3 (D3) knockout mice show regular emotional behaviour.* Pharmacol Res, 2008. **58**(5-6): p. 302-7.

278. Afzelius, P., et al., *The serotonin analogue buspirone increases the function of PBMC from HIV-infected individuals in vitro.* Scand J Infect Dis, 1997. **29**(2): p. 117-20.

279. Freire-Garabal, M., et al., *Effects of buspirone on the immune response to stress in mice.* Pharmacol Biochem Behav, 1995. **51**(4): p. 821-5.

280. Sharma, S., K. Raj, and S. Singh, *Neuroprotective Effect of Quercetin in Combination with Piperine Against Rotenone- and Iron Supplement-Induced Parkinson's Disease in Experimental Rats.* Neurotox Res, 2020. **37**(1): p. 198-209.

281. Dodiya, H.B., et al., *Chronic stress-induced gut dysfunction exacerbates Parkinson's disease phenotype and pathology in a rotenone-induced mouse model of Parkinson's disease.* Neurobiol Dis, 2020. **135**: p. 104352.

282. Garabadu, D. and N. Agrawal, *Naringin Exhibits Neuroprotection Against Rotenone-Induced Neurotoxicity in Experimental Rodents.* Neuromolecular Med, 2020. **22**(2): p. 314-330.

283. Bello-Arroyo, E., et al., *MouBeAT: A New and Open Toolbox for Guided Analysis of Behavioral Tests in Mice.* Front Behav Neurosci, 2018. **12**: p. 201.

284. Crusio, W.E., *Genetic dissection of mouse exploratory behaviour.* Behav Brain Res, 2001. **125**(1-2): p. 127-32.

285. Beck, G., A. Singh, and S.M. Papa, *Dysregulation of striatal projection neurons in Parkinson's disease.* J Neural Transm (Vienna), 2018. **125**(3): p. 449-460.

286. da Silva, W.A.B., et al., *Physical exercise increases the production of tyrosine hydroxylase and CDNF in the spinal cord of a Parkinson's disease mouse model.* Neurosci Lett, 2021. **760**: p. 136089.

287. Zhu, H., et al., *Expression and distribution of all dopamine receptor subtypes (D1–D5) in the mouse lumbar spinal cord: A real-time polymerase chain reaction and non-autoradiographic in situ hybridization study.* Neuroscience, 2007. **149**(4): p. 885-897.

288. Palasz, E., et al., *BDNF as a promising therapeutic agent in Parkinson's disease.* 2020. **21**(3): p. 1170.

289. Reglodi, D., et al., *Pituitary adenylate cyclase activating polypeptide protects dopaminergic neurons and improves behavioral deficits in a rat model of Parkinson's disease.* Behav Brain Res, 2004. **151**(1-2): p. 303-12.

290. Ivashko-Pachima, Y. and I. Gozes, *Activity-dependent neuroprotective protein (ADNP)-end-binding protein (EB) interactions regulate microtubule dynamics toward protection against tauopathy*, in *Progress in Molecular Biology and Translational Science*. 2021, Elsevier. p. 65-90.

291. Hu, Q., et al., *Baicalein inhibits alpha-synuclein oligomer formation and prevents progression of alpha-synuclein accumulation in a rotenone mouse model of Parkinson's disease.* Biochim Biophys Acta, 2016. **1862**(10): p. 1883-90.

292. Carey, G., et al., *Neuroimaging of Anxiety in Parkinson's Disease: A Systematic Review.* Mov Disord, 2021. **36**(2): p. 327-339.

293. He, H., et al., *Progressive brain changes in Parkinson's disease: A meta-analysis of structural magnetic resonance imaging studies.* Brain Res, 2020. **1740**: p. 146847.

294. Villar-Conde, S., et al., *The Human Hippocampus in Parkinson's Disease: An Integrative Stereological and Proteomic Study.* J Parkinsons Dis, 2021. **11**(3): p. 1345-1365.

295. Pagonabarraga, J. and J. Kulisevsky, *Apathy in Parkinson's Disease.* Int Rev Neurobiol, 2017. **133**: p. 657-678.

296. Haider, S., S. Madiha, and Z. Batool, *Amelioration of motor and non-motor deficits and increased striatal APoE levels highlight the beneficial role of pistachio supplementation in rotenone-induced rat model of PD.* Metab Brain Dis, 2020. **35**(7): p. 1189-1200.

297. Samantaray, S., et al., *Calpain inhibition protected spinal cord motoneurons against 1-methyl-4-phenylpyridinium ion and rotenone.* Neuroscience, 2011. **192**: p. 263-74.

298. Martin, L.J., et al., *Parkinson's disease alpha-synuclein transgenic mice develop neuronal mitochondrial degeneration and cell death.* J Neurosci, 2006. **26**(1): p. 41-50.

299. Mendoza-Velasquez, J.J., et al., *Autonomic Dysfunction in alpha-Synucleinopathies.* Front Neurol, 2019. **10**: p. 363.

300. Chen, Z., G. Li, and J. Liu, *Autonomic dysfunction in Parkinson's disease: Implications for pathophysiology, diagnosis, and treatment.* Neurobiol Dis, 2020. **134**: p. 104700.

301. Yanagisawa, N., *Natural history of Parkinson's disease: From dopamine to multiple system involvement.* Parkinsonism & Related Disorders, 2006. **12**: p. S40-S46.

302. Hassan, M.N. and J.H. Thakar, *Dopamine receptors in Parkinson's disease.* Progress in Neuro-Psychopharmacology and Biological Psychiatry, 1988. **12**(2-3): p. 173-182.

303. Neely, M.D., et al., *From the Cover: Manganese and Rotenone-Induced Oxidative Stress Signatures Differ in iPSC-Derived Human Dopamine Neurons.* Toxicol Sci, 2017. **159**(2): p. 366-379.

304. Del Dotto, V., et al., *OPA1: How much do we know to approach therapy?* Pharmacol Res, 2018. **131**: p. 199-210.

305. Mbiydzenyuy, N.E., et al., *Zinc and linoleic acid pre-treatment attenuates biochemical and histological changes in the midbrain of rats with rotenone-induced Parkinsonism.* BMC Neurosci, 2018. **19**(1): p. 29.

306. Rakha, M.K., et al., *Neurotherapeutic Effects of Bee Venom in a Rotenone-Induced Mouse Model of Parkinson's Disease.* Neurophysiology, 2019. **50**(6): p. 445-455.

307. Das, T., J.J. Hwang, and K.L. Poston, *Episodic recognition memory and the hippocampus in Parkinson's disease: A review.* Cortex, 2019. **113**: p. 191-209.

308. Taylor, J.M., B.S. Main, and P.J. Crack, *Neuroinflammation and oxidative stress: co-conspirators in the pathology of Parkinson's disease.* Neurochem Int, 2013. **62**(5): p. 803-19.

309. Castorina, A., et al., *PACAP and VIP expression in the periaqueductal grey of the rat following sciatic nerve constriction injury.* Neuropeptides, 2019. **74**: p. 60-69.

310. de Souza, F.R.O., F.M. Ribeiro, and P.M.D. Lima, *Implications of VIP and PACAP in Parkinson's Disease: What do we Know So Far?* Curr Med Chem, 2021. **28**(9): p. 1703-1715.

311. Dejda, A., P. Sokolowska, and J. Nowak, Z., *Neuroprotective potential of three neuropeptides PACAP, VIP and PHI.* Pharmacol Rep., 2005. **57**(3): p. 307-20

312. Reglodi, D., et al., *Review on the protective effects of PACAP in models of neurodegenerative diseases in vitro and in vivo.* 2011. **17**(10): p. 962-972.

313. Pagonabarraga, J., et al., *Apathy in Parkinson's disease: clinical features, neural substrates, diagnosis, and treatment.* The Lancet Neurology, 2015. **14**(5): p. 518-531.

314. Cannon, J.R., et al., *A highly reproducible rotenone model of Parkinson's disease.* Neurobiol Dis, 2009. **34**(2): p. 279-90.

315. Thomas Broome, S., et al., *Assessing the Anti-Inflammatory Activity of the Anxiolytic Drug Buspirone Using CRISPR-Cas9 Gene Editing in LPS-Stimulated BV-2 Microglial Cells.* Cells, 2021. **10**(6).

316. Bucolo, C., et al., *Dopamine-(3) receptor modulates intraocular pressure: implications for glaucoma.* Biochem Pharmacol, 2012. **83**(5): p. 680-6.

317. Musumeci, G., et al., *Enhanced expression of CD31/platelet endothelial cell adhesion molecule 1 (PECAM1) correlates with hypoxia inducible factor-1 alpha (HIF-1alpha) in human glioblastoma multiforme.* Exp Cell Res, 2015. **339**(2): p. 407-16.

318. Gao, H.-M., et al., *Distinct Role for Microglia in Rotenone-Induced Degeneration of Dopaminergic Neurons.* The Journal of Neuroscience, 2002. **22**(3): p. 782-790.

319. Subhramanyam, C.S., et al., *Microglia-mediated neuroinflammation in neurodegenerative diseases.* Semin Cell Dev Biol, 2019. **94**: p. 112-120.

320. Prut, L. and C. Belzung, *The open field as a paradigm to measure the effects of drugs on anxiety-like behaviors: a review.* European Journal of Pharmacology, 2003. **463**(1-3): p. 3-33.

321. Schneider, R.B., et al., *A trial of buspirone for anxiety in Parkinson's disease: Safety and tolerability.* Parkinsonism Relat Disord, 2020. **81**: p. 69-74.

322. Chauhan, P., et al., *Differential Cytokine-Induced Responses of Polarized Microglia.* Brain Sci, 2021. **11**(11).

323. Mendonca, I.P., et al., *Metformin and fluoxetine improve depressive-like behavior in a murine model of Parkinsons disease through the modulation of neuroinflammation, neurogenesis and neuroplasticity.* Int Immunopharmacol, 2021. **102**: p. 108415.

324. Zhao, X., et al., *Baicalein alleviates depression-like behavior in rotenone- induced Parkinson's disease model in mice through activating the BDNF/TrkB/CREB pathway.* Biomed Pharmacother, 2021. **140**: p. 111556.

325. Ivashko-Pachima, Y. and I. Gozes, *Activity-dependent neuroprotective protein (ADNP)-end-binding protein (EB) interactions regulate microtubule dynamics toward protection against tauopathy.* Prog Mol Biol Transl Sci, 2021. **177**: p. 65-90.

326. Montoya, A., et al., *Dopamine receptor D3 signalling in astrocytes promotes neuroinflammation.* J Neuroinflammation, 2019. **16**(1): p. 258.

327. Miyazaki, I., et al., *Targeting 5-HT(1A) receptors in astrocytes to protect dopaminergic neurons in Parkinsonian models.* Neurobiol Dis, 2013. **59**: p. 244-56.

328. Jiang, X., et al., *Serotonin 1A receptor agonist modulation of motor deficits and cortical oscillations by NMDA receptor interaction in parkinsonian rats.* Neuropharmacology, 2022. **203**: p. 108881.

329. Yu, R., et al., *TAT-tagging of VIP exerts positive allosteric modulation of the PAC1 receptor and enhances VIP neuroprotective effect in the MPTP mouse model of Parkinson's disease.* Biochim Biophys Acta Gen Subj, 2020. **1864**(8): p. 129626.

330. Yang, S., et al., *Pituitary adenylate cyclase-activating polypeptide (PACAP) 38 and PACAP4-6 are neuroprotective through inhibition of NADPH oxidase: potent regulators of microglia-mediated oxidative stress.* J Pharmacol Exp Ther, 2006. **319**(2): p. 595-603.

331. Mandwie, M., et al., *Metformin Treatment Attenuates Brain Inflammation and Rescues PACAP/VIP Neuropeptide Alterations in Mice Fed a High-Fat Diet.* Int J Mol Sci, 2021. **22**(24).

332. Crowe, A.R. and W. Yue, *Semi-quantitative Determination of Protein Expression using Immunohistochemistry Staining and Analysis: An Integrated Protocol.* Bio Protoc, 2019. **9**(24).

333. Sherer, T.B., et al., *Selective microglial activation in the rat rotenone model of Parkinson's disease.* Neuroscience Letters, 2003. **341**(2): p. 87-90.

334. Castorina, A., et al., *Effects of PACAP and VIP on hyperglycemia-induced proliferation in murine microvascular endothelial cells.* Peptides, 2010. **31**(12): p. 2276-83.

335. Giunta, S., et al., *PACAP and VIP affect NF1 expression in rat malignant peripheral nerve sheath tumor (MPNST) cells.* Neuropeptides, 2010. **44**(1): p. 45-51.

336. Delgado, M., G.M. Jonakait, and D. Ganea, *Vasoactive intestinal peptide and pituitary adenylate cyclase-activating polypeptide inhibit chemokine production in activated microglia.* Glia, 2002. **39**(2): p. 148-61.

337. Hirabayashi, T., T. Nakamachi, and S. Shioda, *Discovery of PACAP and its receptors in the brain.* J Headache Pain, 2018. **19**(1): p. 28.

338. Abad, C. and J.A. Waschek, *Immunomodulatory roles of VIP and PACAP in models of multiple sclerosis.* Curr Pharm Des, 2011. **17**(10): p. 1025-35.

339. Masmoudi-Kouki, O., et al., *Role of PACAP and VIP in astroglial functions.* Peptides, 2007. **28**(9): p. 1753-60.

340. Gonzalez-Rey, E., et al., *Neuropeptides as therapeutic approach to autoimmune diseases.* Curr Pharm Des, 2010. **16**(28): p. 3158-72.

341. Carniglia, L., et al., *Neuropeptides and Microglial Activation in Inflammation, Pain, and Neurodegenerative Diseases.* Mediators Inflamm, 2017. **2017**: p. 5048616.

342. Brown, D., et al., *PACAP protects against inflammatory-mediated toxicity in dopaminergic SH-SY5Y cells: implication for Parkinson's disease.* Neurotox Res, 2014. **26**(3): p. 230-9.

343. Korkmaz, O., Ay, H., Ulupınar, E., & Tunçel, N. , *Vasoactive intestinal peptide enhances striatal plasticity and prevents dopaminergic cell loss in Parkinsonian rats.* Journal of Molecular Neuroscience, 2012. **48**: p. 565-573.

344. Wang, G., et al., *PACAP protects neuronal differentiated PC12 cells against the neurotoxicity induced by a mitochondrial complex I inhibitor, rotenone.* FEBS Lett, 2005. **579**(18): p. 4005-11.

345. Maasz, G., et al., *Pituitary adenylate cyclase-activating polypeptide (PACAP) has a neuroprotective function in dopamine-based neurodegeneration in rat and snail parkinsonian models.* Dis Model Mech, 2017. **10**(2): p. 127-139.

346. Contestabile, A., B. Monti, and E. Polazzi, *Neuronal-glial Interactions Define the Role of Nitric Oxide in Neural Functional Processes.* Current neuropharmacology, 2012. **10**(4): p. 303-310.

347. Anja Henn, S.L., Maj Hedtjärn, André Schrattenholz, Peter Pörzgen, Marcel Leist, *The Suitability of BV2 Cells as Alternative Model System for Primary Microglia Cultures or for Animal Experiments Examining Brain Inflammation.* ALTEX : Alternatives to animal experimentation, 2009. **26**(2): p. 83-94.

348. Jayaraj, R.L., et al., *Noscapine Prevents Rotenone-Induced Neurotoxicity: Involvement of Oxidative Stress, Neuroinflammation and Autophagy Pathways.* Molecules, 2021. **26**(15).

349. Zhang, Q., et al., *Pyrroloquinoline Quinone Inhibits Rotenone-Induced Microglia Inflammation by Enhancing Autophagy.* Molecules, 2020. **25**(19).

350. Martinez, C., et al., *Anti-inflammatory role in septic shock of pituitary adenylate cyclase-activating polypeptide receptor.* Proc Natl Acad Sci U S A, 2002. **99**(2): p. 1053-8.

351. Zeng, N., et al., *The pituitary adenylate cyclase activating polypeptide type 1 receptor (PAC1-R) is expressed on gastric ECL cells: evidence by immunocytochemistry and RT-PCR.* Ann N Y Acad Sci, 1998. **865**: p. 147-56.

352. Morales, I., et al., *Astrocytes and retrograde degeneration of nigrostriatal dopaminergic neurons in Parkinson's disease: removing axonal debris.* Transl Neurodegener, 2021. **10**(1): p. 43.

353. Henn, A., et al., *The suitability of BV2 cells as alternative model system for primary microglia cultures or for animal experiments examining brain inflammation.* ALTEX, 2009. **26**(2): p. 83-94.

354. Timmerman, R., S.M. Burm, and J.J. Bajramovic, *An Overview of in vitro Methods to Study Microglia.* Front Cell Neurosci, 2018. **12**: p. 242.

355. Horvath, R.J., et al., *Differential migration, LPS-induced cytokine, chemokine, and NO expression in immortalized BV-2 and HAPI cell lines and primary microglial cultures.* J Neurochem, 2008. **107**(2): p. 557-69.

356. Luo, T., et al., *Propofol limits microglial activation after experimental brain trauma through inhibition of nicotinamide adenine dinucleotide phosphate oxidase.* Anesthesiology, 2013. **119**(6): p. 1370-88.

357. Plastira, I., et al., *1-Oleyl-lysophosphatidic acid (LPA) promotes polarization of BV-2 and primary murine microglia towards an M1-like phenotype.* J Neuroinflammation, 2016. **13**(1): p. 205.

358. Penney, J., W.T. Ralvenius, and L.H. Tsai, *Modeling Alzheimer's disease with iPSC-derived brain cells.* Mol Psychiatry, 2020. **25**(1): p. 148-167.

359. Grenier, K., J. Kao, and P. Diamandis, *Three-dimensional modeling of human neurodegeneration: brain organoids coming of age.* Mol Psychiatry, 2020. **25**(2): p. 254-274.

360. Ke, M., et al., *Comprehensive Perspectives on Experimental Models for Parkinson's Disease.* Aging Dis, 2021. **12**(1): p. 223-246.

361. Suganya, K. and B.S. Koo, *Gut-Brain Axis: Role of Gut Microbiota on Neurological Disorders and How Probiotics/Prebiotics Beneficially Modulate Microbial and Immune Pathways to Improve Brain Functions.* Int J Mol Sci, 2020. **21**(20).

362. Perez-Pardo, P., et al., *Role of TLR4 in the gut-brain axis in Parkinson's disease: a translational study from men to mice.* Gut, 2019. **68**(5): p. 829-843.

363. Procter, A.W., et al., *Topographical distribution of neurochemical changes in Alzheimer's disease.* 1988. **84**(2-3): p. 125-140.

364. Niedzielska, E., et al., *Oxidative Stress in Neurodegenerative Diseases.* Mol Neurobiol, 2016. **53**(6): p. 4094-4125.

365. Ebert, D. and K.P. Ebmeier, *The role of the cingulate gyrus in depression: From functional anatomy to neurochemistry.* Biological Psychiatry, 1996. **39**(12): p. 1044-1050.

366. Castren, E., V. Voikar, and T. Rantamaki, *Role of neurotrophic factors in depression.* Curr Opin Pharmacol, 2007. **7**(1): p. 18-21.

367. Lee, M.R., et al., *Preclinical (1)H-MRS neurochemical profiling in neurological and psychiatric disorders.* Bioanalysis, 2012. **4**(14): p. 1787-804.

368. Hashimoto, H., et al., *Implications of PACAP Signaling in Psychiatric Disorders*, in *Pituitary Adenylate Cyclase Activating Polypeptide — PACAP*, D. Reglodi and A. Tamas, Editors. 2016, Springer International Publishing: Cham. p. 757-766.

369. Decourt, M., et al., *Neuropsychiatric and Cognitive Deficits in Parkinson's Disease and Their Modeling in Rodents.* Biomedicines, 2021. **9**(6).

370. Hanna-Pladdy, B., et al., *Predictors of mild cognitive impairment in early-stage Parkinson's disease.* Dement Geriatr Cogn Dis Extra, 2013. **3**(1): p. 168-78.

371. YorkWilliams, S. and K.L. Poston, *What light have resting state fMRI studies shed on cognition and mood in Parkinson's disease?* J Clin Mov Disord, 2014. **1**: p. 4.

372. Petry-Schmelzer, J.N., et al., *Non-motor outcomes depend on location of neurostimulation in Parkinson's disease.* Brain, 2019. **142**(11): p. 3592-3604.

373. Shimizu, S. and Y. Ohno, *Improving the Treatment of Parkinson's Disease: A Novel Approach by Modulating 5-HT(1A) Receptors.* Aging Dis, 2013. **4**: p. 1-13.

374. Kim, J.K., et al., *Buspirone alleviates anxiety, depression, and colitis; and modulates gut microbiota in mice.* Sci Rep, 2021. **11**(1): p. 6094.

375. Politis, M., et al., *Serotonergic mechanisms responsible for levodopa-induced dyskinesias in Parkinson's disease patients.* J Clin Invest, 2014. **124**(3): p. 1340-9.

376. Shin, E., et al., *Serotonergic and dopaminergic mechanisms in graft-induced dyskinesia in a rat model of Parkinson's disease.* Neurobiol Dis, 2012. **47**(3): p. 393-406.

377. Lindenbach, D., et al., *Side effect profile of 5-HT treatments for Parkinson's disease and L-DOPA-induced dyskinesia in rats.* Br J Pharmacol, 2015. **172**(1): p. 119-30.

378. Iovino, L., M.E. Tremblay, and L. Civiero, *Glutamate-induced excitotoxicity in Parkinson's disease: The role of glial cells.* J Pharmacol Sci, 2020. **144**(3): p. 151-164.

379. Pelletier, M. and R.M. Siegel, *Wishing away inflammation? New links between serotonin and TNF signaling.* Mol Interv, 2009. **9**(6): p. 299-301.

380. Yu, B., et al., *Serotonin 5-hydroxytryptamine(2A) receptor activation suppresses tumor necrosis factor-alpha-induced inflammation with extraordinary potency.* J Pharmacol Exp Ther, 2008. **327**(2): p. 316-23.

381. Hayata-Takano, A., et al., *PACAP-PAC1 Signaling Regulates Serotonin 2A Receptor Internalization.* Front Endocrinol (Lausanne), 2021. **12**: p. 732456.

382. Qamhawi, Z., et al., *Clinical correlates of raphe serotonergic dysfunction in early Parkinson's disease.* Brain, 2015. **138**(Pt 10): p. 2964-73.

383. Wu, H., et al., *Beyond a neurotransmitter: The role of serotonin in inflammation and immunity.* Pharmacol Res, 2019. **140**: p. 100-114.

384. Missale, C., Nash, S. R., Robinson, S. W., Jaber, M., & Caron, M. G., *Dopamine receptors: from structure to function.* Physiological reviews, 1998. **78**: p. 189-225.

385. Reavill, C., et al., *Pharmacological Actions of a Novel, High-Affinity, and Selective Human Dopamine D$_3$ Receptor Antagonist, SB-277011-A.* 2000. **294**(3): p. 1154-1165.

386. Everse, J. and P.W. Coates, *Neurodegeneration and peroxidases.* Neurobiol Aging, 2009. **30**(7): p. 1011-25.

387. Zheng, Y., et al., *The Emerging Role of Neuropeptides in Parkinson's Disease.* Front Aging Neurosci, 2021. **13**: p. 646726.

388. Liao, C., et al., *Targeting the PAC1 Receptor for Neurological and Metabolic Disorders.* Curr Top Med Chem, 2019. **19**(16): p. 1399-1417.

389. Langer, I. and D. Latek, *Drug Repositioning For Allosteric Modulation of VIP and PACAP Receptors.* Front Endocrinol (Lausanne), 2021. **12**: p. 711906.

390. Bourgault, S., et al., *Novel stable PACAP analogs with potent activity towards the PAC1 receptor.* Peptides, 2008. **29**(6): p. 919-32.

391. Chen, W.H. and S.F. Tzeng, *Pituitary adenylate cyclase-activating polypeptide prevents cell death in the spinal cord with traumatic injury.* Neurosci Lett, 2005. **384**(1-2): p. 117-21.

392. Abad, C., et al., *Vasoactive intestinal peptide loss leads to impaired CNS parenchymal T-cell infiltration and resistance to experimental autoimmune encephalomyelitis.* Proc Natl Acad Sci U S A, 2010. **107**(45): p. 19555-60.

393. Deguil, J., et al., *Neuroprotective effects of pituitary adenylate cyclase-activating polypeptide (PACAP) in MPP+-induced alteration of translational control in Neuro-2a neuroblastoma cells.* J Neurosci Res, 2007. **85**(9): p. 2017-25.

394. Reglodi, D., et al., *Review on the protective effects of PACAP in models of neurodegenerative diseases in vitro and in vivo.* Curr Pharm Des, 2011. **17**(10): p. 962-72.

395. Van, C., et al., *Targeted deletion of PAC1 receptors in retinal neurons enhances neuron loss and axonopathy in a model of multiple sclerosis and optic neuritis.* Neurobiol Dis, 2021. **160**: p. 105524.